# METHODS AFFECTING NEURONAL DIFFERENTIATION OF HUMAN ADULT AND PLURIPOTENT STEM CELLS

**John William Thwaites (MRes, BSc Hons.)**

**UCL**

**Engineering Doctorate**

## STATEMENT OF ORIGINALITY

Unless otherwise stated in this text, this thesis is the result of my own work.

John William Thwaites (MRes, BSc Hons.)

## ABSTRACT

Stem cells have significant potential to treat many age-related degenerative disorders that affect increasing numbers of people globally. This thesis investigated the capacity for omnicytes and human pluripotent stem cells (hPSC) to undergo directed differentiation towards neuronal cell types for the treatment of ischemic stroke and Parkinson's disease respectively.

Omnicytes express a range of markers related to pluripotency and plasticity; however they are a challenging cell source to use in the development of cell therapies. Variability in omnicyte quality was associated with patient source, disease type and cryopreservation, all of which affected the reproducibility of data.

Successful generation of dopaminergic neurons was achieved using a suspension-based hPSC culture system, with modified culture medium designed to replicate endogenous signalling during development. Neurons expressing key markers of dopaminergic neurons were generated and were capable of producing dopamine in response to KCl challenge. The work also showed that transfection of saRNA could enhance the expression of key genes i.e. foxa2, lmx1a and TH, relative to mock transfected cultures, although not significantly. Results also showed that the specific hESC line used (Shef6) had a greater propensity for differentiation toward dopaminergic neurons than MSUH001 hiPSC.

This work successfully used saRNA to enhance gene expression, but shows that transfection efficiency is a limiting factor to its use. However, if transfection efficiency can be addressed, saRNA will become a powerful tool in the generation of cell therapies, particularly if it can be applied to suspension cell cultures.

## ACKNOWLEDGEMENTS

I would like to dedicate this work to my late father, William George Thwaites, without whom I would not have realised my love of science: he is the man who inspired and encouraged me to follow my ambitions and dreams.

I would like to express my sincerest appreciation to Dr Ivan Wall and Professor Nagy Habib for their continued support with my research and the writing of this thesis. I have valued your patience, motivation, and advice throughout these four years of research, without which this work would not have been prosperous.

I wish to thank the UCL Department of Biochemical Engineering, namely, Professor Chris Mason, Professor Gary Lye and Professor Nigel Titchener-Hooker and the teams of people within UCL who have supported this work. A special thanks to Ludmila Ruban, who advised and supported me throughout this work and whose patience was a great help in some difficult times.

I thank my fellow laboratory colleagues: Iwan Roberts, Yvonne Pang, Giulia Detela, Nathalie Moens, Shahzad Ali, Kate Fynes, Ben Weil and Vishal Sharma (this is not an exhaustive list), for all those long hours spent in the lab and singing along to Magic FM (you know who you are) and for generally being there to listen. And a big thanks to Owen Bain and Leanne Partington who have been good friends from the first day at UCL; thank you for the food, the wine and the chat.

This work would not have been possible without the generous support of the UK Stem Cell Foundation, Engineering and Physical Sciences Research Council and London Regenerative Medicine Network.

Finally I would like to acknowledge and thank Marieke, Mum and Jenny, for all your support over the last 4 years. You have been the glue that kept this all together, and I thank you for always pushing me to reach for something better. You have taught me that success and happiness come from hard work and dedication.

# TABLE OF CONTENTS

## TABLE OF FIGURES

## LIST OF ACHRONYMS

| Acronym | Full name |
|---|---|
| µL | Microlitre |
| µm | Micrometer |
| $1^{o}$ | Primary |
| 2D | Two Dimensional |
| $2^{o}$ | Secondary |
| 3D | Three Dimensional |
| 5'UTR | 5'Untranslated Regions |
| 6-OHDA | 6-Hydroxydopamine |
| ACT | Advanced Cell Technologies |
| ATP | Adenosine Triphosphate |
| BBB | Blood Brain Barrier |
| BDNF | Brain-Derived Neurotrophic Factor |
| bFGF | Basic Fibroblast Growth Factor |
| BMP | Bone Morphogenic Protein |
| BMSC | Bone Marrow Derived Stem Cell |
| Bn | Billion |
| BSA | Bovine Serum Albumin |
| Ca | Calcium |
| CD-1 | Mouse litter breed CD-1 |
| $CD34^{+}$ | Cluster of Designation 34 |
| CDM | Chemically Defined Media |
| cDNA | Complementary Deoxyribonucleic Acid |
| cm | Centermeter |
| $cm^{2}$ | Centermeter Squared |
| CNS | Central Nervous System |
| $CO_2$ | Carbon Dioxide |
| csFBS | Charcoal Stripped FBS |
| CTI | Cell Therapy Industry |
| D(x) | Day (number) |
| DA | Dopaminergic |
| DAPI | 4,6-Diamidino-2-Phenylindole |
| DAPT | N-[N-(3,5-Difluorophenacetyl)-L-alanyl]-S-Phenylglycine T-butyl ester |
| dbcAMP | N6,2'-O-Dibutyryladenosine 3',5'-Cyclic monophosphate |
| DBS | Deep Brain Stimulation |
| $ddH_2O$ | Double Distilled Water |
| DDM | Dopaminergic Differentiation Media |
| DMEM | Dulbecco's Modified Eagle Medium |
| DMEM/F-12 | Dulbecco's Modified Eagle Medium: Nutrient Mixture F-12 |
| DMSO | Dimethyl Sulfoxide |
| DNA | Deoxyribonucleic Acid |
| DNase I | Anti-Deoxyribonuclease 1 |
| DPBS | Distilled Phosphate Buffer Soluiton |
| DRD | Dopamine Deceptor D1 |
| EDTA | Ethylenediaminetetraacetic Acid |

| | |
|---|---|
| EGF | Epidermal Growth Factor |
| ELISA | Enzyme-Linked Immunosorbant Assay |
| FACS | Fluorescence-Activated Cell Sorting |
| FBS | Foetal Bovine Serum |
| FC-media | Feeder-Conditioned Media |
| FDA | Food and Drug Agency |
| F-DOPA | [$^{18}$F]-dopa |
| FGF2 | Fibroblast Growth Factor 2 or Basic Fibroblast Growth Factor |
| FGF20 | Fibroblast Growth Factor 20 |
| FGF8 | Fibroblast Growth Factor 8 |
| FITC | Fluorescein Isothiocyanate |
| foxa2 | Forkhead box protein A2 |
| G-CSF | Granulocyte-Colony Stimulating Factor |
| gDNA Wipeout | Genomic Deoxyribonucleic Acid Wipeout |
| GFP | Green Flourescent Protein |
| GMEM | Glasgow Minimum Essential Medium |
| GTAC | Gene Therapy Advisory Committee |
| hASC | Human Adult Stem Cell |
| HBSS | Hank's Balanced Salt Solution |
| HCl | Hydrochloric Acid |
| HEPES | 4-(2-Hydroxyethyl)-1-Piperazineethanesulfonic acid |
| hESC | Human Embryonic Stem Cell |
| hiPSC | Human Induced Pluripotent Stem Cells |
| HM | Holding Medium |
| hNSC | Human Neural Stem Cells |
| hPSC | Human Pluripotent Stem Cell |
| Hr | Hour |
| HSC | Haematopoietic Stem Cell |
| ICSD | Initial Cell Seeding Density |
| IGF1 | Insulin-like Growth Factor 1 |
| iMEF | Inactivated Mouse Embryonic Fibroblast |
| KCl | Potassium Chloride |
| KO-SR | Knockout Serum Replacement |
| KO-SRM | Knockout Serum Replacement Media |
| L-DOPA | L-3,4-Dihydroxyphenylalanine |
| LID | L-DOPA Induced Dyskinase |
| lmx1a | Homeoprotein LIM homeobox transcription factor 1α |
| M | Molar |
| MCA | Middle Cerebral Artery infarct |
| MCAO | Middle Cerebral Artery Occlusion |
| MEF | Mouse Embryonic Fibroblast |
| MEF media | Mouse Embryonic Fibroblast Media |
| mesDA | Mesencephalic Dopaminergic neurons |
| Mg | Magnessium |
| Mg | Milligram |
| Min | Minute |
| miRNA | MicroRNA |
| mL | Millilitres |

| | |
|---|---|
| mM | Millimolar |
| $mm^2$ | Millimetre Squared |
| MNC | Mononuclear Cells |
| MOAB | Monoamine Oxidase type B |
| Mock | Mock transfected |
| mRNA | Messenger Ribonucleic Acid |
| MSC | Mesenchymal Stem Cell |
| NEAA | Non-Essential Amino Acid |
| NEM | Neuronal Expansion Media |
| NF | Neurofilament |
| ng | Nanograms |
| NHS | UK National Health Service |
| NIH | National Institute of Health |
| nm | Nanometer |
| NSC | Neural Stem Cell |
| nt | Nucleotide |
| NT2 | NTera2 |
| NT2N | NTera2 Neurons |
| Nurr1 | Nuclear Receptor Related-1 |
| $^oC$ | Degrees Centigrade |
| P(x) | Passage (number) |
| PCR | Polymerase Chain Reaction |
| PD | Parkinson's Disease |
| Penstrep | Penicillin-Streptomycin |
| PET | [$^{18}$F]-dopa Positron Emission Tomography |
| PFA | Paraformaldehyde |
| Pitx3 | Pituitary homeobox 3 |
| PNS | Peripheral Nervous System |
| qPCR | Quantitative Polymerase Chain Reaction |
| RA | Retinoic Acid |
| RNA | Ribonucleic Acid |
| RNAi | RNA Interference |
| rpm | Revolutions Per Minute |
| RPMI | Roswell Park Memorial Institute medium |
| RT | Room Temperature |
| rt-PA | Intravenous Recombinant Tissue Plasminogen Activator |
| rtPCR | Reverse Transcription Polymerase Chain Reaction |
| saRNA | Small Activating Ribonucleic Acid |
| SDF-1 | Stromal cell-Derived Factor-1 |
| sec | Second |
| SHH | Sonic Hedgehog |
| SSEA-1 | Stage-specific Embryonic Antigen-1 |
| SSEA-3 | Stage-specific Embryonic Antigen-3 |
| SSEA-4 | Stage-specific Embryonic Antigen-4 |
| TGFβ | Transforming Growth Factor Beta |
| TH | Tyrosine Hydroxylase |
| TSB | Technology Strategy Board |

| | |
|---|---|
| UK | United Kingdom |
| UPDRS | Unified Parkinson's Disease Rating Scale |
| US | United States |
| USA | United States of America |
| UT | Untransfected |
| VEGF | Vascular Endothelial Growth Factor |
| VM | Ventral Mesencephalon |
| VS1 | Vitrificiation Solution 1 |
| VS2 | Vitrificiation Solution 2 |
| *Wnt5a* | Wingless-related MMTV integration site 5A |
| αMEM | Minimum Essential Medium Eagle Alpha Modification |

# CHAPTER 1 - INTRODUCTION

## 1.1 Regenerative medicine and cell therapy

Regenerative medicine as a discipline includes a number of areas, from the widely known cell transplantation element to synthesised biomaterials including; connecting tissues, matrices and scaffolds. Within this body of work we will be focusing on the cell therapy element and the potential of specific cell types in the development of therapeutically useful cells for the treatment of neurological disorders.

The cell therapy industry (CTI) is presently a very small sector when compared with the pharmaceutical industry ($300billion (Bn) per annum (WHO 2013)). There are approximately 50 publically listed companies across Asia, North America and Europe, with an estimated worth of $7Bn with an estimated increase in revenues of $1Bn per annum (Mason, McCall et al. 2012). This is a rapidly growing and highly lucrative industry that is attracting a lot of investment.

Within the cell therapy sector there is a huge amount of activity. There are a number of adult cell-based and embryonic cell-based products moving through different regulatory frameworks. Within the adult cell arena there a number of key players, for example; Athersys, Mesoblast and Osiris (Brindley and Mason 2012), with Athersys currently moving Multistem® through Phase 2 studies for the treatment of ulcerative colitis and ischemic stroke, with other clinical phase trials on-going for multiple indications (Athersys 2013). There are also number of companies approaching the market with embryonic cell-based products and moving through clinical trials, including, Advanced Cell Technologies (ACT), BioTime, Cell Cure Neuroscience and Pfizer, with ACT, for example, moving through Phase 1/2 studies with their human embryonic cell-based treatment for Stargardt's Macular Dystrophy (Trials.gov 2013) and Age related macular degeneration (Trials.gov 2013). Recently there has been a set back within the embryonic space with Geron exiting this sector to pursue other commercial ventures. Geron was considered to be a front-runner, with its product for the treatment of spinal cord injury

(Keirstead, Nistor et al. 2005) moving well through Phase 1 clinical trials. Thankfully the exit of this player has had limited impact on the market with other companies taking up the mantle.

For this industry to realise its potential and for it to succeed in the healthcare marketplace a number of challenges unique to the CTI must be addressed, including, technological innovation, infrastructure, manufacturing, development of enabling technologies, regulation and reimbursement. This thesis will focus on one of the main challenges of the industry, yield, and the ability to generate appropriate volumes of the desired cell type to allow the generation of a product. This thesis focuses on the potential of specific cell types (stem cells) in the manufacture of therapeutically beneficial neuronal cell types for the treatment of neurological conditions: acute ischemic stroke and Parkinson's disease (PD).

This chapter introduces the background to this work, the cells being utilised and the disease indications that the technology hopes to address. Specific detail will be provided within the various chapter introductions.

## 1.2 Stem cells background

Human stem cells can be broadly placed into three categories: Human embryonic stem cells (HESC), human induced pluripotent stem cells (hiPSC) and human adult stem cells (hASC). These cell types can be either defined as allogeneic, non-patient-derived or autologous, patient derived. These specific cell definitions are explained in more detail below.

### 1.2.1 Autologous and Allogeneic

Cells have been used in medical therapies since the 1960's, with the first bone marrow transplants being carried out on patients with depleted stem cell populations following chemotherapy or radiotherapy treatments for cancer. These early therapies were primarily performed using donor bone marrow (allogeneic). This in turn meant that the donor cells were unlikely to be a perfect genetic match to that of the patient and so immunosuppressant drugs were required to prevent rejection of the graft and to subdue adverse immune responses - graft versus host disease. This though left the patient immune-compromised and exposed to

pathogens and potential secondary complications. More recently autologous cell therapies are preferentially used, whereby the cells are collected from the patient prior to treatment and then administered following chemotherapy or radiotherapy to initiate the repopulation of the bone marrow and the patient's immune system. The advantage of autologous treatment is that this removes the need for immunosuppression, reducing the chance of graft/host rejection. It also bypasses any ethical barriers regarding the use of cells from another individual.

### 1.2.2 Human Embryonic Stem Cells

Embryonic stem cells were first identified and cultured from mouse models in 1981 (Martin 1981). Due to the comparative complexity and ethical issues associated with working with human tissues, it took another two decades for researchers to culture hESCs (Thomson, Itskovitz-Eldor et al. 1998). hESCs are harvested and generated from the blastocyst inner cell mass of an embryo, day 4-5 post fertilisation, at which time the cell mass is relatively low (50-150 cells)(Svendsen C. N. 2008). These cells are then cultured and expanded under hESC conditions (this is described in detail in Chapter 2). hESC have the capacity to form all three germinal layers: ectoderm; endoderm; and mesoderm. These cells have the potential to form any specialised mature cell found in the human body. In normal development they go on to form all the various organs and tissues of the body but *in-vitro* hESC can be cultured and expanded indefinitely under the correct stimuli or induced to form specific cell types.

hESCs present some of the greatest therapeutic potential when looking to generate cell types that are not easily obtainable from donor or autologous sources but their use has created considerable ethical debate. hESC also possess the potential for tumour formation which is a hurdle that needs to be addressed before hESC can be used in any therapeutic intervention. Though hESCs are harvested from human embryos supplied surplus to requirement from *in-vitro* fertilisation, pro-life activists question the morality of their use in research (Svendsen C.

N. 2008). There are strict regulations around the world, with Europe and the USA leading the way in developing and reviewing regulatory frameworks (EuroStemCell 2013, Health 2013).

### 1.2.3 Human induced pluripotent stem cells

In 2006 a new and potentially revolutionary stem cell variation was discovered, hiPSC (Takahashi and Yamanaka 2006). These cells are derived from human fibroblasts that have been induced through genetic manipulation to behave like hESCs. Rather than having only limited differentiation capacity which is characteristic of hASCs, it is thought that they can be directed to differentiate into any cell type. It is unlikely that these will be used in therapeutics for some time, as research is still required to understand the oncogenic status of this cell type and to understand how the genetic manipulation has fully affected the cell. These cells do by-pass the potential ethical and legal issues associated with hESCs.

### 1.2.4 Human Adult Stem Cells

hASCs are found in the majority of organs in the human body (Henry and Asa 2004). They are found within populations of specialised cells but they themselves remain undifferentiated (Health 2009). The main function of adult stem cells is to repair and maintain their tissue type. For example, mesenchymal stem cells (MSC) found in bone marrow differentiate and divide to form bone, cartilage, fat, tendon and muscle (Institute 2013), maintaining and repairing these specific cell types. hASCs can maintain their ability to self-renew and produce specialised adult cells even after long periods of inactivity. This quality of senescence is a key characteristic of stem cells.

hASCs have been a focus of research for the last 50 years and were first used in medical therapeutics in 1968 for bone marrow transplants (Health 2009). There are no ethical issues associated with their use and there is no requirement for immunosuppressant drugs as with autologous cells. They also have the potential for differentiation (Watt, Hogan et al. 2000, Wagers and Weissman 2004) for example hematopoietic stem cells (HSC) have been shown to have the potential to generate cell types outside of their normal linage under the correct

stimuli, for example, the generation *in-vivo* of neurons when implanted into the injured spinal cord of chicken embryos (Sigurjonsson, Perreault et al. 2005).

## 1.3 Stem Cell Characteristics

Stem cells have specific, unique characteristics that make them extremely attractive for incorporation into medical therapies. They are able to undergo self-renewal and retain their undifferentiated state when provided with the correct stimuli but can also differentiate to produce daughter cells with specialised functions. These traits and abilities possessed by stem cells are explained in more detail below.

### 1.3.1 Niche dependency

Whilst the intrinsic genetic programme of the stem cell is critical to its phenotype, environmental stimuli are also thought to be important regulators of behaviour. This environment is commonly referred to as the stem cell niche microenvironment (Schofield 1978, Martinez-Agosto, Mikkola et al. 2007). The niche refers collectively to the chemical and biological signals, along with the physical (mechanical) contact within the immediate environment of the cell. These signals allow stem cells to maintain their identity and prevent the cells from losing their 'stemness'. Niche dependency is best demonstrated by removing the stem cell from its niche. With the loss of the stimuli associated with the niche the cell divides, differentiates or become apoptotic (Scadden 2006). Self-renewal, pluripotency and maintenance/repair are influenced by the stem cell niche, which either maintain the stemness of the cell or causes it to differentiate and specialise. There is one known exception to this rule, HSCs, which are able to enter the circulatory system and then 'home' back to their niche, maintaining their own 'stemness' (Martinez-Agosto, Mikkola et al. 2007).

The characteristics of the niche are simulated or modified in differentiation or expansion protocols. By including or excluding specific stimuli, the cells can be maintained, expanded as a pluripotent cell population or directed towards a desired cell type.

### 1.3.2 Potency

Potency describes a cell's ability to give rise to a variety of mature specialised cell types from one unspecialised stem cell. hESC and hiPSC are thought to have this ability to the greatest degree and are considered to be pluripotent, with the ability to produce over 200 different cell types.

The majority of hASCs are considered multipotent (i.e. HSCs), and are able only to produce a limited number of different cell types connected to their particular lineage, under normal, niche, conditions. Other tissue specific cell populations are more restricted still, for instance neural stem cells (NSC) found within the hippocampus are believed to have the potential to produce purely neurones (Martinez-Agosto, Mikkola et al. 2007).

### 1.3.3 Cell maintenance and repair

Through asymmetric division stem cells produce daughter cells to maintain their population to repair areas of damage within the tissue. As cells are removed from the niche they mature and differentiate into the required cell type through external stimuli (Martinez-Agosto, Mikkola et al. 2007).

### 1.3.4 Self-renewal

Where in cell maintenance and repair, stem cells produce specialised daughter cells through asymmetric division, they are also able to self-renew, through symmetric division. This process enables stem cells to maintain their population and expand it within the niche (Martinez-Agosto, Mikkola et al. 2007). The mitotic spinal during division remains parallel to the niche, ensuring that the daughter cell maintains in contact with the niche and its stimuli. Through this process the progeny produced are identical to the parent cell, retaining their stem cell characteristics.

### 1.3.5 Quiescence

Stem cells are thought to be relatively quiescent, and under normal physiological conditions proliferate and divide infrequently (Morshead, Reynolds et al. 1994). This characteristic is

considered important to maintain cell homeostasis and reduce the probability of mutagenic events. The molecular pathways that control quiescence are closely related to the stem cell niche interaction, when separated from niche stimuli, as is the case for asymmetric division, quiescence is interrupted and the cells differentiate.

### 1.4 Acute ischemic infarct (Stroke)

Stroke is the fourth most common cause of mortality in the United Kingdom (UK). There are approximately 150,000 incidences of stroke (Association 2013) per annum and stroke accounts for approximately 50,000 deaths every year in England (Association 2013). It is also the leading cause of long and short term disability globally (Deb, Sharma et al. 2010). There is a 33% mortality rate associated with stroke one year post incidence (Foundation 2009) and one third of the surviving patients left with disabilities including speech and vision difficulties, difficulty with mental processes, tiredness and weakness associated with one side of the body. The financial burden of stroke on the UK National Health Service (NHS) and economy via lost productivity is considerable and estimated at £7Bn annually (Excellence 2010). The number of incidences of stroke is only anticipated to increase in the future due to the global aging population. Therefore, the development of new and innovative therapies for the stroke is of paramount importance.

There are a number of risk factors associated with stroke which include; social, ethnic, pharmacological and physiological factors, resulting from the individual or the environment. Social factors include; drug use, drinking, smoking and the use of the contraceptive pill and there is evidence to suggest that some ethnic groups may be at higher risk. Other factors include but are not limited to hypertension, arterial fibrillation and diabetes (Adina Michael-Titus 2007, Choices 2012).

There are two main types of stroke that result in an interruption of the blood supply to the brain, ischemic and haemorrhagic, both can lead to infarction and cell death. Ischemic stroke, caused by a blockage within a vessel of the brain, accounts for approximately 87% of stroke

cases; with haemorrhagic stroke, the bursting of a vessel, accounting for the remainder (Lopez, Mathers et al. 2006, Association 2012).

Due to its prominence and the proposed mechanism of treatment, cell replacement, this thesis focuses on acute ischemic stroke, and the development of a cell therapy from omnicytes to treat the condition.

### 1.4.1 Pathophysiology

The human circulatory system pumps blood around the body, providing oxygen and nutrient to cells and removing metabolic waste products, such as carbon dioxide ($CO_2$). Though the brain only constitutes 2% for the body's mass it utilises 20% of the available oxygen content of the circulatory system (Adina Michael-Titus 2007). This is because the brain is solely dependent on aerobic respiration to provide energy to support its intensive metabolism; other organs have the capacity for anaerobic respiration. This makes the brain extremely vulnerable to the consistent supply of oxygen (Thwaites, Reebye et al. 2012).

Ischemic strokes occur when the blood to an area of the brain is restricted (by approximately 50%) and can be caused by the narrowing of the arteries through atherosclerosis or blocked as a result of an embolus. Though these are the primary causes of an ischemic stroke, it can also be caused by systemic hypofusion (the blood flow to the whole body is reduced), typically caused by heart failure (Association 2012). Atherosclerosis is the build-up of plaque within the lumen of the artery, which can lead to the formation of a thrombus, blocking the lumen of the vessel and restricting blood flow (Adina Michael-Titus 2007). Atherosclerosis can occur as a result of high blood pressure, cholesterol, smoking or high sugar intake. Embolic strokes are caused by the movement of an embolus formed elsewhere in the body to the brain and blocking the vessels. The majority of embolus strokes occur in the morning when the victim undergoes a sudden transition from rest state, characteristic of sleep, to the physical activity of awake, resulting in fluctuations in blood pressure, dislodging the embolus present.

The severity of an ischemic stroke differs depending on the area of the brain that has been effected and the duration of the ischemia (Mitsios, Gaffney et al. 2006). An area of the brain that is starved of blood for 20 seconds becomes anoxic (oxygen starved) and lapses into unconsciousness. If the ischemia continues for up to five minutes, the cells in the effected regions will die (Mitsios, Gaffney et al. 2006). This is due to the reduction in available adenosine triphosphate (energy) which results in reduced energy dependent functions such as membrane ionic pump function triggering membrane depolarisation, failure of ion homeostasis and release of glutamate (Dirnagl, Iadecola et al. 1999). These processes, which happen between 1- 2 hours (hr) (Mitsios, Gaffney et al. 2006), trigger a cascade of other effects which result in cell apoptosis and necrotic cell death. In the immediate region (the core), cells are instantly dead. The region surrounding the core (the penumbra) experiences significantly reduced blood flow and it is here that energy dependant functions fail and apoptosis occurs. The longer the duration of the incidence the greater the damage in this region (Deb, Sharma et al. 2010). The penumbra and the surrounding tissue are the targets of cell therapy, to prevent or reduce cell death within these regions or replace the cells lost.

### 1.4.2 Current treatment

There is currently only one Food and Drug Agency (FDA, United States) approved drug treatment for stroke. Approved in 1996, intravenous recombinant tissue plasminogen activator (rt-PA) (Albers, Bates et al. 2000) has a treatment window of 6hrs after stroke onset and is ideally administered within 3hrs (Association 2013). This time limit inevitably means that the majority of patients cannot benefit from the treatment. Pharmaceutical treatments in development are targeting early onset stroke, and focus on anticoagulants and antiplatelet, but have been shown to have limited impact on the revascularisation of the affected area. In addition to the pharmaceutical intervention techniques mentioned there are also two mechanical treatments available. These function to attach to the insulting embolism or thrombus and allow manual removal. FDA approved devices include: the Mechanical Embolus

Removal of Cerebral Ischemia and the mechanical thrombectomy device; the Penumbra system (Bose, Henkes et al. 2008, Cohen, Itshayek et al. 2011).

### 1.4.3 Cellular therapies for Ischemic Stroke

With currently available pharmacological and surgical treatments having a number of limitations, namely their short administration window, the advent of cell transplantation and the potential for long term regeneration through the use of stem cells is an attractive adjuvant to stroke patients. Candidate cell types have the potential to act in two modes; they can function in a trophic, neuroprotective capacity to subdue the impact of the ensuing stroke and reduce the level of cell death experienced, otherwise stem cells have the potential to be administered at a later stage to replace non-viable cells and tissues and to restore function.

### 1.4.4 In-vitro investigation

The ability to generate neurons *in-vitro* has evolved from being a niche expertise to a widely used technique within many laboratories. The potential of stem cells in the treatment of neurological conditions is coming closer to being realised. The ability to generate neurons from a number cell sources including; hESC, hiPSC, immortalized cell lines and hASC has been shown by different groups around the world.

hESC are an extremely attractive source of cells for this type of differentiation due to their ability for expansion and pluripotency. It was demonstrated by Reubinoff *et al.* that it was possible to generate an enriched population of neuronal progenitors that were capable of undifferentiated proliferation from a starting population of HES-1 (Reubinoff, Pera et al. 2000). Similarly Chambers *et al.* described a protocol that claimed to be able to differentiate hESC into functional neurons at an efficiency of 80% using two inhibitors of smad signalling; noggin and SB431542 (TGF-β inhibitor) (Chambers, Fasano et al. 2009).

There is a drive to try to avoid the use of hESC in the development of treatments due to their ethical status and their potential for tumour formation. With this in mind researchers have also started work to investigate other adult cell populations.

One promising source of cells includes immortalized cell lines. An example is NTera2 (NT2), which was established from a human testicular germ cell tumour and has been shown to be exclusively committed to the neuronal lineage upon exposure to retinoic acid (RA) (Andrews, Damjanov et al. 1984). The resulting cells, NT2N, display functional neuronal progenitor and terminally differentiated cell characteristics (Pleasure, Page et al. 1992, Pleasure and Lee 1993).

hASC have also been shown to have potential within this field, marrow subpopulation MSCs have been differentiated successfully into neuron-like cells. These neuron-like cells expressed neuron-specific endonuclease, NeuN and Neurofilament-M (Woodbury, Schwarz et al. 2000). Hermann *et al*. (Hermann, Gastl et al. 2004) showed that MSCs could be differentiated into neuronal-like progenitors when cultured in basic fibroblast growth factor 2 (FGF2) and epidermal growth factor (EGF), which then required maturation using other factors such as brain derived neurotrophic factor (BDNF) and RA. It is clear that hASC have potential within this field and that they possess some ability to be differentiated towards a neuronal linage; however it is also clear that other factors are required to completely commit these cells to the relevant differentiation pathways.

### 1.4.5 Preclinical investigations

Specific cell types have been shown to have potential in brain repair following ischemic attack. A number of pre-clinical trials have been carried out on autologous derived adult stem cells with some success. Groups have shown that the administration of rat derived MSCs into rats subjected to middle cerebral artery occlusion (MCAO) resulted in significant recovery over the control arms of the investigation (neurological severity scores, adhesion removal and rota-rod tests analysis techniques were assessed). It was also shown that the administered cells localised to the site of infarct, resulting in an up-regulation of astrocyte and neuronal markers as well as reducing scaring levels (Chen, Li et al. 2001, Shen, Li et al. 2007).

Bone marrow derived HSC have also been investigated for the potential in brain repair following ischemic attack. HSCs isolated from bone marrow biopsies or by mobilisation through Granulocyte colony-stimulating factor (GCS-F) stimulation have both been studied. HSC have been shown to 'home' to a site of injury and to secrete trophic factors such as vascular endothelial growth factor (VEGF), FGF2 and insulin-like growth factor 1 (IGF1), which promote revascularization and the protection of damaged tissues (Taguchi, Soma et al. 2004). Taguchi *et al*. showed that mice following MCAO, injected with HSC showed enhanced angiogenesis and neurogenesis at the site of infarct. It was also shown that treated mice compared to the control showed lower levels of behavioural abnormalities (Taguchi, Soma et al. 2004). Similar results were shown by Schwartin *et al*. who investigated the anti-inflammatory effects of purified HSC in MCAO treated mice. Post-mortem studies showed that administered HSC migrated to the peri-infarct regions significantly reducing the infarct volumes and reducing the level of apoptotic cell death, this was in part thought to be due to a subdued immune response caused by the administered HSC (Schwarting, Litwak et al. 2008).

Human neural stem cells (hNSC) have also been investigated. hNSC are derived from foetal or embryonic central nervous system (CNS) and cultured and expanded *in-vitro*. It was shown in rats subjected to MCAO that cultured hNSC administered to the non-ischemic zone migrated towards the infarct area and started to express mature neuronal markers. Though this shows some potential for this cell type in the treatment of ischemic stroke the use of hNSC in routine clinical use is questionable due to their derivation from foetal or embryonic tissues, raising ethical issues but also logistic issues in maintaining availability and quality control.

### 1.4.6 Clinical trials

Bone marrow derived and immortalised cell lines are being investigated within clinical trials in the UK (Catapult 2013). The inclusion of bone marrow derived MSCs in the treatment of ischemic stroke was first reported in 2005 by Bang *et al*. (Bang, Lee et al. 2005) who performed a phase 1 safety and efficacy trial on 30 patients that had suffered a middle cerebral artery

infarct (MCA). A defined number of autologous cells were injected intravenously and patients were examined against the Barthel index and Rankin Score one year post administration. It was observed that the treated group steadily improved in both indices and that there was no adverse reactions to the treatment. A similar investigation was performed on 52 patients over a five year period with similar findings. The improvements were thought to be associated with increased Stromal cell-derived factor-1 (SDF-1) levels in the patient serum and the involvement of other areas of the brain, namely the sub ventricular region of the lateral ventricle (Lee, Hong et al. 2010). Improvements were also observed by Savitz *et al.* in a patient group injected with autologous mononuclear cells (MNC). Patients showed enhanced improvement on the Barthel index, with no adverse effects associated with the administration of the cells (Savitz, Misra et al. 2011).

There are two clinical trials associated with stroke that have recently finished in the UK; a phase 1 trial based at Hammersmith Hospital, Imperial College London finished in 2014 (Banerjee, Bentley et al. 2014) and a commercial trial, PISCES, by ReNeuron Group Plc. (Therapy 2013). Imperial College London's trial involved the administration of *in-vitro* expanded Cluster of designation 34 $(CD34)^+$ cells within 7 days of the event. It involved 10 patients and commenced in 2007. PISCES, authorised by the Gene Therapy Advisory Committee (GTAC, UK) investigated the safety and feasibility of their immortalized NSC line, ReN001, derived from foetal brain tissue. The company has now been awarded £1.5 million grant by the Technology Strategy Board (TSB) to support the Phase 2 trial of ReN001 (ReNeuron 2013).

### 1.5 Parkinson's disease

PD is a progressive, neurodegenerative disorder first identified in 1817 by James Parkinson (Parkinson 1917), caused by the gradual degeneration of neurons in the substantia nigra pars compacta (Davie 2008) and results in reduced levels of the neurotransmitter dopamine. This leads to the gradual loss of control over motor function and the ability to initiate movement.

PD is not fatal but patients deteriorate physically and mentally over time and so the disease has a significant impact on the quality of life for the patient.

In the UK, approximately 127,000 people suffer from the disease, this equates to 1 in 500 people nationally (UK 2013). The financial burden of PD including costs incurred from GP visits, hospital visits, drugs, and other professional health service, and indirect costs associated with loss of productivity of the sufferer and impact on those close to sufferers are significant. Depending on the measure and assumptions, Findley *et al*. estimates the cost of PD to the UK to be in a range between £449million and £3.3Bn (Findley 2007). The cost of PD to society is anticipated to increase due to the average age of the population increasing, and the prevalence of PD increasing with age. As the cost of care increases with severity of the condition, treatments that can reduce symptoms or delay the disorder's progression will have a positive impact on the health service and national economic system. The development of new therapies has been recognised by global governments, non-government organisations and industry as of paramount importance, with the level of investment and support being moved into this area increasing annually.

PD symptoms worsen as the disease develops and are categorised as either motor or neuropsychiatric (Massano and Bhatia 2012). Motor symptoms include tremors, postural instability, slowness in movement and physical rigidity. Resting tremors are a characteristic symptom associated with the disease and occur late in the disease progression. Early symptoms can include but are not exclusive to expressionless face, cramped handwriting, minor shakes and difficulty rising from a chair (UK 2013). Neuropsychiatric symptoms manifest in the form of cognitive impairments as well as mood and behaviour problems. As the disease advances it can cause cognitive disturbances and can result in problems involving planning, rule acquisition and the control of appropriate and inappropriate action, speed of thinking and memory (Massano and Bhatia 2012). Later in the stages of the disease, psychotic symptoms including hallucinations and delusions can also develop (Friedman 2010).

### 1.5.1 Pathophysiology

PD can either be idiopathic, arising from an unknown cause, or hereditary, where the patient has a genetic predisposition to the disease. Suffers are typically diagnosed with the disease later in life (>50 years old), with only 5% of patients diagnosed below the age of 40 (UK 2013). Diagnosis is often made when symptomatic changes alert patients to consult their health practitioners; unfortunately by this time, the level of neurological-degeneration is usually in its advanced stages and it is estimated up to 80% of the dopamine producing neurons are lost (Lees, Hardy et al. 2009). This loss results in one of the most characteristic symptoms of PD, the loss of motor function; this symptom is directly linked to the loss of dopaminergic (DA) neurons and their presence in the striatum, resulting in the disruption and diminished control of the motor circuitry due to reduced levels of dopamine neurotransmitter present (Obeso, Rodriguez-Oroz et al. 2000). There are currently no definitive diagnostic tests for Parkinson's disease; diagnosis is primarily done through historical analysis of the family and positron emission tomography (PET Scanning) to elucidate the number of surviving dopaminergic neurons; brain scans are also used to rule out other causes of the symptoms (Massano and Bhatia 2012).

### 1.5.2 Current treatments

Current treatments for PD involve either drug administration or surgical intervention, with treatments tailored to the individual patient. Although there are several drug treatments available for PD (Lindvall and Kokaia 2006, Lindvall and Kokaia 2009, UK 2010, UK 2013) they do not function to slow the progression or cure the disease, they only provide symptomatic relief. Surgical techniques such as deep brain stimulation (DBS) have also been found to give relief to advanced stage PD suffers (Hellmann, Djaldetti et al. 2006, Lindvall and Kokaia 2006, Lindvall and Kokaia 2009) and rehabilitation such as exercise, physiotherapy, speech therapy and diet can also help to relieve symptoms (UK 2010).

The gold-standard pharmacological treatment is a dopamine replacement, a treatment discovered in the 1950's by Arvid Carlsson. The treatment involves the administration a dopamine precursor L-3,4-dihydroxyphenylalanine (L-DOPA) that passes through the blood brain barrier (BBB) and is catalysed by dopa carboxylase to synthesise dopamine, and has been found to reduce some of the symptoms of PD (Carlsson, Lindqvist et al. 1958, Cotzias, Van Woert et al. 1967). L-DOPA has a vital role currently in the treatment of PD due to its ability to pass through the BBB; dopamine administered itself is unable to do this and so is of no therapeutic use. L-DOPA is an effective treatment for reducing the symptoms caused by PD but prolonged use of the drug can lead to the development of L-DOPA induced dyskinesia (LID). LIDs are a result of abnormal motor outputs from the striatum that result in the involuntary movements, caused by the sensitivity of the neurons to the treatment after prolonged use. A second side effect resulting from the use of L-DOPA and the variability in levels between administration is known as the 'on/off' response (Thanvi, Lo et al. 2007). The on/off response is shown through ease of mobility during the 'on' phase and stiffness and bradykinetic movements during the 'off' phase, when the levels of L-DOPA are low.

Developing on the success of L-DOPA is a new drug, Duodopa, this is a new formulation of L-DOPA (carbidopa/levodopa) which is delivered via a novel intra-intestinal pump which is surgically inserted and programmed to deliver a dose which can be modified using an external controller, in a non-invasive way (Karlsborg, Korbo et al. 2010).

Two pharmacological treatments used separately, or in conjunction with L-DOPA have also had positive results. Dopamine receptor antagonists can be used to bind to the dopamine receptors in the brain and mirror the effect of dopamine (Burton and Calne 1984). Monoamine oxidase type B (MOAB) inhibits the breakdown of neurotransmitters and has been shown to reduce the breakdown of endogenous dopamine (Ives, Stowe et al. 2004). These treatments have some success in reducing symptoms, particularly in the early stages of PD, but neither is as effective as L-DOPA in relieving and reducing symptoms.

Surgical intervention as an option for treatment involves DBS and was first reported in the 1980s by Brice *et al*. (Brice and McLellan 1980). DBS involves the implantation of electrodes to stimulate the neurons within specific regions of the brain, two targets for implantation have been identified including to the globus pallidus and the sub thalamic nucleus of the basal ganglia motor circuitry. DBS excites or inhibits neurons in the vicinity of the electrodes and is controlled by the duration and intensity of the stimulation, which is controlled by a DBS pacemaker (Vitek 2008).

### 1.5.3 Cellular therapies for Parkinson's disease

The idea of substituting lost DA neurons with a donor source has been around since the 1970s where it was first explored in Sweden and the United States of America (USA) using rats with 6-hydroxydopamine (6-OHDA) induced lesions. Although, the use of donor human foetal grafts was held back for ethical reasons in a number of countries; in 1985 the Lund group received permission to use human foetal tissue to show good survival in the stratum of 6-OHDA lessoned rats. It was shown that the introduced donor cells were able to innervate the host striatum and reverse lesion induced motor deficits (Brundin, Nilsson et al. 1986, Brundin, Barbin et al. 1988). In 1986 the Ethical Delegation of the Swedish Society of Medicine endorsed the use and issued guidelines for the use of human foetal tissue harvested from aborted foetus in transplantation therapies, and shortly afterwards, trials showed significant and sustained improvements in a number of parameters associated with dopamine management, including improved [$^{18}$F]-dopa positron emission tomography (PET) uptake. The results of the trial indicated good survival and growth of the grafted DA neurons (Lindvall, Brundin et al. 1990, Lindvall, Widner et al. 1992) and, further, post mortem studies of the subjects showed good graft survival and robust innervation (Kordower, Rosenstein et al. 1996). These positive outcomes supported a change in policy in the USA, where regulation was adapted to allow the National Institute of Health (NIH) to fund 2 placebo controlled trials in 1993. Since these initial transplantations between 300-400 patients have received this treatment, either in open label or placebo surgery controlled trials (Lindvall and Kokaia 2009). Results have shown that cell

replacement of mesencephalic dopaminergic neurons (mesDA) neurons can be beneficial. Results have varied between open-label trials but benefits have been witnessed through patient symptomatic relief as well as increased L-DOPA intake indicating successful engraftment and graft survival (Lindvall and Kokaia 2009).

There is currently one on-going open-label clinical trial in the UK based at Cambridge University in this area. The trial is a Phase 1/2 trial investigating the use of foetal brain tissue in 40 PD patients. The patients have been pre-screened through the Transeuro observational study and have been selected to participate. Participants will be monitored for up to 36 months and will be measured according to outcomes such as Unified Parkinson's Disease Rating Scale (UPDRS) change, Dyskinesia, L-DOPA usage and PET analysis (ClinicalTrials.gov 2013).

Though findings of cellular replacement therapies for PD are promising, there are a number of issues associated with using cells from human foetal tissue; including patient variability, graft-induced dyskinesia and the consistency of foetal tissue as a material: obtaining source material in great enough numbers is difficult; the quality can be highly variable; the cells are almost impossible to standardize; and finally in many countries, harvesting tissues from aborted foetuses is highly controversial and in some cases illegal. These matters have driven a push to develop other sources of DA neurons, including via stem cell advances in technology. Cells that can be sourced from none ethically controversial sources that can be standardised in number and quality controlled; stem cells have been identified as a likely candidate.

### 1.5.4 Preclinical Investigations

The characteristics of PD make it a target for stem cell therapy. If it is possible to replace the lost cells with differentiated stem cells, it may be possible to alleviate or even cure the disease and achieve long-term, sustainable relief for patients. It is important that any treatment that is developed far exceeds the current capabilities of pharmaceutical or surgical based interventions. The ultimate goal is for cells to be able to: secrete dopamine in a regulated

manner; respond to stimuli; express morphological and genetic similarity to mesDA neurons; reverse symptoms caused by the disease; and be able to integrate into existing circuitry, becoming functionally active. Stem cells would also have to be expandable in culture, survive long-term in the patient's brain once engrafted, and behave and express all markers and functional similarities with mesDA neurons *in-vitro*. It is likely that DA neurons derived from stem cells are going to have to be of human origin, due to the risk of inter species disease transmission.

A number of groups have shown the ability to generate DA-like neurons through the manipulation of stem cell populations. Kim *et al*. (Kim, Auerbach et al. 2002) demonstrated in hESC that over-expression of Nuclear receptor related-1 (Nurr1), using plasmid technology and electroporation, could differentiate hESC into midbrain neural stem cells. These progenitor cells went on to produce tyrosine hydroxylase (TH) positive cells. The resulting cells were investigated *in-vivo* in mice treated with 6-OHDA lesions. Animals were screened to detect the graft placement and after 4 to 8 weeks the number of neurons present did not change, indicating the stability of the graft. Over this period there was also no observation of teratoma formation and neurons formed functional synapses and showed the relevant electrophysiological properties that are expected of mesDA neurons. The group also tested for behavioural improvements and found significant improvements in various behaviour tests in the treated population. While the study was promising for cell therapy, the publication identified a need for further studies into the long-term safety of the protocol along with efficacy of implantation.

Work performed on primate embryonic stem cells (ESCs) by Takagi *et al.* (Takagi, Takahashi et al. 2005) showed that monkey ESCs could be induced to differentiate into dopamine neurons through co-culture with stromal cells (P6 stromal cells), supplemented with fibroblast growth factor 20 (FGF20) and FGF2 to increase the overall yield. These cells were transplanted into *Macaca fascicularis* that had been treated with 1-methyl-4-phenyl-1,2,3,6-tetrahydropyridine

resulting in a primate PD model. At 10 weeks significant improvements in neurological score for treated animals were observed over that of control animals and imaging during the experiment showed that cells were functioning as dopamine producing cells once administered.

Though hESCs have been investigated for this purpose, there are obstacles in their use, their ethical status is questionable and their potential for teratoma formation is concerning, especially in a non-terminal diseases such as PD. These concerns have led research to a move towards hASC as a cell source. DA neuronal differentiation is being investigated using a number of sources including, CNS tissue (Shim, Park et al. 2007), bone marrow derived stem cells (BMSC) (Dezawa, Kanno et al. 2004) and hiPSC (Chambers, Fasano et al. 2009).

### 1.5.5 In-vitro & In-vivo investigation

Investigators have shown that over expression of various transcription factors can induce differentiation of cell types into DA neurons. As described previously, the over-expression of *nurr1* can be used to generate DA precursors from hESCs (Kim, Auerbach et al. 2002) and similar findings have been found with other cell sources. Adult CNS derived cells showed that with over-expression of *nurr1* and the addition of growth factors they could be differentiated towards a DA cell type (Shim, Park et al. 2007). Embryonic or foetal CNS cells have also been shown to differentiate into DA neurons with the over-expression of either *Wnt5a* (Parish, Castelo-Branco et al. 2008) or Pituitary homeobox 3 (P*itx3)* (O'Keeffe, Scott et al. 2008), and *notch1* over-expression has been found to have the same effect on bone marrow derived cells (Dezawa, Kanno et al. 2004) when co-cultured with various growth factors. In the majority of these examples the procedure was only investigated using animal stem cells, with further work needed to investigate the impact on human stem cells.

The use of animal products and retroviruses within these studies present their own obstacles that need to be addressed before these protocols can move forwards, the risk of xeno-transmission of disease and the genomic instability caused through DNA modification of the

genome needs to be investigated. This said, a Phase I trials has previously been done using a gene therapy in PD and so may address this concern (Fiandaca, Forsayeth et al. 2008).

Fu *et al*. (Fu, Cheng et al. 2006) investigated the use of MSCs isolated from the Wharton's jelly of human umbilical cord as a source for differentiating DA neurons. The group found that through culture with neuronal conditioned medium supplemented with growth factors sonic hedgehog (SHH) and fibroblast growth factor 8 (FGF8) they were able to differentiate MSCs into DA neurons. Cells cultured with the additional growth factors were found to secrete dopamine whereas cells that had not been cultured with them, did not secrete. These cells were implanted into rat models treated with 6-OHDA lesions and were found to be viable 4 months after transplantation without the need for immunosuppression within the animals. No tumour formation was identified. Despite this success, behavioural analysis of the animals, showed no improvement over the control animals. It was thought this result may be due to inadequate cell transplantation, as it contradicted other studies which showed that implanted DA neurons help to alleviate PD symptoms. Fu *et al*. also suggest it may take time for administered cells to integrate into the host brain and there were concerns for the viability of the introduced cells. The group suggest further work is needed to assess cell number requirement and a greater understand of the factors being utilised, so to mitigate any toxicity.

Work done by Wernig *et al.* (Wernig, Zhao et al. 2008) demonstrated that iPSC could be efficiently differentiated into neuronal precursor cells, and once implanted *in-vivo,* these cells were observed to migrate and integrate into the host brain tissue, differentiating into mature neurons and glial cells. Wernig *et al* also demonstrated through electrophysiological recording and morphology analysis that iPSC could be directed to differentiate into DA neurons *in-vitro* and once implanted into a PD model improve the behaviour of the host rat when compared to the control rats.

## 1.6 Thesis aims

This thesis investigates the potential of both hASC (omnicytes) and hPSC (hESCs and hiPSC) for the differentiation of neuronal populations for therapeutic use. Specifically, omnicytes will be assessed for their ability to differentiate into neuronal populations through both media and molecular manipulation; and hPSCs will be investigated for their ability to form specialised DA neurons through media manipulation. We will then go onto investigate the use of small activating RNA (saRNA) to enhance gene expression of differentiating populations and to increase the yield of DA neurons produced

# CHAPTER 2 - MATERIALS AND METHODS

This thesis investigates two specific cell types; hASC, namely omnicytes, and hPSC types including hESC and hiPSC. The two bodies of work were carried out at separate locations; UCL laboratories (2nd floor, Robert building, London) and Omnicyte laboratories (Hammersmith hospital, London). Due to this work being carried out in different laboratories and on different cell types, different protocols were used to culture the cells and analyse the products of the experiments. In this materials and methods, general protocols associated with working on human pluripotent cell types in the UCL laboratories are described first. Protocols used at the Omnicyte Ltd. facility whilst working on omnicytes are described in the second part of the chapter.

In working with both cell types, methodologies and protocols were refined to optimise the outcome; this process of optimisation was informed by literature, lab work and collaboration.

**UCL BASED CULTURE AND ANALYTICAL TECHNIQUES**

This section describes the culturing and analytical techniques that were used whilst experimenting with hPSCs; hESC and hiPSC.

## 2.1. General Human iPSC and ESC Culture Techniques

### 2.1.1 Human iPSC and ESC Culture

Undifferentiated hPSC, MSUH001 (hiPSC, acquired from Michigan State University, USA) and Shef6 (hESC, acquired from UK Stem Cell Bank) were cultured in T25 culture flasks (Nunc). VWR International Ltd, Leicestershire, UK). Cells were co-cultured with Mitomycin-C (0.01mg/mL Sigma-Aldrich, Poole, UK) inactivated mouse embryonic fibroblasts (iMEF, Ref. 2.1.4) in knockout serum replacement media (KO-SRM) comprising of: KnockOut™ DMEM (KO-DMEM, Life Technologies, Paisley, UK) supplemented with 20% KnockOut™ Serum Replacement (KO-SR, Life Technologies); 1% Glutamax™ (Life Technologies); 1% non-essential amino acids (NEAA, Life Technologies); 100mM β-Mercaptoethanol (Life Technologies). hESC

and hiPSC medias was supplemented with 4 & 10ng/mL basic fibroblast growth factor (bFGF, Prospec-Tany Technogene Ltd. East Brunswick, USA) respectively.

Cells were incubated in a HERAcell 150 incubator (ThermoFisher Scientific, Loughborough, UK) at 37$^{o}$C and 5% $CO_2$ and media was changed on a 24hrs cycle, replacing spent media with 5mL of fresh KO-SRM. Pluripotent cells were passaged onto freshly prepared iMEFs every 3-4days by mechanical dissection of colonies into smaller sections using sterile 3mL fine tip pasteur pipette (StarLab, Milton Keynes, UK). hESC colonies were dissected using this technique but were additionally treated with 0.125mg/mL Collagenase Type IV (Life Technologies) for 5min at 37$^{o}$C prior to dissection. Dissected colonies were transferred onto fresh iMEF cultures at typically a 1:2 or 1:3 split.

### 2.1.2 Vitrification of hESCs

To allow long-term storage of hESC, cells were vitrified using the following method. hESC colonies were first treated with 0.125mg/mL Collagenase IV and incubated at 37$^{o}$C for 5min followed by a rinse with KO-SRM. Colonies were then dissected in 1mL KO-SRM using a sterile micro pipette into clumps containing ~100-200 cells each. Vitrification comprised of 4 steps: (i) clumps were stored in Holding medium (HM, Table 1), whilst alongside, sterile 4.5mL cryovials (Nunc.) were prepared in order to record cell line details, date and passage number; vials were also perforated with a sterile hypodermic needle to aid air displacement when submersed in liquid nitrogen; (ii) using a 20µL pipette (StarLab) 8-10 clumps were transferred to Vitrification solution 1 (VS1, Table 1) and incubated at room temperature (RT) for 1min; (iii) clumps were then transferred to Vitrification Solution 2 (VS2, Table 1) and held for 25 seconds at RT; (iv) clumps were transferred using a pipette onto the lid of the plate being used with minimal VS2 transfer; (v) using capillary straws (Corning, Flintshire, UK), cells were drawn into the straws; (vi) straws were immediately plunged into liquid nitrogen and transferred to the storage cryovials (prepared in step (i)) for long-term storage. The whole process was performed in less than 3min. Samples remained cryogenically frozen until use.

| | |
|---|---|
| **HM** | D-MEM containing HEPES (10mM HEPES, Life Technologies)<br>20% FBS |
| **VS1** | HM<br>10% DMSO (Dimethyl sulfoxide, Sigma-Aldrich)<br>10% Ethylene glycol (Sigma-Aldrich) |
| **VS2** | HM<br>20% DMSO<br>20% Ethylene glycol<br>0.5mol/L Sucrose (Sigma-Aldrich) |

**Table 1 - Vitrification solution compositions**
Basic composition of the solutions used in the vitrification of hESC.

### 2.1.3 Thawing of vitrified cells

Straws of cryogenically frozen cells were carefully removed from the liquid nitrogen and the cryovials and immediately submerged in HM supplemented with 0.2molar (M) sucrose to expel the cell clumps. Cells were incubated in HM for 1min at RT and then transferred to HM supplemented with 0.1M sucrose and incubated for 5min. Cells were washed twice in clean HM solution and incubated for 5min before being transferred into fresh T25 culture flasks and co-cultured with iMEF. Cells would typically attach to the culture surface overnight and required passaging within 7 days.

### 2.1.4 Inactivated mouse embryonic fibroblast protocols

To allow co-culture of hESC and hiPSC with iMEF, mouse embryonic fibroblasts needed to be isolated, expanded and inactivated. This section will describe the protocols used.

#### 2.1.4.1 Isolation of mouse embryonic fibroblasts

Mouse embryos from females (Strain: CD-1) at embryonic day E12.5-13 were obtained. Embryos were separated using sterile tweezers from the placenta and the surrounding membranes. The embryo sac was cut open using sterile fine surgical scissors and the brain and dark organs removed. The embryos were rinsed in distilled phosphate buffer solution (DPBS, Sigma-Aldrich) and then transferred into 0.25% Trypsin/Ethylenediaminetetraacetic acid (EDTA) (Sigma-Aldrich) for 15min at 37$^{o}$C. After incubation the solution and cell suspension was collected and mixed with mouse embryonic fibroblast (MEF) media consisting of Dulbecco's modified eagle medium (DMEM), with 4.5 g/L D-Glucose, 584 mg/L L-Glutamine,

(Life Technologies) supplemented with 10% foetal bovine serum (FBS, Life Technologies) and NEAA. The FBS contained within the MEF media quenched the trypsin, stalling the enzymatic function of the enzyme. The cell suspension was then centrifuged at low speed (1,200 revolutions per minute (rpm), Centrifuge 5810 R, Eppendorf, Stevenage, UK) for 3min. The supernatant was removed and the pellet re-suspended in fresh MEF media. Cells were then split into T75 culture grade T-flasks (Nunc.) and incubated for 4 days at 37$^{o}$C and 5% $CO_2$. Once cultures reached confluence the cells were prepared for long-term storage in liquid nitrogen. Flasks were trypsined in 0.25% Trypsin/EDTA for 5min at 37$^{o}$C, and then centrifuged at 1,200rpm for 3min. The supernatant was aspirated and the cell pellet re-suspended in freezing media: FBS supplemented with 10% DMSO. The cell suspension was then immediately aliquoted into 1mL cryovials (Nunc.) and frozen using 'Mr Frosties' (ThermoFisher Scientific, Loughborough, UK) in -80$^{o}$C for 24hrs. Frozen vials were then transferred to the liquid nitrogen stores for long-term storage, denoted as P0 MEF with the date of harvesting. Cell samples were also taken to screen for mycoplasm contamination. This screening process was outsourced.

#### 2.1.4.2 iMEF preparation

MEF were cultured from passage 0 (P0) and iMEF were generated from P1 – P6. iMEF were produced every 3-4 days and always 1 day prior to hPSC passaging. MEF were inactivated by adding 4mL of pre-diluted 0.01mg/mL Mitomycin-C to the flask and incubating for 2hrs at 37$^{o}$C. Cells were washed 3 times in DPBS and trypsinized for 3min at 37$^{o}$C. Trypsin was quenched using MEF media and the cell suspension centrifuged at 1,200rpm for 3min. The cell pellet was then re-suspended in 10mL of fresh MEF media and the number of cells found using a haemocytometer (Figure 1). iMEF were seeded onto gelatin (Sigma-Aldrich) coated T25 flasks at a density of 9.2x10$^{4}$ iMEF/cm$^{2}$ and cultured overnight at 37$^{o}$C and 5% $CO_2$ to allow iMEF to adhere to the surface prior to seeding hPSC.

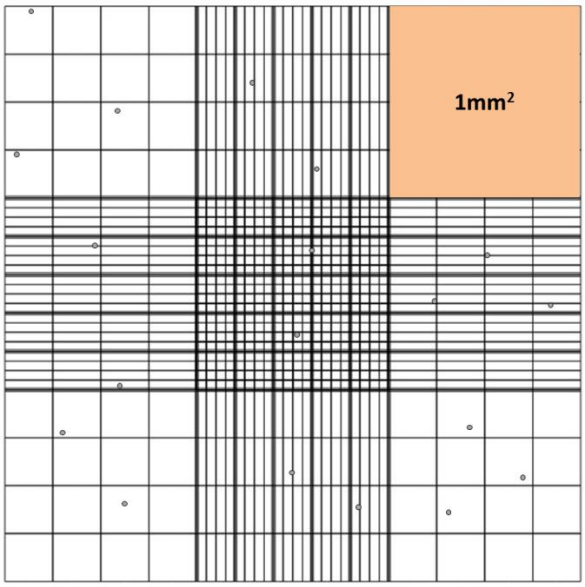


**Figure 1 - Haemocytometer counting strategy**
Cartoon depicting a typical haemocytometer chamber, the pink square denotes a 1mm$^2$ area; grey circles depict distribution of single cell suspension. The average number of cells per large square (i.e. pink square) was found and multiplied by 10,000 to calculate the volume of cells per 1mL.

## 2.2 Characterisation of hPSC protocols

### 2.2.1 Spontaneous differentiation

hPSCs were co-cultured with iMEF in standard KOSRM supplemented with 10ng/mL bFGF until seeding. Following mechanical passage, clumps were seeded onto iMEF in gelatin coated 21cm$^2$ easy grip culture dishes (BD Falcon) and cultured for 5 days. Media was aspirated and replaced with KOSRM without bFGF and cultured for 27 days changing media every two days. All incubation steps were carried out at 37$^o$C and 5% $CO_2$. Cultures were fixed in 4% PFA for 10min at RT and stored at 4$^o$C. Cultures were assessed for differentiation into endoderm, ectoderm and mesoderm linages using immunocytochemistry (Chapter 2, 2.2.6).

### 2.2.2 PA6 co-culture

Co-culture with PA6 was used to provide proof of concept that the hPSC used within this work have the potential to differentiate toward (TH$^+$) DA neurons. It was reported by Zeng *et al*. (Zeng, Cai et al. 2004) that following co-culture with PA6 stromal cells, ~87% of their differentiated hESC colonies contained TH$^+$ cells.

PA6 stromal cells (obtained from Clinical Neurosciences, UCL) were maintained in DMEM supplemented with 10% FBS and 50µg/mL penicillin-streptomycin (Penstrep, Invitrogen). PA6 cells were passaged using 5min trypsin treatment and passaged 1:5 into T75 flasks and expanded for 4 days. PA6 were inactivated using 0.01mg/mL Mitomycin-C and incubated for 2hrs at 37$^{o}$C. Cells were washed three times in DPBS and trypsinized for 3min at 37$^{o}$C. Trypsin was quenched using MEF media and the cell suspension centrifuged at 1,200rpm for 3min. Inactivated PA6 (iPA6) cells were split, one T75 flask into three gelatin coated T25 flasks; this produced confluent monolayers of iPA6 cells in each flask. Cultures were incubated overnight to allow iPA6 to adhere.

hPSCs were co-cultured with iMEF in standard KOSRM and supplemented with 10ng/mL bFGF until seeding. To start co-culture with iPA6 cells, hPSC colonies were mechanically passaged and seeded onto iPA6. Following this transfer, cells were cultured in media consisting of Glasgow Minimum Essential Medium (GMEM) supplemented with 10% KOSR, 2mM L-glutamine, 1mM sodium pyruvate and 0.1mM β-mercaptoethanol. Media was changed after 4 days post seeding and changed every 2 days thereafter. Cultures were grown for 4 weeks and then fixed using 4% PFA for immunocytochemistry staining.

### 2.3 Aggregate-based hPSC dopaminergic differentiation

This section will describe the protocol for the aggregate-based hPSC DA differentiation programme. Suspension culture was used for the majority of the programme to expand and induce the hPSC towards a neuronal and DA lineage. On D24, aggregates were stuck down and directed to mature in a chemically defined medium. The individual sections of the process are represented diagrammatically in Figure 2 and described in detail in the following section. Media was changed ever 2-3 days or as required by the cultures.

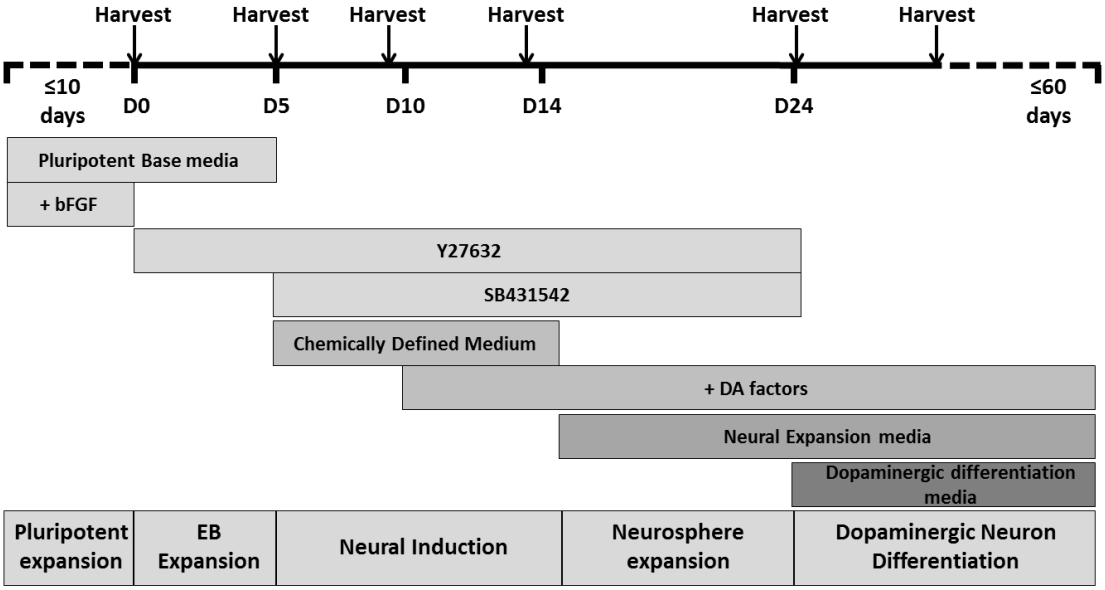


**Figure 2 - Aggregate-base dopaminergic differentiation programme**
Schematic showing the individual step performed during the aggregate-base dopaminergic differentiation programme, indicating the main constituents of the culture media and the points at which cell samples were harvested.

### 2.3.1 Pluripotent cell expansion

Pluripotent hESC (p73-75) and hiPSC (p66-68) were cultured according to the protocols described above and passaged mechanically. Upon initiating the investigation, colonies were plated onto iMEF in 21cm$^2$ easy grip culture dishes, approximately 15-20 clumps per dish and cultured in KOSRM supplemented with 10ng/mL bFGF at 37$^o$C and 5% $CO_2$. Cultures were expanded for up to 10 days or until colonies reached optimal size and morphology with minimal differentiation, an example is shown in Figure 3, B.

### 2.3.2 Cell aggregate formation and neural priming

Differentiation was initiated by transferring the colonies from adherent culture into suspension culture, this processes required colonies from approximately 10x 21cm$^2$ culture plates. hPSC colonies were assessed (Figure 3, B) and a liquid waste trap with a dissecting tool attached used to remove differentiated colonies (Figure 3, A). Colonies were kept moist during dissection using sterile DPBS and then incubated in collagenase IV (2mg/mL, Invitrogen) at 37$^o$C for 10min until colony edges started to detach from the culture surface. Collagenase was aspirated and colonies detached using gentle agitation and were transferred to a sterile vial after which they were centrifuged at 500g for 5min (Centrifuge 5810R. Eppendorf). Colonies

were then transferred to 60x15mm petri dishes (BD Flacon), residual media was aspirated, and colonies were dissected using a sterile McIlwain tissue chopper (Mickle Laboratory Engineering Company, Guildford, UK) set to 150nm. Colonies were dissected, the plate rotated 90$^{o}$, and dissected again (Figure 3, C).

Aggregates were finally transferred into polyHEMA coated T12.5 flasks (DB Falcon) and re-suspended in KOSRM (~8mL) supplemented with ROCK inhibitor (10nM, Y-27632) to reduce apoptosis (Claassen, Desler et al. 2009), 1x Penstrep and incubated at 37$^{o}$C at 20% $CO_2$ for 5 days.

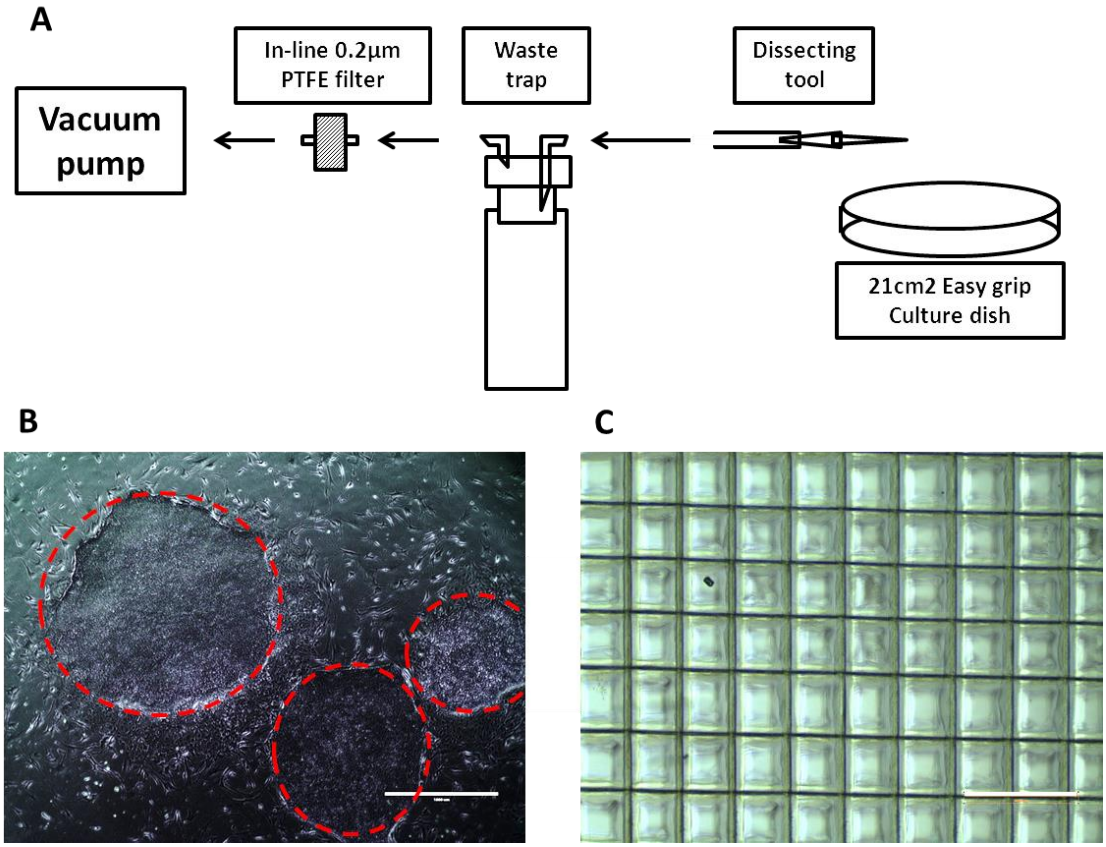


**Figure 3 - Aggregate-based dopaminergic differentiation - Neuralisation**
**A)** Schematic of the liquid waste trap and dissecting tool used to dissect differentiated cells from expanded hPSC colonies prior to chopping using the McIlwain tissue chopper. **B)** Representative image of typical hPSC colonies prior to removal of differentiated cells. All cells immediately outside of the red circles were removed (Scale bar = 1000µm). **C)** Bright field image of petri dish post dissection with McIlwain tissue chopper. The blade of the McIlwain tissue chopper produced uniform score lines 150nm apart (Scale bar = 400µm).

### 2.3.3 Neural Induction

Embryo bodies (EB)/cell aggregates were transferred from the T12.5 flask to a 15mL flacon tubes post priming and EBs were left to collect at the bottom for 5mins. The media was aspirated and replaced with chemically defined neural induction medium (CDM, Table 2) to initiate neural induction and cultured for 9 days. Media was changed when its colour indicated that the media was spent (yellow/plum colouring), typically every 3 days. From D5 of the 9 days in CDM, media was supplemented with the following DA factors to condition the cultures toward DA differentiation:

1. 100ng/mL fgf8a (R&D systems)
2. 2µM Purmorphamine (Cambridge Bioscience)
3. 0.2mM Ascorbic acid (Sigma)

| Reagent | Volume/concentration (50mL total) | Supplier |
|---|---|---|
| IMDM + GlutaMAX | 25mL | Invitrogen, UK |
| F12 + GlutaMAX | 25mL | Invitrogen, UK |
| Albumax II (200 mg/mL) | 100µL | Invitrogen, UK |
| Lipid concentrate | 500µL | Invitrogen, UK |
| Monothioglycerol (100%) | 1.95µL | Sigma, UK |
| Insulin (10 mg/mL) | 35µL | Sigma, UK |
| Transferrin (12.5mg/mL) | 60µL | Sigma, UK |
| SB431542 (10mM) | 20µM | Tocris, UK |
| Y27632 (ROCK inhibitor) (10mM) | 10µM | Tocris, UK |

**Table 2 - Neural induction CDM composition**
Composition of neural induction CDM, with volumes or final concentrations required for a 50mL total volume.

### 2.3.4 Expansion stage

On D9 of neural induction, EBs were transferred to a 15mL falcon tube and the media replaced with expansion media (Table 3). Neurospheres were primed and cultured in these conditions for an additional 10 days. On D10 of expansion SB431542 and Y27632 were removed from the media composition for extended culture.

| Reagent | Volume/concentration | Supplier |
|---|---|---|
| **Neuronal expansion Media Base** | (300mL total) | |
| KODMEM | 210mL | Invitrogen, UK |
| F12 + Glutamax | 90mL | Invitrogen, UK |
| Penstrep | 3mL | Invitrogen, UK |
| Glutamax | 2.1mL | Invitrogen, UK |
| **Expansion Media Supplements** | | |
| B27 | 2% | Invitrogen, UK |
| Heparin | 5µg/mL | Sigma-Aldrich, UK |
| FGF2 | 20ng/mL | R&D Systems, UK |
| FGF8a | 100ng/mL | R&D Systems, UK |
| Purmorphamine | 2mM | R&D Systems, UK |
| Ascorbic acid | 0.2M | Sigma-Aldrich, UK |
| SB431542 | 20µM | R&D Systems, UK |
| Y27632 | 10µM | R&D Systems, UK |

**Table 3 - Expansion media composition**
Composition of neural expansion media for a total volume of 300mL with final concentrations of the supplements.

### 2.3.5 Stick down

Stick down was performed in DA differentiation media (DDM, Table 4). Neurospheres were plated onto sterile glass cover slips (VWR) treated with poly-D-Lysine (PDL, Sigma) and coated in laminin (1:100 dilutions, Sigma). Neurospheres were plated in 250µL DDM for 16hrs, allowing the colonies to settle and adhere. Media was topped up to 400µL at 24hrs and the cells were cultured at 37$^{o}$C in 20% $CO_2$ for 14 or 28 days. Media was changed every 3 days or when the media colour indicated that the media was spent.

| Reagent | Volume/concentration | Supplier |
|---|---|---|
| Neural expansion Media Base | (Table 3) | |
| **Supplements** | | |
| FGF8a | 100ng/mL | R&D systems, UK |
| Purmorphamine | 2mM | R&D systems, UK |
| Ascorbic Acid | 0.2M | Sigma-Aldrich, UK |
| BDNF | 20ng/mL | Peprotech, UK |
| GDNF | 20ng/mL | Peprotech, UK |
| TGFβ3 | 1ng/mL | R&D systems, UK |
| dbcAMP | 0.5mM | Sigma-Aldrich, UK |
| DAPT | 10nM | R&D systems, UK |

**Table 4 - Dopaminergic differentiation media composition**
Composition of dopaminergic differentiation media and final concentrations required.

## 2.4 saRNA experimental protocols

### 2.4.1 Designing short activating RNA oligonucleotides

The proteins; TH, lmx1a and foxa2 were selected for the design and generation of saRNA, with the intention for specific activation of their respective genes. saRNA sequences were designed and generated by a collaborator of Omnicyte Ltd. and only recently has the method been reported within two papers by Reebye *et al.* (Reebye, Saetrom et al. 2013, Reebye, Saetrom et al. 2013). Briefly the algorithm identifies the gene of interest, locates its promoter and generates candidate antisense sequences that overlap or are in the close vicinity or in some way thought to interact with the gene promoter. This work was done in collaboration with another research laboratory, Pål Sætrom, Department of Cancer Research and Molecular Medicine and Department of Computer and Information Science, Norwegian University of Science and Technology.

### 2.4.2 saRNA preparation

saRNA were synthesised by Invitrogen (foxa2) and Eurogentec (TH and lmx1a, Southampton, UK) and reconstituted in 5x Universal siMAX siRNA buffer (Eurofins MWG operon, Ebersberg, Germany). Stock saRNAs were reconstituted at RT to a concentration of 20µM and aliquoted for storage at -80$^{o}$C. One working aliquot at a time was utilised, with freeze-thaw cycles kept to a minimum, stored at -20$^{o}$C.

Lipid-oligonucleotide complexes were formed through the combination of transfection reagent and saRNA oligonucleotides. Briefly, the appropriate transfection reagent: Nanofectin (PAA Laboratories Ltd, Staffordshire, UK), ICAfectin 442 (Eurogentec, Hampshire, UK) or FuGene (Roche, Sussex, UK)) (3µL/mL) and saRNA (50nM) were individually diluted in base media (no serum) and gently vortexed. The saRNA solution was then added to the transfection reagent solution, gently vortexed and complexed at RT for 15min. Following incubation the solution was vortexed again and applied to the culture flasks and the flasks mixed gently by rocking back and forth and side to side 20 times (Figure 7, B).

### 2.4.3 saRNA transfections

Cell cultures were prepared and cultured as described above in the experimental materials and methods. Three investigation arms were created; un-transfected (UT), aggregates were differentiated normally with no addition of saRNA; transfected, aggregates were differentiated normally and transfected with saRNA every 3 days; and mock transfected (Mock), aggregates were differentiated normally and treated with nanofectin alone.

### 2.4.4 hiPSC aggregate formation using Aggrewell

hiPSC were used to assess the impact of cell aggregate size on transfection efficiency. hiPSC colonies were disassociated using Tryple Express into a single cell suspension and passed through a 100nm cell strainer prior to manufacture of aggregates using the aggrewell 400EX (Stemcell Technologies, Manchester, UK) plate. Cells were then centrifuged (Centrifuge 5810 R) at 1,200rpm for 3min and the supernatant aspirated. Cells were re-suspended into KOSR supplemented with 10nM ROCK inhibitor and the cells counted using a haemocytometer. The aggrewell was prepared by dispensing 2mL of 10% pluronic acid into each well and the plate centrifuged at 4,000rpm for 5min, to remove any bubbles found in the bottoms of the aggrewell units. The pluronic acid was then aspirated and the whole well rinsed with KOSR. Cells were seeded into the wells at $4.7x10^6$ cells per well to produce 1000 cells/aggregate and $9.4x10^6$ cells per well to produce 2000 cells/aggregate. The plate was centrifuged gently at 500rpm for 3min to evenly precipitate the cells into each conical unit, as demonstrated in Chapter 6, section 6.5, and then incubated at $37^oC$ and 5% $CO_2$. After 24hrs aggregates were harvested by agitating the plate and aspirating the aggregates in suspension. Aggregates were transferred to low adherent bacteria culture dishes in KOSR supplemented with ROCK and cultured for a further 24hrs.

### 2.4.5 hiPSC aggregate transfection assessment

To transfect the aggregates, they were transferred to polyHEMA coated T12.5 flasks and treated with siGLO transfection reagent daily for 3 days and incubated at $37^oC$ and 5% $CO_2$.

Every 12hrs, following transfection the media was aspirated and changed prior to the next transfection. At the end of the experiment aggregates were aspirated and the cells disassociated and processed using flow cytometry.

## 2.5 ICSD experimental protocols

### 2.5.1 Conditioned media preparation

iMEF were generated and inactivated as described above. Mitomycin-C was discarded and the cells washed three times in DPBS. iMEF were then trypsinised, centrifuged (Eppendrof centrifuge 5810R) and counted using a haemocytometer and then plated into gelatin-coated T75 flasks at a density of $2.0x10^4/cm^2$. iMEF cultures were incubated in MEF media for 12hrs to allow iMEF to adhere and then the media was removed and replaced with 35mL KSRM media supplemented with 4ng/mL bFGF. Cultures were incubated for 3 days at which time media was aspirated and replaced, this was repeated three times. The aspirated iMEF conditioned media (FC-media) was filter sterilised (Millipore, 0.22µm filter) and stored at -20$^oC$ until use.

### 2.5.2 ICSD Differentiation Protocol

Priming briefly consisted of the hPSCs being expanded using T25 flasks and cultured in KO-SRM supplemented with bFGF, until colonies compacted. Upon initiation of priming, cells were disassociated into single cell suspension using Tryple Express and passed through a 40µm cell strainer to ensure a single cell suspension. Cells were re-suspended in filter sterilised FC-media, supplemented with 10ng/mL bFGF and 10nM Y27632 (FC/ROCK media) and plated onto gelatin-coated 6 well plates (Nunc) followed by incubation at 37$^oC$ for 1hr. Non-adhered hPSC were aspirated and the wells rinsed gently with fresh complete FC-media to remove any remaining non-attached cells. iMEF remained adhered to the gelatin-coated surface. Pluripotent cell suspensions were centrifuged at 1,200rpm for 3min, re-suspended in FC/ROCK media and then counted using a haemocytometer. The hPSC populations were plated onto matrigel (BD) pre-coated 24 well plates (Nunc) at ICSD of $10k/cm^2$, $18k/cm^2$ and $25k/cm^2$ and

cultured in FC/ROCK media. Experimental ICSD wells were setup in duplicate. Media was changed after 24hrs, removing the Y-27632 supplement.

On D3 of population expansion the media was changed to initial differentiation media; KO-SRM supplemented with noggin (500ng/mL, R&D Systems) and TGF-β inhibitor (10µM, SB431542, Miltenyi Biotec), known as priming D0. On D1 media was supplemented with sonic hedgehog (100ng/mL, SHH) and Purmorphamine (2µM, Miltenyi Biotec). Media was maintained until D3, when CHIR99021 (3µM, Miltenyi Biotec) was added. After an additional 2 days the media was changed and modified to contain 25% N2, neuronal supplement (PAA,) in addition to factors: Noggin, SHH, Purmo and CHIR, but excluding SB4314542. N2 concentration was incrementally increased over the following 6 days (to D11) to 25%, 50% and 75% of the media constituent, while the media was changed every 2 days. This process is depicted in Figure 4.

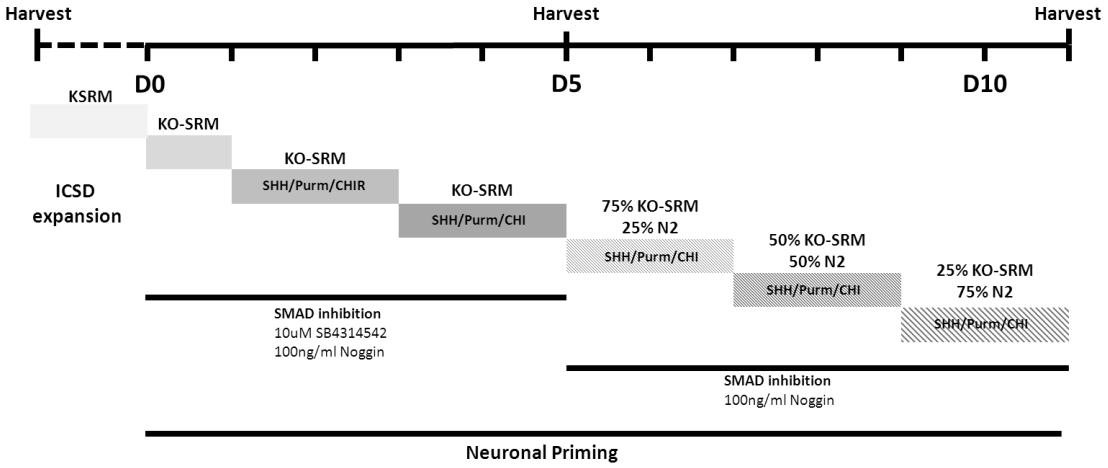


**Figure 4 - Neuronal priming timeline**
Diagram showing the stages of the neuronal priming protocol carried out with hPSC. The days when cells were harvested are labelled above the time line.

### 2.5.3 Confluence Analysis

Analysis of confluence was performed using a phase contrast microscope (Nikon, Eclipse TI-E) with an inbuilt automated platform. 20 images (x10 magnification) were taken of each duplicate well daily. Images were processed using the PHANTAST software (Jaccard, Griffin et al. 2014). Briefly, cell regions were characterised by high variations in intensity on the phase contrast microscopy images and detected using a local contrast filter. Image confluence was

computed as the ratio of the number of cell pixels to the total number of pixels. Images of biological duplicates were processed and averages were taken of all readings for a given ICSD. Readings were taken over 7 days, to ascertain the growth profile of the two hPSC lines and to determine the appropriate time point to commence priming the cells.

## 2.6 Pluripotent Cell Analytical Techniques

### 2.6.1 Cell Harvesting

At specific times during an experimental protocol, cells were harvested for extraction of total ribonucleic acid (RNA) for subsequent messenger RNA (mRNA) analysis. This was performed using quantitative polymerase chain reaction (qPCR) to assess target gene expression relative to the starting pluripotent population.

Cells were mechanically harvested for qPCR using the flat end of a 1mL sterile syringe plunger (BD, Oxford, UK). Disrupted cells were transferred immediately to RNAse free eppendorfs (Starlab), centrifuged to 8,000rpm for 5sec, the supernatant was aspirated and the resulting cell pellet was snap frozen in liquid nitrogen and transferred to -80$^{o}$C until processing.

### 2.6.2 RNA extraction

Total RNA was extracted from the cell pellet using RNAqueous micro kit (Applied Biosystems, Warington, UK). Briefly, the pelleted cells were re-suspended in cell lysis buffer (provided by the kit) and mechanically disrupted using QIAshredder columns (Qiagen, Manchester, UK). Total RNA was then precipitated with 99% Ethanol (Sigma-Aldrich), followed by affinity separation and elution with RNA columns as provided by the kit. Total RNA content and purity was then quantified using a Nanodrop 1000 spectrophotometer (Thermo Fisher Scientific). For the sample to be valid for analysis a 260/280nanometer (nm) absorbance ratio was required to be between 1.9 - 2.1. RNA samples were kept on ice or immediately stored at -80$^{o}$C until required for complementary deoxyribonucleic acid (cDNA) synthesis.

### 2.6.3 cDNA Synthesis

RNA (typically 100-500ng of each sample) was reverse transcribed to cDNA in order that the sample could be processed using qPCR. Reverse transcription was achieved using QuantiTect Reverse transcription Kit (Qiagen). Briefly, in stage 1, RNA was mixed with gDNA wipeout reagent to degrade any contaminating genomic deoxyribonucleic Acid (gDNA) present. The mixture was then incubated at 42$^{o}$C for 2min as set out in Table 5, stage 1. Stage 2 involved mixing the resultant solution with Quantiscript Reverse Transcriptase, Quantiscript RT buffer and RT primer mix (Table 5, Stage 2, all reagents are included within the kit), and incubating the samples at 42$^{o}$C for 15min and at 95$^{o}$C for 3min at to inactivate the enzymes. Immediately following incubation, the samples were processed using qPCR and then stored on ice or stored at -20$^{o}$C for short-term use. Temperature cycling was performed using a Veriti 96-well thermal cycler (Model 9902, Applied Biosystems).

**Stage 1**

| Reagent | Volume per reaction |
|---|---|
| **gDNA Wipeout** | 2µL |
| **Molecular grade water** | Total 12µL (including RNA volume added) |
| **Sample RNA** | 100-1000ng |

**Stage 2**

| Reagent | Volume per reaction |
|---|---|
| **RT master mix** | 1µL |
| **Quantiscript buffer** | 4µL |
| **Quantiscript primer** | 1µL |
| **gDNA wipeout treated RNA** | 14µL |

**Table 5 - Table of cDNA synthesis reaction mix**
Table describes the reaction mixes used during the QuantiTect reverse transcription reaction to synthesise cDNA from extracted sample mRNA. Stage 1 shows the reagents used during the gDNA wipeout step and Stage 2 shows the composition of the cDNA synthesis step (all Qiagen).

### 2.6.4 Quantitative PCR

Gene expression analysis was executed using QuantiFast SYBR Green PCR Kit (Qiagen). Briefly, cDNA was diluted (1:5) in molecular grade water (Sigma-Aldrich) and stored on ice ready for use. A master mix was composed as described in Table 6 (all reagents provided in the kit). 20µL of master mix was aliquoted into each qPCR plate well and 5µL of pre-diluted cDNA added. All qPCR primers were purchased from Qiagen and are listed in Table 7. qPCR cycling was

performed using a BioRad CFX Connect Real-Time System (BioRad, Hertfordshire, UK) as described in Table 6. All samples were processed in duplicate and analysis was performed using the CFX manager and gene study programme (BioRad) as described below.

| Stage | Temperature | Duration |
|---|---|---|
| **Activation** | 95°C | 5min |
| **Two-step cycling** | | |
| **Denaturation** | 95°C | 10sec |
| **Combined annealing/extension** | 60°C | 30sec |
| **Number of cycles** | 35-45 | |

| Reagent | Volume per reaction |
|---|---|
| **Quantifast master mix** | 12.5µL |
| **Quantitech primer** | 2.5µL |
| **Molecular grade water** | 5µL |
| **cDNA (1:5 dilution)** | 5µL |

**Table 6 - Table of qPCR reaction mixture + cycling conditions**
Tables describe the cycling conditions used during qPCR analysis of experimental cDNA and the reaction mix used per reaction (all Qiagen).

### 2.6.5 qPCR data analysis

qPCR data collected through the BioRad CFX Connect Real-Time System was categorised and processed using CFX Manger Data analysis software. The samples were categorised using a number of criteria:

1) Biological set (biological replicate number)
2) Cell type
3) Technical replicate
4) Target gene
5) Sample name

Statistical significance analysis was performed using CFX Manager Data analysis. Relative quantification/fold-difference between samples was determined using reference genes, namely *GAPDH, β-Actin* and *UBC* to normalise the starting template (cDNA) volume. The relative quantity was determined by analysing the $C_T$ for each sample/target gene/replicate and then calculating the relative quantity based on the difference between the $C_T$ values of the target and reference genes.

The BioRad CFX Manager DATA analysis software automatically calculated the normalised relative expression (ΔΔCT) of the target genes (using the criteria listed above to categorise) relative to a designated reference gene or sample on the plate. Statistical testing was based on the 2-tailed T-test with p-value then calculated to understand the significance of the findings. When the p-value was found to be $p \leq 0.05$, i.e. the probability of this situation occurring by chance being less than 5%, significance was ascertained.

For further details please refer to the BioRad supporting documentation: CFX96 Touch, CFX96 Touch Deep Well, CFX Connect, and CFX384 Touch Real-Time PCR Detection Systems Instruction manual.

| Primer target | Primer ID | Function |
|---|---|---|
| **Glyceraldehyde-3-Phosphate Dehydrogenase (GAPDH)** | Hs_GAPDH_2_SG | House keeper gene |
| **β-ACTIN** | Hs_ACTB_2_SG | House keeper gene |
| **Polyubiquitin-C (UBC)** | Hs_UBC_1_SG | House keeper gene |
| **NANOG** | Hs_NANOG_2_SG | Pluripotency |
| **octamer-binding transcription factor 4 (OCT4)** | Hs_POU5F1_1_SG | Pluripotency |
| **Sex determining region Y-box 2 (SOX2)** | Hs_SOX2_1_SG | Pluripotency |
| **Fibroblast growth factor 5 (FGF5)** | Hs_FGF5_1_SG | Epiblast |
| **BRACHYURY** | Hs_T_1_SG | Mesoderm |
| **Sex determining region Y-box 17 (SOX17)** | Hs_SOX17_1_SG | Endoderm |
| **NESTIN** | Hs_NES_2_SG | Ectoderm |
| **Sex determining region Y-box 1 (SOX1)** | Hs_SOX1_2_SG | Ectoderm - early neuronal |
| **Nuclear receptor related 1 (NURR1)** | Hs_NR4A2_1_SG | Dopaminergic system maintenance |
| **Orthodenticle homeobox 2 (OTX2)** | Hs_OTX2_1_SG | VTA mdDA neurogenesis |
| **Engrailed-1 (EN1)** | Hs_EN1_1_SG | mdDA devlopment |
| **Forkhead box protein A2 (FOXA2)** | Hs_FOXA2_1_SG | DA neuron marker |
| **Homeoprotein LIM homeobox transcription factor 1α (LMX1A)** | Hs_LMX1A_1_SG | DA neuron marker |
| **Tyrosine hydroxylase (TH)** | Hs_TH_1_SG | DA neuron marker |
| **Dopamine receptor D1 (DRD)** | Hs_DRD1_1_SG | Dopamine receptor |

**Table 7 - List of primers used in qPCR analysis**
List of qPCR primers used to analyse experimental samples. The table includes the target gene name and descriptor, Quantitech primer ID (All Qiagen) and function of the target gene. The qPCR cycle recommended by the manufacturer, Qiagen, was used standardly for all primers.

### 2.6.6 Basic Immunocytochemistry

Experimental cultures were fixed in-situ with 4% paraformaldehyde (PFA, Sigma-Aldrich) for 10min before being permibilized in 0.5% Triton X-100/DPBS for 10min and blocked with 5% FBS/DPBS blocking solution for 30min (all Sigma-Aldrich). When detecting surface markers the permibilization step was omitted from the protocol due to the damage caused to the cell membranes by detergents. The samples were incubated with 300µL of primary ($1^{o}$) antibody (Table 8) and incubated at $4^{o}$C overnight. $1^{o}$ antibodies were diluted in blocking solution. Cells were then washed in 2mL of DPBS three times to remove any residual $1^{o}$ antibody and then incubated with 300µL of secondary ($2^{o}$) antibodies, diluted in blocking solution (Table 9) and incubated for 1hr. The cells were then washed 3 times in DPBS and incubated with 4,6-diamidino-2-phenylindole (dapi, Life Technologies, 1:1000) for 5min. All incubation steps were performed at RT unless otherwise stated. Fluorescence images were acquired using a fluorescence microscope (Eclipse TE2000-U, Nikon, Kingston-upon-Thames, UK) and analysed with NIS-element software. This protocol was used throughout this work unless otherwise stated.

| Function | Target | Location | Species | Isotype | Dilution |
|---|---|---|---|---|---|
| **Nuclei** | DAPI | Nucleus | | | 1:1000 |
| **Pluripotency** | OCT3/4 | Nucleus | Mouse | IgG2b | 1:200 |
| | TRA-1-60 | Surface | Mouse | IgM | 1:200 |
| | SSEA4 | Surface | Mouse | IgG3 | 1:200 |
| **Early differentiation** | SSEA1 | Surface | | | 1:100 |
| **Germ Layer** | NESTIN | Cytoplasm | Mouse | IgG | 1:100 |
| | BRACHYURY | Nucleus | Mouse | IgG2a | 1:200 |
| **Neural** | SOX1 | Nucleus | Rabbit | IgG | 1:200 |
| | PAX6 | | Mouse | IgG1 | 1:200 |
| | β-III-TUBLIN (TU-20 clone, C-terminus of the neuron specific beta III isoform) | Cytoplasm | Mouse | IgG1 | 1:200 |
| **Neuronal** | EN1 | Nucleus | Mouse | IgG2a | 1:200 |
| **Dopaminergic** | LMX1A | Cytoplasm | Rabbit | IgG | 1:300 |
| | TH | Cytoplasm | Chicken | Polyclonal | 1:200 |
| | FOXA2 (HNF-3β) | Nucleus | Mouse | IgG2a | 1:100 |

**Table 8 - List of $1^{o}$ antibodies used in immunocytochemistry analysis**
Table showing the $1^{o}$ antibodies used to analyse marker expression in cell cultures. Listed are the functions, target antigens, species reared in, isotype and the dilution used. Antibodies were supplied by Abcam (Cambridge, UK) or Millipore (Merck, Hertfordshire, UK).

| Secondary raised in | Affinity | Isotype | Excitation frequency |
|---|---|---|---|
| goat | chk | igy | 488 |
| goat | rb | igg (H+L) | 555 |
| goat | ms | igg (H+L) | 488 |
| Donkey | goat | igg (H+L) | 488 |
| goat | mouse | igg (H+L) | 555 |

**Table 9 - Compilation 2$^{o}$ antibodies for basic immunocytochemistry**

Table describing the antibodies used for immunocytochemical analysis during this work. Describing the 2$^{o}$ antibodies used to in conjunction with the 1$^{o}$ antibodies, the species it was raised in, the species it has affinity to, its isotope and the excitation frequency it is visualised at.

### 2.6.7 Bright field microscopy

Bright field microscopy was typically performed on live cells during an experimental procedure using the bench top AMG EVOSx1 (Peqlab ltd, Sarisbury Green, UK) at x10 or x20 magnification.

### 2.6.8 Immunocytochemical staining for confocal imaging

Confocal imaging was only performed later in the work when differentiating DA neurons using a cell aggregate based method. The method used to stain the samples for this process is slightly different from the method otherwise used in this work (and described above).

When differentiating DA neurons, neurospheres were terminally differentiated whilst adhered to a laminin coated coverslip and visualised using confocal microscopy. To enable the immunocytochemical staining of neurospheres the basic protocol was modified due to the highly delicate nature of the samples and the fragility of the filaments protruding from the main body. The steps involved in the protocol were reduced significantly to limit agitation and the antibodies were applied alongside permibilization solution to aid in the penetration of the antibody into the aggregate cell mass.

Cells were fixed in-situ with 4% PFA for 10min before being permibilized in 0.5% Triton X-100/DPBS for 20min and blocked with 5% goat serum/DPBS blocking solution for 30min. The samples were incubated with 300µL of 1$^{o}$ antibody (Table 10) and incubated for 3hrs. 1$^{o}$ antibodies were diluted in 0.1% triton X-100 solution. Cells were then washed in 1mL of DPBS to remove and dilute any residual 1$^{o}$ antibody and then incubated with 300µL of 2$^{o}$ antibody

(Table 10) for 90min. 2° antibodies were diluted in 0.1% Triton X-100. The cells were washed 1mL DPBS and incubated with dapi for 3min and then washed. All incubation steps were performed at RT unless otherwise stated. Images were acquired using a Leica TCS SP8 microscope (Leica microsystems, Milton Keynes, UK) and analysed using LIECA LAS AF (Leica microsystems) imaging software.

**A. Primary antibodies**

| Target | Supplier | Species | Isotype | Dilution | Location |
|---|---|---|---|---|---|
| TH | Abcam | Chicken | Poly | 1:200 | Cytoplasm |
| Foxa2 (HNF-3β) | Santa Cruz Biotechnology | Mouse | IgG2a | 1:100 | Nucleus |

**B. Secondary antibodies**

| Target | Supplier | Species | Excitation frequency | Dilution |
|---|---|---|---|---|
| Anti-Chicken | Abcam | Goat | Alexa-488 | 1:200 |
| Anti-mouse IgG2a | Millipore | Goat | Alexa-555 | 1:200 |

**Table 10 - Compilation of 1° and 2° antibodies for confocal analysis**
Table **A)** describes the 1° antibodies used during confocal analysis of the differentiated neurosphere population, listing the target protein, supplier, the species the antibody was raised in, isotype, dilution used and its cellular location. Table **B)** lists the 2° antibodies used in conjunction with the 1° antibodies to visualise the proteins, the table lists the target species, supplier, excitation wavelength and the dilution used.

### 2.6.9 Confocal Imaging

Images were taken for both qualitative and quantitative analysis of co-associated staining.

Quantitative images were taken from representative adhered neurospheres that had been co-stained for both TH and foxa2. Images were taken for each experimental condition at four locations of each neurosphere; top, bottom, right and left (Figure 5). The quantitative images taken at these sites maintained a constant Z-stack of the following physical characteristics; ~30µm in depth, 30 slices of which each layer was ~1µm in depth and the lens, laser, filter parameters described in Table 11. To allow direct comparison across the biological replicates and experimental conditions the analysis criteria described remained constant. Staining rich areas were targeted at each location.

Analysis of co-associated of TH and foxa2 was processed using an image analysis software, Volocity 3D image analysis software (PerkinElmer, Cambridge, UK).

Representative qualitative images were taken to demonstrate the variety and types of morphologies and staining that were observed within the adhered neurosphere culture.

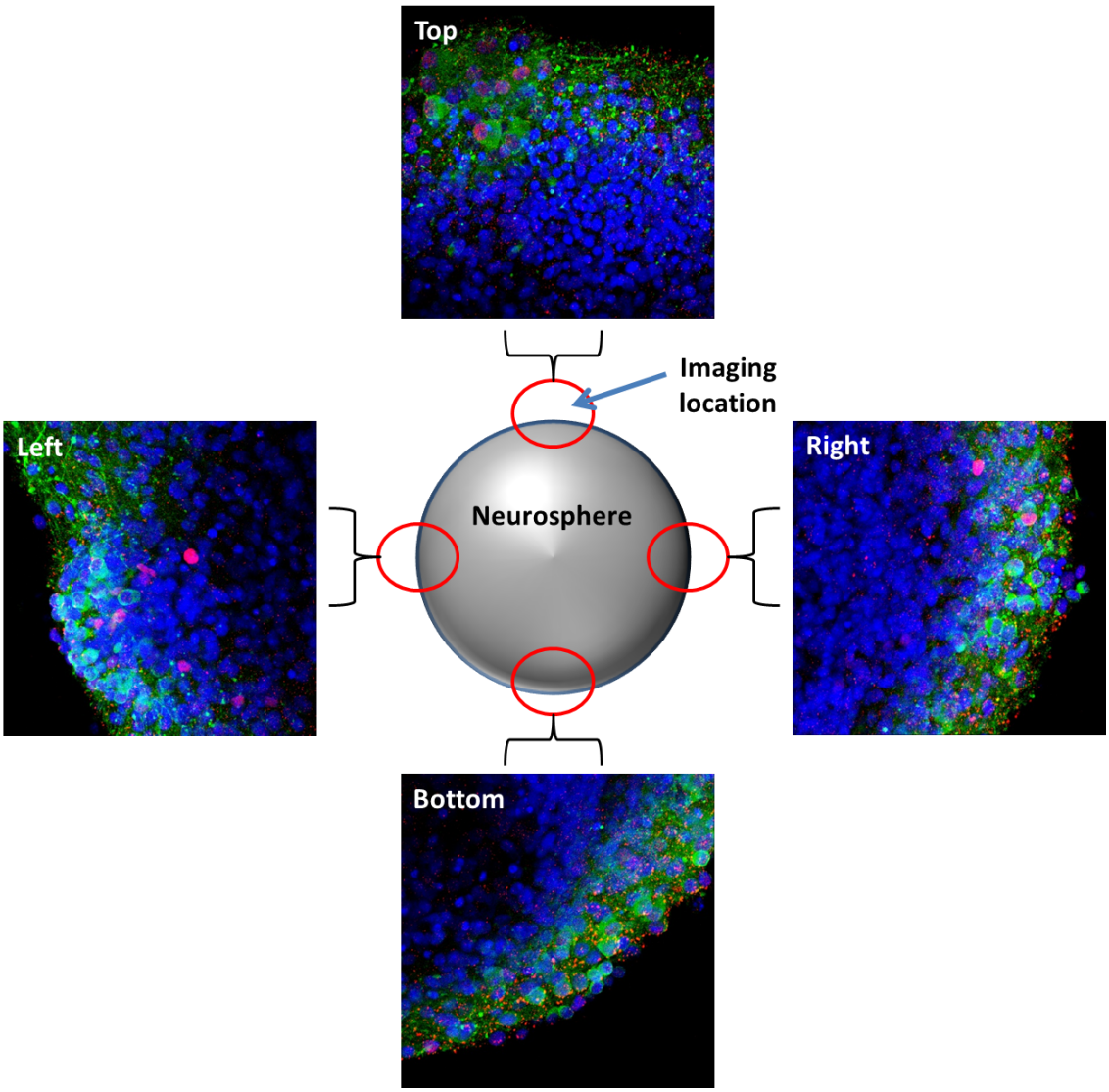


**Figure 5 - Schematic of the imaging locations for co-localisation analysis**
The schematic shows a representative neurosphere, depicted onto which are the four locations at which images (top, bottom, right and left) were captured for quantitative analysis. At each of these locations the z-stack remained constant to allow direct comparison with other images. Images were taken for each experimental condition; untransfected and saRNA transfected and each condition was processed in triplicate.

| | |
|---|---|
| **Microscope** | Leica TCS SP8 |
| **Lens** | X25 water immersion 0.95NA |
| **Frequency + magnification** | 1000Hz x2.95 magnification |
| **Green filter** | Laser power-30% Gain -953% Offset-0.14 Leica Alexa 488 |
| **Red filter** | Laser power-47.5% Gain -35% Leica Alexa 561 |
| **Dapi filter** | Laser-8.34% Gain-90% Leica Dapi |

**Table 11 - Confocal microscope parameters**
The table describes the parameters used during confocal analysis of the adhered neurospheres. Describing the microscope and lens utilised as well as the frequency and magnification used. Described also are the three filters used, green, red and blue (dapi) and the laser power utilised with each of the individual filters, the gain and the filter name/manufacturer.

### 2.6.10 Co-association analysis - Volocity

Volocity co-association analysis was performed on each quantitative image acquired from confocal microscopy. All images were of the same dimensions and were normalised using the nuclear stain dapi to control for number of cells analysed in each photo. Certain criteria were used within volocity image analysis to allow maximum accuracy (Figure 6, A). Dapi staining analysis utilised a maximum size guide allowing the program to differentiate between cells that were touching. The software was programmed to disregard dapi staining of $<25\mu m^3$, this reduced the possibility of DNA fragments obscuring analysis. Similar criteria were used in the analysis of foxa2 and TH staining; please refer to Figure 6 for more details. Co-association was analysed for nuclei_Foxa2 (Figure 6, B, ii), nuclei_TH (Figure 6, B, iii) and Foxa2_TH (Figure 6, B, iv) and the results were normalised and reported using the following equations shown in Figure 6, C.

**A**

| Staining analysed | Localised | Criteria |
|---|---|---|
| Nuclei (Dapi) | Nuclei | Solid form where pixles are touching |
| | | Definition - separate touching objects - maximum size 300µm$^3$ |
| | | Exclude background - exclude background objects <25um3 |
| Foxa2 | Nuclei (some cytoplasmic & extracellular) | Definition - separate touching objects - maximum size 300µm$^3$ |
| | | Intensity - 79<br>Offset - 0 |
| TH | Cytoplasmic | No criteria |

**B**

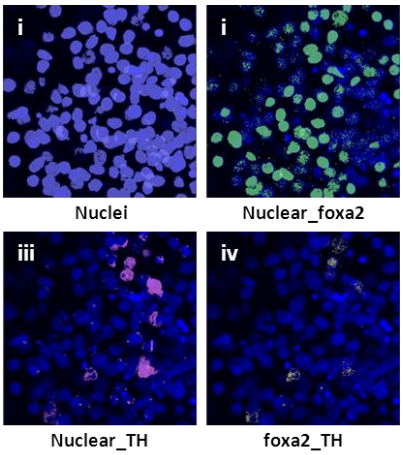


**C**

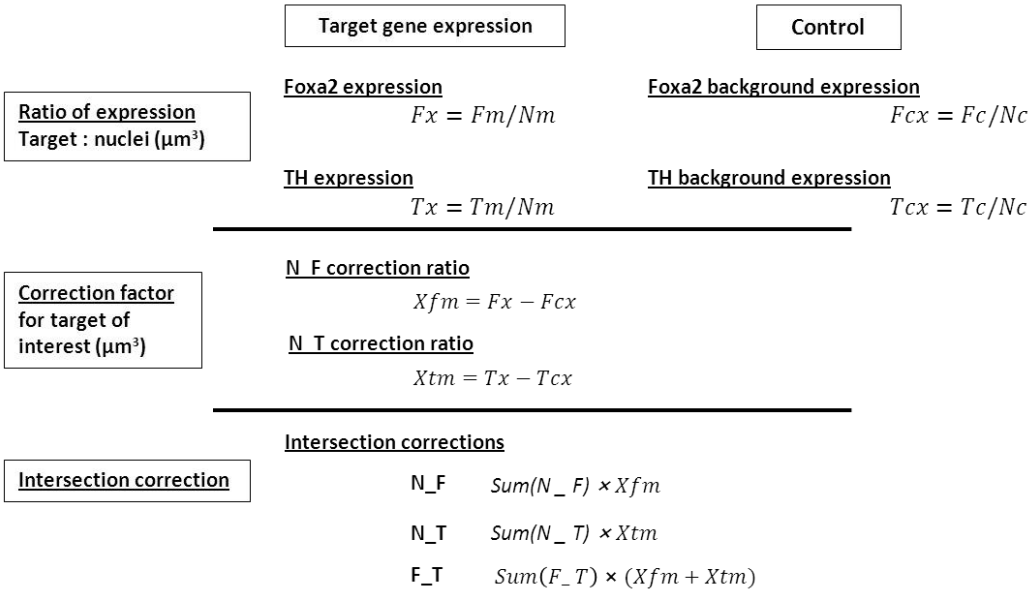


**Figure 6 - Volocity analysis criteria**

The parameters used during Velocity analysis are defined in **A**, described are the stains analysed, the localisation of the stain and the criteria Velocity used in its analysis of dapi, Foxa2 and TH. Shown in **B** are representative images generated using the criteria shown, **$B_i$)** shows nuclei identification, where individual nuclei are distinguished from touching nuclei using the criteria described in **A**. Co-association of **($B_{ii}$)** nuclei_Foxa2 and **($B_{iii}$)** nuclei_TH are shown in green and pink respectively allowing the total volume of co-association to be elucidated. Image **($B_{iv}$)** indicates were co-association of Foxa2_TH within the image. **C** describes the steps undertook to normalise each of the images and to calculate the relative total volume of each protein and the co-associated volume.

### 2.6.11 Enzyme-Linked Immunosorbant Assay (ELISA)

#### 2.6.11.1 Dopamine stimulation

Neurospheres were differentiated for 28 days after 'stick down' onto laminin coated cover slips in 4 well plates (2 neurospheres per well). Cells were washed once with Hank's Balanced Salt Solution (HBSS, containing phenol red, magnesium$^+$ (Mg) and calcium$^+$ (Ca), Sigma-Aldrich) before 300µL of HBSS was added to each well. To stabilise the dopamine released from the neurospheres EDTA was supplemented into the media to a final concentration of 0.1millimolar

(mM). Dopamine release was stimulated by supplementing potassium chloride (KCl) to the well to a final concentration of 56mM. In each run, one well remained unstimulated to show base level dopamine release. Cells were incubated at 37$^{o}$C for 15min and the media immediately removed and snap frozen in liquid nitrogen and stored at -80$^{o}$C until ELISA analysis.

#### 2.6.11.2 Dopamine assay procedure

The ELISA was performed using the dopamine ELISA Kit supplied by Abnova (Novus Biologicals, Cambridge, UK). Briefly, reagents were equilibrated to RT before use. 10µL of each of the standards and controls and 300µL of each of the experimental media samples were pipetted into their respective wells of the extraction plate (supplied in the kit). To the standards and controls 250µL of distilled water was added. 50µL of assay buffer and 50µL of extraction buffer was added to all the wells sequentially and the plate covered with the supplied adhesive foil and incubated at RT for 30min on a shaker (600rpm). Following incubation the wells were emptied onto an absorbent towel and residual liquid removed by tapping. 1mL of wash buffer was added to each well and the plate incubated for 5min at RT on a shaker. Contents were again emptied and the wash process repeated. 150µL acylation buffer was added to each well followed by 25µL acylation reagent and incubated for 15min at RT on a shaker. Contents were emptied from the wells and 175µL hydrochloric acid (HCl) pipetted into each well and covered with adhesive foil and incubated at RT for 10min. Following incubation the foil was removed and the remaining liquid was used in the dopamine ELISA described next (all reagents were provided with the kit).

#### 2.6.11.3 Dopamine ELISA protocol

To prepare the wells of the dopamine ELISA strips, 25µL of enzyme solution was pipetted into each well. 25µL of the standards and controls and 50µL of extracted experimental media were pipetted into their respective wells and 25µL of HCl was added to each. The plate was incubated at RT for 30min on a shaker. 50µL of dopamine antiserum was added to each well and the wells covered with adhesive foil and incubated at RT for 2hrs on a shaker. The foil was

removed and the liquid aspirated from the wells. Wells were washed with 300µL wash buffer three times and blotted dry to remove any residual liquid. 100µL of enzyme conjugate was added to each well and incubated on a shaker for 30min. The enzyme was aspirated and the wells washed three times with wash buffer. The wells were emptied and 100µL of substrate added to each and incubated on a shaker for 25min (avoiding any direct sun light exposure). 100µL of stop solution was added to each well and the plate shaken to ensure homogenous mixing of the liquids (all reagents were provided with the kit).

Absorbance was read within 10min of stopping the reaction using a Safire2 microplate reader (Tecan, Reading, UK) set to 450nm with a reference wavelength of 620nm.

### 2.6.12 Flow cytometry

Cultures were disassociated into a single cell suspension using Tryple express (Life Technologies) and flowed through a cell strainer (40µm apertures, BD). Live cells were used for all characterisation flow cytometry. Cells were blocked using 5% FBS and stained using conjugate antibodies (Table 12), cell suspensions were incubated with conjugate antibodies for 1hr on ice, washed in DPBS and then immediately processed using Coulter Epics XL•MCL flow cytometer (Beckman Coulter, High Wycombe, UK). A minimum cell count of 10,000 cells was used to ensure a good population representation. Side and forward scatter were adjusted according to the experimental population but between comparable runs these were maintained to allow for direct comparison. Readings were made at excitation 488nm.

| Function | Target | Species | Isotype |
|---|---|---|---|
| **Pluripotent antibody** | Anti-TRA-1-60 | Mouse | IgM, FITC conjugate |
| **Pluripotent antibody** | Anti-SSEA-4-PE | Mouse | IgG3, clone MC-813-70 |
| **Conjugate control** | IgM/FITC | Anti-Mouse | |
| **Conjugate control** | IgG | Anti-Mouse | |

**Table 12 - Table of pluripotent conjugate antibodies**
List of pluripotent conjugate antibodies used for flow cytometry and their associated conjugate controls.

**OMNICYTE LTD. BASED CULTURE AND ANALYTICAL TECHNIQUES**

This section describes the culture and analytical techniques utilised whilst working and experimenting on the hASC, omnicyte. Within this body of work a number of cancer cell lines were also utilised due to the limited availability of the omnicyte cell type. Culturing protocols of the cancer cell lines are also described in this section.

## 2.7 Omnicyte culture techniques

### 2.7.1 Omnicyte isolation and culture

Omnicytes are a sub population of the HSC population they are isolated from patient samples using the same protocol as that used to isolate HSC. The HSCs are then further purified to isolate the omnicyte population.

The HSCs used in this investigation were obtained with the written consent of neutropenic patients undergoing therapy for haematological malignancies. Patients were pre-treated with G-CSF (Life Technologies) to enhance bone marrow secretion of HSCs into their peripheral blood prior to leukapheresis.

MNCs were isolated from the whole aspirate, post leukapheresis, by centrifugation on an isosmotic medium (Lymphoprep$^{TM}$, Axis-Shield, Cambridgeshire, UK) and incubated with magnetically conjugated anti-CD34 antibody (Miltenyi Biotec, Germany). $CD34^+$ cells were then immunoaffinity purified by passing through a magnetic column (MACS Separator LS, Miltenyi Biotec).

Omnicytes were isolated by re-suspension in minimum essential medium eagle alpha modification (αMEM, Life Technologies) media and plated at a density of $2.5\times10^5$ cells per $2cm^2$ (24 well plate, Nunc.). Following incubation at $37^oC$ with 5% $CO_2$, non-adherent cells were washed away in DPBS. Adherent $CD34^+$ cells were cultured in serum free medium (CellGro, CellGenix, London, UK) with additional cytokine factors, 250ng/mL interleukin-6, 250ng/mL stem cell factor, and 250ng/mL interleukin-3 (all Life Technologies or Cellgenix) with 0.5%

penicillin/streptomycin antibiotics (Life Technologies), known as expansion media. Cells were cultured at 37$^{o}$C in 5% $CO_2$.

### 2.7.2 Long-term storage for CD34$^{+}$ purified cells

For long-term storage, fresh media comprising of 90% FBS (PAA, Austria) and 10% DMSO (freezing media) was made for each application. CD34$^{+}$ cells were pelleted (2,500rpm at RT) and the supernatant discarded. The cells were then gently re-suspended in freezing media at a cell density of approximately $1\times10^{7}$ cells per mL and transferred into 2mL cryovials. These were then wrapped in tissue to allow gradual freezing at -80$^{o}$C before being transferred into liquid nitrogen storage.

### 2.7.3 Defrosting of CD34$^{+}$ purified cells from long-term storage

Although cell survival during the freeze/thaw process is generally low, the method described was developed by Omnicyte Ltd. to optimise the number of viable cells recovered following cryopreservation.

Defrosting was performed using a 'thaw mix' solution at ×5 concentration; this solution contained Roswell Park Memorial Institute medium (RPMI, Life technologies), antibiotics (Life technologies) and Anti-Deoxyribonuclease I (DNase1, Sigma-Aldrich). The frozen sample was snap thawed by placing it into a 37˚C water bath before being transferred to the thaw mix solution. The cells were then pelleted by centrifugation (Microfuge, Eppendorf, 2,500rpm at RT) and the supernatant discarded. The cells were then washed in the thaw mix solution twice, centrifuged and re-suspended in αMEM. A viable cell count was established using trypan blue (Life Technologies) exclusion and a haemocytometer (Figure 1). Cells there then immediately processed for 'Omnicyte' isolation using the 'stick down' protocol described above.

### 2.7.4 Cancer Cell Line Culture

Undifferentiated human neuroblastoma, SH-SY5Y cells (passage 40-49), were cultured in Dulbecco's Modified Eagle Medium: Nutrient Mixture F-12 (DMEM/F-12, Life Technologies) supplemented with 10% FBS, 0.5% NEAA and antibiotics. Human hepatocarcenoma, HEPG2

(passage 10-20) and Human T-Lymphocyte cells, Jurkat (Passage 1-20) were cultured in RPMI supplemented with 10% FBS and antibiotics. Cultures were passaged every 3 days when 90% cell confluence was achieved, adherent cultures were passaged using 0.25% Trypsin/EDTA for 5 min at 37$^{o}$C to disassociate the cell monolayer and split 1:3. Suspension cultures were aspirated, centrifuged and re-suspended in fresh media and split 1:3. All cultures were incubated at 37$^{o}$C, 5% $CO_2$.

### 2.7.5 Experimental preparation - cancer cell lines

Cell lines were harvested from the main culture via trypsinisation, if required, and the used media removed and cells re-suspended in fresh media. Cell were then seeded into individual wells of a 24 well culture plate (Costar, UK) at a seeding density of $2.5\times10^5$/well (all cell types) 12hrs following seeding, the culture media was replaced with either serum containing culture media (unsynchronised) or starvation media consisting of the appropriate base media (no phenol red, Life Technologies) and charcoal stripped FBS (csFBS, Life Technologies), cultures were then incubated for another 12hrs. Starvation was used to induce cell cycle arrest, resetting the entire culture to G0 (Chen, Huang et al. 2012), whereas cells in serum-containing media cultures remained unsynchronised, containing cells at all stages of the cell cycle. Following 12hrs of incubation, cultures were transferred back into normal media for the experiment.

### 2.7.6 Cell line plasmid transfection optimisation experiment

Lipid-plasmid complexes were formed using the same protocol as described for lipid-oligonucleotide complex formation. Plasmid and lipid reagent solutions were prepared separately and the plasmid solution added to lipid solution carefully. The solution was then gently vortexed and incubated for a minimum of 15 min at RT. The complexed solution was applied to the culture wells in a spiral motion and the plates agitated side to side to ensure an even distribution (Figure 7, B).

Cell line transfections were optimised using 200ng GFP-pSG5 plasmid and pSG5ø negative control (Figure 7, A, Omnicyte Ltd., London, UK). Omnicyte transfections were optimised using siGLO transfection control reagent (GE Lifesciences, Little Chalfont Bucks, UK).

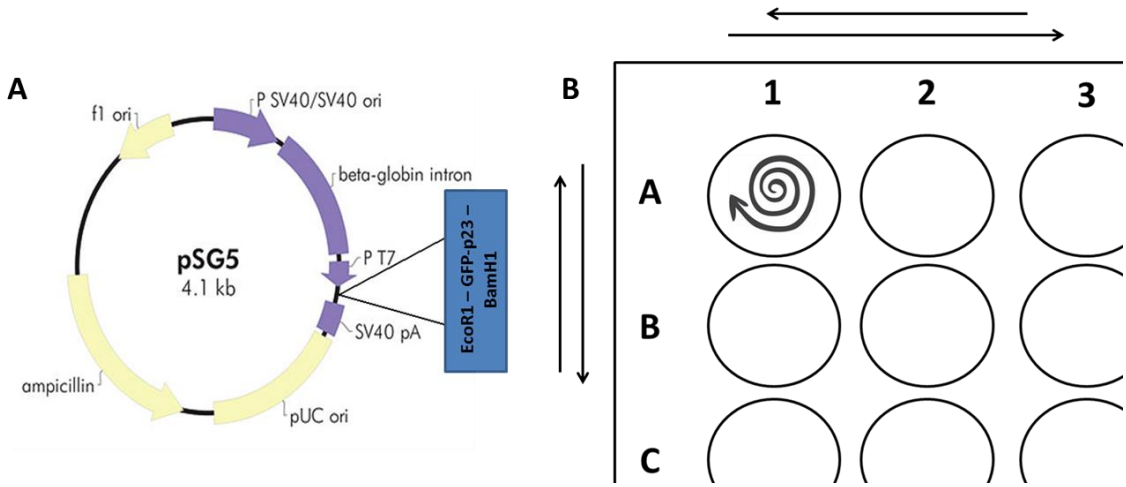


**Figure 7 - GFP containing plasmid and well transfection method**
**A)** Schematic showing the plasmid used during cancer cell line transfection optimisation, the plasmid was designed to contain an EcoR1-GFP-p23-BamH1 element that once taken up by the cell would allow the synthesis of GFP within the cell. **B)** Lipid-oligonucleotide/plasmid complexes were applied to the experimental wells in a circular motion and then the whole plate rocked side to side to avoid creating a vortex.

## 2.8 Omnicyte Analytical Techniques

### 2.8.1 WST-1 cell proliferation assay

Cells were cultured in micro-plates (96 wells) prior to WST-1 analysis. WST-1 reagent was added to cultured cells at 5µL per 100µL culture media and incubated at 37$^{o}$C, 5% $CO_2$ for 3hrs prior to measuring the absorbance (450nm) with a reference wavelength of >600nm using a uQuant microplate spectrophotometer (BioTek, Potton, UK) and analysed with KC4 version 3.4 (BioTek). Standard curves were produced for each cell type and blank (no cells) controls were used to obtain a background/baseline reading.

### 2.8.2 Harvesting of cell cultures and RNA extraction

At specific time points, and at the end of experiments, cells were harvested for extraction of total RNA for subsequent mRNA analysis. This process allowed analysis of target genes throughout the course of an experiment.

Adherent cells were harvested mechanically using a cell scraper to disrupt the cell monolayer. Cold DPBS was used to transfer the cells into RNAse free eppendorfs. To harvest suspended cells, the cell suspension was carefully transferred to RNAse free eppendorfs. For both methods the cell suspension was centrifuged at 8,000rpm for 3min and the supernatant discarded, the cell pellet was snap frozen in dry ice and ethanol and stored at -80$^{o}$C until RNA processing.

RNA was extracted using an RNAqueous micro kit (Applied Biosystems). Briefly, the pelleted cells were resuspended in cell lysis buffer (provided by the kit) and mechanically disrupted on ice using a sonicator (Misosonic Inc) with 3 pulses at output 3. Total RNA was then precipitated with 99% Ethanol (Sigma-Aldrich) followed by affinity separation and elution with RNA columns as provided by the kit. Total RNA content and purity was then quantified using a Nanodrop 1000 spectrophotometer. RNA samples were kept on ice at all times or immediately stored at -80$^{o}$C until required. For very short-term storage, RNA samples were stored at -20$^{o}$C (but only for a very limited time to avoid damage to the RNA).

### 2.8.3 Reverse transcription polymerase chain reaction (rtPCR)

cDNA synthesis was performed on a CX1000 thermocycler (Biorad) using Omniscript kit (Qiagen) following the manufacturer's protocol. Subsequent to this, semi-quantitative polymerase chain reaction (PCR) of the cDNA was performed using Taq Polymerase (Qiagen) for the following genes: *β-Actin, sox1, otx2, pax6, nestin, TH, lmx1a, foxa2,* with *β-Actin* serving as the internal control (Table 13) using the CX1000 thermocycler (Biorad, Hertfordshire, UK). PCR cycles and optimal conditions were optimised per primer set.

Amplified products were visualised using 2% agarose (Sigma-Aldrich) gels stained with ethidium bromide (Sigma-Aldrich) enabling labelling of the PCR products. Gels were analysed using a UV reader (UVP VisionWorks LS v6.2, Cambridge, UK).

| | Primer Sequence | PCR conditions |
|---|---|---|
| **β-actin** | Forward | (37 cycles) |
| | 5'-GAG AAA ATC TGG CAC CAC ACC-3' | 95°C - 5min |
| | Reverse | 95°C - 45sec |
| | ATA CCC CTC GTA GAT GGG CAC-3' | 60°C - 30sec |
| | | 70°C - 45sec |
| | | 72°C - 10min |
| **Sox1** | Forward | (45 cycles) |
| | 5'-CAA TGC GGG GAG GAG AGG TC-3' | 95°C - 5min |
| | Reverse | 95°C - 45sec |
| | 5'-CTC TGG ACC AAA CTG TGG CG-3' | 58°C - 40sec |
| | | 60.7°C - 1min |
| | | 60.7°C - 10min |
| **Otx2** | Forward | (40 cycles) |
| | 5'-CAA CAG CAG AAT GGA GGT CA-3' | 95°C - 5min |
| | Reverse | 95°C - 45sec |
| | 5'-CTG GGT GGA AAG AGA AGC TG-3' | 55°C - 30sec |
| | | 62°C - 45sec |
| | | 62°C - 10min |
| **Pax6** | Forward | (35 cycles) |
| | 5'-GGC AAC CTA CGC AAG ATG GC-3' | 94°C - 5min |
| | Reverse | 94°C - 45sec |
| | 5'-TGA GGG CTG TGT CTG TTC GG-3' | 64°C - 1min |
| | | 66°C - 1min |
| | | 66°C - 10min |
| **Nestin** | Forward | (45 cycles) |
| | 5'-GCC CTG ACC ACT CCA GTT TA-3' | 95°C - 5min |
| | Reverse | 95°C - 1min |
| | 5'-GGA GTC CTG GAT TTC CTT CC-3' | 57°C - 45sec |
| | | 60°C - 1min |
| | | 60°C - 10min |
| **Nanog** | Forward | (35 cycles) |
| | 5'-AAT ACC TCA GCC TCC AGC AGA TG-3' | 95°C - 5min |
| | Reverse | 95°C - 45sec |
| | 5'-TGC GTC ACA CCA TTG CTA TTC TTC-3' | 60°C - 30sec |
| | | 66°C - 45sec |
| | | 66°C - 10min |
| **TH** | Forward | 94°C - 5min |
| | 5'-AGC TGT GAA GGT GTT TGA GAC-3' | 94°C - 30sec |
| | Reverse | 57°C - 45sec |
| | 5'-TCG AGG CGC ACG AAG TAC T-3' | 62°C - 45sec |
| | | 62°C - 3min |
| | | (39 cycles) |
| **Foxa2** | Forward | 95°C - 3min |
| | 5'-CCC GCC CAC TCC AAC TAC CG-3' | 95°C - 40sec |
| | Reverse | 55°C - 40sec |
| | 5'-GCG CCC ACG TAC GAC GAC AT-3' | 62.5°C - 40sec |
| | | 62.5°C - 3min |
| | | (39 cycles) |
| **Lmx1a** | Forward | 95°C - 3min |
| | 5'-AAC GAC AGC TTC TGG CAT GA-3' | 95°C - 40sec |
| | Reverse | 55°C - 40sec |
| | 5'-TCA AGA TGG TTC TCG GAC GT-3' | 62.5°C - 40sec |
| | | 62.5°C - 3min |
| | | (39 cycles) |

Table 13 - PCR primers, sequences and cycle conditions

Table describes the PCR primers utilised for mRNA interrogation. Listed are the genes targeted, sequences for both forward and reverse primers and the optimised PCR cycling conditions used; melting, annealing, extending and the number of cycles performed.

### 2.8.4 Agarose gel manufacture

Agarose gels were produced in-house to assess the expression of target genes amplified using PCR. 1g of agarose was diluted in 49mL double distilled water ($ddH_2O$). Agarose was dissolved on a heated stirring platform and then cooled to a workable temperature (~60$^{o}$C). 5µL of ethidium bromide was pipetted into the solution and mixed well before pouring into moulds and allowed to set at RT. PCR products were loaded following mixing with Orange-G loading buffer and ran at 70volts for 15min (timing adapted as appropriate)

Ethidium bromide (Sigma-Aldrich) labelled PCR products were then analysed using a UV reader (UVP VisionWorks LS v6.2).

### 2.8.5 Quantitative PCR

Quantification of gene expression was executed using QuantiFast SYBR Green PCR Kit (Qiagen, Chapter 2, 2.2.4). Briefly, cDNA was synthesised using Omniscript kit and stored on ice ready for use. A quantifast master mix was prepared for the gene of interest and the mix then transferred to the PCR wells. Samples were processed in duplicate. 24µL of master mix was aliquoted into each well and to this 1µL of pre-diluted cDNA added. qPCR cycling was performed using an Applied Biosystems 7500 Fast Real-Time PCR System (Applied Biosystems). Analysis was processed using SDS 2.4 (Applied Biosystems). The same Quantitech primers were used as described in Table 7: TH, Lmx1a and Foxa2.

### 2.8.6 Immuno-fluorescent staining

Cells were fixed for 10min at RT using 4% PFA and fixed onto glass cover slides. Cells were permeabilised using 0.05% triton-X solution, and blocked with 3% goat serum. Staining was performed using the appropriate 1$^{o}$ antibody i.e. β-III-Tubulin, MAP2 and TH. 2$^{o}$ antibodies (Alexa Fluors®). -488, 594, Cell Signalling Technology, Leiden, Netherlands) were incubated at RT for 1hr at a dilution of 1:600. Dapi nuclear staining was incubated for 10min at RT at a dilution of 1:1000. Between all staining procedures cells were stored in DPBS. Slides were visualised and analysed on a Leica DM4000 (Leica) at x60 magnification.

### 2.8.7 Flow Cytometry Analysis

Cells were fixed and permeabilized using Fix&Perm® fixation medium according to the manufacturer's protocol. Briefly, cells were harvested through trypsin digestion, incubating at 37$^{o}$C for a maximum of 5min, cells were then washed in DPBS and then resuspended in 100µL of reagent A (fixation medium), for 15min at RT. Cells were rinsed with DPBS and resuspended in 100µL reagent B (permeabilization medium) and incubated for 10min at RT. Cells were resuspended in blocking buffer comprising of DPBS, 4% FBS and 3% Bovine serum albumin (BSA, Sigma-Aldrich) and incubated for 15min. Finally cells were stored in DPBS at 4$^{o}$C for a maximum for 48hrs before processing.

Cells were analysed using the BD LSRII flow cytometer (BD) to view the Alexa Fluors®. A minimum of 10,000 cells were collected for each test sample to a maximum of 50,000 to ensure a sufficient number of positive stained cells. FlowJo 7.6 software (TreeStar, USA) was used for further analysis.

### 2.8.9 Automated media analysis

Media samples were collected from cultures at specific time points during the procedure. These were centrifuged at high speed in a microfuge (Eppendorf, 13,000 rpm) to pellet and remove any cells and debris in suspension and the supernatant transferred to a sterile storage tube and snap frozen in liquid nitrogen and stored at -80$^{o}$C until processing. Upon processing samples were defrosted in a water bath at 37$^{o}$C and immediately analysed using an YSI 2700 Select Dual Channel Analyser (YSI Bioanalytical Products, Hampshire, UK). This allowed the measurement of D-glucose (g/L) and L-lactate (g/L). Values were normalised using the baseline measurement of the specific media type being analysed.

### 2.8.10 Growth scoring

Growth scoring was performed by two colleagues who graded growth of specific culture wells and scored them between 1-10. Scoring was performed blinded (assessors did not know the conditions the cultures were exposed to). Averages were taken of the awarded scores.

# CHAPTER 3 - THE POTENTIAL OF OMNICYTES IN NEURONAL DIFFERENTIATION

## 3.1 Introduction

As briefly discussed in chapter 1, hASCs may have regenerative capacity within the ischemic stroke environment. hASCs regenerative potential lies in their capacity to secret paracrine factors (Taguchi, Soma et al. 2004) that aid in endogenous angiogenesis and neurogenesis. They have also been shown *in-vivo* to home to the site of damage and express neuronal and glial cells markers reducing scar formation, this will be discussed within this introduction.

HSCs are one of the best described groups of adult stem cells in mammals and have been widely studied. They have a unique ability during early development to leave their tissue of origin, circulate in the blood and relocate to other niche environments to develop new pools of HSCs (Mikkola and Orkin 2006). They retain this ability during adulthood to an extent, enabling them to 'home' back to the niche within the bone marrow after being in circulation (Lam and Adams 2010). The capacity to mobilise, circulate and return has been exploited for clinical use, for example the intravenous infusion of HSCs following myeloablative therapies to repopulate the patient's bone marrow.

HSCs are a heterogeneous population of cells that express, amongst other antigens, the cell surface marker CD34, and are typically non-adherent to culture vessel plastic. Taguchi *et al* (Taguchi, Soma et al. 2004) reported that $CD34^+$ cells *in-vivo* enhanced neovascularisation in the ischemic brain, this in turn enhanced cerebral blood flow; as well as enhanced cortical expansion, likely reflecting endogenous neurogenesis. There was evidence of an increased number of neural progenitors migrating to the infarct following treatment and it was also noted that animals that did not receive $CD34^+$ cells showed significant behavioural abnormalities after 90 days, whereas those receiving $CD34^+$ cells, did not. The conclusion of the study was that administration of $CD34^+$ cells when compared to $CD34^-$ cells and sham

treated animals resulted in accelerated neuronal regeneration and improved recovery after ischemia.

### 3.1.1 Experimental trials using HSC

The use of HSCs as therapeutic treatments for ischemic stroke has been widely speculated. Their characteristics that make them particularly attractive as a cell therapy; including their ability to 'home' to the area of injury, and their secretion of neuroprotective compounds including, VEGF, FGF2, IGF-1, stem cell factor and granulocyte colony-stimulating factor (G-CSF) (Taguchi, Soma et al. 2004, Kawada, Takizawa et al. 2006), which aid endogenous repair and trigger the mobilisation of bone marrow cells to the brain. These characteristics have particularly focused study on the potential of HSCs in both early stage onset stroke as well as late stage stroke. Early stage treatment focuses on trying to prevent the wave of damage from extending outwards from the infarct site through the provision of trophic, transient support. Late stage administration could function to directly replace neurons lost during the stroke. This late stage intervention could be achieved in two ways: by differentiating the cells *in-vitro* prior to transplantation or by the direct transplantation of $CD34^+$ cells followed by specialisation *in-vivo* via endogenous signalling (Sigurjonsson, Perreault et al. 2005).

### 3.1.2 Omnicytes

A small sub-population of $CD34^+$ cells called omnicytes has been identified (Gordon 1994, Zuba-Surma, Kucia et al. 2009) with promising characteristics for ischemic stroke therapy. They were identified based on their adherence to culture plastic and their expression of the CD34 antigen. $CD34^+$ cells are typically non-adherent, and this property has long been used to separate $CD34^+$ from $CD34^-$ cells such as MSCs. However it was discovered by Gordon *et al.* that a sub-population of $CD34^+$ cells adhered to plastic that constitutes approximately 1% of the whole $CD34^+$ population. Omnicytes have morphology consistent with a primitive stem cell population; they have a small lymphocyte-like morphology with high nuclear/cytoplasm ratio, attributes that are not characteristic of $CD34^+$. Once isolated, the adherent population was

99% pure with low expression of CD38, CD33 and HLA-DR, differing from their fellow non-adherent population that had high variability in expression of these antigens. It was hypothesised that the regenerative capabilities of the total $CD34^+$ population lay within this small sub-population of cells (Gordon 1994, Gordon, Levicar et al. 2006).

As well as the primitive morphology, these cells also expressed a number of genes indicating their potential to differentiate towards different lineages and cell types (Cross and Enver 1997). Gordon *et al.* showed that omnicytes expressed genes associated with all three germ layers, including genes associated with cardiovascular, pancreatic, muscle and nerve lineages (Table 14). They also expressed genes associated with pluripotency including *Nanog* and *Oct4*. Evidence suggests that this small sub-population is a putative stem/progenitor cell population that may have the potential to form a range of cells from the 3 embryonic germ layers (Gordon 1994, Gordon, Levicar et al. 2006).

| Stem cell | Pancreas | Cardiovascular | Nerve |
|---|---|---|---|
| CD34 | Pdx-1 | Nkx2.5 | Endolase |
| CD133 | NGN-3 | MEF-2C | Nestin |
| Rex-1 | Insulin | MEF-2D | Dopamine |
| Oct-4 | | Phosholamban | Serotonin |
| Nanog | | VEGF | NGN3 |
| Tie-2 | | KDR | |
| Angiopoietin | | PECAM | |
| TAL-1 | | VE-cadherin | |
| CXCR4 | | | |

**Table 14 - Endogenously expressed genes associated with freshly isolated omnicytes**
Genes observed by Gordon *et al.* to be endogenously expressed by fresh omnicytes, genetic analysis done using rt-PCR.

Omnicytes taken through phase 1 safety trials in liver failure patients were found to be to have no adverse effects on patients (Gordon, Levicar et al. 2006, Levicar, Pai et al. 2008, Pai, Zacharoulis et al. 2008). This confirms the safety profile and justifies their use in further human trials to investigate their therapeutic potential.

In light of *in-vivo* studies demonstrating that $CD34^+$ cells aid in angiogenesis and neovascularisation following ischemic stroke (Chen, Zhang et al. 2003, Taguchi, Soma et al. 2004), it is thought that using omnicytes could aid and enhance patient recovery, as was

investigated in a phase 1 trial by Imperial College London in 2013 (Catapult 2013, Banerjee, Bentley et al. 2014).

### 3.1.3 Neuronal priming through the use of growth factor and cytokine manipulation

Omnicytes have potential to differentiate into all three germ layers, including ectoderm, indicated by the endogenous gene expression of *nestin, endolase, dopamine, serotonin* and *NGN3* (Gordon, Levicar et al. 2006). This work investigates the effectiveness and impact of protocols that were developed for the differentiation of hPSC into neuronal populations on omnicytes. With the aim of understanding if omnicytes could be used to generate neuronal population for the treatment of ischemic stroke.

One published protocol that was investigated, reported the ability to produce >80% neuronal precursors ($pax6^{+}$) from hPSCs (Chambers, Fasano et al. 2009). Neuronal conversion was achieved by inhibiting transforming growth factor beta (TGFβ) signalling by blocking downstream smad signalling pathways using Noggin and SB431542. TGFβ signalling promotes differentiation towards endoderm and mesoderm fates, inhibiting these pathways via smad inhibition blocks endoderm and mesoderm differentiation thereby encouraging the ectoderm lineage.

Under a separate investigation, later stage growth factor manipulation was performed on omnicyte cultures to investigate the hypothesis that omnicytes are already primed for neuronal differentiation (Gordon, Levicar et al. 2006). Factors, sonic hedgehog (SHH), fgf8 and brain derived neurotrophic factors (BDNF) were used to provide the appropriate cues to induce midbrain neuron phenotypes (Jiang, Henderson et al. 2003).

### 3.1.4 RNA mediated manipulation of omnicyte neuronal fate

Neural circuitry has been traditionally studied in the terms of conserved signalling pathways and neurogenic transcription factors. To exploit these pathways scientist were limited to adapting culture media and using growth factors and cytokines. Recently, groups of conserved non-coding RNAs that are highly influential post transcriptionally have been discovered, these

RNAs modify protein expression through the inhibition or degradation of messenger RNA (mRNA) and include, Piwi-interacting RNA (pirRNA) (Siomi, Sato et al. 2011), small-interfering RNA (siRNA) and RNA interference (RNAi) (Dogini, Pascoal et al. 2014). Studies have also shown the existence of a highly conserved noncoding regulatory RNA group known as microRNAs, these are discussed in the next section.

#### 3.1.4.1 MicroRNA background

MicroRNAs are short noncoding nucleotide sequences that have been found to be essential in the regulation of gene expression (Ameres and Zamore 2013). This work investigates whether by using microRNAs, omnicytes can be driven towards a neuronal lineage.

MicroRNA function by targeting mRNA once they are exported from the nucleus, and inhibiting their translation into functional protein. MicroRNAs are endogenous 20-24 nucleotide (nt) long RNA elements and were originally thought to be possessed only by higher organisms, essential only for complex characteristic expression. It has now been found that microRNAs are highly conserved across the phylogeny indicating their importance in cellular function (Meza-Sosa, Pedraza-Alva et al. 2014). It has been hypothesised through bioinformatics that thousands of microRNAs have regulatory functions within the human body and are thought to be involved in almost every function and cellular process (Bartel 2004). Expression has been found to be highly specific, with microRNA's being exclusive to particular cell types and some transiently expressed during different stages in development. This characteristic suggests an important role for microRNAs in cellular homeostasis.

MicroRNAs function by inhibiting specific mRNA expression post-transcriptionally, this is a result of either degrading of the mRNA or by inhibiting/blocking of translation. The inhibitive interaction between the microRNA and their target mRNA is dependent on two factors: homology at the 5' seed region of the microRNA (usually 2-8 nt) target site of the mRNA – Watson-Crick pairing; and the mismatching and bulging at the centre region, allowing

endonucleolytic cleavage of target mRNA by Ago2 (Slicer) (Pillai, Bhattacharyya et al. 2007, Filipowicz, Bhattacharyya et al. 2008).

#### 3.1.4.2 Candidate microRNA

It is understood that there are distinct microRNA expression profiles during mammalian brain development (Martino, di Girolamo et al. 2009) and in the mature brain, these expression profiles are tightly regulated. Approximately half the known microRNA identified are found within the brain (Shao, Hu et al. 2010), indicating the vital role they play in the brains function and development.

The focus of this work will be two key neuronal microRNAs; microRNA 9 (miR9) and microRNA 124 (miR124). miR124 is the most abundantly found microRNA in the brain, and accounts for approximately 25% of the microRNA expressed. It is found to be perfectly conserved throughout species, from worms to humans and exists in three forms, 124-a,-b,-c, all resulting in identical mature microRNA. In murine models miR124 has been identified to be involved in the differentiation of neurons and are predominantly expressed in mature and differentiating neurons (Cheng, Pastrana et al. 2009). *In-vivo* miR124 expression occurs with the initial differentiation of neurons from neural progenitor cells (Krichevsky, Sonntag et al. 2006), indicating miR124 plays a key role in the differentiation of neural progenitor cells into neurons. It is thought it does this by repressing the expression of a large number of non-neuronal genes (Conaco, Otto et al. 2006, Cheng, Pastrana et al. 2009). Knockdown studies and over expression studies have shown that increased levels of miR124 drove cells towards a neuronal lineage and knockdown showed a 30% reduction in functional neurons produced.

MiR9 is primarily expressed in the brain as a mediator of neurogenesis (Krichevsky, Sonntag et al. 2006, Packer, Xing et al. 2008). The expression of this microRNA is variable throughout differentiation from neural progenitor to more mature cell types, the highest level of expression is found in mature cell types (Krichevsky, King et al. 2003). A key function of miR9 is thought to involve the regulation of *TLX*, an orphan nuclear receptor involved in proliferation

and self-renewal (Zhao, Sun et al. 2009). Over expression of miR9 leads to a down regulation of *TLX* and reduced levels of proliferation, pushing cells out of proliferation and into differentiation.

## 3.2 Aim

The aim of this chapter will be to assess the potential of omnicytes for neuronal differentiation and the production of neuronal cells for the treatment of ischemic stroke. Initial work by Gordon *et al.* has indicated the potential of omnicyte for neuronal differentiation. We will investigate the potential of this cell type in both neuronal progenitor production and later specialised cell induction, forgoing the progenitor stage. The impact of media manipulation (smad inhibition and later growth factor modification) and microRNAs will be investigated.

## 3.3 Results

### 3.3.1 Omnicyte expansion and endogenous gene expression

Due to the low yield of omnicytes (~1% of total $CD34^+$ population) from a primary cell source it was important to be able to expand the starting population to a number that could be of therapeutic value and of use in differentiation experiments. It was found that by using 'expansion mix' (Chapter 2, section 2.7.1) it was possible to expand the starting population by approximately 6-fold over the course of 6 days (Figure 8, A). This enabled the investigation of various differentiation protocols from a very low starting population. Omnicytes were screened at day 0 (D0) for their endogenous gene expression to assess their potential for neuronal differentiation. It was shown by Gordon *et al*. that omnicytes express ectoderm associated genes including; *Nestin, Dopamine and Serotonin* (Gordon, Levicar et al. 2006). In this work omnicytes were assessed for their expression of a number of other neural markers and found positive for *sox1, sox2, otx2* and *nurr1* (Figure 8, B), a number of these were shown to be maintained over the 6 days of expansion in expansion media (Figure 8, C). Day 5 was deemed to have the greatest potential with the majority of the target genes still expressed (Figure 8, C). Omnicytes were found to show negative expression of neural markers *pax6, foxa2* and *TH* (Figure 8, B).

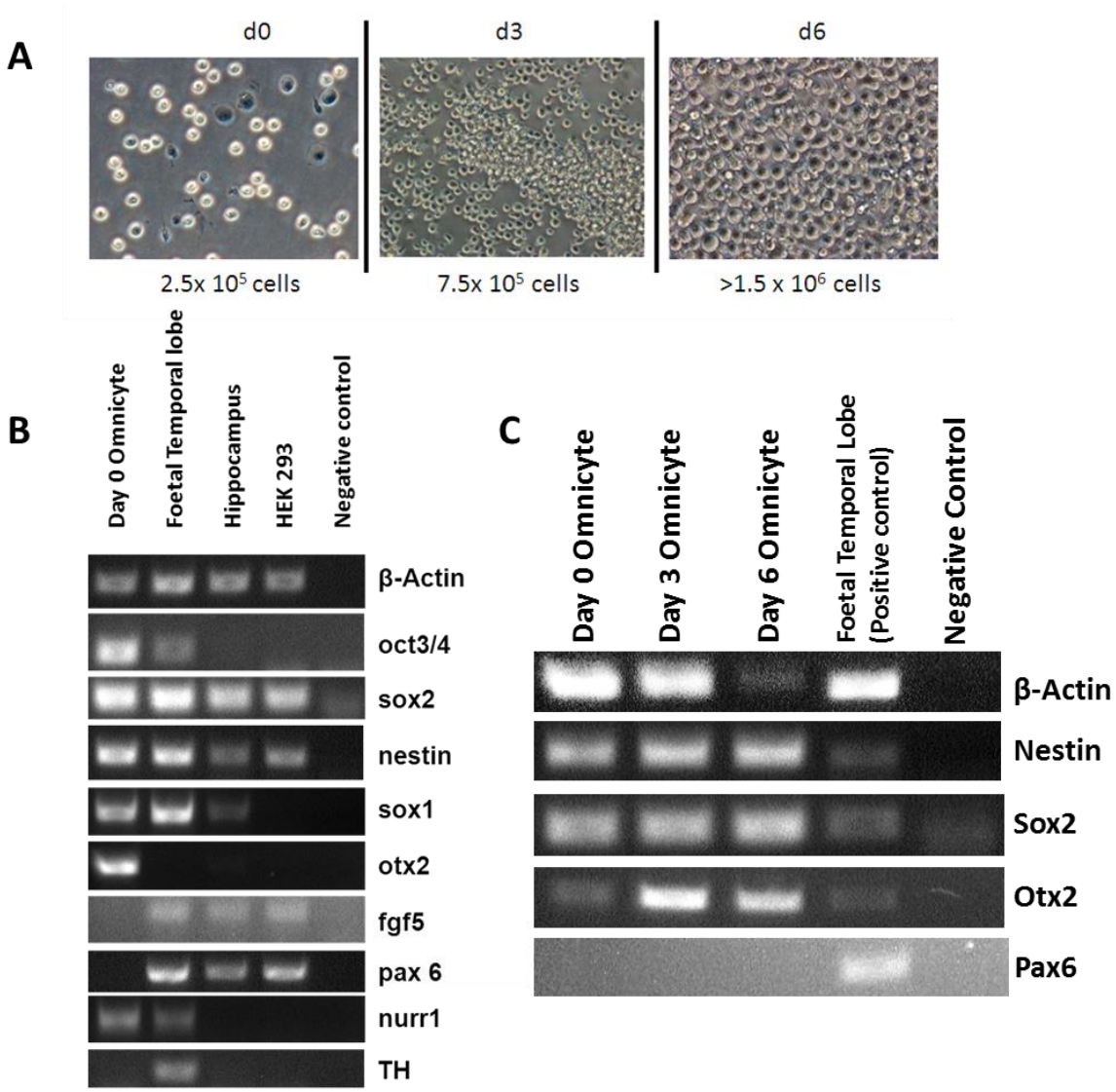


**Figure 8 - Omnicyte expansion and endogenous gene expression**
**A)** Representative bright field images of omnicytes expanded in expansion media over 6 days showing approximately a 6-fold increase in cell number. **B)** rtPCR primer optimisation and screening of endogenous omnicyte gene expression of target genes. **C)** rtPCR for target neuronal genes during 6 days of expansion of omnicytes in expansion media.

### 3.3.2 Effects of cryopreservation on omnicyte expansion potential

Due to the infrequency of patient samples being available for research (Figure 9, C) the effects of retrieval from storage at -80$^{o}$C on omnicyte expansion potential was investigated. Cryopreserved and fresh omnicytes were seeded at 3.7x10$^{4}$ cells per well (96 well plate) and cultured over a 6 day period. WST-1 analysis (Figure 9, A) shows that the sample that had been exposed to cryopreservation was severely limited in its ability to stick down and expand over the first 6 days when compared with fresh samples.

Media analysis was also performed to assess dextrose consumption and lactate production over a 9 day culture period. It was shown that over the first 48 hours dextrose consumption and lactate production remained low. After 48hrs dextrose levels were observed to drop and lactate levels rise in line with omnicyte cell expansion. Media dextrose levels were shown not to drop below 2.5g/L over this culture period with only 1 addition of fresh media at day 6 (Figure 9, B). The same trend was observed in two independent samples characterised over the first 5 days.

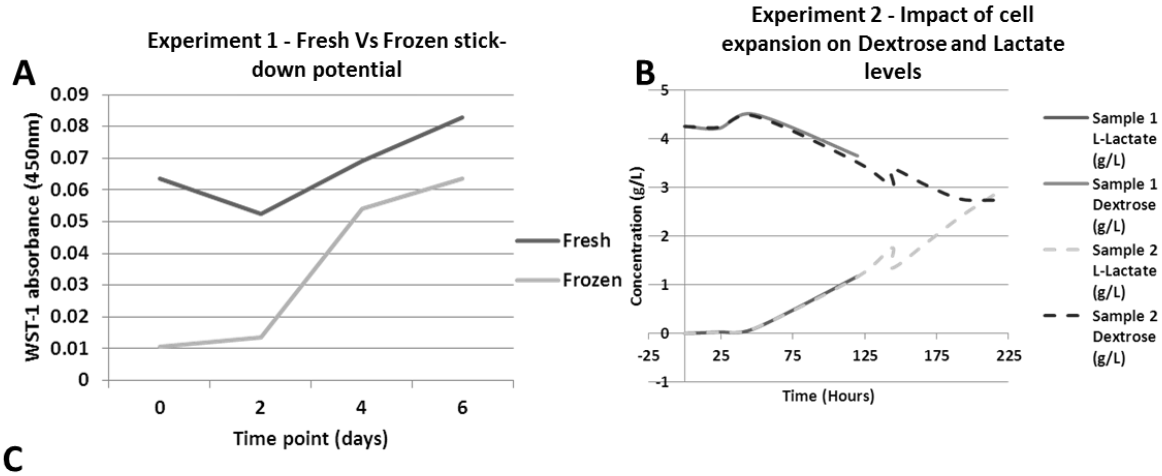


C

| Year | Allogeneic | Myeloma | Lymphoma |
|---|---|---|---|
| 2009 | 6 | 7 | 8 |
| 2010 | 8 | 8 | 7 |
| 2011 | 6 | 7 | 6 |

**Figure 9 - Basic omnicyte culture over time**

**A)** Shows WST-1 readings for fresh versus frozen omnicytes over 6 days (3 hour WST-1 incubation, n=1) **B)** Automated media analysis (Sample 1 & 2, solid and dashed line respectively) under normal culture conditions 37$^{o}$C 5% $CO_2$. Lactate production (g/L) and Dextrose consumption (g/L) is shown over 125hrs (n=2). **C)** Table showing the number $CD34^{+}$ patient samples donated to Omnicyte Ltd. over a three year period, categorised by disease type.

## 3.4 Growth factor and cytokine manipulation of omnicytes

### 3.4.1 Priming omnicytes towards a neuronal lineage using smad signalling inhibition

Omnicytes were manipulated using conditions similar to those described by Chamber *et al.* (Chambers, Fasano et al. 2009). Smad inhibition was used to drive omnicytes down the ectoderm lineage whilst restricting both endoderm and mesoderm differentiation by blocking Activin/BMP signalling pathways. The conditions described in Figure 10, A, allowed the screening of three base media alongside the influence of the smad inhibition; DMEM (DMEM/KO-SR + Factors), αMEM (αMEM/KO-SR + Factors) and an in-house expansion media

(Expansion/KO-SR + Factors). Serum (+ve growth control, DMEM/FBS) and serum-free conditions (DMEM/KO-SR) were used as experimental controls.

Cell cultures were analysed qualitatively (Figure 10, B) and blind scored for morphology change and cell culture proliferation following 3 days in the experimental conditions (Figure 10, C).

Expansion/KO-SR + Factors resulted in the highest level of population expansion and the greatest level of morphological change during the 3 days of culture and the serum positive control (DMEM/FBS) showed a level of proliferation and morphological change greater than the other experiential conditions investigated over the 3 days of culture (Figure 10, B, C).

**A**

| | DMEM/FBS | DMEM/KO-SR | DMEM/KO-SR + Factors | αMEM/KO-SR + Factors | Expansion/KO-SR + Factors |
|---|---|---|---|---|---|
| **Day 0** | DMEM + FBS | DMEM + Knockout Serum **NO** factors | DMEM + KO **PLUS** factors | αMEM + KO **PLUS** factors | Expansion media + KO **PLUS** factors |
| **Day 2** | DMEM + FBS | DMEM + Knockout Serum **NO** factors | DMEM + KO **PLUS** factors | αMEM + KO **PLUS** factors | Expansion media + KO **PLUS** factors |
| **Day 3** | **Analysed** | **Analysed** | **Analysed** | **Analysed** | **Analysed** |

**B**

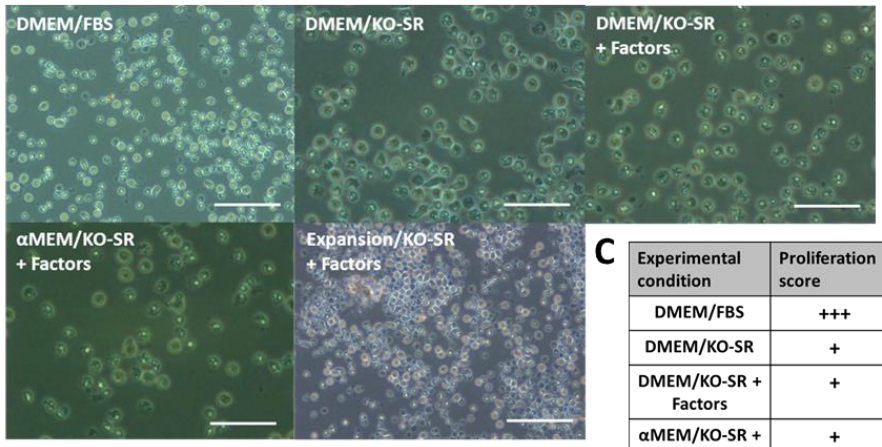


**C**

| Experimental condition | Proliferation score | Morphological change score |
|---|---|---|
| DMEM/FBS | +++ | ++ |
| DMEM/KO-SR | + | + |
| DMEM/KO-SR + Factors | + | + |
| αMEM/KO-SR + Factors | + | + |
| Expansion/KO-SR + Factors | ++++ | +++ |

**Figure 10 - Effect of smad inhibition and different media compositions on omnicyte morphology and proliferation over 3 days**

**A)** Schematic of the experimental protocol used to screen initial conditions for the smad inhibition investigation. Serum (DMEM/FBS) and serum-free (DMEM/KO-SR) controls were used as controls to assess cell growth in unmodified conditions. αMEM and DMEM + smad fact investigated base medium use and expansion media assessed the use of the proprietary in-house expansion mix with omnicytes (factors included noggin (500ng/mL) and SB431542 (10μM)). **B)** Representative bright field images (x20 (DMEM/FBS, Expansion/KO-SR + Fact., scale bars = 100μm) and x40 (DMEM/KO-SR, DMEM/KO-SR + Fact. and αMEM/KO-SR + Fact., scale bars = 50μm) magnification) following 3 days in experimental media. **C)** Blind scoring for proliferation and morphology change for each experimental condition.

To further investigate the effects of the previous experiment, 2 experimental conditions were taken forward: i) Expansion/KO-SR + factors given the proliferation and morphological scorings

observed; and ii) DMEM/KO-SR + factors, so to assess the impact of expansion media. DMEM/KO-SR was used as the experimental control. The culture period was extended to 7 days to allow the effects of the smad inhibition on cell morphology to be assessed over a longer period of time.

Morphology changes were observed in all conditions (Figure 11, A-H). The greatest level of change was observed in Expansion/KO-SR + factors (Figure 11, C, G and I), where approximately 11% of cells were found to morphologically change; either elongated or adhered to the culture plastic and extending projections (Figure 11, H, I).

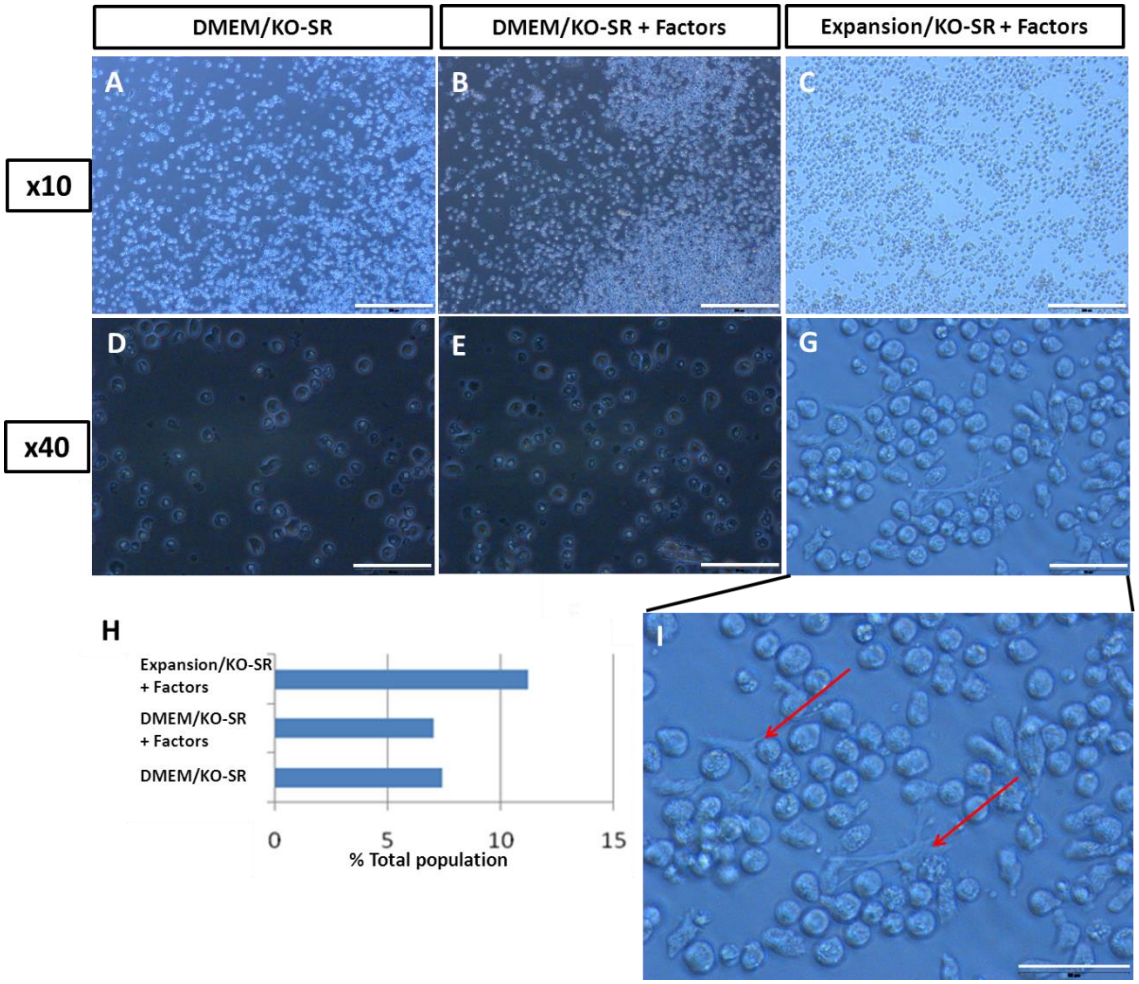


**Figure 11 - Effect of smad inhibition on omnicyte morphology after 7 days of culture**
Representative bright field images of day 7 **(A/D)** DMEM/KO-SR, **(B/E)** DMEM/KO-SR + Factors and **(C/G)** Expansion/KO-SR + Factors cultures. (x10 and x40 scale bars = 200µm and 50µm respectively). **H)** Blind scoring of observed morphological changes following 7 days culture in experimental conditions. **I)** Enhanced bright field image of Expansion/KO-SR + Factors, red arrows highlight adhered omnicytes with transformed morphologies (Scale bar = 50µm).

### 3.4.2 Impact of smad signalling inhibition on the neuronal gene expression of omnicytes

With similarly insignificant morphological changes being  were observed in both DMEM/KO-SR with or without smad inhibitors, it was decided that further experiments would focus on the use of Expansion media with and without smad inhibition (Figure 12, A).

Real-time PCR was used to assess the molecular changes induced in culture populations over time. It was previously shown that *sox1* and *otx2* were endogenously expressed by omnicytes (Figure 8); therefore we investigated whether these genes would be stably expressed throughout 9 days of culture or whether they would be affected by smad inhibition. We also looked to understand whether a longer culture period could result in neuronal progenitor marker *pax6* expression.

Analysis showed that *sox1* was maintained throughout the 9 days of culture irrespective of the condition. *Oxt2* was shown only to be maintained in expansion media without smad inhibition factors (Figure 12, B). The inclusion of factors resulted in a marked decrease in band intensity by D3 and no expression by D9 (Figure 12, B). *Pax6* was not expressed at any time point of the experiment. Pluripotency marker *nanog* was found to decrease by D3 but returned to D0 levels by D9 in expansion media without smad inhibitors but additions of inhibitors appeared to reduce *nanog* expression (Figure 12, B).

**A**

| | -ve control | Adapted |
|---|---|---|
| Day 0 | Expansion media + Knockout Serum<br>NO factors | Expansion media + KO<br>PLUS factors |
| Day 7 | Expansion media + Knockout Serum<br>**NO** factors | Expansion media + KO<br>**PLUS** factors |
| Day 9 | Harvest | Harvest |

**B**

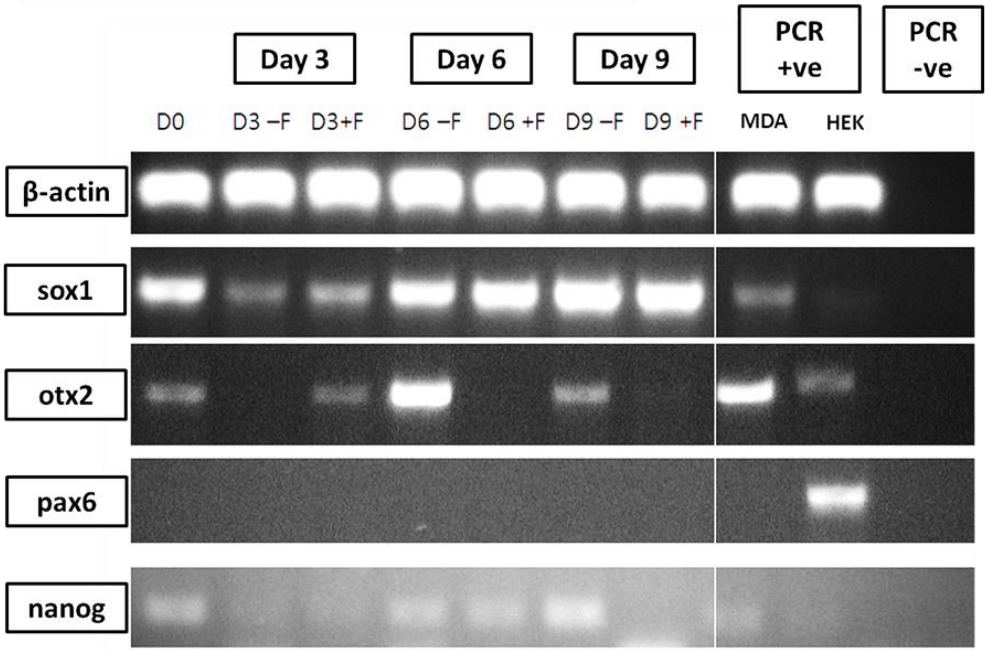


**Figure 12 - Smad inhibition - Molecular analysis at over 9 days (n=2)**
**A)** Schematic of 9 day smad inhibition investigation using expansion media as the base medium. Factors included Noggin (500ng/mL) and SB431542 (10μM) **B)** rt-PCR for mRNA analysis of target neuronal genes over the 9 days of differentiation. Target genes used include; *β-actin* (housekeeping gene), *sox1* (early ectoderm marker), *otx2* (sensory organ development and neuronal patterning), *pax6* (neuronal progenitor) and *nanog* (pluripotency). Positive controls were developed for each PCR primer set, for *sox1, otx2* and *nanog* MDA-MB-231 breast cancer cell line was used and HEK-293 cell line for *pax6*.

### 3.4.3 Neuronal differentiation of omnicytes using later stage neuronal growth factors

The effect of specific neuronal growth factors (SHH, FGF8, BDNF) on neuronal differentiation of omnicytes were also assessed. This work was modelled on research by Jiang *et al.* (Jiang, Henderson et al. 2003) that differentiated neuroectoderm from mouse multipotent progenitor cells. It was thought that the endogenous expression of early neural markers *sox1* and *sox2* by omnicytes could indicate that omnicytes are already primed for differentiation and that early neuronal progenitor manipulation was unnecessary.

We designed an experiment to determine the effects of different supplements on the seeded cells, including +/- neuronal supplement N2 (Life Technologies, Figure 13, A, shaded) and +/- fibronectin (5μg/mL, Sigma) coating of plates (Figure 13, A). The experiment was performed

over 28 days and non-adherent cells were harvested for PCR analysis. Adherent cells were not harvested, due to low cell numbers and with the intention of allowing these cells to mature fully over 28 days.

**A**

| | Negative control (without factors) | Growth factors only | Growth factors + fibronectin | Growth factors + N2 | Growth factors + N2 + fibronectin |
|---|---|---|---|---|---|
| **Plate coating** | | | | Fibronectin | Fibronectin |
| **Base media** | αMEM + 20% FBS | αMEM + 20% FBS | αMEM + 20% FBS | αMEM + 20% FBS | αMEM + 20% FBS |
| **Day 0** | Expansion mix | Expansion mix | Expansion mix | Expansion mix | Expansion mix |
| **Day 6** | | Supplements: bFGF 100ng/ml | Supplements: bFGF 100ng/ml | Supplements: N2 bFGF 100ng/ml | Supplements: N2 bFGF 100ng/ml |
| **Day 13** | | Supplements: SHH 100ng/ml FGF8 10ng/ml | Supplements: SHH 100ng/ml FGF8 10ng/ml | Supplements: N2 SHH 100ng/ml FGF8 10ng/ml | Supplements: N2 SHH 100ng/ml FGF8 10ng/ml |
| **Day 21** | | Supplements: BDNF 10ng/ml | Supplements: BDNF 10ng/ml | Supplements: N2 BDNF 10ng/ml | Supplements: N2 BDNF 10ng/ml |
| **Day 28** | **Molecular and Immunocytochemical analysis** | | | | |

**B**

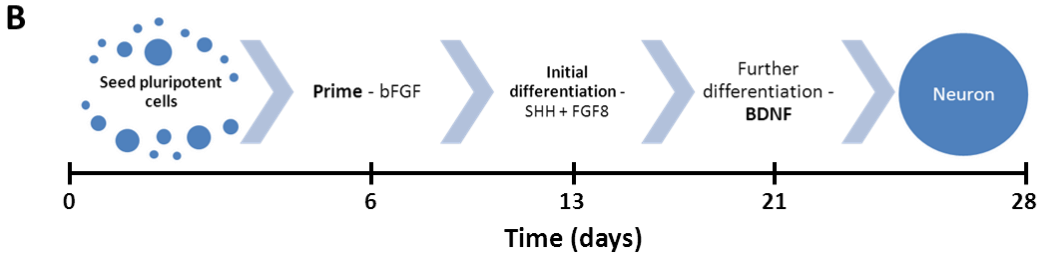


**Figure 13 - Growth factor manipulation schematic**
**A)** Schematic describing the experimental conditions used to investigate the utilisation of growth factors for inducing omnicyte neuronal differentiation. 'Negative control' utilised base media only to provide a baseline for comparison, unshaded columns (without N2) and shaded columns (with N2) allowed the investigation of the growth factors alongside condition types, +/- fibronectin and +/- N2 supplement. **B)** Depiction of the anticipated protocol stages of differentiation.

### 3.4.4 Morphological analysis of growth factor manipulation of omnicytes

Omnicytes were efficiently expanded during the first 6 days (Figure 14, A) and split into wells to investigate the effects of the experimental conditions previously described. Bright field images are shown in Figure 14, B-F. During the initial 7 days of differentiation following growth in the expansion media (i.e. D6 to D13 of the experiment), the cells were exposed to bFGF. Upon stimulation with bFGF, cells started to assume fibroblast-like morphologies, consistent with those observed by Gordon *et al* during normal expansion, elongated or flattened

spherical cells. During this time the cell population grew dramatically with cells being released into suspension. These non-adherent cells were harvested periodically for total RNA extraction and subsequent mRNA analysis but by D11 cell numbers unexpectedly decreased, not allowing further molecular analysis (Figure 15, B). Progressive cell morphologies were continually observed over culture period (Figure 14, B-F) until D28 where samples were shown to have adherent spindle-shaped morphologies (Figure 15, A).

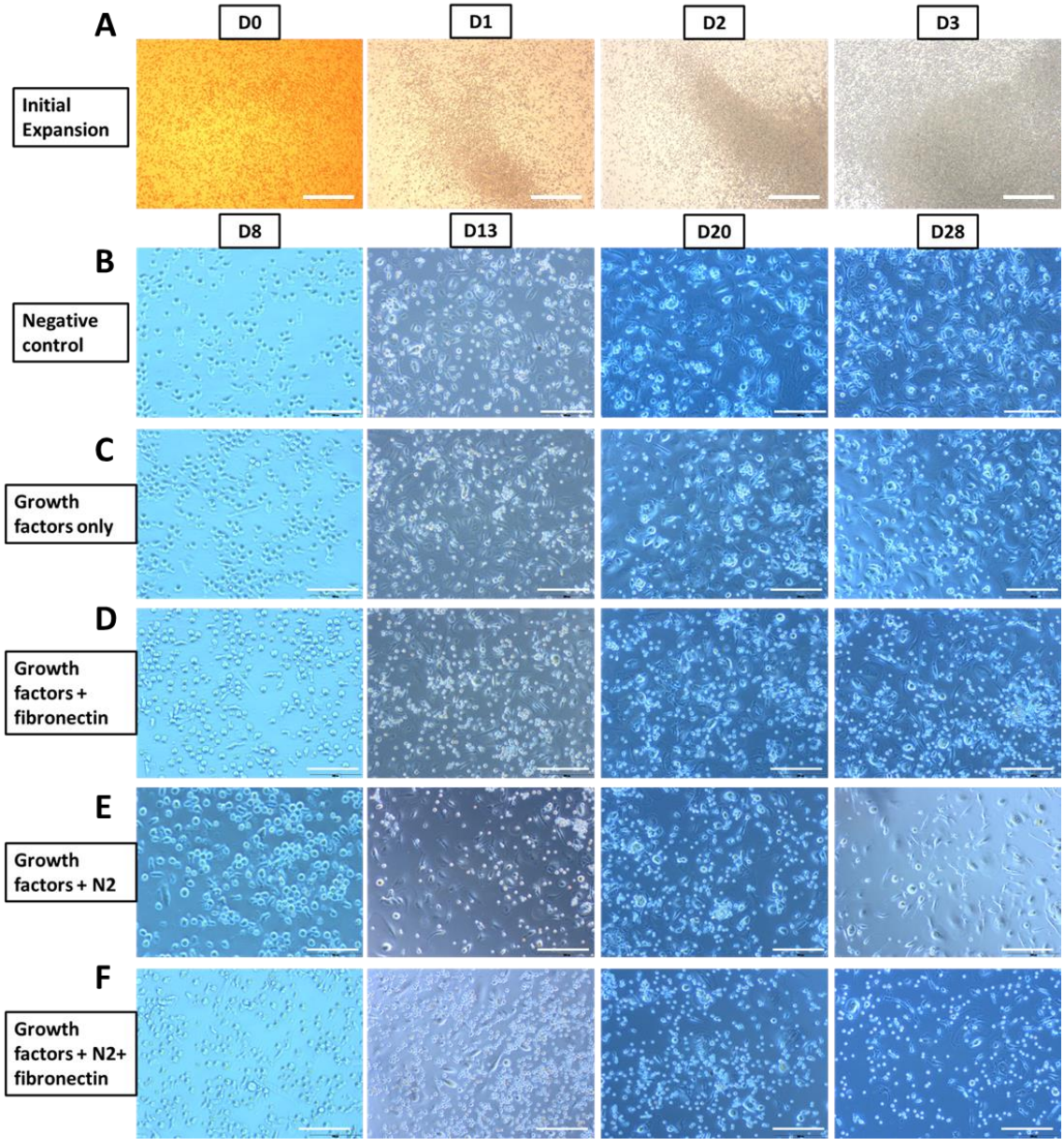


**Figure 14 - Growth factor manipulation - cell morphology images**
**A)** Representiative bright field images of the first 3 days of the initial expansion stage (Scale bars = 1000µm). Representiative bright field images of culturing conditions; (**B**) negaitive control, (**C**) growth factors only, (**D**) growth factors + fibronectin, (**E**) growth factors + N2 and (**F**) growth factors + N2 + fibronectin at day 8, 13, 20 and 28. (Scale bars = 200µm).

By D23 of the experiment, cells had acquired the various morphologies as shown in Figure 15, A. The negative control used exhibited a number of cell types but predominantly adherent circular cells were observed (Figure 15, A, indicated by the red arrow). Cultures without fibronectin coating also exhibited this cell type but the majority were found to be long spindle like cells (Figure 15, A, indicated by the green arrow) with N2 addition reducing the number of cells present and stunting the cellular protrusions (Figure 15, A, indicated by the yellow arrow). The addition of fibronectin appeared to affect viability, with low cell densities being observed in both conditions including the substrate. Growth factors + N2 + fibronectin showed the lowest viable cell population.

PCR analysis revealed that *sox1* and *otx2* expression was generally stable across the majority of conditions, with *sox1* increasing or remaining stable over time in all conditions. *Otx2* appeared to be transiently expressed with reduced levels around D9 of culture. *Pax6* analysis indicated instability of the cDNA synthesised with unstructured banding observed. At D13 *pax6* banding could be observed in 'negative control', 'growth factors only' and 'growth factors + N2' but was questionable in most conditions. There was also evidence of early expression in 'growth factors + fibronectin' but this appeared to have dropped by D13 (Figure 15, B). It was not possible to analyse cells after D13 due to cell numbers being too low. This experiment was repeated with three omnicyte samples; however there was no consistency of gene expression or trends observed across the samples.

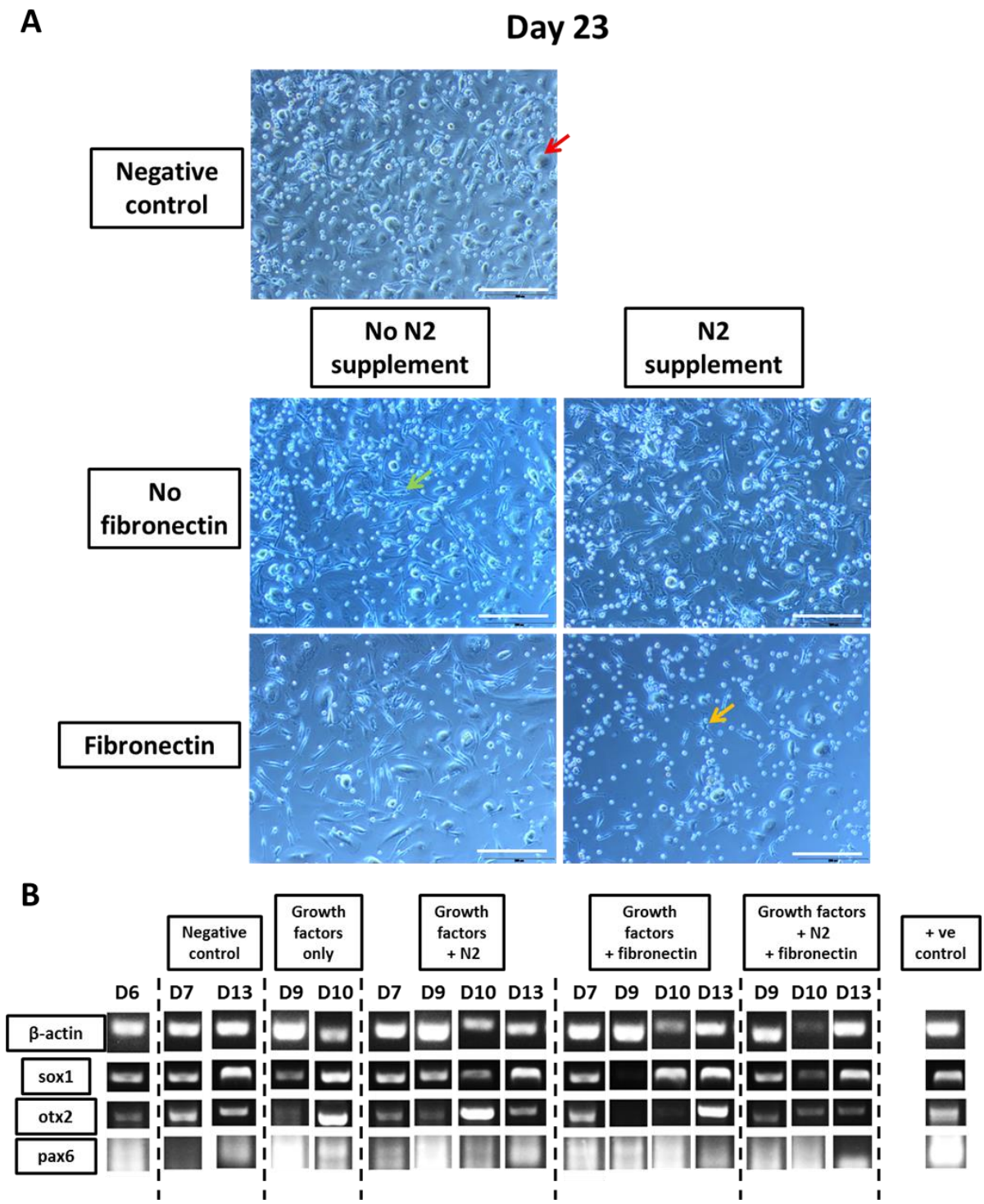


**Figure 15 - Growth factor manipulation - Enhanced day 23 morphology images and RT-PCR analysis**
**A)** Enhanced bright field images of day 23 cultures in the different experimental conditions (Scale bars = 200µm). **B)** Composite image of RT-PCR results of mRNA analysis of target neural genes over 13 days of the growth factor differentiation. Target genes used include; housekeeping gene, *β-actin* and neuronal genes, *sox1*, *otx2* and *pax6* (n=1).

As previously described non-adherent cells were harvested for molecular analysis but adherent cells were cultured for the full 28 days. To analyse these adherent cells

immunocytochemistry (ICC) was carried out. Due to the very low cell number PCR was felt not to be feasible.

Cultures were assessed for expression of neuronal markers β-III-Tubulin (microtubule, neuron specific) and MAP2 (mature neuronal) using ICC (Figure 16). It was observed that on fibronectin coated plates β-III-Tubulin$^{+}$ cells were present though these were found at very low frequencies. MAP2$^{+}$ cells were observed in Growth factor + N2 cultures. Unfortunately staining was not successful for any of the other experimental condition investigated (Growth factors only and Negative control).

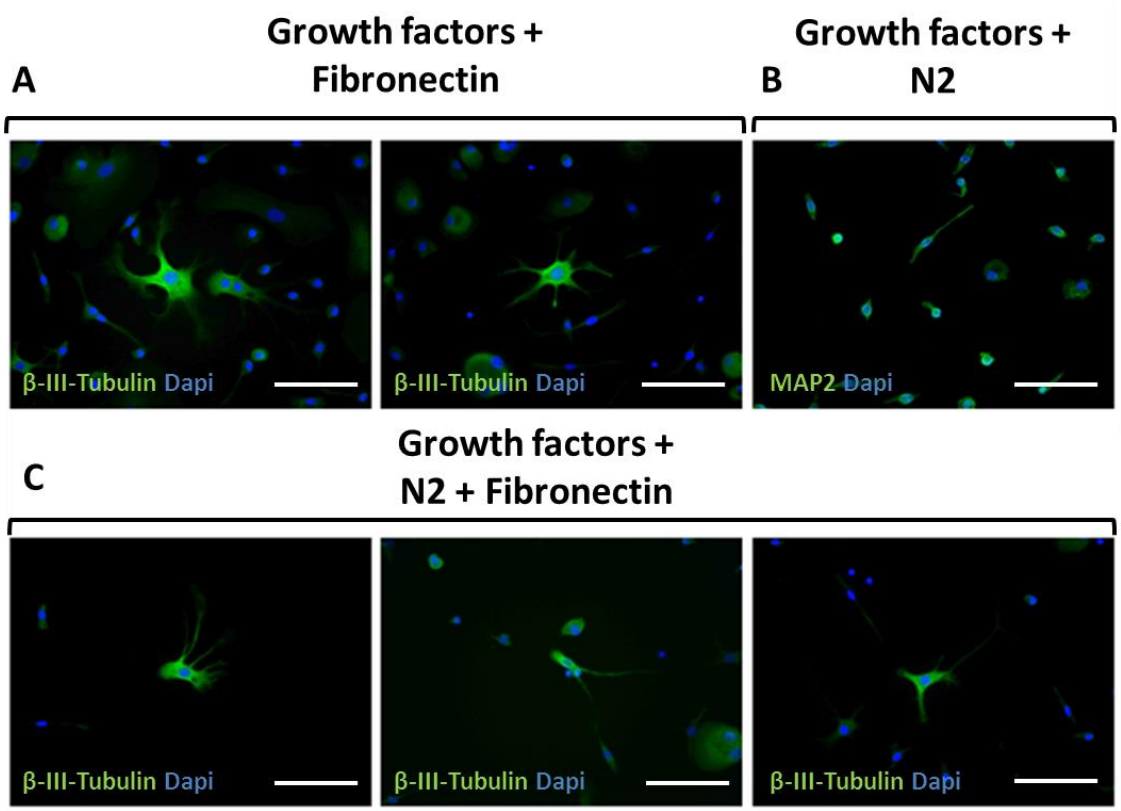


**Figure 16 - Immunofluorescent labelling of growth factor manipulated omnicytes**
Representative ICC images of β-III-Tubulin (microtubule, neuron specific) staining of **(A)** growth factors + fibronectin and **(C)** growth factors + N2 + fibronectin. MAP2 (mature neuronal) staining was processed for **(B)** growth factors + N2 (Scale bars = 50μm).

### 3.5 Utilisation of microRNAs to modify omnicytes gene expression and drive them towards a neuronal lineage

The effects of microRNA124 and microRNA9 on the neuronal gene expression of omnicytes were investigated (Figure 17). Omnicytes were seeded in expansion media with SHH supplemented, SHH has been shown to have a strong proliferation impact on adult neural

progenitors, and it was thought this would prime the cell towards a neuronal lineage (Lai, Kaspar et al. 2003). On day 2 and 3 cultures were transfected with microRNAs or microRNA-negative reagent as a control. The negative control allowed the assessment of the effects of transducing cells alone and the two single microRNA transfections allowed the effects of the individual microRNAs to be assessed.

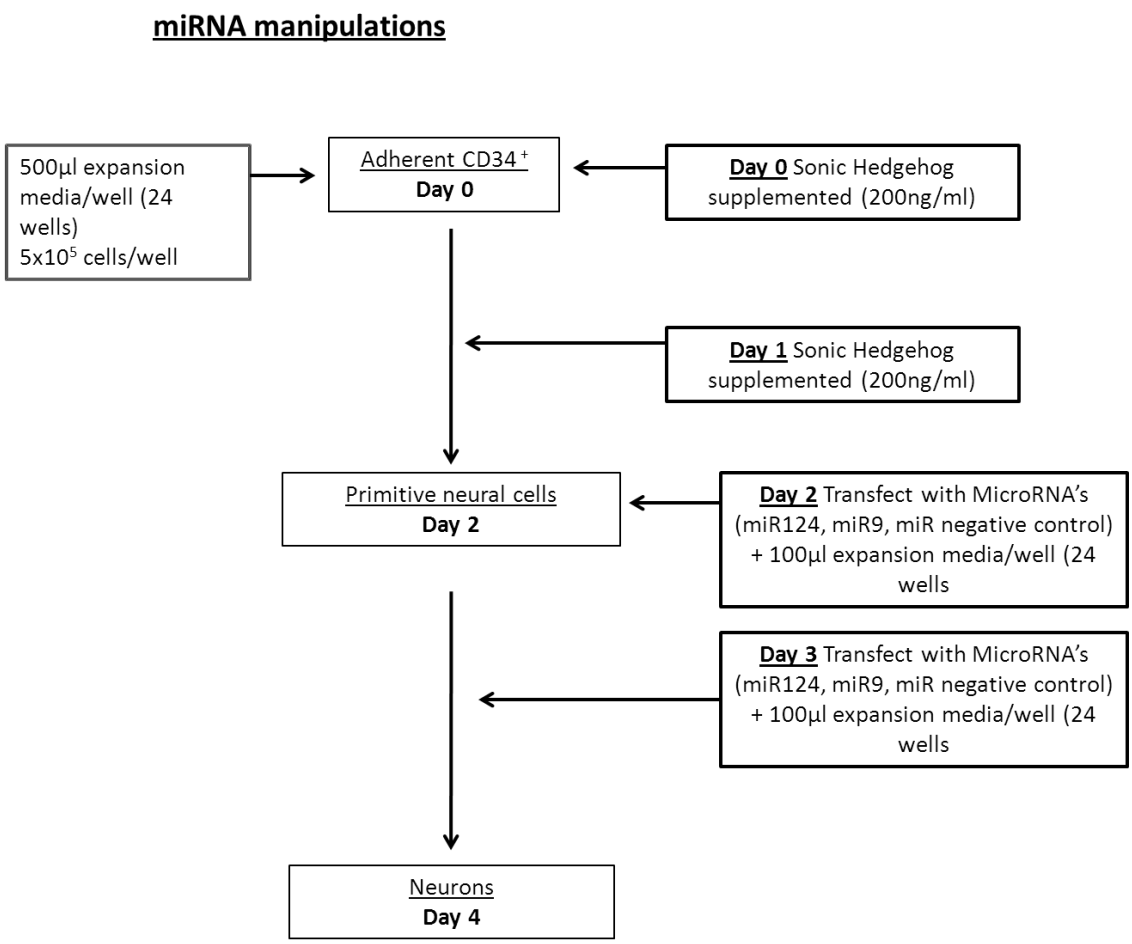


**Figure 17 - Schematic of microRNA work**
Schematic of the experimental protocol used to investigate the utilisation of microRNAs to modify omnicyte gene expression and direct them towards a neuronal lineage, indicating the anticipated stages of the differentiation. Cultures were grown over 4 days in expansion media and supplemented with SHH for the first 2 days. Experimental cultures were then transfected with either miR124 or miR9 to assess the effects of the individual microRNAs. Transfection with miR-negative reagent (100nM) or untreated (negative control) were used as negative controls.

PCR was used to assess the effects of microRNAs on neuronal gene expression in cryopreserved omnicytes. Initial experiments were performed to assess the effects of introducing SHH to the cultures over the first 2 days (Figure 18, A). During this stage *sox2* was found to be stably expressed, *nestin* was found to be amplified in most of the cultures compared with the experimental negative. *Otx2* expression was up regulated consistently

across all the cultures and *Nurr1* only expressed strongly in miR9 transfected cultures. By D4 following transfection, *sox2* and *nestin* were only expressed in miR9 and miR-negative cultures but conversely *otx2* was only expressed in miR124 transfected cultures. *Foxa2* was not expressed by omnicytes under any condition. D0 samples were not collected for this early experiment hindering gene expression analysis over time compared with endogenous expression, D0 expression this was addressed in later experiments (Figure 18, A).

The same protocol was repeated using fresh omnicytes and showed differing results. *Sox2* and *nestin* were expressed across all experimental conditions. *Otx2* was up-regulated in all conditions except miR124 transfected cultures. *Nurr1* showed faint banding at D0 but this low level of expression was lost by D2. Expression levels of *TH* were negative (Figure 18, B).

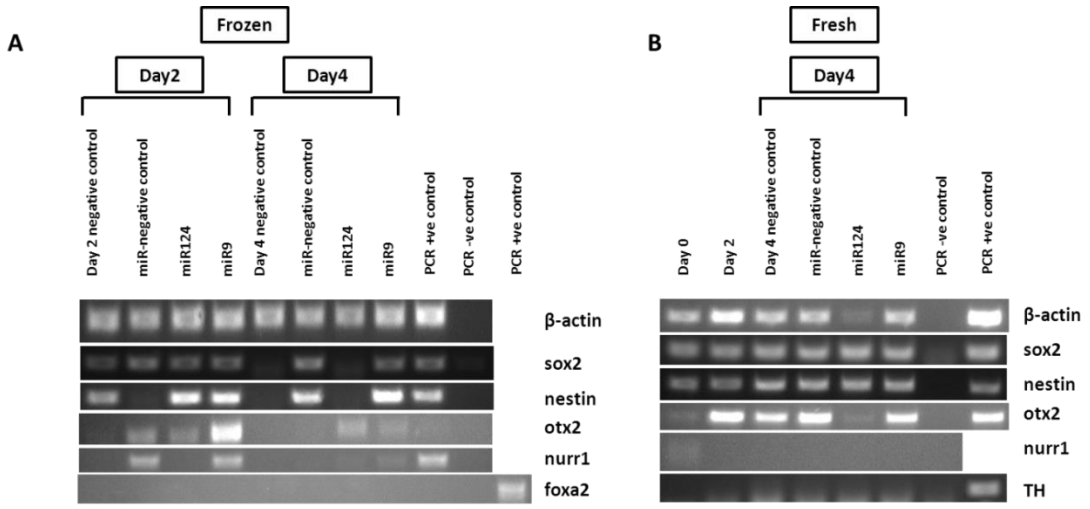


**Figure 18 - RT-PCR analysis of microRNA manipulation of omnicytes**
**A)** RT-PCR analysis of frozen omnicyte expression of target genes (*β-actin, sox2, nestin, otx2, nurr1* and *foxa2*) over 4 days, investigating four conditions. D2 shows the effects of supplementing the experimental media with SHH, D4 represent the individual effects of each experimental condition on target gene expression. **B)** RT-PCR for mRNA analysis of fresh omnicyte target gene expression (*β-actin, sox2, nestin, otx2, nurr1* and *TH*). Negative controls represent cells cultured in expansion media alone. PCR +ve controls were processed using commercially available human foetal temporal lobe DNA.

To build on the variability observed in the previous two experiments (cryopreserved versus fresh), two fresh patient samples received at the same time were used to investigate the variability between patients. *Nestin* was observed to be unaffected by patient variability when considering the level of *β-actin* expression for each sample. Expression across the different conditions showed that neither miR9 nor miR124 showed higher expression than the microRNA-negative control. *Sox2* expression appears to be highly variable with sample A

indicating similar expression levels for both miR124 and miR9 transfected cultures and sample B showing substantially higher expression in miR9 transfected cultures than miR124. *Otx2* also showed no consistency with expression levels per conditions varying widely. *Nurr1* expression was found to be highly variable at D2 and at D4 only miR124 transfected cultures expressed *nurr1* (Figure 19). TH is consistently not expressed.

For both patient samples it was observed that transfection with miR124 resulted in the greatest increase in target gene expression when compared with miR9 (Figure 19).

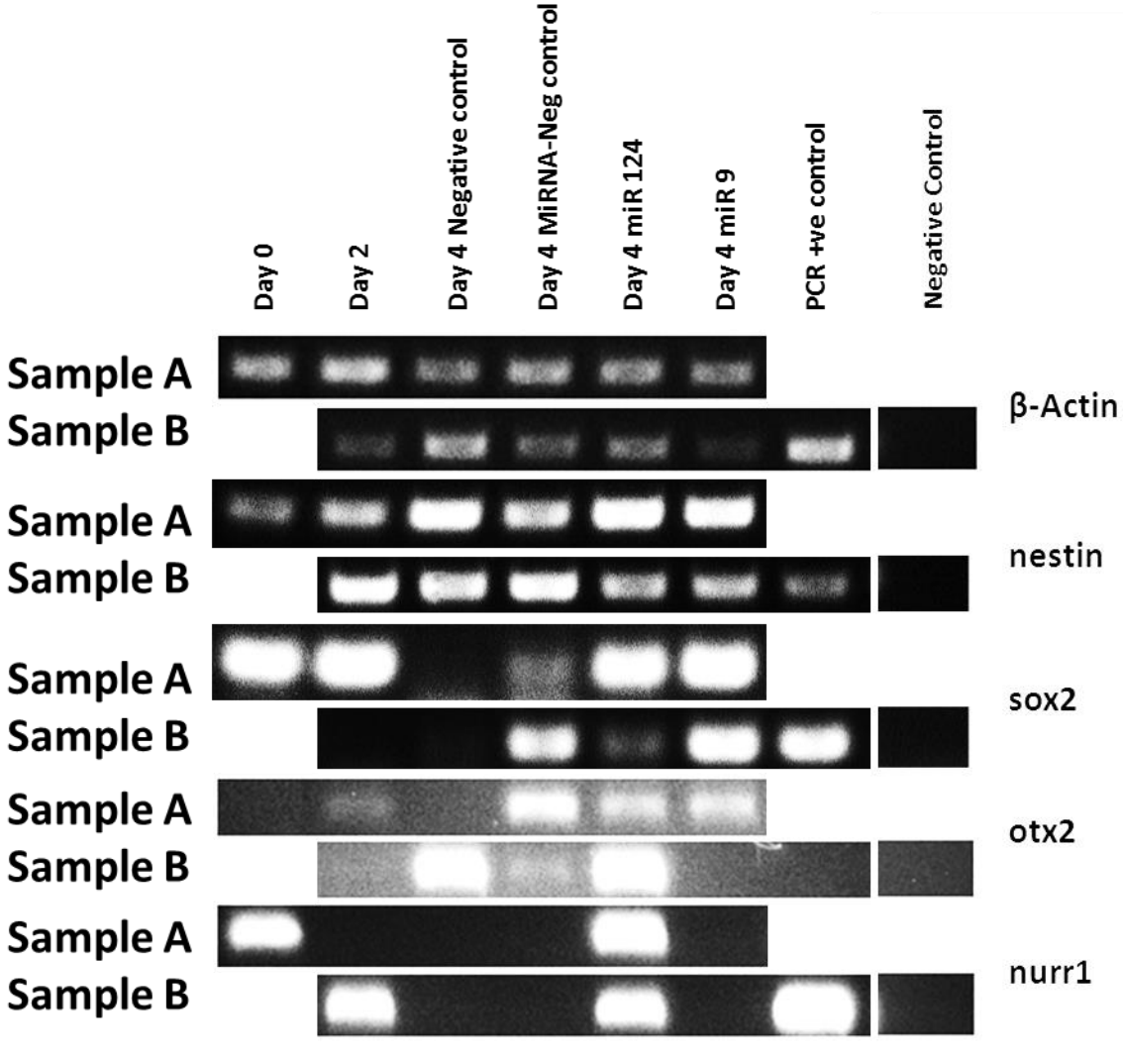


**Figure 19 - microRNA transfections using fresh cells**
RT-PCR analysis of two patient samples (samples A and B). Samples were cultured over 4 days in identical experimental conditions and harvested at D2 and D4 to assess the expression of target genes (*β-actin, nestin, sox2, nestin, otx2* and *nurr1*) over the course of the experimental procedure. One representative D0 sample was harvested due to restricted availability of samples. The PCR +ve were achieved through the use commercially available human foetal temporal lobe DNA.

We then investigated the expression of target neural genes (*sox2, nestin, nurr1* and *TH*) in the two patient samples. Samples were either cultured with expansion media alone or transfected with miR124. This was done to understand the impact of the culture media on gene expression, over that of miR124. miR124 was selected due to the level of expression observed in the previous work (Figure 19) when compared with miR9.

mRNA analysis (Figure 20, A) demonstrated a low consistency in expression of *sox2* and *nestin* with results shown to be contradictory to previous findings. The morphological effects of transfection were clear, in expansion media only cultures single cells were observed (Figure 20, B); but in transfected cultures, cells clumped to form cell aggregates (Figure 20, C).

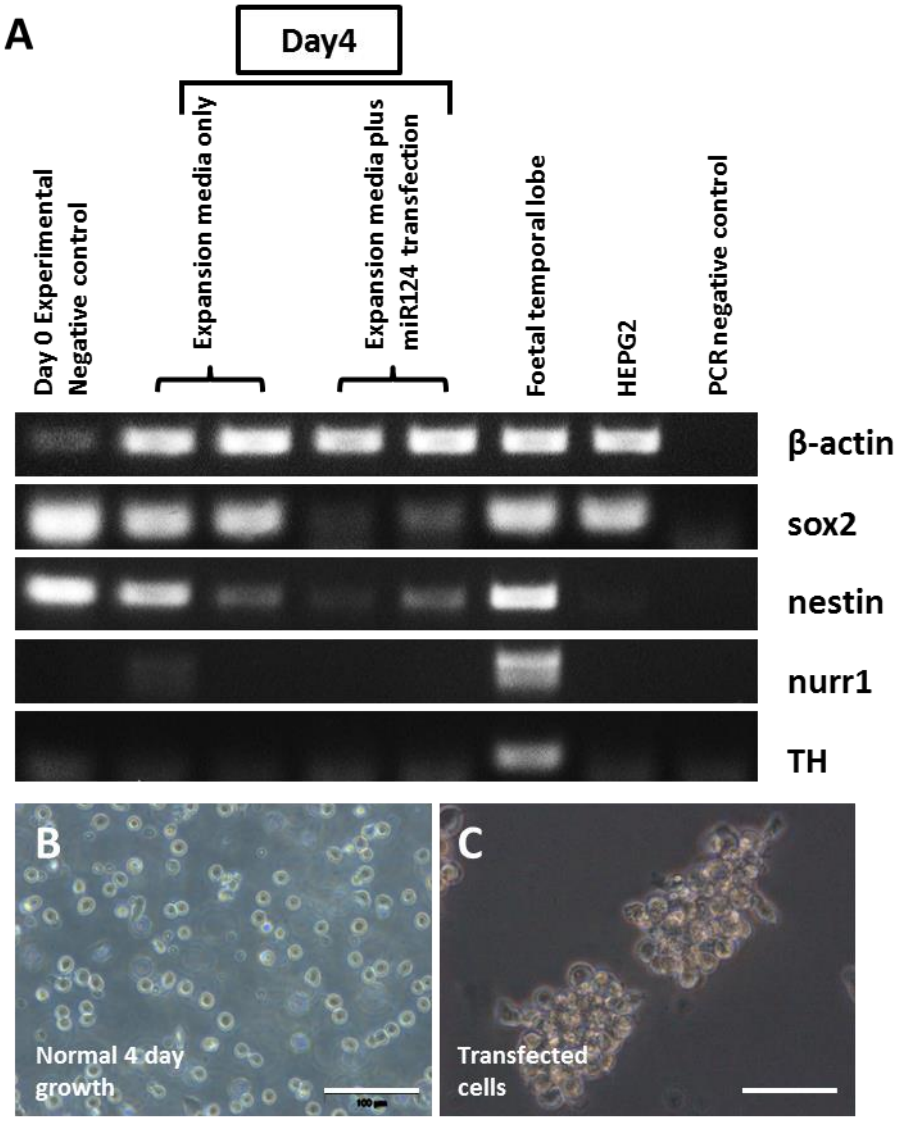


**Figure 20 - Cell culture with expansion media versus culture expansion media and transfection of miR124**

**A)** RT-PCR analysis comparing the effects of expansion media and expansion media plus miR124 on omnicyte gene expression. Representative bright field images of omnicyte cultures in expansion media **(B)** and expansion media transfected with miR124 **(C)** at day 4 of culture (Scale bars = (B) 100µm (C) 50 µm, n=2).

## 3.6 Discussion

This chapter investigated the use of omnicytes (adherent $CD34^+$ cells) as a cell source to generate neuronal populations. It has been shown through *in-vivo* studies (Taguchi, Soma et al. 2004) that administration of $CD34^+$ cells post ischemic attack can have beneficial effects; reduced scaring, increased neovascularization and increased endogenous neurogenesis. Trials are on-going to investigate the benefit of $CD34^+$ cell mobilisation and administration in humans (Therapy 2013, Banerjee, Bentley et al. 2014).

It was thought that by utilizing omnicytes as the cell source for neuronal differentiation, undifferentiated cells following the differentiation process would have a restorative effect and differentiated omnicytes would integrate and have a regenerative effect.

### 3.6.1 Endogenous omnicyte gene expression and their ability for expansion

$CD34^+$ cells are isolated from patient donated bone marrow aspirates or G-CSF stimulated, mobilised bone marrow samples. Omnicytes are a sub-population of this $CD34^+$ population, accounting for around 1% of the whole $CD34^+$ population (Gordon 1994, Gordon, Levicar et al. 2006). This presents a challenge as the initial population for investigation is extremely small and so requires expansion to be viable for investigation. Omnicyte Ltd. developed a propriety expansion media that enabled the expansion of the omnicyte population six-fold over the course of 6 days (Figure 8, A). We found that during these 6 days of expansion in the media, seeding remained appropriate for cell growth. However, as the population increased (Figure 9, A) lactate levels increase and dextrose levels decrease (Figure 9, B). Cell expansion appeared not to be hindered (Figure 9, A).

Due to the rarity of sample acquisition (Figure 9, C) the majority of experiments were carried out on ‘long term’ stored samples and this led us to question how cryopreservation might affect cell viability. We found the level of adherence, ‘stick down’ following cryopreservation was greatly diminished when compared to fresh samples and that population expansion was delayed (Figure 9, A). This needed to be taken into account when initiating experiments.

It was found by Gordon *et al*. (Gordon, Levicar et al. 2006) that omnicytes express a number of neural marker genes. We also assessed gene expression and whether these genes continued to be expressed during the expansion phase. Omnicytes were found to endogenously express two key pluripotency markers; *oct4* and *sox2*, affirming their identification as pluripotent progenitors. It was found that omnicytes expressed a number of neural genes including; *nestin, sox1, otx2* and *nurr1*, supporting the hypothesis that these cells have the potential for neuronal differentiation (Cross and Enver, 1997). Omnicytes were found to not endogenously express *pax6, fgf5* or *TH* (Figure 8), indicating that they are not neuronal progenitors (*fgf5*$^{+}$, *pax6*$^{+}$), or express genes associated with dopaminergic neurons (TH$^{+}$). Expansion was shown to support the expression of the pluripotency gene *sox2* as well as the neural genes *nestin* and *otx2*, indicating that with the genes assessed, expansion could support omnicyte's endogenous neural gene expression profile.

### 3.6.2 The effect of smad signalling inhibition on omnicyte morphology, proliferation and neuronal gene expression

Due to omnicytes being found to endogenously express a number of neuronal genes it was hypothesised that they were primed for differentiation towards a neuronal lineage. To exploit this theory smad inhibition was used to try to direct the cultures away from endoderm and mesoderm lineages and to differentiate them down the ectoderm lineage.

Initial work was designed to assess the effects of different conditioning factors on omnicyte proliferation and morphology over 3 days. Morphological and proliferation blind scoring showed that expansion media plus smad inhibition resulted in the greatest proliferation levels and morphological changes; this was closely followed by serum (FBS) control (Figure 10). This observed proliferation might be expected due to optimised capabilities of expansion media, and serum's common use in cell culture and expansion for this attribute. The use of serum in translatable therapy is avoided where possible due to the increased chance of transmission of xeno-disease to humans, and also because of its uncontrolled consistency. Where possible,

serum is removed from experimentation within this work. Expansion media on the other hand is a chemically defined media (described in the chapter 2, 2.7.1) and is manufactured to be GMP compliant. Other than expansion media, all other conditions showed little to no effect on proliferation of cells, with the exception of DMEM/FBS which was later excluded.

Culture time was extended to 7 days to further investigate these findings. The conditions taken forward included DMEM/KO-SR with/without smad inhibition and expansion media with smad inhibition. Serum was withdrawn for the reasons mentioned above and αMEM/KO-SR with smad inhibition excluded because it was observed to have no greater impact over that of DMEM/KO-SR alone. Findings from this investigation confirmed the observations from the previous screening: expansion media plus smad inhibition resulted in the greatest morphological change with DMEM/KO-SR with/without smad showing no difference, indicating that smad inhibition had no effect over that of the base media alone (Figure 11, A-G/H). In the condition expansion media plus smad inhibition cell morphology could be found to alter in approximately 11% of the cells observed (Figure 11, H).

Following the finding that smad inhibition alone in basal media (DMEM/KO-SR) led to no change in morphology over that observed in the negative control, it was decided that the work would focus solely on expansion media and the inclusion and exclusion of smad inhibition. We investigated the impact of inclusion of smad inhibition over the course of 9 days and assessed its inclusion by looking at the effect on neuronal gene expression; *sox1, otx2* and *pax6* (Figure 12). Relative to D0, *sox1* was found to decrease by D3 but returned to prior levels by D6 then increase in level to D9 where expression was observed to be equal in +/- conditions and enhanced relative to D0, indicating that the culture had moved towards an ectoderm lineage. *Otx2* was expressed at D0 but by D3 *otx2* was found only to be expressed in smad inhibitive cultures. This was reversed by D6, where expression was shown to be enhanced only in expansion media (-factors) cultures and lost in smad inhibitive cultures. Expression was found to decrease again by D9 to D0 levels in smad negative cultures and was observed not to be

expressed in smad inclusive cultures. This indicates that the inclusion of smad inhibition with omnicytes does not promote differentiation towards a neuronal lineage. *Pax6* (Walcher, Xie et al. 2013), an early neuronal progenitor marker, was considered the first milestone in moving omnicytes towards a neuronal cell type (Chambers, Fasano et al. 2009). However in this experiment it was not expressed at any time, under any condition. Screening of the pluripotency marker *nanog* showed that expression increased by D9 in smad negative cultures; this could potentially corroborate the idea that cultures in this condition are maintained in their pluripotent state and not differentiated towards any lineage in particular.

This investigation into the use of smad inhibition alongside expansion media was repeated twice but results were not reproducible. In all experiments, *pax6* was not expressed and so this method of neuronal induction was perceived as unsuccessful and not continued.

### 3.6.3 The effects of growth factor manipulation on neuronal gene expression of omnicytes

It was hypothesised that the lack of neuronal differentiation witnessed using smad inhibition may be due to intervention and manipulation occurring too early in the neuronal differentiation process. This section of work focused on using patterning growth factors to influence the cells and stimulate neuronal progenitors.

The growth factor investigation was designed to test the impact of a number of variables including the use of fibronectin as surface matrix, N2 supplement and the addition of growth factors (Figure 13). It was hypothesised that the addition of the fibronectin would improve cell adhesion and differentiation, through cell-substrate interaction. It has been shown by Nakajima *et al.* that fibronectin can support neuronal cell growth and aids maturation (Nakajima, Ishimuro et al. 2007), supporting this hypothesis. N2 was investigated as it has been shown to support primary neuronal cultures and it was hypothesised that its addition would support the primed omnicytes as they differentiated and matured into neurons.

Omnicytes were observed to expand over the first 6 days in expansion media prior to being split for the experiment (Figure 14). Up to D13, whilst being supplemented with bFGF, the

cultures were found to expand dramatically; cells were also observed to adhere to the culture surface and assume fibroblast-like morphologies similar to findings by Gordon *et al*. During this time, as cells were released into suspension, they were harvested for mRNA analysis. Adhered cells were not harvested as we were limited by the number of experimental replicates and harvesting the adhered cells would have impacted on the scope of the work. Following the addition of SHH and fgf8a on D13, cell numbers dramatically decreased until D21. Alongside this observation, in conditions including fibronectin and N2 supplement (Figure 14), the number of adhered cells was greatly reduced when compared with no addition of fibronectin. Suggesting that omnicytes do not adhere well to fibronectin and that conditions suitable for primary neuronal populations (including N2) are not beneficial to the omnicyte derived population.

At D23 a number of different morphologies were observed. The negative control allowed us to elucidate the impact of the growth factors and additives. Within the negative control, cells adhered and assumed 'fried egg' morphologies (Figure 15), with a smaller proportion presenting elongated morphologies. Within experimental cultures, elongated cells were shown to be the prominent cell type, over that of the 'fried egg' morphology. Both of these morphologies are consistent with observations made by Gordon *et al* in 2006. The exclusion of N2 resulted in the greatest proportion of elongated cells with inclusion of fibronectin resulting in this cell type being the dominate morphology (Figure 15).

Gene expression was assessed over the first 13 days, *sox1* appeared to be maintained up to D13 in all conditions but with reduced expression around D9 or D10 (Figure 15). This trend was also observed with *otx2*. *Pax6* screening did not yield viable results as it appeared that sample RNA or primer had degraded prior to screening but slight banding was observed in all conditions except those including fibronectin. This may indicate that cells exposed to fibronectin mature faster, passing the neural progenitor (*pax6*$^{+}$) stage and this is supported by the protein expression observed. Maturity of the cells in fibronectin coated wells was

confirmed by staining of MAP2 (mature neuronal marker) and β-III-Tubulin (neuronal microtubule marker). $MAP2^+$ and β-III-$Tubulin^+$ were only observed in fibronectin coated conditions (Figure 16), however it is difficult to draw conclusions from this outcome because staining failed in a number of conditions.

The inability to generate convincing neuronal cell types from omnicytes is consistent with literature and other studies that show that the generation of neuronal cells *in-vitro* from whole $CD34^+$ populations or purified HSC populations is generally unsuccessful (Roybon, Ma et al. 2006). Other work has shown in chicken that $CD34^+$ cells can be induced to express neuronal markers though only when implanted directly into the injured embryonic CNS (Sigurjonsson, Perreault et al. 2005). This suggests that to succeed in differentiating $CD34^+$ cells *in-vitro,* factors may need to mimic the injured brain rather than signally during development, which was attempted in this work.

### 3.6.4 The influence of microRNA on omnicyte neuronal gene expression

Finally, the work investigated molecular manipulation, using microRNA, of omnicyte cultures to achieve neuronal differentiation.

The potential of microRNAs as post-transcriptional controlling elements was only just being realised at the time of this work and we attempted to use these elements to modify omnicyte gene expression at a molecular level. A review of the literature highlighted the potential of two candidate microRNA; miR124 (Conaco, Otto et al. 2006, Cheng, Pastrana et al. 2009) and miR9 (Krichevsky, Sonntag et al. 2006; Packer, Xing et al. 2008) that had been shown to be highly influential in the development of neuronal cell types.

A protocol was designed that would prime the cells before transfecting with miR124 and miR9 to drive omnicytes down a neuronal lineage (Figure 17). SHH was supplemented to the cultures at D0 and on D2 cultures were transfected with either the experimental microRNA or miR-negative to assess the impact of the transfection method and the RNA element. An

untreated arm (no SHH or transfection) was used to assess endogenous gene expression over the culture period (Figure 17).

The initial screen was designed to assess the impact of microRNA transfection (D4) on (fresh) omnicyte gene expression. Gene expression was observed to fluctuate between sample times, with expression in miR124 transfected cultures showing variable expression of *sox2* and *nestin* from D2 to D4. However, when the protocol was repeated, on frozen samples, the expression of these genes was found to show the reverse. This experiment was repeated but results were found to be highly variable, this was thought in part to be due to the effects of cryopreservation (Figure 18).

This work then compared the effects of microRNA in two fresh patient samples; this allowed us to interrogate the impact of patient variability on results (Figure 19). Results were found to vary between samples. *Nestin* expression appeared to be relatively constant across both groups of conditions but expression of other genes (*sox2, otx2* and *nurr1*) varied widely. These results, though not conclusive, led us to believe that patient variability and sample storage has an impact on omnicyte gene expression.

The final experiment we performed assessed the effects of miR124 transfection against expansion media alone (Figure 20). Once again results varied from those previously achieved with expansion media alone enhancing gene expression more than in cultures that had been transfected. These findings further supporting the move away from this cell type within the work.

From research performed since this investigation, we now know that miR124 and miR9 can be used to differentiate functional neurons. Yoo *et al.* showed that these two microRNAs can be used in conjunction to differentiate fibroblasts into functional neurons (Yoo, Sun et al. 2011). This would suggest that this technology could still be used with omnicytes though a consistent source of cell needs to be found to reduce the impact of patient variability.

## 3.7 Conclusion

A number of methods were employed in an effort to drive omnicytes down a neuronal lineage including: varying the conditions used; the length of culture; and the stage at which the manipulation occurred (whether this involved signalling pathway manipulation or molecular modification). In none of these situations were gene profiles thought to be indicative of neuronal populations or reproducibly switched on. This finding is in line with other groups that have investigated $CD34^+$ purified populations for the differentiation of neuronal populations (Roybon, Ma et al. 2006).

This analysis was able to show a high level of patient variability associated with omnicytes, however, due to the rarity of the samples, analysis was restricted. The scarcity of the cell type encouraged the use of cryopreserved samples, further restricted analysis as we were able to demonstrate that there was significant variability compared to fresh samples, further impacting on the consistency of the results. These results are in line with the findings of Reebye *et al.* (Reebye, Saetrom et al. 2013, Reebye, Saetrom et al. 2013), that fresh cells yield the best results.

The results of this work challenge the potential of omnicytes as a cell source, certainly under these protocols. To develop the overall goal of directing cells towards a neuronal lineage, the rest of this thesis focuses on the use of a readily available cell source, hPSCs.

# CHAPTER 4 - DIRECT DOPAMINERGIC DIFFERENTIATION OF HUMAN PLURIOPOTENT STEM CELLS

## 4.1 Introduction

Due to the lack of success using omnicytes for the derivation of neuronal populations it was decided that the research would move to use different cell types, namely, human embryonic stem cells and human induced pluripotent stem cells.

At this stage in the work the sponsoring company, Omnicyte Ltd. was refocusing their resources to investigate the use of small activating RNAs, and their utilisation in deriving DA neuronal subpopulations. The intended purpose of this work was to improve the yield of differentiated DA neurons and so to move research one step closer to the development of a treatment for Parkinson's disease. This work was carried out at the UCL laboratories using the methods and protocols available within that facility.

To allow us to investigate the use of saRNA within a pluripotent population we needed to be able to generate DA neurons through conventional means. This functioned to reassure us that firstly, the cell types being used (Shef6 (hESC) and MSUSH001 (hiPSC)) could generate DA populations and secondly, give us a base level of differentiation that was already primed to allow us to assess the function of saRNA in enhancing differentiated yields.

There are a growing number of research groups attempting to generate therapeutically beneficial neuronal subsets, including DA neurons from pluripotent cells (Kriks, Shim et al. 2011, Theka, Caiazzo et al. 2013). One method was of particular interest given its potential scalability of expansion of embryo bodies and was developed by a collaborator's laboratory (unpublished). The DA differentiation protocol used by the laboratory was designed to mimic signalling pathways that neurons are exposed to during the endogenous generation of DA neurons. The protocol was developed to allow the expansion of the pluripotent population

using typical expansion techniques, and then induce neuronal differentiation, expand this population and terminally differentiate these primed cells into DA neurons.

The pluripotent expansion process utilised adhered co-culture with iMEF which mimicked how the cell populations had previously been cultured so to avoid any adverse effects. The populations were then assessed for differentiation and any differentiated cells or colonies removed prior to being put into suspension as cell aggregates. Neural induction was modified from a protocol developed by Joannides's *et al*. ((Joannides, Fiore-Heriche et al. 2007))and was used to select for a neural lineage using SB431542 to block the endoderm and mesoderm lineages and selecting ectoderm as the default (Inman, Nicolas et al. 2002, Laping, Grygielko et al. 2002), similar to the investigation and work described in chapter 3 using omnicyte. The neuronal primed population was then expanded using bFGF which has elsewhere been shown to stimulate proliferation of hPSC-derived neurosphere populations (Gensburger, Labourdette et al. 1987), prior to maturation and terminal differentiation. During maturation cultures were conditioned towards a DA final population through the addition of fgf8a, purmorphamine and ascorbic acid. Both fgf8a and purmorphamine have been shown to be involved endogenously in the development of the mesencephalon (Alves dos Santos and Smidt 2011) and the generation of ventral midbrain neurons (Roelink, Augsburger et al. 1994, Marti, Bumcrot et al. 1995). Ascorbic acid was included for its neuroprotective qualities and its ability to increase differentiation yields of $TH^+$ neurons (Cooper, Hargus et al. 2010). This treatment commenced on D10 and continued until the neurospheres were terminally differentiated into DA neurons after 24 days. Neurospheres were directed finally toward terminal DA differentiation using a chemically defined medium including transforming growth factor betas (TGFβ), GDNF, BDNF, dbcAMP and DAPT, each with their own function in the differentiation including, cell survival, DA neuronal differentiation (TGFβ and GDNF (Krieglstein, Henheik et al. 1998)), promotion of $TH^+$ cell differentiation (BDNF (Hyman, Hofer et al. 1991)), apoptosis prevention (dbcAMP (Hartikka, Staufenbiel et al. 1992)) and restriction of differentiation potential (DAPT (Crawford and Roelink 2007)).

## 4.2 Aim

In this chapter we investigate the potential of two human pluripotent stem cell lines, MSHU001 (hiPSC) and Shef6 (hESC), to differentiate into neuronal subsets expressing DA markers. To do this we firstly investigated the population's ability for self-renewal under typical culture conditions and their ability to differentiate into the three germ layers. We then assessed the cell population's ability under chemically defined conditions to differentiate into neuronal populations that express DA molecular markers and express DA associated protein markers.

## 4.3 Results

### 4.3.1 Normal hPSC culture and characterisation

hPSCs were co-cultured with iMEF and passaged mechanically to maintain their pluripotency. Both cell types are defined by their ability to self-renew and to differentiate to form cells from the three germ layers. Pluripotency of both hiPSC and hESC was assessed at a molecular and protein level through the detection of pluripotent markers using qPCR and immunocytochemical assays. The ability of these cell types to generate the three germ layers; endoderm, mesoderm and ectoderm was assessed by allowing these cultures to spontaneously differentiate *in-vitro* and then test for the expression of germ layer markers, nestin, sox17 and brachyury using immunocytochemistry.

### 4.3.2 hPSC colony morphology

hPSC were typically expanded then passaged every 3-4days. The mechanically passaged clumps were seeded onto fresh iMEF and the progressive colony morphology assessed over 4 consecutive days (Figure 21). By day 3-4, cell density within the colonies was high and the nuclei compacting and becoming visible (Figure 21, D & E).

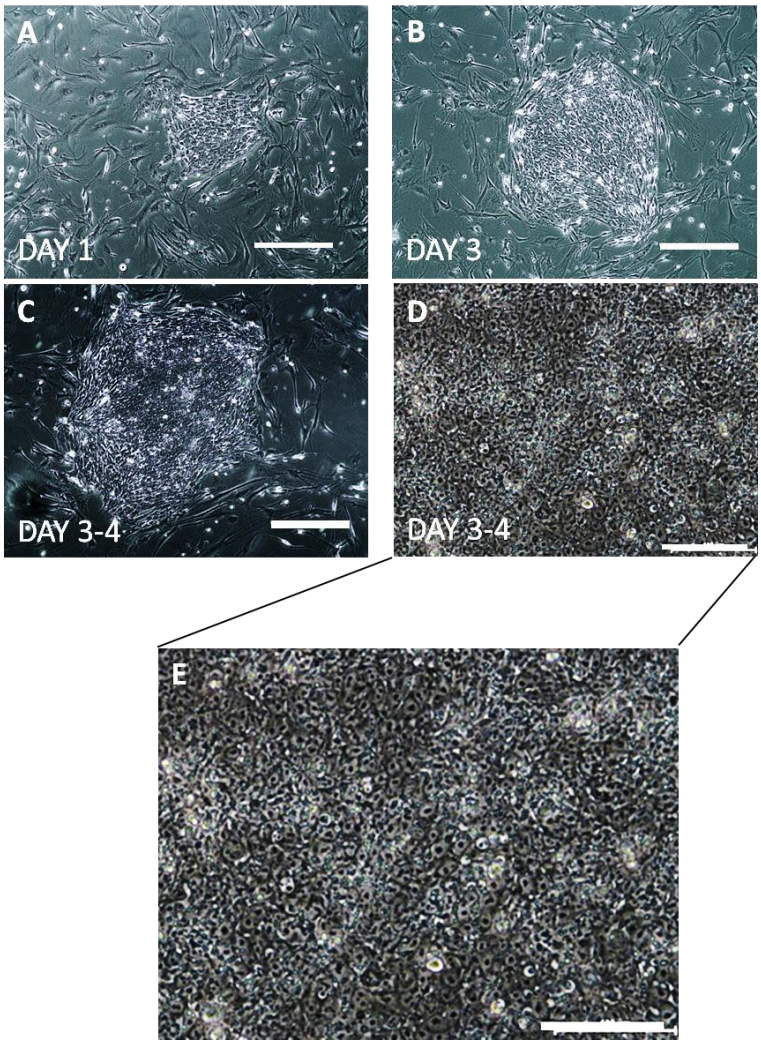


**Figure 21 - Representative images of colony morphology during general culture**
Bright field images of typical hPSC colony morphology during culture. **A)** Initial seeding saw small fragmented cell clumps which **(B-D)** developed and expanded in diameter over time. Once colony mass reached a high level the edges of the colonies started to push against the surrounding iMEF resulting in compaction of the colony centre **(E)** (Scale bars A-C = 400µm, D & E = 100 µm).

### 4.3.3 Confirmation of pluripotent marker expression in hPSC

Pluripotent marker expression by hPSCs was assessed using immunofluorescent labelling, screening for surface (TRA-1-60, Figure 22, B & D/E) and intracellular (Oct4, Figure 22, A & D/E) pluripotent markers. Early differentiation of hESC was visualised through the expression of SSEA1 (Figure 22, C) and was typically found expressed by cells that were removed from the main colony mass, this population was also observed to express reduced levels of Oct4 (Figure 22, A).

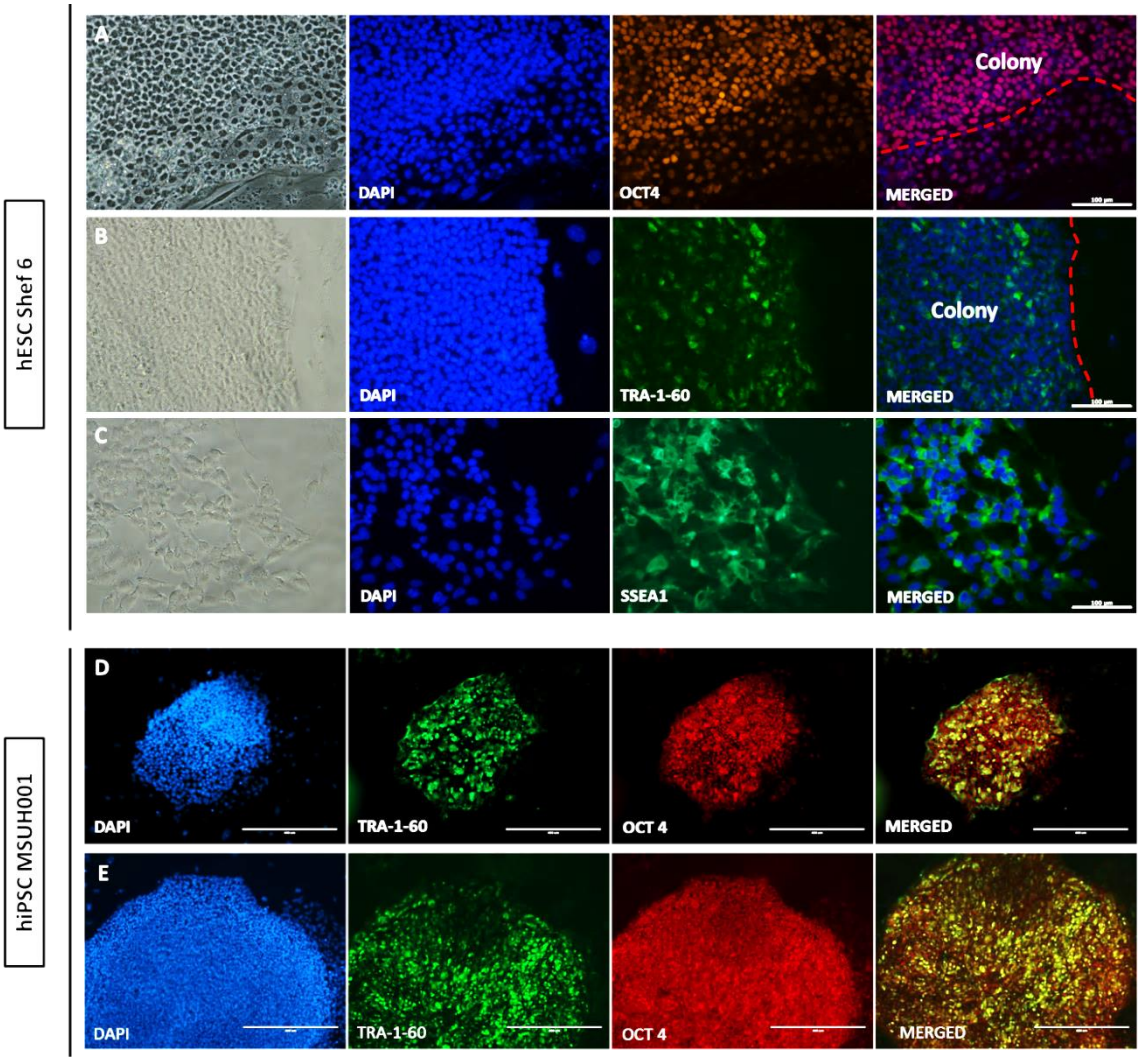


**Figure 22 - hPSCs maintained pluripotent surface marker expression in culture**
Representative images of immunofluorescent labelling of pluripotent markers, **(A)** Oct4**, (B)** TRA-1-60 and early differentiation marker **(C)** SSEA1 in hESC cultures (Scale bar = 100µm). **D-E)** Immunofluorescent labelling of pluripotent markers, TRA-1-60 and Oct4 for hiPSC (Scale bar = 400µm).

### 4.3.4 Quantification of pluripotent marker expression in hPSC

Conjugate surface pluripotent markers were used to quantify the proportion of hPSC that expressed pluripotent markers in culture. SSEA4 and TRA-1-60 can be seen to be expressed in ≥90% of the cultures screened in hESC and hiPSC (Figure 23).

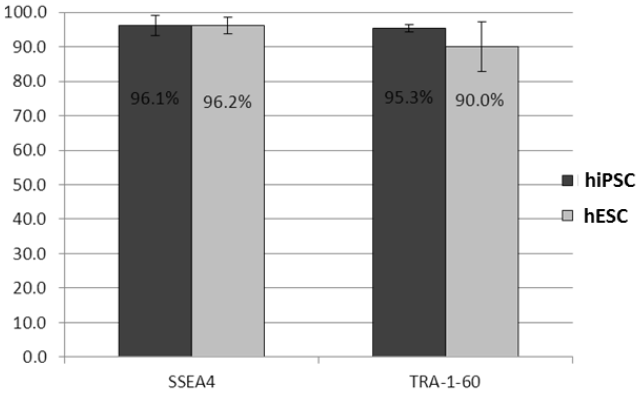


**Figure 23 - Flow cytometry analysis of pluripotent surface markers**
Graphs representing flow cytometry data for hESC and hiPSC culture expression of pluripotent surface markers SSEA4 (n=3) and TRA-1-60 (n=2). Error bars represent SD±1

### 4.3.5 hPSC culture pluripotent gene expression

Three key pluripotency genes were assessed at the start of each experiment; *nanog*, *oct4* and *sox2.* Pluripotency genes were all expressed in both hESC (Figure 24, A) and hiPSC (Figure 24, A) however, relative to the combined housekeeping genes, hiPSC exhibited lower expression of the pluripotency genes.

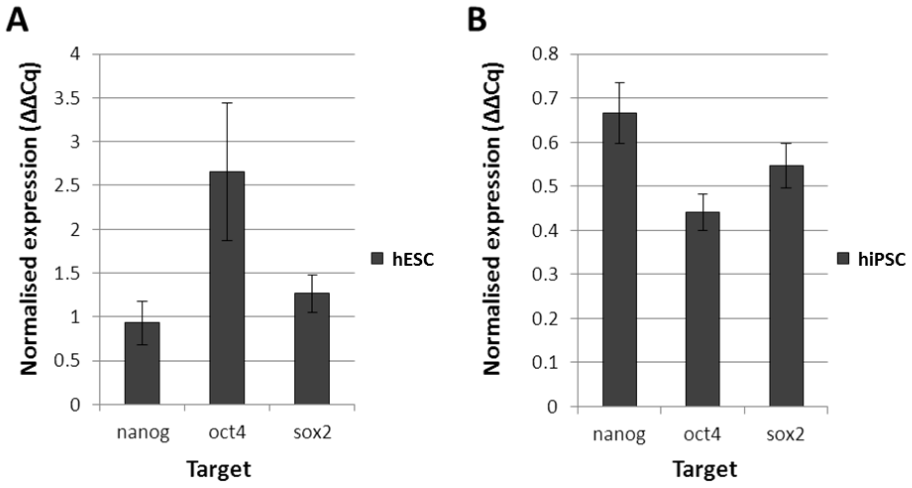


**Figure 24 - Endogenous pluripotent gene expression in hPSC**
qPCR data for pluripotency gene expression of *nanog*, *oct4* and *sox2* in hESC **(A)** and hiPSC **(B)** cell lines. Data was normalised against *β-Actin, GAPDH* and *UBC*. Error bars = SEM±1 (n=3)

### 4.3.6 Spontaneous differentiation of hPSC can generate cells of all germ layer lineages

Cultures were spontaneously differentiated to examine the pluripotent nature of both hESC and hiPSC. This was done by removing bFGF from the culture media (KOSRM) and culturing cells for 27 days without passage. hPSC cultures were shown to express mesoderm marker, Brachyury (Figure 25, A & D), ectoderm marker, Nestin (Figure 25, B & E) and endoderm

marker, Sox17 (Figure 25, C & F), demonstrating the ability of hESC and hiPSC to form cells from all three germ layers.

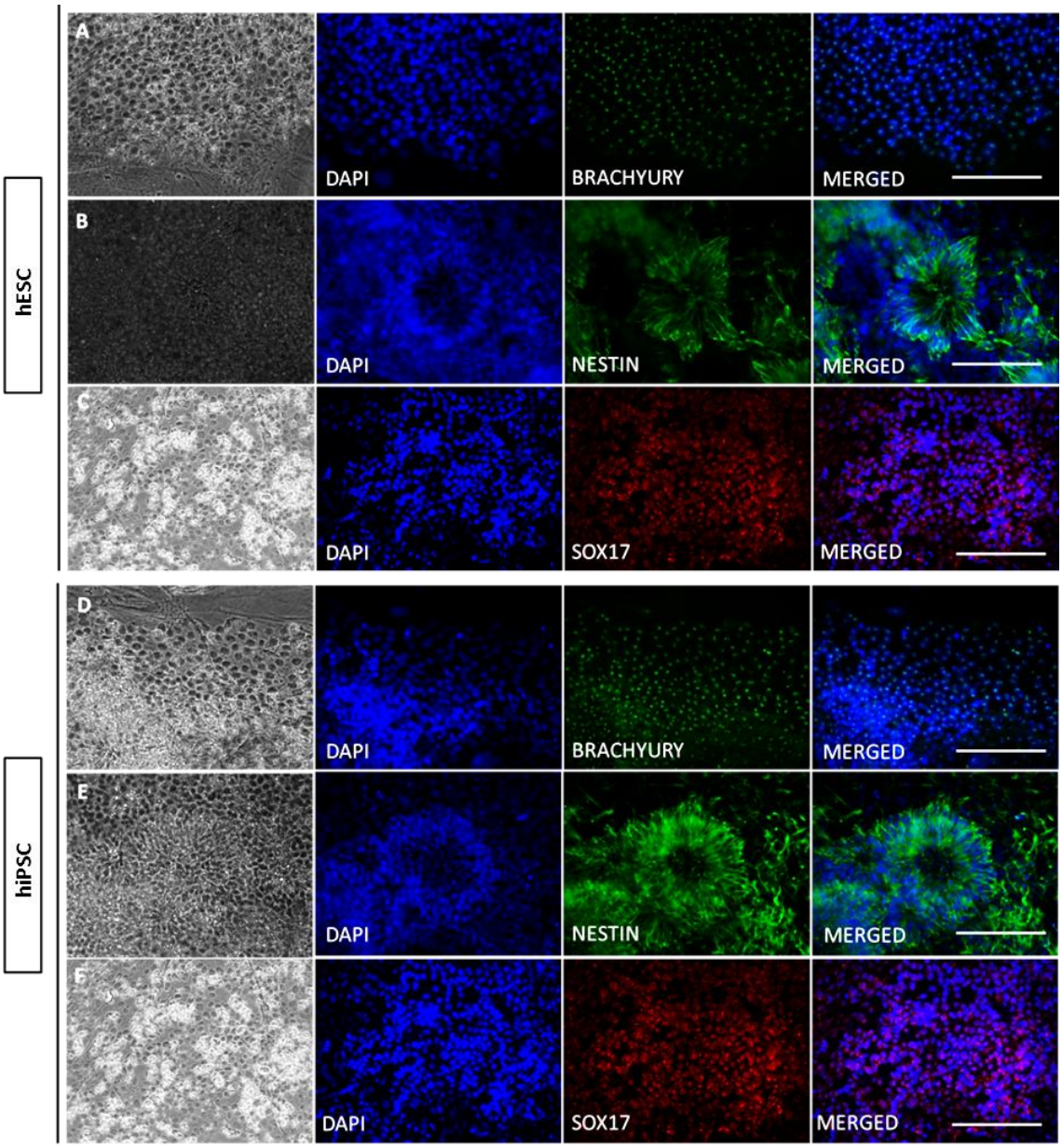


**Figure 25 - Immunocytochemistry staining of spontaneously differentiated hPSCs**
Representative images of immunofluorescent labelling of hPSC cultures for mesoderm, ectoderm and endoderm markers; Brachyury, Nestin and Sox17 in hESC **(A-C)** and hiPSC **(D-F)** (Scale bar = 400µm).

### 4.3.7 Neuronal differentiation of hPSC through co-culture with PA6 stromal cells

hPSC's ability to differentiate towards ($TH^+$) DA neuron specification was examined through co-culture with mouse PA6 stromal cells. After 4 weeks in co-culture, colonies were screened for evidence of DA neuron differentiation (i.e. the co-localisation of β-III-Tubulin and TH) (Figure 26, A & D). In addition, the general neural marker Nestin was assessed in hESC (Figure 26, B-C).

The cell colonies expressed all these specialised markers confirming their ability to differentiate along the neuronal lineage towards specialised $TH^+$ cell types.

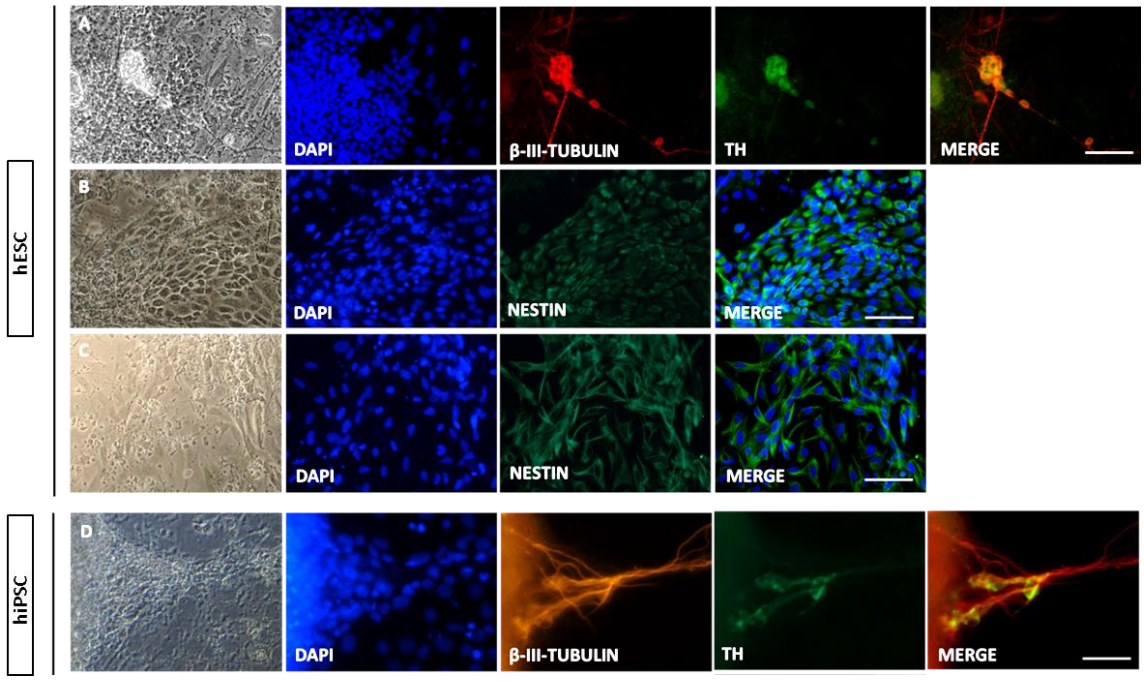


**Figure 26 - Immunocytochemistry staining of PA6 co-cultured hPSC**
**A) Representative immunocytochemistry images of β-III-Tubulin and TH co-staining and B-C) neuronal marker Nestin in hESC cultures. Immunocytochemistry images for and neuronal markers D) β-III-Tubulin, TH staining in hiPSC (Scale bars = 400µm).**

## 4.4 Differentiation of hPSC-derived dopaminergic neurons from hPSCs

Following the characterisation work we investigated the potential of hPSCs to generate DA neurons. hPSCs were cultured according to the protocol described in Chapter 2, section 2.3. Briefly, cells were expanded normally, co-cultured with iMEF to achieve sufficient pluripotent cell numbers. Cultures were then dissected and cultured in suspension (feeder-free) whilst being exposed to a number of different culture conditions as shown in Figure 2. Cell samples were harvested for each major stage in the protocol; D5, D9, D13, D23 and D30, allowing the influence of each stage of the protocol to be assessed. The method also allowed the analysis of extended culture past D24 (the typical termination point) which will be discussed later in this chapter.

### 4.4.1 Aggregate morphology during hPSC dopaminergic differentiation

Aggregate morphology of the cultures was assessed over the 24 days prior to stick down (Figure 27). We found that neurospheres from both hESC and hiPSC formed aggregates which

increased in diameter over time (Figure 27). Although the McIlwain tissue chopper was used to provide uniform aggregate formation variation was observed at D4 onwards (Figure 27).

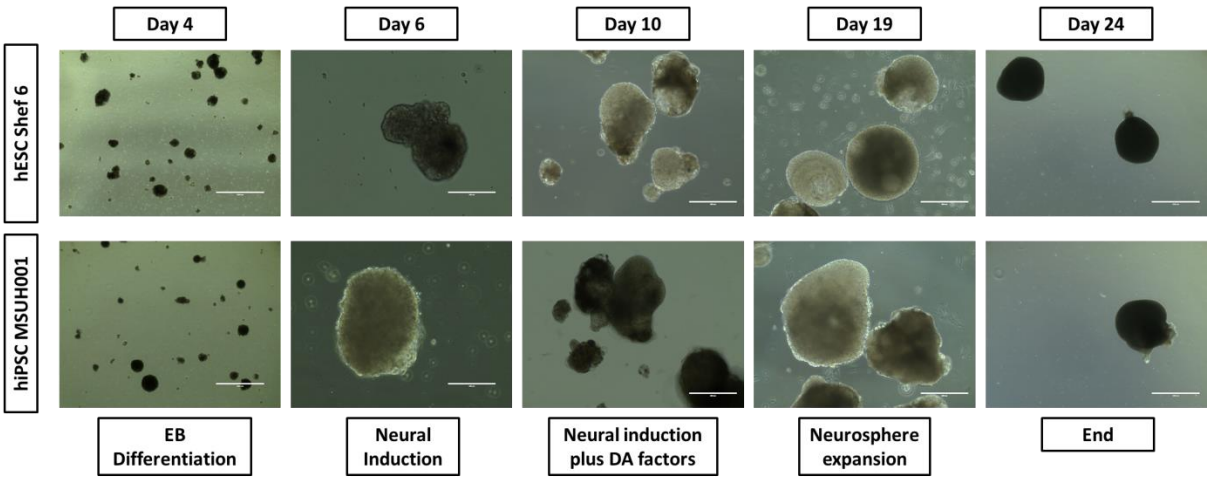


**Figure 27 - hPSC suspension culture dopaminergic differentiation**
Representative images showing the growth of hPSC derived neurospheres during the aggregate-based dopaminergic differentiation process (24 days) (Scale bars = (Day 4 & 24) 1000µm, (Day 10 & 19) 400 µm and (Day 6) 200µm).

### 4.4.2 Differentiation of hPSC-derived aggregates towards dopaminergic neurons: pluripotent gene expression

To assess the impact of the protocol on the pluripotency of hPSC, the relative expression of pluripotent genes *nanog*, *oct4* and *sox2* were measured. By D5 both *nanog* and *oct4* were observed to significantly drop in expression in both hESC (Figure 28, A & B) and hiPSC (Figure 28, D & E), except in the case of hiPSC, where *oct4* expression only significantly dropped following neural induction (D9) (Figure 28, E, $p \leq 0.01$). *Sox2* expression significantly increased in hESCs during neural induction (Figure 28, C) and was maintained until D23, where expression dropped. *Sox2* expression in hiPSC culture was observed to significantly decrease during EB expansion (Figure 28, F) and was never found to significantly exceed that of D0 levels.

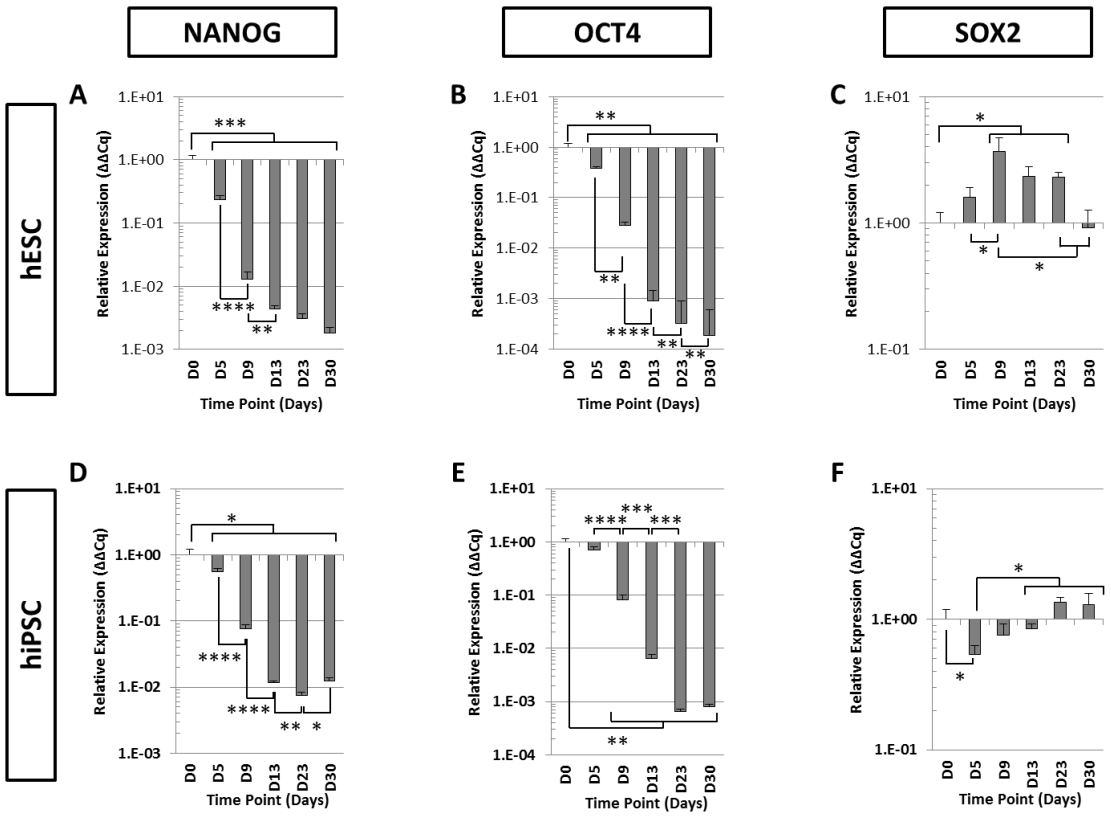


**Figure 28 - qPCR analysis of pluripotent gene expression during aggregate-base dopaminergic differentiation of hPSC**

qPCR analysis of pluripotent mRNA expression over the course of aggregate-base dopaminergic differentiation. hESC and hiPSC derived neurosphere expression of *nanog* **(A/D)**, *oct4* **(B/E)** and *sox2* **(C/F)** are shown relative to D0 expression. Data was normalised using *GAPDH* expression (* p< 0.05, ** p<0.01, ***p<0.001 and **** p<0.0001. Bars = Mean ± SEM. n=3).

### 4.4.3 Differentiation of hPSC-derived aggregates towards dopaminergic neurons: epiblast fgf5 gene expression

Analysis of *fgf5* expression over time showed expression in hESC cultures did not significantly change during the differentiation programme (Figure 29, A); however, hiPSC expression was found to drop during EB expansion (Figure 29, B) and thereafter significantly increase throughout the protocol. (Figure 29, B).

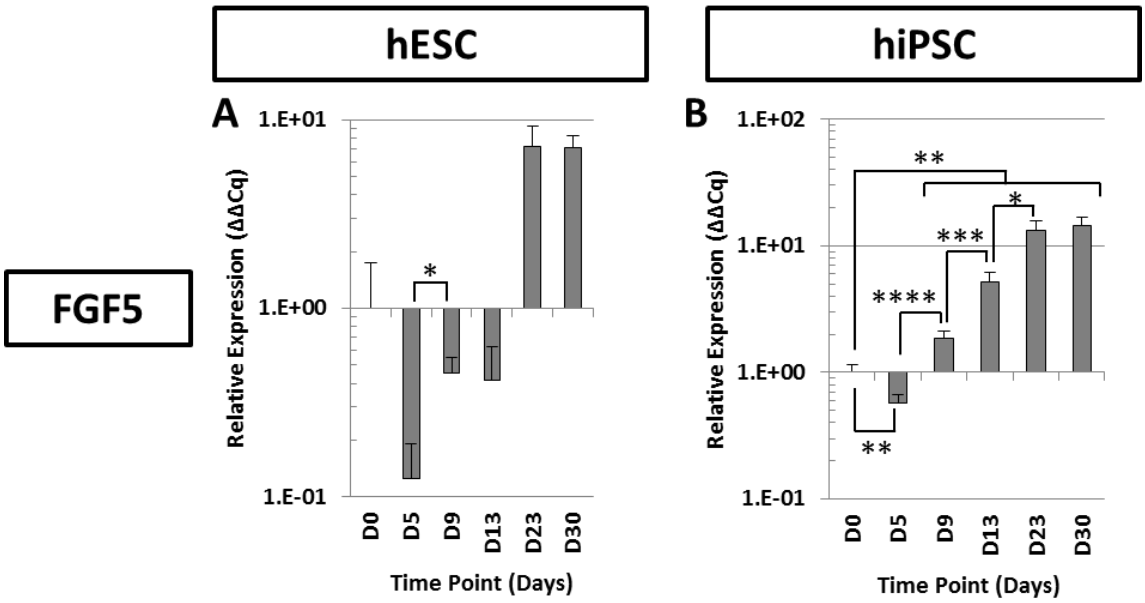


**Figure 29 - qPCR analysis of *fgf5* gene expression during aggregate-base dopaminergic differentiation of hPSC**

qPCR analysis of *fgf5* mRNA expression over the course of aggregate-base dopaminergic differentiation. hESC and hiPSC derived neurosphere expressions of *fgf5* (**A/B** respectively) are shown relative to D0 expression. Data was normalised using *GAPDH* expression (* p< 0.05, ** p<0.01, ***p<0.001 and **** p<0.0001. Bars = Mean ± SEM. n=3).

### 4.4.4 Differentiation of hPSC-derived aggregates towards dopaminergic neurons: germ layer gene expression

Analysis of germ layer genes indicated that *brachyury* (mesoderm) was down-regulated in hESC, yet underwent transient up-regulation in hiPSC (

Figure 30, A&D) during the protocol. *Sox17* (endoderm) was constantly down-regulated for both cell types (

Figure 30, B&E) whereas *sox1* (ectoderm) was up-regulated significantly over time (

Figure 30, C&F).

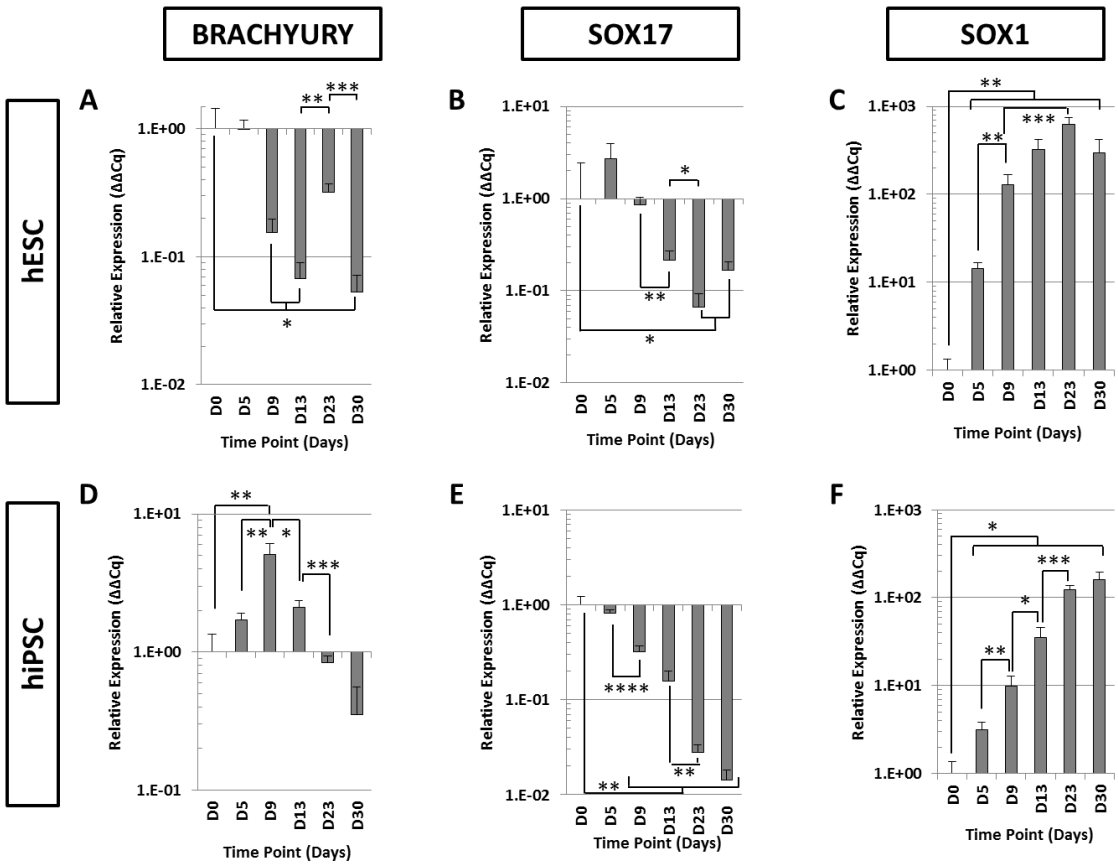


**Figure 30 - qPCR analysis of germ layer gene expression during aggregate-base dopaminergic differentiation of hPSC**

qPCR analysis of germ layer mRNA expression over the course of aggregate-base dopaminergic differentiation. hESC and hiPSC derived neurosphere expression of *brachyury* **(A/D)**, *sox17* **(B/E)** and *sox1* **(C/F)** are shown relative to D0 expression. Data was normalised using *GAPDH* expression (* p< 0.05, ** p<0.01, ***p<0.001 and **** p<0.0001. Bars = Mean ± SEM. n=3).

### 4.4.5 Differentiation of hPSC-derived aggregates towards dopaminergic neurons: neuronal gene expression

Analysis of neuronal genes revealed an up-regulation in all genes screened in hESC cultures (Figure 31, A-C). However *nurr1* expression (not statistically significant) was observed to fluctuate throughout culture; increasing throughout neuronal induction (D9), decreasing with addition of DA factors (D13) then increasing on neurosphere expansion (D23) (Figure 31, A). *Otx2* levels significantly increased during neural induction (D9), after which time, continued to decrease in expression (Figure 31, B). *En1* levels remained increased relative to D0 throughout the whole culture period (Figure 31, C) but fluctuated in alignment with *nurr1*. In hiPSCs, *nurr1* and *otx2* decreased during the culture period (Figure 31, D&E), whereas, expression of *en1* increased during EB expansion and remained increased for the duration of the culture (Figure

31, D). Due to the number of biological repeats no statistical significance could be ascertained for *nurr1* and *en1* qPCR results.

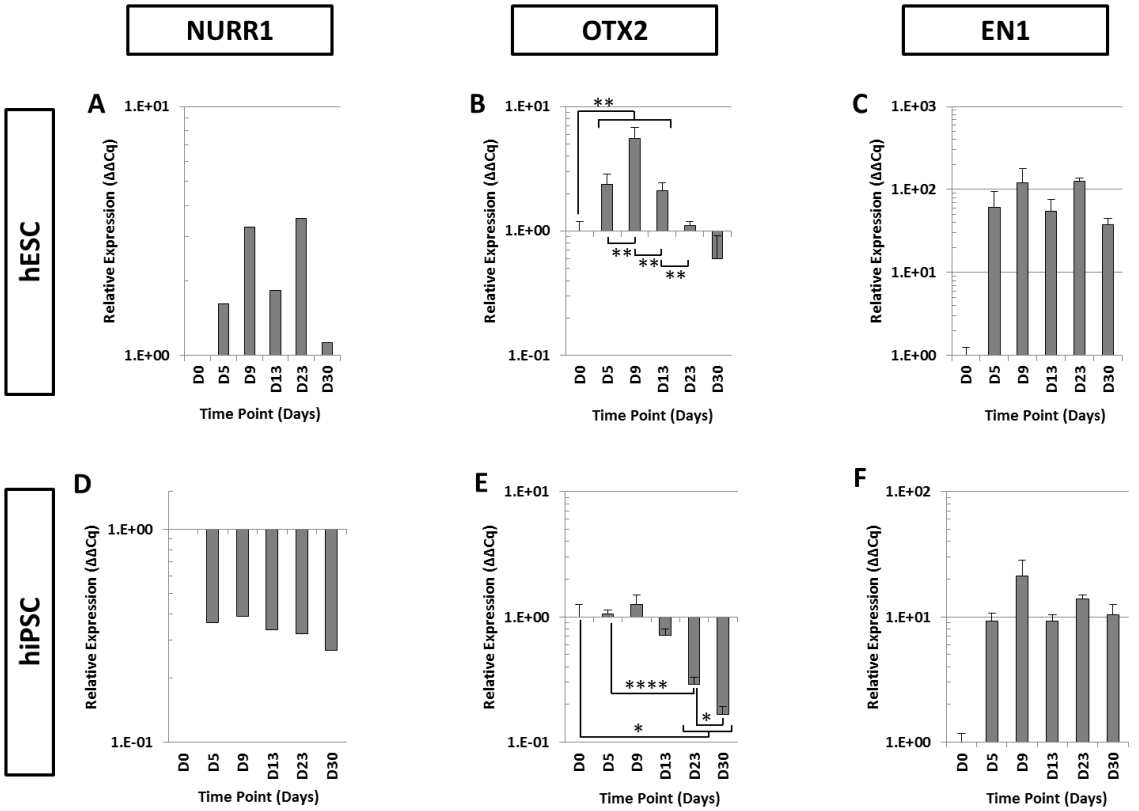


**Figure** 31 - qPCR analysis of neuronal gene **expression during aggregate-base dopaminergic differentiation of hPSC**

qPCR analysis of neuronal mRNA expression over the course of aggregate-base dopaminergic differentiation. hESC and hiPSC derived neurosphere expression of *nurr1* **(A/D,** n=1**)**, *otx2* **(B/E,** n=3**)** and *en1* **(C/F** n=2**)** are shown relative to D0 expression. Data was normalised using *GAPDH* expression (* p< 0.05, ** p<0.01, ***p<0.001 and **** p<0.0001. Bars = Mean ± SEM).

### 4.4.6 Differentiation of hPSC-derived aggregates towards dopaminergic neurons: dopaminergic neuron gene expression

Analysis of DA neuron genes showed that all genes generally increased in hESC cultures over time (Figure 32, A-D). *Lmx1a* expression declined following D13 (Figure 32, B) and *TH* and *DRD* had the greatest expression at later time points (Figure 32, C&D). *Foxa2* was the most delayed DA gene assessed with expression increasing only following neurosphere expansion (Figure 32, A, D23).

hiPSC generally mirrored this pattern, particularly with expression for both *TH* and *DRD* (Figure 32, G&H). *Foxa2* expression was found to decease during culture and was never up-regulated relative to D0 (Figure 32, E).

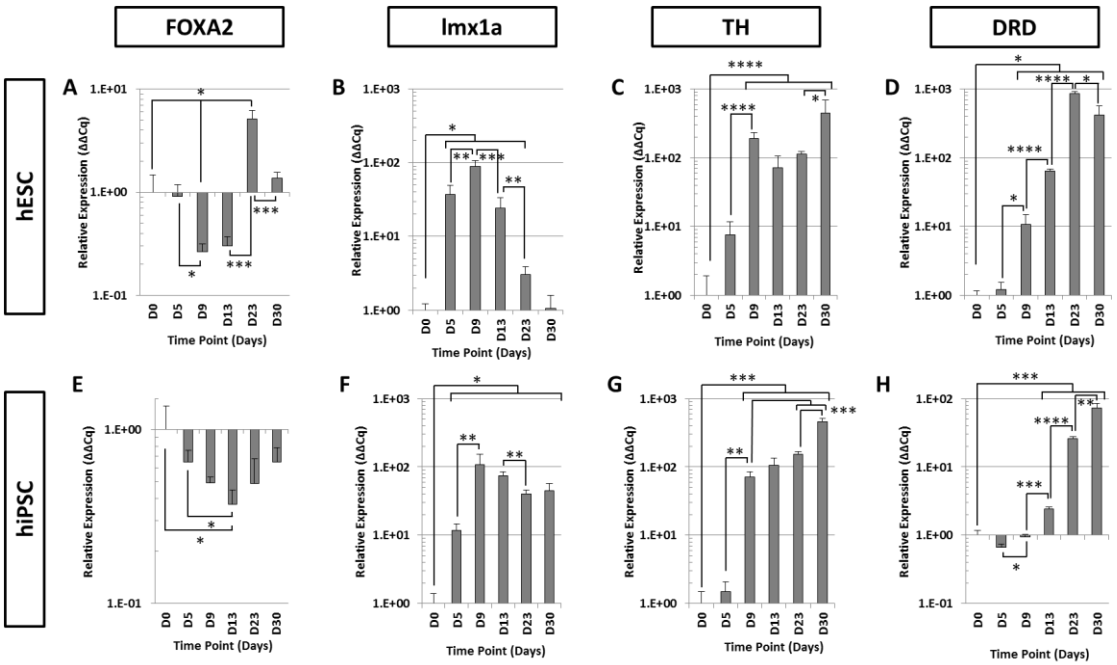


**Figure 32 -** qPCR analysis of dopaminergic gene **expression during aggregate-base dopaminergic differentiation of hPSC**

qPCR analysis of dopaminergic mRNA expression over the course of aggregate-base dopaminergic differentiation. hESC and hiPSC derived neurosphere expression of *foxa2* **(A/E)**, *lmx1a* **(B/F),** *TH* **(C/G)** and *DRD* **(D/H,** n=2**)** are shown relative to D0 expression. Data was normalised using *GAPDH* expression (* p< 0.05, ** p<0.01, ***p<0.001 and **** p<0.0001. Bars = Mean ± SEM. n=3).

### 4.4.7 Morphology assessment of adhering neurospheres upon 'stick down'

To assess the morphology of neurospheres during the 'stick down' maturation protocol, bright field images were taken over 14 days. Neurospheres from both hESC and hiPSC cultures were observed to adhere to the laminin surface substrate and by D7 projections extend away from the main body of the neurosphere resulting in extensive projections by D14, as shown in Figure 33.

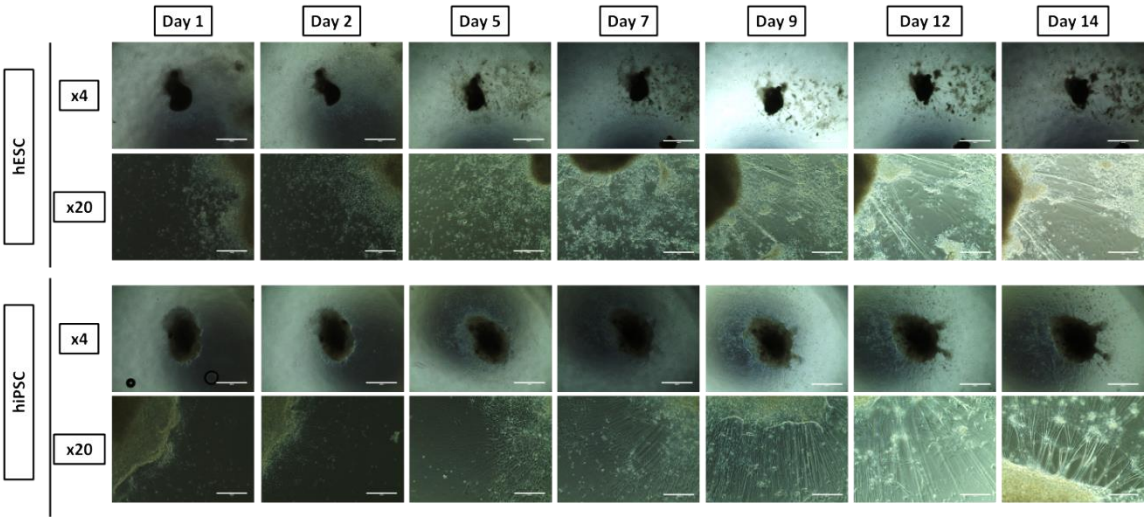


**Figure 33 - Stages of 14 day stick down protocol**

Representative bright field images of hPSC derived neurospheres during the 'stick down' process (14 days), whilst being patterned through the addition of dopaminergic differentiation media (Scale bars = (x4) 1000µm and (x20) 200µm).

### 4.4.8 Confocal imaging of 14 day differentiated neurospheres following 'stick down'

Cultured neurospheres were plated onto laminin coated coverslips on D24 of neurosphere expansion and cultured in DDM for 14 days. Colonies were then fixed using 4% PFA and immunofluorescent labelling performed to assess neuronal differentiation and the efficiency in producing DA neurons ($TH^+$/$foxa2^+$).

First differentiation of hPSC towards a neuronal lineage was confirmed using Nestin immunofluorescent labelling. Both hESC and hiPSC were confirmed as $Nestin^+$ (Figure 34). Cell projections were seen projecting from the main neurosphere body, connecting different bodies of cells.

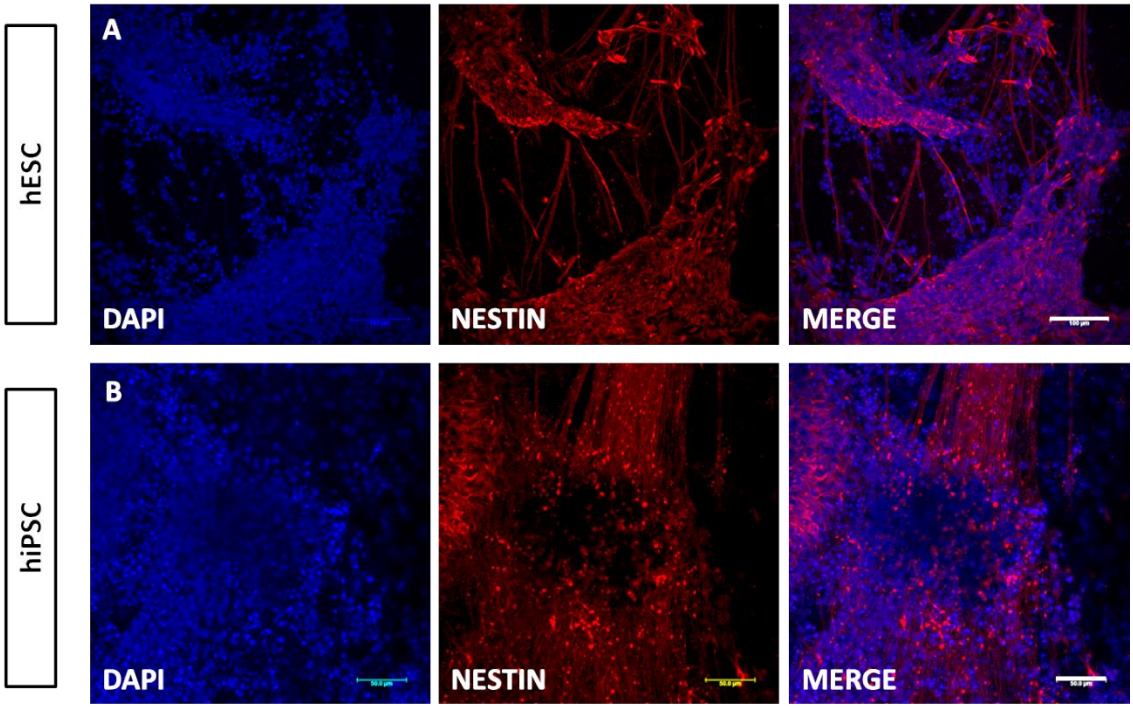


**Figure 34 - Confocal images of Nestin stained differentiated neurospheres**
Representative confocal images of neural marker, Nestin, in 14 day differentiated neurospheres for **(A)** hESC (Scale bar = 100µm) and **(B)** hiPSC (Scale bar = 50µm).

To ascertain whether DA neurons had been produced during the protocol, adhered neurosphere cultures were assessed for TH (green) and Foxa2 (red) markers. hESC cultures could be shown to contain $TH^+$ cells and $Foxa2^+$ cells. TH was found in the cytoplasm of the cells whilst Foxa2 was co-localised with dapi to the nuclei (Figure 35, A-E). The majority of cells were found to be $TH^-/Foxa2^-$ but pockets of cells were $Foxa2^+$ (Figure 35, D). Association of Foxa2 and TH within a single cell was very limited. hiPSCs appeared to have a slightly higher level of co-labelled cells (Figure 35, H) though more commonly cells were defined as either $TH^+$ or $Foxa2^+$ (Figure 35, F & G).

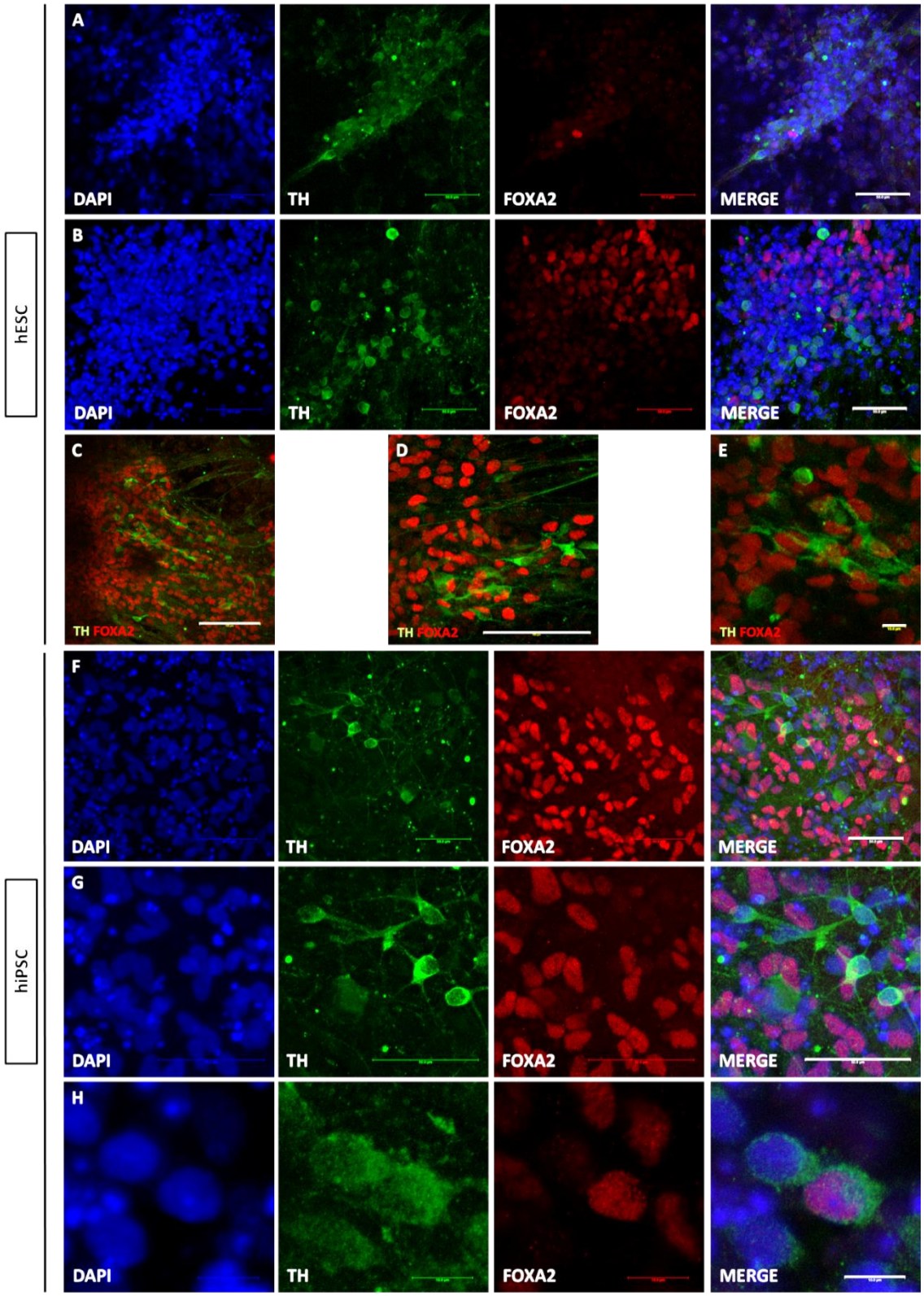


**Figure 35 - Confocal images of TH and foxa2 stained differentiated neurospheres**

Representative confocal images of hESC **(A-E)** and hiPSC **(F-H)** adhered neurosphere cultures. Differentiated neurospheres were staining for Foxa2 (red), TH (green) and dapi (blue). Scale bars = 50nm (A-B & F-G), 100nm (C-D) and 10nm (E & H).

### 4.5 Dopamine release from hPSC-derived differentiated neurospheres

To verify whether the differentiated hPSC-derived neurospheres were functional and contained cells that were able to synthesise dopamine, two neurospheres were plated onto laminin coated coverslips at D24 and differentiated for 4 weeks in DDM. Neurospheres were then stimulated using potassium chloride (KCl) and the media collected and stored at -80$^{o}$C until processing.

ELISA analysis revealed that basal level dopamine was ~7.8ng/mL in hESC, increasing to ~18.6ng/mL on stimulation with KCl (Figure 36, A). Basal dopamine levels from hiPSC were shown to be ~5.8ng/mL, increasing to ~12.9ng/mL on stimulation (Figure 36, B).

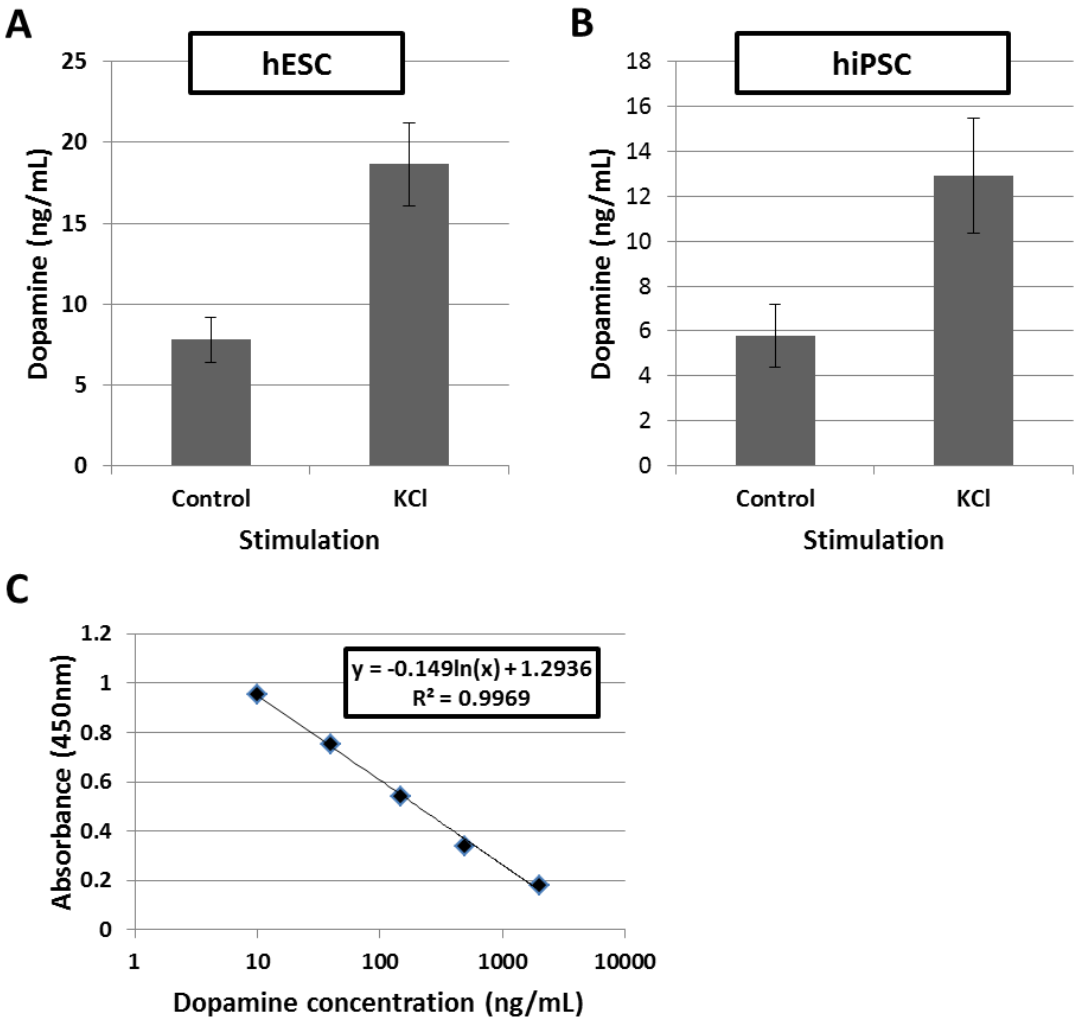


**Figure 36 - Dopamine release from 4-week matured neurospheres**
Dopamine release from two hPSC-derived 4-week matured neurospheres, showing dopamine release from both un-stimulated (control) or stimulated with the addition of 56mM KCl. Detection was performed using ELISA for hESC **(A)** and hiPSC **(B)**. **C)** A standard curve was generated from using standards provided in the ELISA kit, $R^2$ = 0.9969.

### 4.5.1 Effect of extended neurosphere culture on resulting dopaminergic gene expression

Neurospheres were cultured for an extended period before 'stick down' to assess its effect on DA gene expression. Gene expression was assessed at D0 and D14 of adherent culture relative to experimental D0 levels. Expression of *foxa2* by hESC was observed to drop to negative levels when seeded at times after D24 (Figure 37, A). The ability to express *foxa2* gradually decreased following extended periods of culture and by D55 no recovery of *foxa2* expression was observed following culture in DDM. hESC expression of *lmx1a* and *TH* was observed to increase in expression following stick down at all seeding time points (Figure 37, B&C). Both genes were seen to consistently increase to D14 following culture in DDM except at D55 where *lmx1a* showed reduced expression.

Expression of *foxa2* in hiPSC was shown to be lower than the experimental control (D0 pluripotent cells) for all stick down time points except D55 which showed enhanced expression (Figure 37, D). *Lmx1a* and *TH* expression as with hESC were shown to increase following stick down, though hiPSC expression of *lmx1a* did not consistently increase following 14 days in DDM (Figure 37, E). *TH* was shown to mirror the pattern on hESC with enhance expression following 14 days in culture (Figure 37, F).

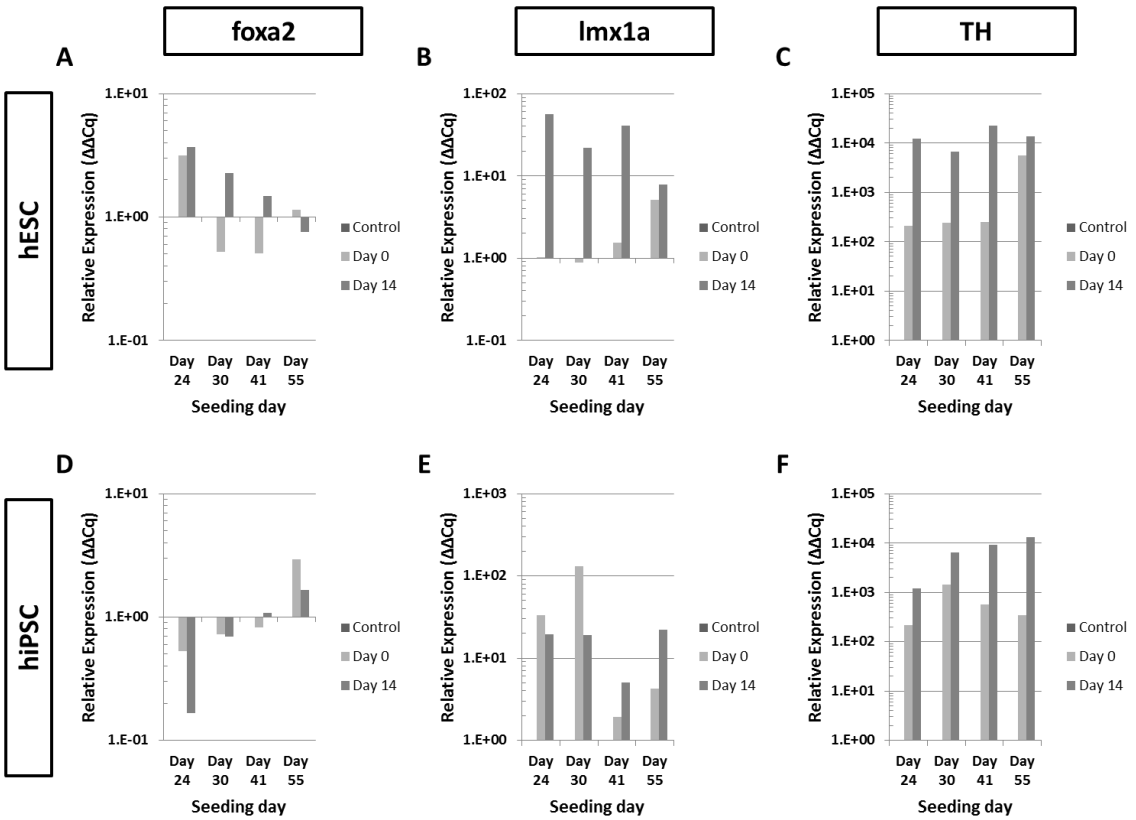


**Figure 37 - qPCR analysis of dopaminergic gene expression following 'stick down' at different time points**

qPCR analysis of dopaminergic mRNA expression following extended suspension culture (24days, 30days, 41days and 55days) then followed by 14 days of stick down and culture in DDM. hESC and hiPSC derived neurosphere expression of *foxa2* **(A/D)**, lmx1a **(B/E),** and *TH* **(C/F)** are shown relative to control (experimental D0) expression. Data was normalised using *GAPDH* expression (n=1).

### 4.5.2 The effect of extended 'stick down' culture on dopaminergic gene expression

To assess the effect of extended culture in DDM on DA gene expression, neurospheres were adhered for a prolonged period of time (up to 28 days). In hESC, the expression of all the genes increased relative to the control up to D14, but then tailed off to D28 (Figure 38, A). Expression of target genes in hiPSC followed a similar path to hESC, with all genes showing increased expression relative to control, but reducing following stick down (D0). Again, an exception was with expression of *TH* which increased consistently to D28 whilst in culture with DDM (Figure 38, B).

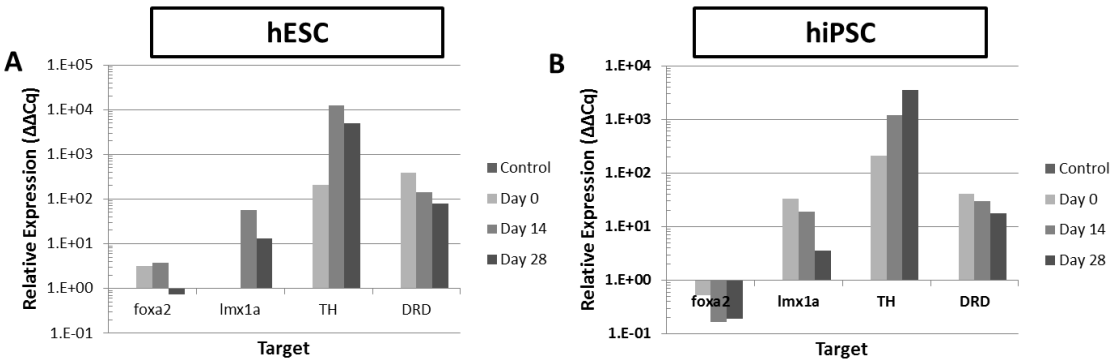


**Figure 38 -** qPCR analysis of dopaminergic gene expression during extended stick down

qPCR analysis of dopaminergic mRNA expression during extended stick down culture (up to 28 days) in DDM. hESC **(A)** and hiPSC **(B)** derived neurosphere expression of *foxa2*, lmx1a**,** and *TH* are shown relative control (experimental D0) expression. Data was normalised using *GAPDH* expression.

## 4.6 Discussion

### 4.6.1 Pluripotent hPSC culture and expansion

It is essential in the development of new and innovative cell therapies based on the use of stem cells that we are able to confirm the identity of the pluripotent base population. This work showed that we are able to co-culture hPSCs with iMEFs to maintain an $Oct4^{+}$/$TRA\text{-}1\text{-}60^{+}$ cell population in both hESC and hiPSC (Figure 22). We were also able to confirm that as cells migrated out of the colony they became $SSEA1^{+}$ and showed reduced levels of Oct4 expression, indicating a loss of pluripotency. To quantify these findings, TRA-1-60 and SSEA4, both surface markers, were used for live cell flow cytometry. Results confirmed that cultures were maintained so that the majority of cells (≥90%) were positive for the pluripotent markers investigated (Figure 23).

Finally, pluripotency was confirmed at the molecular level. Gene expression analysis showed that both hESC and hiPSC cultures were positive for pluripotent markers; *nanog* (Chambers, Colby et al. 2003, Mitsui, Tokuzawa et al. 2003)*, oct4 and sox2* (Masui, Nakatake et al. 2007) (Figure 24), all considered to be essential for pluripotent maintenance and used regularly within research literature to confirm population pluripotency.

Although it is widely considered that pluripotency can only be confirmed using *in-vivo* teratoma assays to determine products of all three germ layers (Wesselschmidt 2011), in this study we assessed the ability to produce cell types of all three germ layer; ectoderm, mesoderm and endoderm lineages following spontaneous differentiation for 27 days (Figure 25) and showed that both hESC and hiPSC were able to form $Nestin^{+}$ neural rosettes indicative of ectoderm. Rosettes were shown to be present in high density 3D structures within the colonies under staining. Brachyury was also abundantly present indicating mesoderm was present at the edges of the colonies in a monolayer tiled formation. Staining was found to be located to the nuclei, characteristic of Brachyury staining. Sox17 was also present at high levels in the cultures and like brachyury, localised to the edges of colonies as very distinctive

spherical cells. This work confirmed that the hPSCs being utilised were pluripotent and able to form all three germ layers (Figure 25).

Directed differentiation of hPSC was also performed by co-culturing hPSC with iPA6 mouse stromal cells. iPA6 cells were used instead of iMEF because they have been shown to generate $TH^+$ cells from hESC (Zeng, Cai et al. 2004). We used this method to confirm that the hPSC used within this investigation were capable of differentiating to a neuronal lineage and further towards a $TH^+$ cell specification. Results confirmed that hPSCs were capable of differentiating toward a neuronal cell type ($Nestin^+$) and acquired a β-III-$Tubulin^+$ and $TH^+$ phenotype (Figure 26). These results indicate that hPSC had differentiated into $TH^+$ neurons and they imply that the cells are capable of differentiating towards specialised DA neurons.

### 4.6.2 Differentiation of dopaminergic neurons from hPSC

The investigation attempted to differentiate hPSC towards a DA phenotype using an aggregate-based protocol adjusted with growth factors and media modification to mimic the endogenous signalling that DA neurons are exposed to during development. This method was chosen due to the potential for scale-up, by incorporating bioreactors within the process. We showed that it was possible to form cell aggregates following colony segmentation using the McIlwain tissue copper and culture these aggregates in suspension over a 24 day period (Figure 27). Aggregates were shown to increase in diameter over time, reaching up to 1mm by D24. In spite of the even spacing (150µm) of the cutting blade incisions, the resulting aggregate diameters were heterogeneous, illustrating a key process variable that would benefit from better control. If this protocol was to be used for longer than the 24 days of this investigation, aggregates should be passaged using the McIlwain tissue chopper to reduce the size within the population, though this is an open process and risks infection. The size of the aggregate is important as it has a significant impact on oxygen transfer and growth factor diffusion to the centre of the aggregate (Van Winkle, Gates et al. 2012). The effect of the size of aggregates on culture differentiation efficiency was not investigated within this body of

work but will be discussed in the final discussion of the thesis for its potential within future work.

### 4.6.3 qPCR analysis of target genes during dopaminergic differentiation

Molecular analysis of harvested cultures showed that pluripotency genes *nanog* and *oct4* significantly decreased in hESC and hiPSC cultures following EB formation and expansion (Figure 28). This signified that the cultures were moving away from a pluripotent state and differentiating. *Sox2*, also a marker of pluripotency because of its role in regulating *oct4* (Masui, Nakatake et al. 2007), rather than decreasing, significantly increased in hESC following neural induction (Figure 28). This may be due to the role of *sox2* in maintaining the neural progenitor state (with its further loss associated with neuronal differentiation) (Graham, Khudyakov et al. 2003), however, hiPSC results did not mirror this pattern. In hiPSC, *sox2* expression dropped significantly during EB expansion and then gradually increased, although never significantly exceeding levels of D0 pluripotent cells. This increase in *sox2* expression might reflect neural progenitors in culture.

The assessment of *fgf5* expression also supported the theory that neuronal precursors were present within the experimental populations. *Fgf5* is associated with early stages of lineage commitment (Lowell, Benchoua et al. 2006) and is also reported to be a neural precursor marker, found in primitive ectoderm (Hitoshi, Seaberg et al. 2004). Similar results were seen for both hESC and hiPSC with initial *fgf5* expression being reduced but then increasing significantly compared to D0 levels over the culture period (Figure 29). For both hPSC types, the initial drop may indicate lineage commitment of pluripotent cells and the following up-regulation suggest neural precursors in the population. The increase in *sox1* expression following EB expansion (Figure 30) further corroborates the generation of neural precursors, as *sox1,* like *sox2* and *fgf5* is an early neuronal marker (Brafman 2014).

Following EB expansion, expression of *brachyury* and *sox17* fell in the hESC cultures confirming that the protocol directs ectoderm specification and inhibits mesoderm and endoderm.

However in hiPSC, *brachyury* expression increased following EB expansion, suggesting that contaminating mesoderm cells were present in culture. Expression of s*ox17* in hiPSCs decreased following EB expansion suggesting that endoderm lineage cells were not present in culture (Figure 30).

The expression of *nurr1, otx2* and *en1,* key neuronal patterning genes important to DA neuron specification were also investigated. *Nurr1* plays a key role in the maintenance of the DA phenotype (Sacchetti, Carpentier et al. 2006); *otx2* is considered the 'master' anterior-posterior patterning module gene (Omodei, Acampora et al. 2008) confirming that the protocol mimics conditions found at the midbrain-hindbrain boundary; and *en1* is associated with proliferation and survival of the ventral midbrain neurons and is also midbrain marker (Gale and Li 2008).

Results from hESC analysis indicated that expressions of all three genes were increased over time. *Nurr1* appeared to be transiently expressed with expression peaking during neural induction (D9) and neurosphere expansion (D23) (Figure 31). *Otx2* expression increased then dropped away to D24 (Figure 31) suggesting that the cells produced were not of the appropriate phenotype. Initial enhancement in expression does suggest the protocol was directing them correctly but following neural induction the marker was lost; inclusion of DA factors appeared to change the course of expression. Expression of *en1* was shown to increase significantly throughout the duration of the experiment for both cell types (Figure 31) suggesting a midbrain phenotype was achieved. It is difficult to draw a solid conclusion from this data, though it is appears that this protocol is driving the cells down a midbrain lineage, results suggest that it is not generating the desired A9 DA neurons. Further optimisation of the patterning procedure is required.

A number of key identifiers have been recognised for the characterisation of therapeutically valuable DA neurons and have been assessed within this work, these include: *foxa2 lmx1a* and *TH*. *Foxa2* has been found to be important in the differentiation of DA neurons and associated

with a loss of proliferative neuronal precursors (Lee, Bae et al. 2010), it also works synergistically with *nurr1* in the development of the DA phenotype. *Lmx1a* is an early regulator of midbrain dopamine neural progenitor phenotype specification and has been shown in mouse embryonic development to regulate maturation of DA neurons (Chung, Kim et al. 2012). Finally, *TH* is a key rate limiting enzyme in the synthesis of dopamine and so an essential marker for any viable DA neuron. Also assessed was dopamine receptor D1 (*DRD)* gene expression; the most abundant dopamine receptor in the central nervous system and found to regulated neuronal growth and development (O'Keeffe, Barker et al. 2009).

Results from hESC analysis showed that DA genes (*foxa2 lmx1a* and *TH*) were significantly up-regulated by D23 of the protocol (Figure 32). *Lmx1a* was observed to significantly rise during EB expansion and peak during neural induction. *DRD* was observed to increase significantly during neural induction, with inclusion of DA factors enhancing this further to D23. This may corroborate *lmx1a's* involvement in early regulation of DA development and the expression of DRD following neural induction. The increase in *DRD* was mirrored by that of *TH*, which increased significantly following neural induction and was maintained throughout the experiment. *Foxa2* was transiently expressed, initially dropping during neural induction only to significantly increase to D23. This is in line with our collaborators findings (unpublished), that *foxa2* expression requires longer culture to be induced. hiPSC's expression of *lmx1a* appeared more stable than in hESC cultures, expression was observed to increase significantly during EB expansion, rising to D9 levels and remaining at significantly high levels for the remainder of the protocol. *TH* mirrored this, increasing following neural induction and remaining stable until the end of the protocol. *DRD* levels were significantly up-regulated following DA factor additions although this was delayed compared to hESCs. Contrary to these other positive results *foxa2* levels decreased throughout the protocol, this indicated that although a number of appropriate makers were switched on during directed differentiation of hiPSC, the protocol requires significant optimisation to correctly specify DA neurons from MSUH001 cells. Timing of delivery of certain factors may need to be altered for this particular cell line.

Confocal imaging confirmed Nestin$^{+}$ cells were generated (Figure 34) indicating that neurospheres were correctly directed towards a neuronal lineage. Neurospheres were also assessed for TH and Foxa2 expression and although both markers were shown to be expressed by different individual cells, co-expression was rare. It was interesting to see the level of co-localisation in hiPSC as qPCR data had suggested a lack of gene expression for *foxa2*. Even though gene expression is important for protein synthesis, ultimately it is protein expression and localisation that enables function.

Extending culture of the neurospheres past D24 resulted in a varying ability of neurospheres to adhere and produce transcripts for *foxa2/lmx1a/TH* (Figure 37). All stick down days up to D41 resulted in high expression of *foxa2/lmx1a/TH* relative to D0. Both *lmx1a* and *TH* expression increased following stick down (Figure 37) suggesting prolonged culture of hESC is possible. Due to time constraints the experiment was only performed once and so solid conclusions cannot be drawn. This would be an interesting extension to this work if long-term culture within bioreactors were to become an option.

### 4.6.4 Gene expression and dopamine release from differentiated neurospheres

Gene expression analysis of the extended stick down neurospheres for the purpose of ELISA showed that hESC and hiPSC expression of key genes, *lmx1a, foxa2* and *DRD* all decreased to D28 of extended culture. This suggests that this time point may be too late for ELISA analysis as neuronal function may have been compromised.

Though gene expression analysis suggested a reduction in DA markers, ELISA analysis at D28 revealed that cells in both hESC and hiPSC cultures responded to stimulation and released dopamine. Resulting in background levels of 7.8ng/mL and 5.8ng/mL respectively, increasing to 18.6ng/mL and 12.9ng/mL (Figure 36) after stimulation. This result combined with the molecular and protein analysis suggests that dopamine releasing neurons were generated under this protocol.

## 4.7 Conclusion

The work in this chapter shows it is possible to direct neuronal specification in hPSC types using a feeder layer and subsequent aggregate-based differentiation procedure. This might enable scalable production using 3D bioreactor based method in the future.

The experiments also show that it is possible to produce neuronal phenotypes with characteristics of DA neurons. Although we did not conclusively produce a valid DA neuronal product that could be tested *in-vivo*, we did show we were able to generate cell types that express the genes of interest, enabling the incorporation of saRNA.

Systematic optimisation of the long, complex culture method and assessment of other pluripotent cell lines would inevitably improve the production of DA neurons and future work could follow these avenues.

# CHAPTER 5 - OPTIMISATION OF SMALL ACTIVATING RNA USING CANCER CELL LINES AND OMNCIYTES

## 5.1 Introduction

Though our ability to generate specific cells types including DA neurons *in-vitro* has become a widely used research methodology, the ability to generate large and consistent yields of target cell types remains elusive, hindering the movement of this technology toward a therapeutically beneficial product. Groups have reported variable efficiencies of generating $TH^+/Tuj^+$ cells ($TH^+$ neuronal cells) of between 3 - 30% from hPSC, using media conditioning and smad inhibition (Yan, Yang et al. 2005, Stanslowsky, Haase et al. 2014). To address the issue of yield and consistency, researchers are investigating a number of methods, including bioreactor culture (Van Winkle, Gates et al. 2012) and genetic modification (Park, Lim et al. 2012). Within this chapter we will investigate the potential of saRNA for enhancing target gene expression and identify the optimal saRNA candidate for use in collaboration with the aggregate-based DA differentiation protocol investigated in Chapter 4.

Since the publication of the human genome (Lander, Linton et al. 2001) and the development of RNA interference (RNAi)(Agrawal, Dasaradhi et al. 2003), our ability to understand and manipulate gene and protein expression has greatly increased. It was previously thought that there were few mechanisms of gene regulation, for example chromatin remodelling and DNA methylation (Geiman and Robertson 2002). However it is now recognised that a new powerful class of regulators in the form of small RNA elements exists. What were once thought to be non-coding 'junk' RNA sequences have now been demonstrated to play key roles in the regulation of gene expression through the repression of transcription or translation.

Recently there has been the discovery of a new regulatory element, saRNA. saRNA are able to modify gene expression at the transcription stage, targeting activation sites and amplifying the expression of specific genes. These molecules allow the directed up-regulation of specific

target genes within cell populations without the use of plasmids and viral transfection (Reebye, Saetrom et al. 2013, Reebye, Saetrom et al. 2013). This approach is preferable to the DNA- and viral-based approaches as synthetic mRNA modifications are thought not to impact on the genetic integrity of the cell genome (Steichen, Luce et al. 2014).

saRNAs were identified and developed as part of this investigation to specifically target genes with an expression associated with DA neuronal specification. Within this work we focused on three genes; forkhead box protein A2 (*foxa2*), Homeoprotein LIM homeobox transcription factor 1α (*lmx1a*) and tyrosine hydroxylase (*TH*) (Caiazzo, Dell'anno et al. 2011, Pfisterer, Kirkeby et al. 2011).

*Lmx1a* has been shown to promote neuronal midbrain DA neuron differentiation by repressing other neuronal differentiation pathways (Cai, Donaldson et al. 2009), for example down-regulating the floor plate marker *Nkx6* which is involved in ventral neural patterning (Sander, Paydar et al. 2000, Cai, Donaldson et al. 2009, Kriks, Shim et al. 2011). Forkhead/winged helix transcription factor, *foxa2,* has been shown to be influential in the specification of DA neurons (Ferri, Lin et al. 2007, Lin, Metzakopian et al. 2009) and the determination of mesencephalon floor plate cell fate in cooperation of *lmx1a/b* (Akashi, Traver et al. 2000). Lastly, *TH* is essential in the normal functioning of the nervous system and is a rate limiting component of the pathway that produces an important group of hormones called catecholamines (Figure 39) and is involved in the synthesis of dopamine, essential in a functional DA neuron.

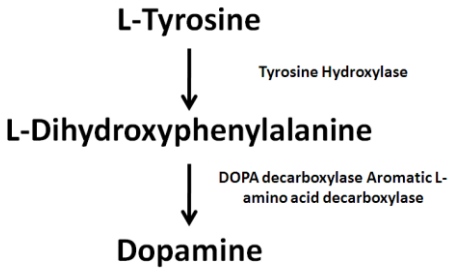


**Figure 39 - Dopamine synthesis pathway**
L-Tyrosine is converted into L-Dihydroxyphenlalanine by an enzymatic reaction involving Tyrosine Hydroxylase. DOPA decarboxylase Aromatic L-amino acid decarboxylase then converts L-Dihydroxyphenlalanine into the functional neurotransmitter dopamine which is the essential for the normal functioning of the nervous system.

## 5.2 Aim

This chapter investigates the use of saRNAs and their efficiency in up-regulating three target genes; *foxa2*, *lmx1a* and *TH*. The initial assessment was done through the use of epigenetically positive cell lines to illuminate the best variant saRNA. It then investigates the potential to transfer these findings into omnicytes, a cell type considered to have great potential within the cell therapy environment.

## 5.4 Results

### 5.4.1 Cell line culture and lipid-based transfection reagents optimisation

The ability of candidate saRNA to modify target gene expression were first assessed using cell lines SH-SY5Y (Figure 40), HepG2 (Figure 42) and Jurkat (Figure 44). Due to their anticipated endogenous expression of the target genes *TH, foxa2* and *lmx1a* respectively, it was thought that the cells would be amenable to gene manipulation and not be hindered by any epigenetic fingerprint.

To allow analysis of the impact of the saRNAs, PCR primers (forward and reverse) were designed in-house or taken from peer reviewed papers and optimal PCR cycling conditions established by cycle optimisation of the annealing temperature ($T_a$). *TH* and *foxa2* PCR cycling conditions were optimised against SH-SY5Y (Figure 40, C/D) and HepG2 synthesised cDNA from total extracted RNA (Figure 42, C/D). *Lmx1a* primers were optimised against foetal temporal lobe (Figure 44, B/D).

To optimise the impact of the saRNA transfections, SH-SY5Y seeding density and growth rate were initially assessed. WST-1 analysis revealed that $2.5x10^4$ cells/well (microplate) resulted in optimal growth over 72hrs and provided the maximum number of cells for lipid-oligonucleotide endocytosis. Higher seeding at $5x10^4$cells/well resulted in growth inhibition by 50hrs and viable cell reduction to 72hrs (Figure 40, B). Visual analysis showed that $2.5x10^4$ resulted in good surface coverage and allowed continuous proliferation over the culture period.

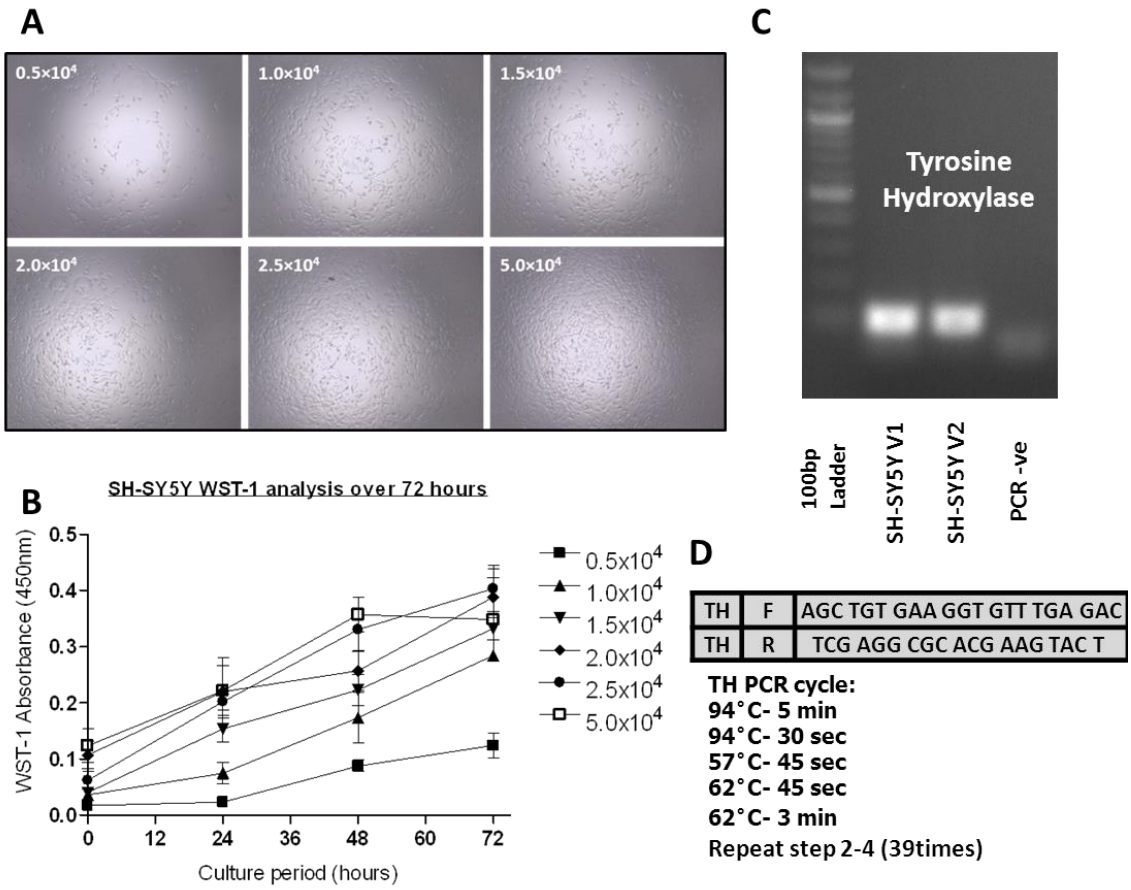


**Figure 40 - SH-SY5Y seeding density and TH PCR optimisation**

**A)** Representative images showing SH-SY5Y at varying seeding densities at 24hrs (x4 magnification). **B)** WST-1 analysis of SH-SY5Y at different seeding densities over a 72hr culture period (n=2). **C)** Optimisation of Tyrosine hydroxylase PCR primers against SH-SY5Y total RNA, with primer dimers observed in the -ve control **(D)** Table showing primer sequences for TH PCR primers and optimal thermo cycling conditions

It was thought that the individual cell types may exhibit different behaviours in each lipid transfection reagents and for this reason we investigated the use of three reagents for each cell line. To allow us to visualise and assess the efficiency of each transfection reagent we used a green fluorescent protein (GFP) labelled plasmid provided by Omnicyte Ltd., pSG5-GFP. The non-fluorescent, GFP -ve plasmid, øpSG5, was used as the negative control. Efficiency of the transfection of SH-SY5Y was assessed using flow cytometry, the difference between pSG5-GFP (+ve) and øPSG5 (-ve) represented transfection efficiency (Figure 41, A). Data indicated that ICAfectin was the most efficient at transfecting the pSG5-GFP plasmid into SH-SY5Y cells (Figure 41, B) with 28.0% (σ ±0.23) of cells showing positively for GFP. Confocal analysis showed that the neuroblastoma cell line was capable of producing GFP (Figure 41, C).

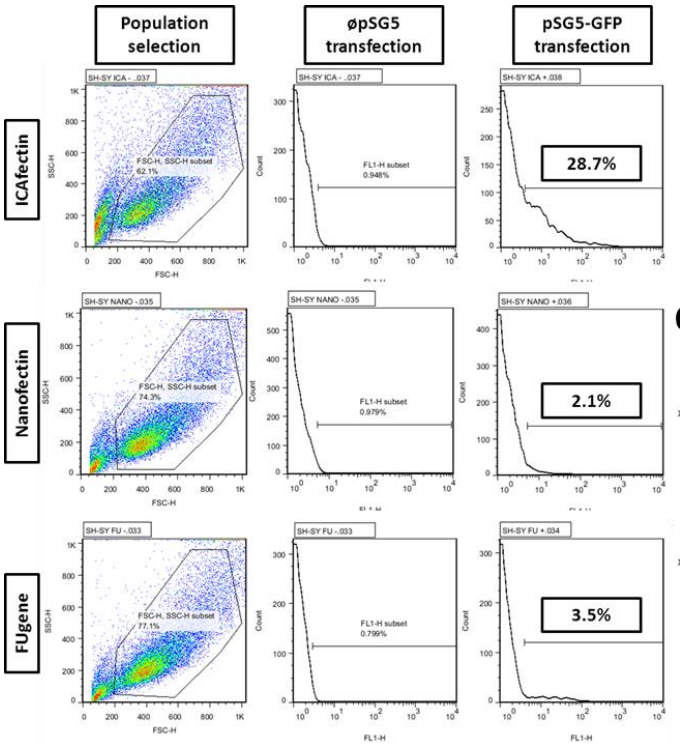


| Transfection reagent | Average Efficiency |
|---|---|
| ICAfectin | 28.7% (±0.23) |
| Nanofectamin | 2.1% (±0.17) |
| FUgene | 3.5% (±0.75) |

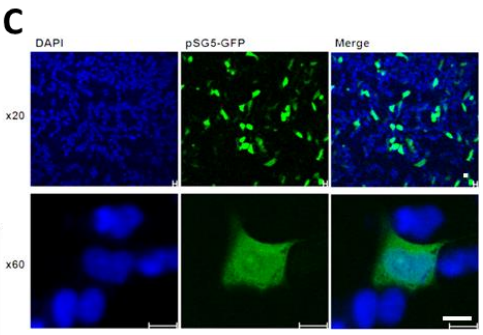


**Figure 41 - SH-SY5Y transfection reagent optimisation**

**A)** Flow cytometry results for SH-SY5Y transfection reagent optimisation, cells were either transfected with a GFP containing plasmid, GFP-pSG5 or the negative, pSG5. **B)** Compilation of transfection optimisation results (n=3). **C)** Representative confocal microscopy images of ICAfectin transfected SH-SY5Y cells with the plasmid, pSG5-GFP. Images show DAPI nuclear staining, pSG5-GFP expression and merged images. Images were taken at both at x20 and x60 magnification (Scale bar = 10µm).

HepG2 density and proliferation were assessed to find the maximum cell seeding density whilst allowing viable cell proliferation over the 72hrs of culture and maximising lipid-oligonucleotide endocytosis. WST-1 analysis revealed that $2.5x10^4$ cells per well resulted in optimal growth over 72hrs. A seeding density of $2.5x10^4$ resulted in a similar end absorbance result to that of the higher seeding density and made setting up of experiments more efficient when done alongside the SH-SY5Y cell line (Figure 40, B). Visual analysis showed that $2.5x10^4$ resulted in good culture surface coverage and allowed continuous proliferation during culture. PCR primers were confirmed against HepG2 with the cycling conditions optimised for the primer set (Figure 42, C/D).

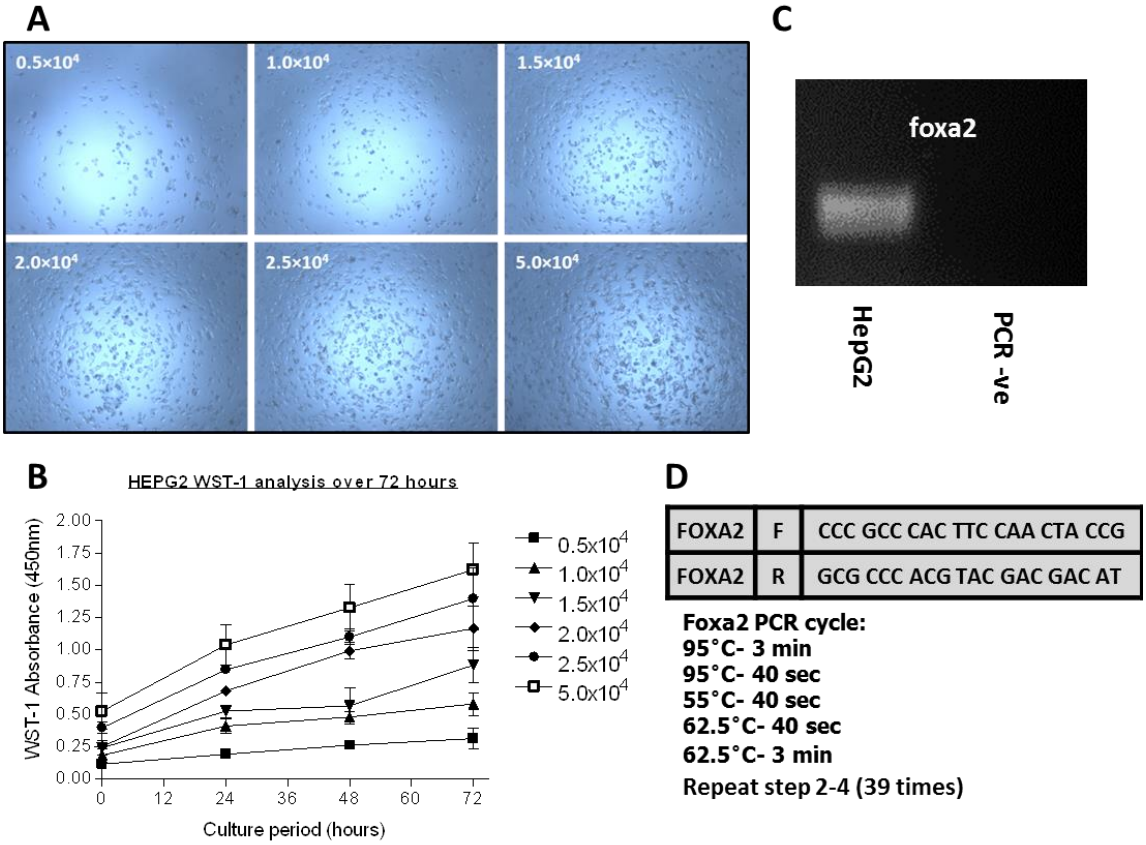


**Figure 42 - HepG2 seeding density and foxa2 PCR optimisation**
**A)** Representative bright field images showing HepG2 at varying seeding densities at 24hrs (x4 magnifications). **B)** WST-1 analysis of HepG2 at different seeding densities over a 72hr culture period (n=3). **C)** Foxa2 PCR primers were optimised against HepG2 total RNA and the cycling conditions shown in **D**.

HepG2 cell line transfection efficiency under this protocol was less than 1.9% (Figure 43, A/B) for each reagent. Confocal imaging however, showed that GFP was being generated by the cells in isolated pockets (Figure 43, C) throughout the cytoplasm and surrounding the cells, suggesting that the HepG2 cells generated and secreted the GFP protein. The presence of GFP indicates that transfection had been successful but it was not possible to quantify.

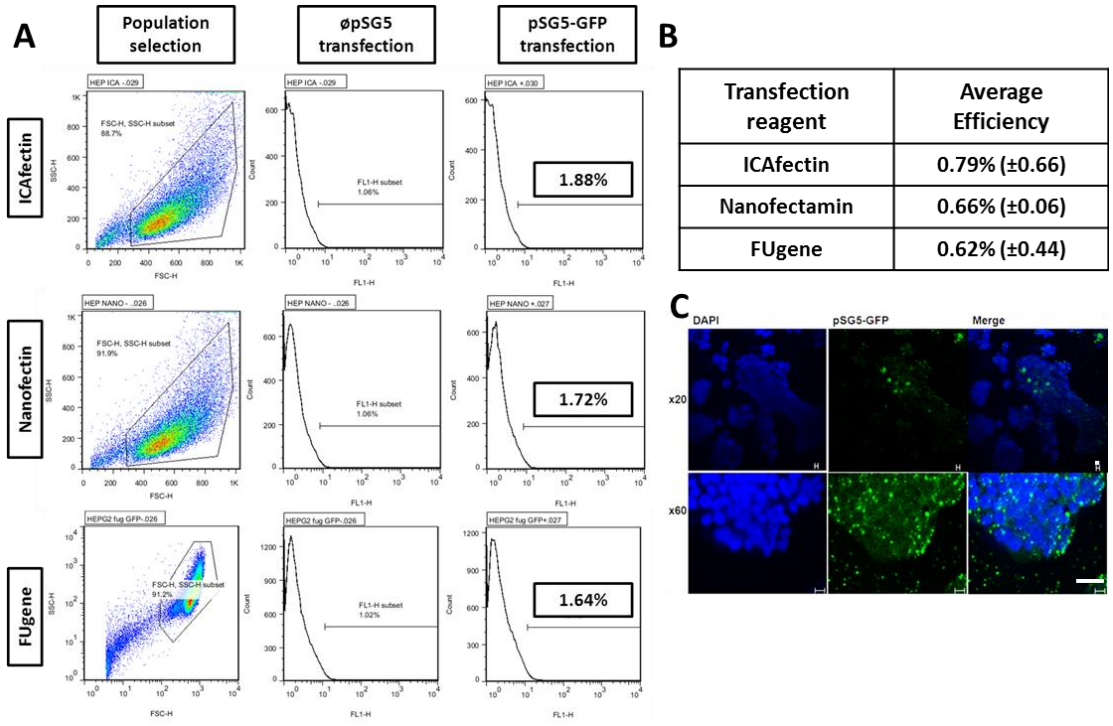


| Transfection reagent | Average Efficiency |
|---|---|
| ICAfectin | 0.79% (±0.66) |
| Nanofectamin | 0.66% (±0.06) |
| FUgene | 0.62% (±0.44) |

**Figure 43 - HepG2 transfection reagent optimisation**

**A)** Flow cytometry results for HepG2 transfection reagent optimisation, cells were either transfected with a GFP containing plasmid, GFP-pSG5 or the negative, pSG5. **B)** Compilation of transfection optimisation results (n=3). **C)** Representative confocal microscopy images of ICAfectin transfected HepG2 cells with the plasmid, pSG5-GFP. Images show DAPI nuclear staining, pSG5-GFP expression and merged images. Images were taken at both at x20 and x60 magnification (Scale bar = 10µm).

Jurkat density and proliferation was also assessed. WST-1 analysis revealed that $2.5x10^4$ cells/well resulted in optimal growth over 72hrs (Figure 44, C) with reasonable cell density observed that would allow continuous proliferation over the experimental time frame. Lmx1a PCR primers were optimised against foetal temporal lobe because Jurkat was found not to express *lmx1a* (Figure 40, B/D). The absence of *lmx1a* expression was not expected as Jurkat lysate is commonly used as a positive control for lmx1a protein assays (abcam 2014). Despite this finding, we continued to use this cell type to assess lmx1a saRNA efficiency with the expectation that the saRNA technology could overcome this barrier. Transfection efficiency experiments were not carried out due to time constraints.

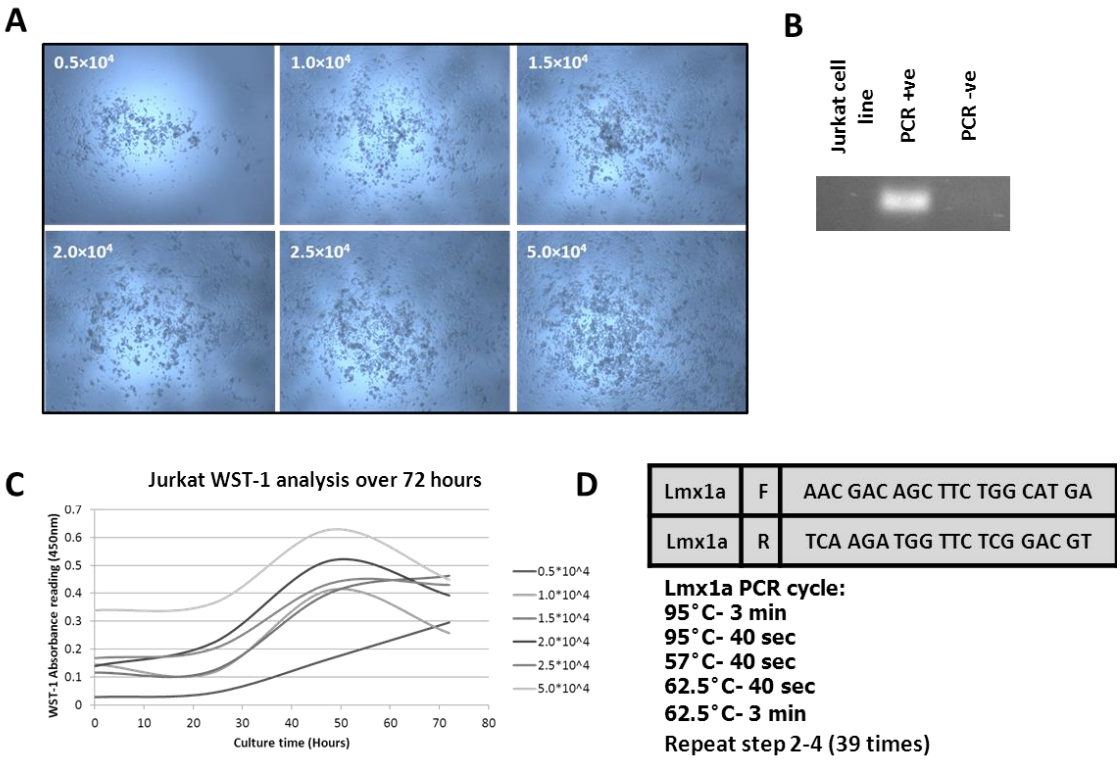


| | | |
|---|---|---|
| Lmx1a | F | AAC GAC AGC TTC TGG CAT GA |
| Lmx1a | R | TCA AGA TGG TTC TCG GAC GT |

**Figure 44 - Jurkat seeding density and TH PCR optimisation**
**A)** Representative bright field images showing Jurkat at varying seeding densities at 24hrs (x 4 magnifications). **C)** WST-1 analysis of Jurkat at different seeding densities over a 72hr culture period (n=3). **B)** *lmx1a* PCR primer was optimised against foetal temporal lobe DNA and the optimal cycling conditions are shown in **D**.

### 5.4.2 PCR analysis of saRNA transfected cell lines

Cells were transfected with their relevant saRNA at 24hrs and 48hrs alongside 'Un-transfected', lipid transfection reagent alone and 'Scramble', random RNA sequences that have no specific target, using ICAfectin. Scramble acted as a true negative, allowing assessment of the effects of the transfection reagent and the RNA molecule without a targeted impact on the gene of interest. These controls also worked to assess the component's effect on cell viability. Transfections were performed on cultures that were either unsynchronised or synchronised.

Total RNA was harvested at 72hrs and rtPCR performed to assess the expression levels of the genes of interest. Unsynchronised cells were found to produce variable results with no consistency across repeated experiments (Figure 45, A-B, n=2). Cultures were then synchronised as it was thought the inconsistencies might be a result of different cell cycle positions throughout the populations of unsynchronised cells (Figure 45 A-B). Following synchronisation, cultures were found to be uniform in expression for *foxa2. TH* results are not

shown as these were inconclusive, thought to be due to RNA or primer degradation. There was no observable impact of saRNA. *Lmx1a* was not observed to be expressed by Jurkat under any condition, with the performance of the lmx1a PCR primers confirmed using foetal temporal lobe DNA (Figure 46, D/E).

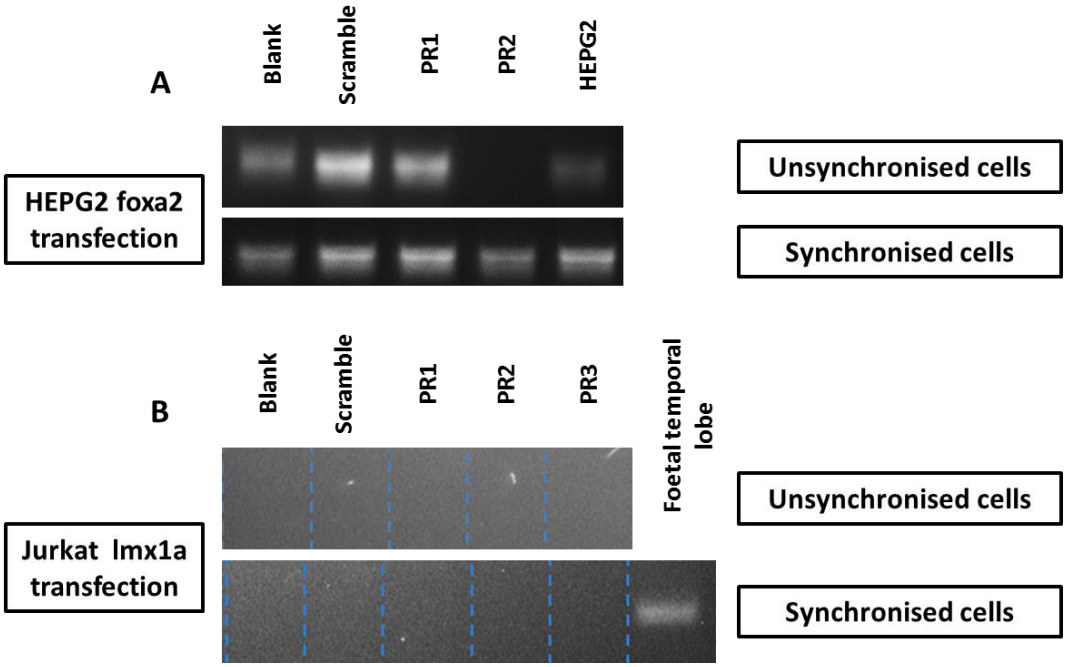


**Figure 45 - RT-PCR mRNA analysis of transfected cell lines**
rtPCR mRNA analysis of HepG2, SH-SY5Y and Jurkat expression of target genes; **(A)** *foxa2* and **(B)** *lmx1a* respectively. Cultures were treated with different conditions; untransfected, scramble and the available saRNA variants for that target gene (PR1-PR3). The figure shows a comparison of results from unsynchronised (n=2) and synchronised (n=1) cultures. *TH* results are not shown as these were inconclusive. PCR primer functionality was confirmed using cDNA from target gene positive sources; HepG2, SH-SY5Y and foetal temporal lobe DNA respectively.

### 5.4.3 Lipid-base transfection reagent optimisation for omnicytes

Due to the inconclusive results using cell lines it was agreed that the saRNA candidates would be screened using omnicytes. The efficiency of the transfection reagents at transfecting omnicytes was investigated using siGLO green fluorescent transfection. This is a small molecule of a similar size to that of siRNA and saRNA elements (~20nt) and is used regularly in RNAi experiments; it was thought that this would give a more accurate representation of transfection efficiency of the reagents. SiGLO allowed the visualisation of transfected cells and quantification using flow cytometry.

Flow cytometry data showed that efficient transfection could be achieved using both nanofectin (99.1%) and ICAfectin (92.6%) (Figure 46, A/B). Confocal imaging following

transfection with nanofectin confirmed that siGLO was internalised and was located to the cytoplasm (Figure 46, C).

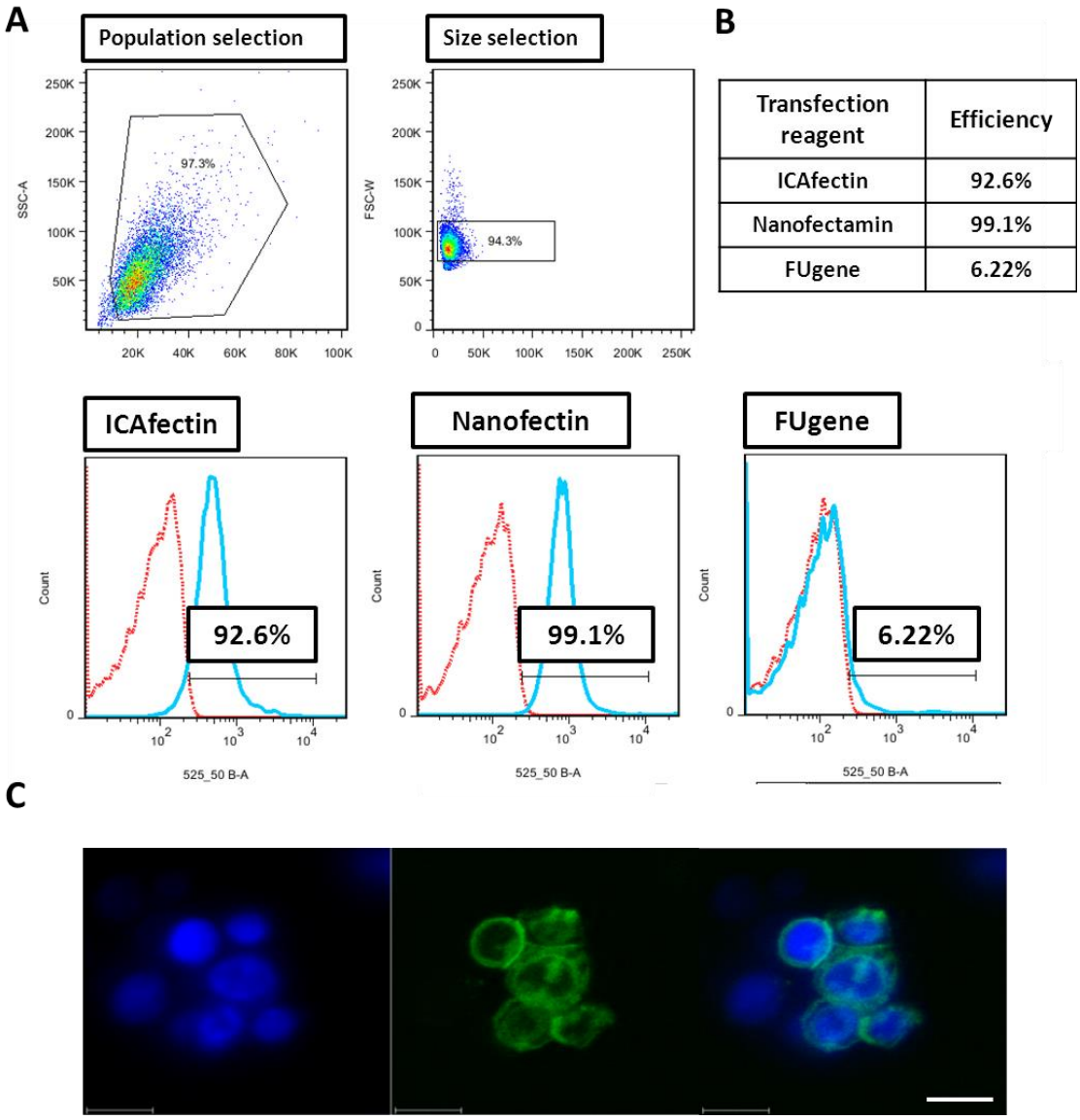


**Figure 46 - Optimisation of omnicyte transfection**
**A)** Omnicyte transfection reagent optimisation using a frozen lymphoma sourced omnicyte cell sample. Cells were transfected with siGLO fluorescent transfection control and efficiency assessed using flow cytometry **B)** Table showing the compiled transfection efficiencies for omnicytes using different lipid-based transfection reagents (n=1). **C)** Confocal images of omnicyte transfected cells at x60 magnification (n=1) (Scale bars = 10µm).

During this stage of the investigation an opportunity arose to work with two known disease type omnicyte samples. This allowed us to investigate the impact of disease type on transfection efficiency, gene expression and the efficacy of the saRNA.

The omnicyte disease samples were transfected twice with candidate saRNA, as depicted in Figure 47, A. Briefly, $CD34^+$ were seeded at a density of $2.5x10^5$cells/well and omnicytes

isolated, then expanded for 24hrs in proprietary expansion media. Cultures were then transfected twice over a 48hrs period using nanofectin and cultured for a further 24hrs. Cultures were then mechanically harvested and gene expression assessed using qPCR. Parallel to the saRNA experimental transfections, both myeloma and lymphoma cell types were transfected with siGLO allowing visualisation of the transfection efficiency. It was observed that myeloma cells showed significantly better transfection ability when compared with lymphoma (Figure 47, B).

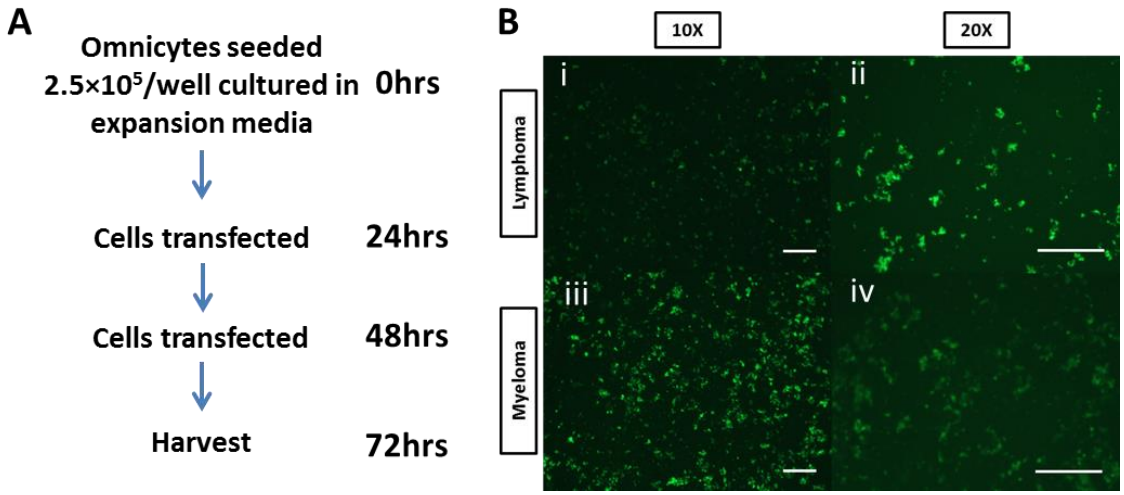


**Figure 47 - Transfection protocol schematic and siGLO of omnicytes**
**A)** Omnicytes were seeded into wells (24 well plate) and expanded in expansion media and expanded for 24hrs. Cultures were then transfected with saRNA over the next 48hrs and mechanically harvested for mRNA analysis at 72hrs. **B)** Myeloma and lymphoma omnicyte samples were transfected over 72hrs with siGLO transfection control, figures show representative x10 and x20 magnification fluorescent images of the cell populations (Scale bars = 100µm).

### 5.4.4 Molecular analysis of omnicyte target gene expression following saRNA transfection

qPCR data was collected for both myeloma and lymphoma omnicyte samples and interrogated for the target genes of interest for each transfection set. As a general trend it was found that myeloma sourced omnicytes showed greater variation when transfected with the relevant saRNA when compared with lymphoma, with the exception of lymphoma when transfected with TH saRNA. *TH* expression in lymphoma following TH saRNA transfection showed the greatest enhancement in PR1 (Figure 48).

Through this experiment it was observed that lymphoma and myeloma sourced omnicytes responded differently to the addition of saRNA. It was therefore decided that the use of this

cell type for the work would be unproductive until a consistent non-disease-type omnicyte cell source could be obtained.

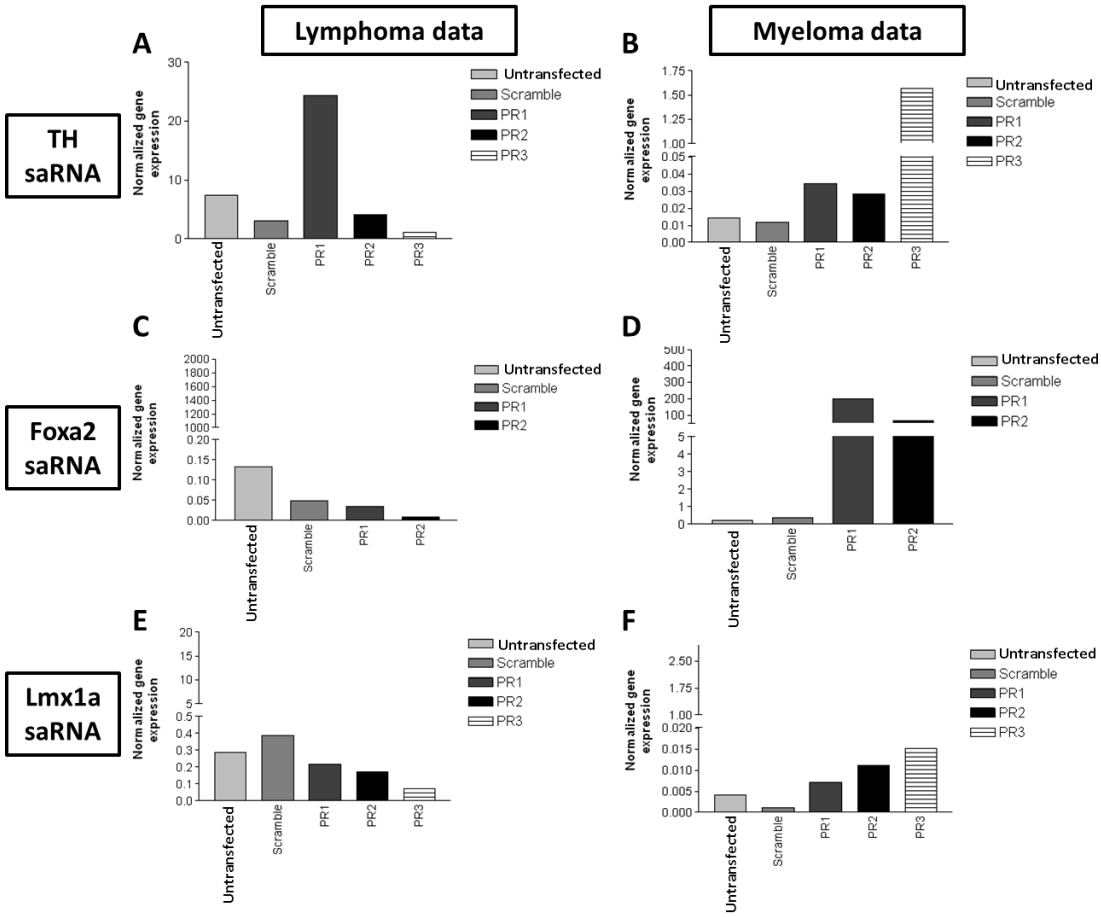


**Figure 48 - qPCR analysis of saRNA transfected lymphoma and myeloma omnicyte samples**
Lymphoma and myeloma sourced omnicyte cells were transfected with TH (**A/B** respectively), foxa2 (**C/D** respectively) and lmx1a (**E/F** respectively) saRNAs and harvested and analysed after 72hrs. Results were normalised against *β-actin* expression and controlled against 'untransfected', transfected with Nanofectin alone, 'scramble', transfected with Nanofectin and scramble RNA and saRNA variants (PR1 - 3)(n=1).

## 5.5 Discussion

Due to the limited availability of omnicytes, it was decided that initial optimisation of the saRNA candidates would be done using cell lines that were thought to endogenously express the genes of interest. This was done as it was thought that these cells would contain no epigenetic factors that might inhibit the transcription of the target genes and obscure the impact of the saRNA.

Two cell lines, HepG2 and SH-SY5Y, were found to be positive for the targets *foxa2* (abcam 2014) and *TH* (abcam 2014) at a protein level. The expression of the target genes was confirmed at a molecular level using rtPCR for both cell types (Figure 40/Figure 42). A similar search was used to identify Jurkat as being positive for *lmx1a* expression (abcam 2014) though confirmation at a molecular level was negative. *Lmx1a* PCR cycling was optimised against foetal temporal lobe RNA that was purchased commercially.

A seeding density of $2.5x10^4$cell/well (24 well plate), as determined by WST1 analysis, was used as the standard density for all of the cell lines, allowing continuous cell proliferation over 72hrs culture. Through visual assessment, this initial seeding density also resulted in a good cell density at 24hrs when the cells were transfected using a lipid-base reagent, maximising lipid-cell interaction and endocytosis (Figure 40/Figure 42/Figure 44) (Ziello, Huang et al. 2010).

Cell lines were individually assessed for their efficiency to be transfected using three reagents; ICAfectin, Nanofectin and FUgene, using a GFP containing plasmid, pSG5-GFP, and non-GFP containing control, øpSG5, to visualise and quantify the efficiency of the transfection reagents. pSG5-GFP is approximately 4kb in size, significantly larger than the candidate saRNA (20nt) elements, providing a rigorous test of transfection efficiency. Following optimisation it was decided that ICAfectin would be used for all cell types, because SH-SY5Y showed the greatest efficiency using ICAfectin (28.7% efficiency) and the HepG2 assessment was inconclusive

although GFP was present in ICAfectin transfected cultures when assessed using confocal microscopy (Figure 41/Figure 43).

PCR results from both Jurkat and SH-SY5Y based transfection experiments were inconclusive. Unsynchronised cells, showing variability across all variants and controls assessed. This was thought to be due to cells within culture being at different stages of the cell cycle, impacting on efficiency of the saRNA and the expression of target genes, this is supported by findings of Chen *et al.* (Chen, Huang et al. 2012). Chen *et al.* found retroviral infection was significantly affected by cell culture synchronisation. To overcome this, cells were synchronised using starvation media which resulted in uniform expression across all experimental conditions. This was thought to be a result of endogenous gene expression masking the effects of the saRNA. The lack of conclusive results was thought to be, in part, a result of the insensitivity inherent to the rtPCR method. We expect that changes in the expression levels of the target genes were too subtle and could not be distinguished. At this stage of the work the use of qPCR became available, allowing sensitive and quantitative analysis of any molecular changes within the cells.

It was decided further optimisation of saRNA would be carried out using omnicytes as this was a potential cell source for use within the development of a therapeutic product.

Transfection optimisation work was performed using a green fluorescent molecule, siGLO, which better represented the saRNA molecules (Figure 45, C). Transfection was found to be most efficient when using nanofectin (Figure 46) and so this reagent was used in all further investigations.

The omnicytes available for screening of the saRNAs at this stage of the work were sourced from two diseased donors, one myeloma and one lymphoma. Following the discovery in Chapter 3 that disease type influenced cell behaviour and molecular gene expression it was decided that these cell types would be ran in parallel and their results assessed separately. Transfection efficiency was found to be affected by disease type with lymphoma showing

significantly lower transfection efficiency than that of myeloma (Figure 47, B). qPCR data also showed a high degree of variability depending on which disease type was transfected, with both TH and lmx1a saRNAs producing distinctive results dependant on disease type (Figure 48, A/B & E/F). Foxa2 transfected cells showed some consistency with PR1 showing an increase in expression for both disease types though the expression level difference was dramatic with lymphoma and myeloma showing 0.05 and >175 fold increases in expression, respectively. This could be a result of disease modification of the gene activation sites, as it has been found by another group that only 9% of small nucleotide polymorphisms (SNPs) associated with disease are found in the protein coding region the rest are found in the activation sites (Hindorff, Sethupathy et al. 2009), this could impact on the binding of the saRNA at the activation site and their functionality. This limitation of diseased cells should be investigated if this work is to be taken forwards (Figure 48, C/D).

Due to the lack of availability of 'normal', non-disease omnicyte cells and the variability of the results from disease types and patient variability (discussed in Chapter 3) observed, it was decided that for this work to progress a different experimental cell type would need to be used. This thesis continues this work on saRNA using hPSCs, hESC and hiPSC, in conjunction with the DA differentiation protocol described and investigated in Chapter 4.

## 5.6 Conclusion

SaRNAs were shown in these limited experiments to have variable impact on gene expression when source cells were of different disease types. As the experiment was only repeated once due to limited sample availability these results should be interpreted with caution. It was found that the use of rtPCR to screen and understand the effects of saRNA in cell types is unsuitable due to the low sensitivity of this method.

Due to the lack of availability of the omnicytes and the variability observed across all the work done with this cell type, whether because of patient variability or the disease type, experimental work with this cell type is challenging and could not be addressed in the timescale of this doctorate.

In the following chapter (Chapter 6) we show how saRNAs can be included into an hPSC-based DA differentiation protocol and we will investigate if saRNA can have an impact on gene expression and differentiation yield.

# CHAPTER 6 - POTENTIAL OF SARNA FOR ENHANCING TARGET GENE EXPRESSION DURING AGGREGATE-BASED DOPAMINERGIC DIFFERENTIATION

## 6.1 Introduction

Our ability to derive specific neuronal cell types from hPSCs has developed from niche expertise based on the fundamentals of developmental biology into a widespread laboratory methodology increasingly adopted by translational scientists. It is now possible to stimulate a cell population to express DA genes, *TH, lmx1a and foxa2*, through a number of protocols (Chambers, Fasano et al. 2009, Kriks, Shim et al. 2011); however as discussed in Chapter 5, the efficiency of these protocols remains low. The lack of an efficient protocol has hindered progress to clinic and the development of robust cell lines for drug screening. The low purity of the differentiation process means, additional purification and packaging steps and increased input cell numbers at the initial stages of the process will be required. Contaminating cell types, including pluripotent, germ layer and incorrectly differentiated cells, also need to be removed from the dose to eliminate tumorigenic risk, again reducing the output of the process.

We know through the work presented in Chapter 4, that the generation of specific, DA-like neuronal cell types from hPSC populations is possible using a suspension-based culture system. Within the differentiated populations pluripotent and non-ectoderm germ line marker expressions were shown to reduce and the expression of key DA marker genes, including, *lmx1a, TH* and *DRD* to increase. This work also showed that while we can now generate cell populations that express the desirable markers required, we cannot achieve efficient co-expression of the target proteins in all the cells. Through collaboration with Omnicyte Ltd. this project was able to use the novel technology, saRNA, to modify targeted gene expression transiently and attempt to enhance the efficiency of the protocol. Pilot work was performed

on cancer cell lines and omnicytes as described in Chapter 5. This work proved inconclusive on these cell lines, however the technology has been shown to influence genes and protein expression and proof of principal confirmed through work done to improve liver function, inhibit live carcinogenesis *in-vivo* and target and modify the specific Islet beta-cell transcription factor MafA in $CD34^{+}$ cells (Reebye, Saetrom et al. 2013, Reebye, Saetrom et al. 2013); indicating that there is potential for this technology to be used to enhance hPSC differentiation yields.

## 6.2 Aim

Having generated hPSC products that express DA genes, and given the reported stimulatory effect of saRNAs on differentiation and reprogramming, the aim of this chapter was to determine whether combination effects of standard differentiation protocols and neuron-specific saRNA treatment can enhance the expression of key markers *TH, lmx1a* and *foxa2* in hPSC cell lines.

## 6.3 Results

### 6.3.1 saRNA transfection optimisation

Transfection of hESC and hiPSC with nanofectin, a lipid-base reagent, was assessed using the transfection control reagent, siGLO, which fluoresces green for visual confirmation of transfection. Both hESC and hiPSC were successfully transfected with siGLO relative to UT and Mock transfected controls (Figure 49, C & F). Transfection with siGLO appeared to impact on cell growth with lower colony density observed when compared with both mock and UT cultures.

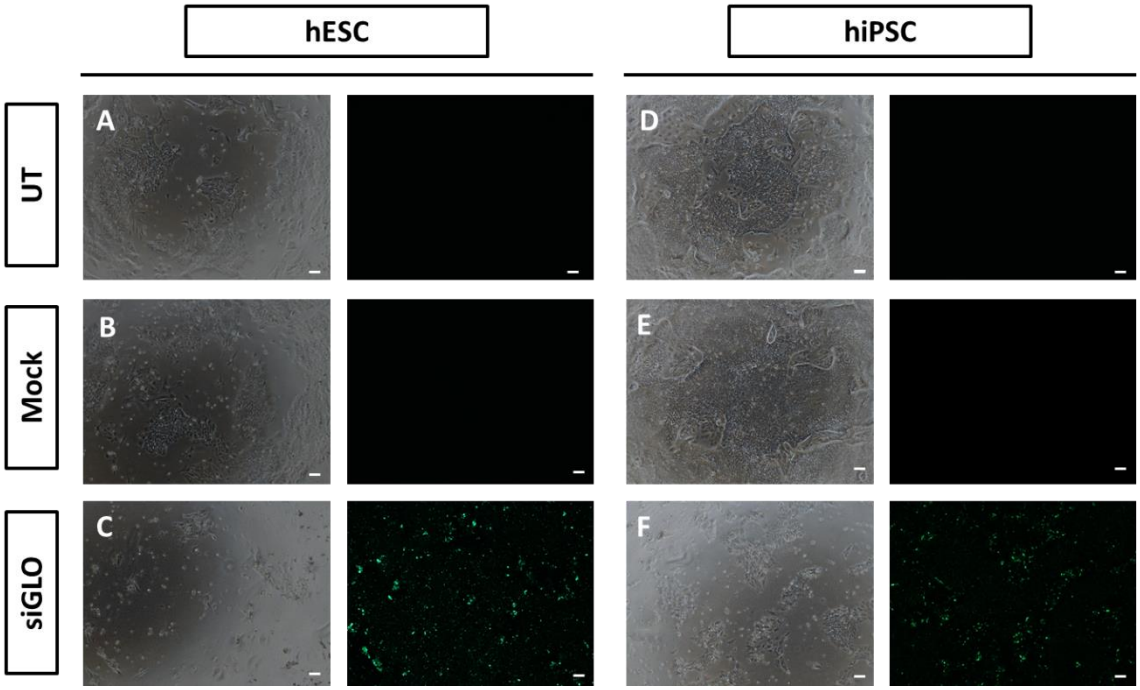


**Figure 49 - Nanofectin transfected hPSC with fluorescent element siGLO**
Representative bright-field and fluorescent images of hPSC cultures transfected using nanofectin. hESC and hiPSC were negative for green fluorescence when cultured un-transfected **(A/D)** and mock transfected **(B/E)**. Cells transfected with siGLO **(C/F)** emitted green fluorescence (495nm/519nm, n=1) (Scale bar = 100µm).

To assess the impact of the candidate saRNAs on target gene expression, saRNAs were tested in hiPSC. hiPSC were transfected, using nanofectin, with either individual saRNA or all three saRNA together. Cultured cells were mechanically harvested for qPCR analysis 72hrs after transfection. All the genes showed the greatest expression increase following transfection with all three candidate saRNAs (Figure 50, A-C). Transfection at the higher concentration resulted

in a greater increase in expression for *foxa2* (Figure 50, A), and a slight increase in *TH* (Figure 50, C). *Lmx1a* expression was not impacted by saRNA concentration (Figure 50, B).

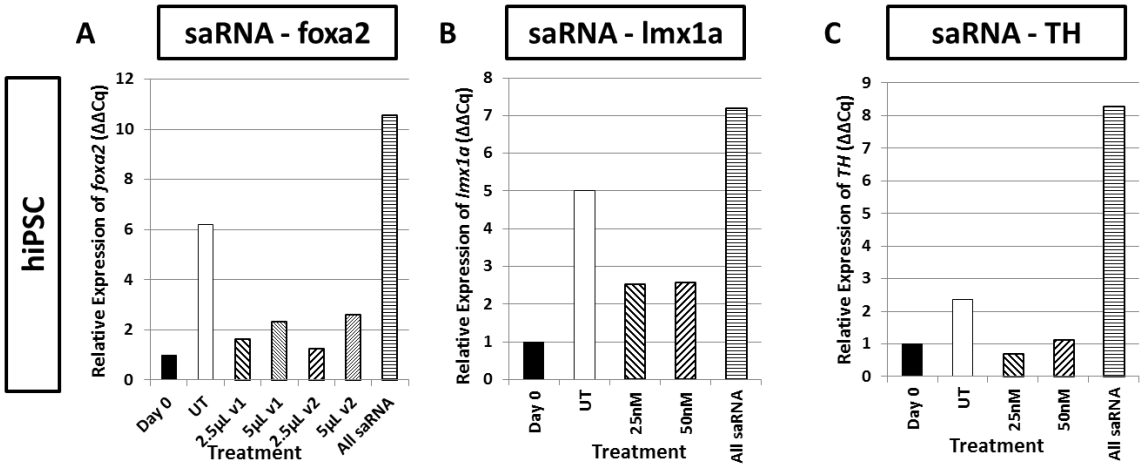


**Figure 50 - saRNA optimisation using hiPSC**

qPCR analysis of mRNA expression in saRNA transfected hiPSC cultures. hiPSC were transfected with **A)** foxa2, **B)** lmx1a and **C)** TH saRNA either individually or combined over 72hrs (3 x transfections) at two concentrations; 25nM or 50nM. Foxa2 **(A)** was assessed for two candidates (v1 & v2); volume was used to alter concentration levels (2.5µL or 5µL). Investigations were controlled against UT cultures, cultured in KOSRM.

### 6.3.2 Impact of combined saRNA addition during dopaminergic differentiation at the molecular level

The impact of saRNA transfection was assessed at a molecular level using qPCR. Pluripotent, germ layer, neuronal and DA marker gene expression levels were assessed at a population level throughout the differentiation process. Samples were harvested at D0, D24 and D38, i.e. before differentiation, following suspension culture and following adhered maturation of the neurospheres. Transfection of the hPSC aggregates was confirmed in hiPSC using the siGLO transfection control. Control suspension cultures were transfected over the course of 24 days, mimicking the transfection regime of the saRNA samples. Qualitative analysis of the cultures confirmed that the aggregates positively fluoresced when transfected with siGLO whilst UT aggregates did not fluoresce (Figure 51).

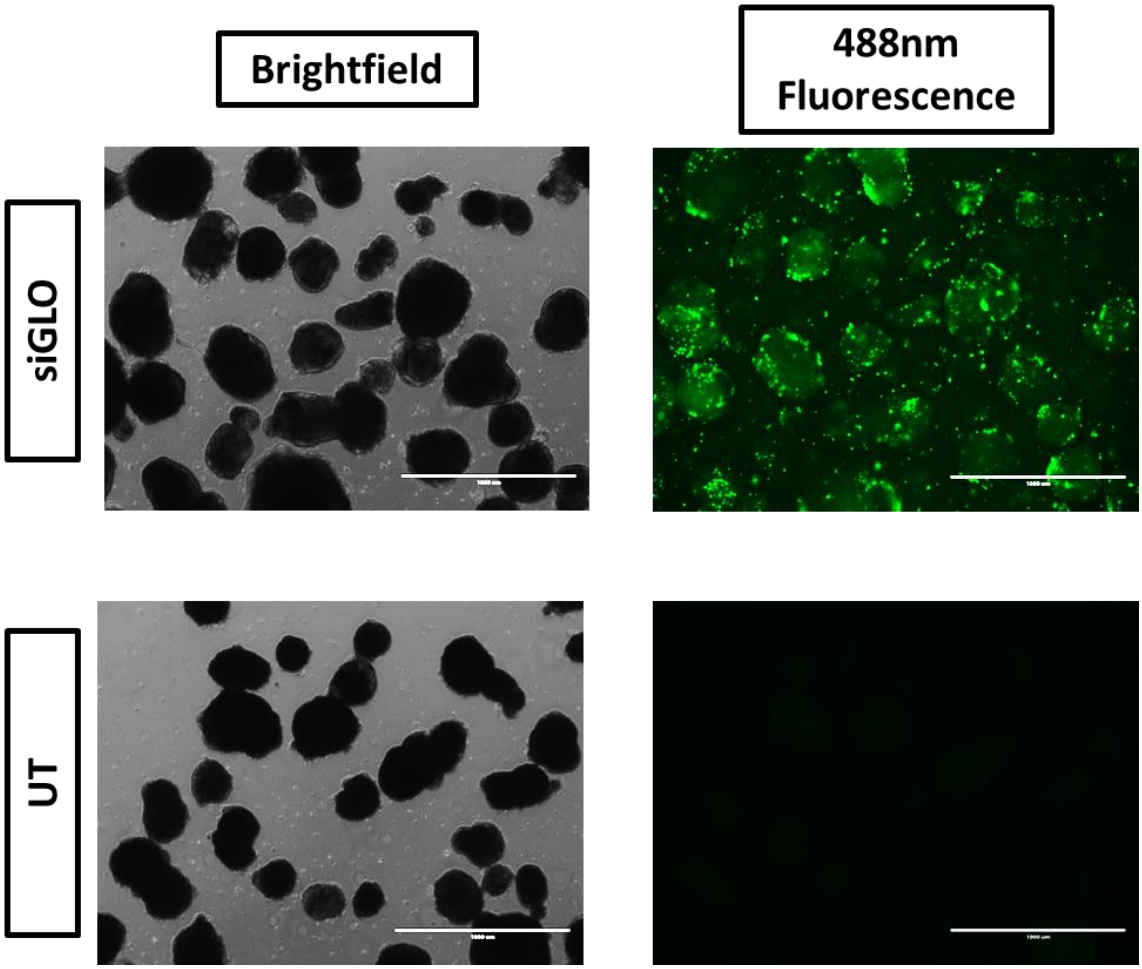


**Figure 51 - Representative image of siGLO transfected hiPSC neurospheres**
Representative bright field and fluorescent images of transfected (siGLO) and UT hiPSC aggregates (Scale bars 1000µm).

### 6.3.3 Impact of transfecting saRNAs during the dopaminergic differentiation protocol - pluripotent gene expression

Pluripotency genes, *nanog* and *oct4,* were significantly down-regulated over time in hESC and hiPSC (Figure 52, A-B & D-E); however the addition of saRNA did not induce substantial changes when compared to mock or UT. Indeed in hiPSC, mock transfected conditions appeared to result in the greatest measurable down-regulation, though not statistically significant.

In the case of *sox2*, gene expression was up-regulated at D24 relative to D0 in hESC but by D38 *sox2* was significantly down-regulated in all conditions (Figure 52, C). *Sox2* expression in hiPSC was found not to change substantially from D0 levels at any point during culture (Figure 52, F).

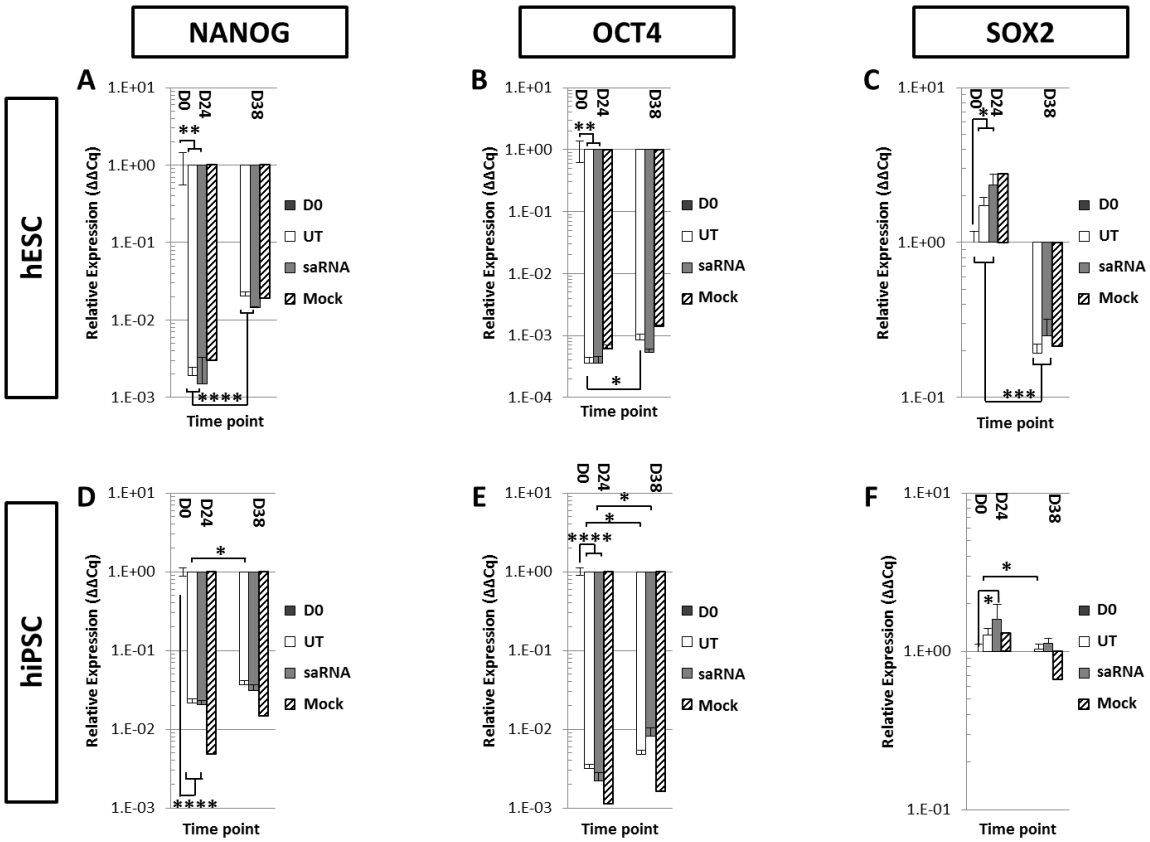


**Figure 52 - qPCR analysis of pluripotent gene expression following the inclusion of saRNA during dopaminergic differentiation and maturation**

qPCR analysis of pluripotent mRNA expression following dopaminergic differentiation (D24) and adhered maturation in DDM (D38). hESC and hiPSC derived neurosphere expression of *nanog* **(A/D)**, *oct4* **(B/E)** and *sox2* **(C/F)** are shown relative to D0 expression. Data is normalised using *GAPDH, β-Actin and UBC* expression (* p< 0.05, ** p<0.01, ***p<0.001 and **** p<0.0001. Bars represent Mean ± SEM. All UT and saRNA cultures n=3, hESC mock culture n=1 and hiPSC mock culture n=2).

### 6.3.4 Impact of transfecting saRNAs during the dopaminergic differentiation protocol - *fgf5* gene expression

Expression of *fgf5* in both hESC and hiPSC significantly increased in all experimental conditions relative to D0 over the duration of culture, though hiPSC was shown to increase faster than hESC by D24 (Figure 53, A & B). Transfection with saRNAs was not observed to increase the expression of *fgf5* compared with control arms in either cell type.

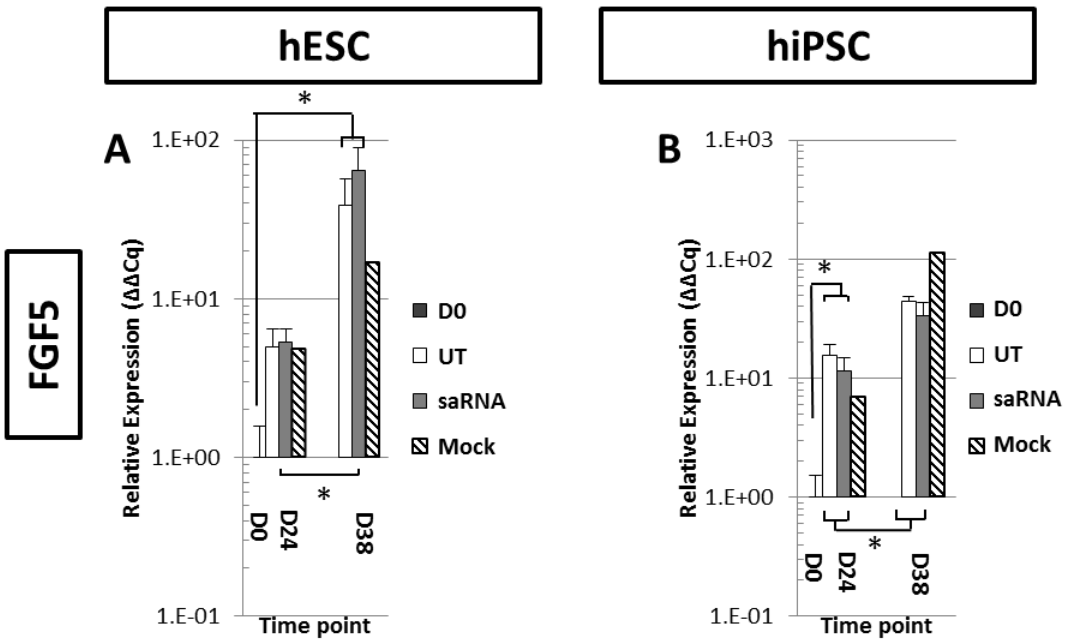


**Figure 53 - qPCR analysis of *fgf5* expression following the inclusion of saRNA during dopaminergic differentiation and maturation**

qPCR analysis of *fgf5* mRNA expression following dopaminergic differentiation (D24) and adhered maturation in DDM (D38). hESC and hiPSC derived neurosphere expression of *fgf5* (**A/B** respectively) is shown relative to D0 expression. Data is normalised using *GAPDH, β-Actin and UBC* expression (* p≤0.05 and ** p≤0.01. Bars represent Mean ± SEM. All UT and saRNA cultures n=3, hESC mock n=1 and hiPSC mock n=2).

### 6.3.5 Impact of transfecting saRNAs during the dopaminergic differentiation protocol - germ layer gene expression

Contaminating germ layer markers *brachyury* and *sox17* were shown to be down-regulated in both hESC and hiPSC following differentiation (Figure 54, A-B & D-E). *Sox17* was shown to be significantly reduced in hESC by D38 and in hiPSC by D24. *Nestin* expression increased significantly in all conditions by D24 (Figure 54, C & F) for hiPSC, and in hESC it was shown to decrease by D38. Transfection of saRNA did not reduce expression of *brachyury* and *sox17* or increase the expression of *nestin* over that of the control arms.

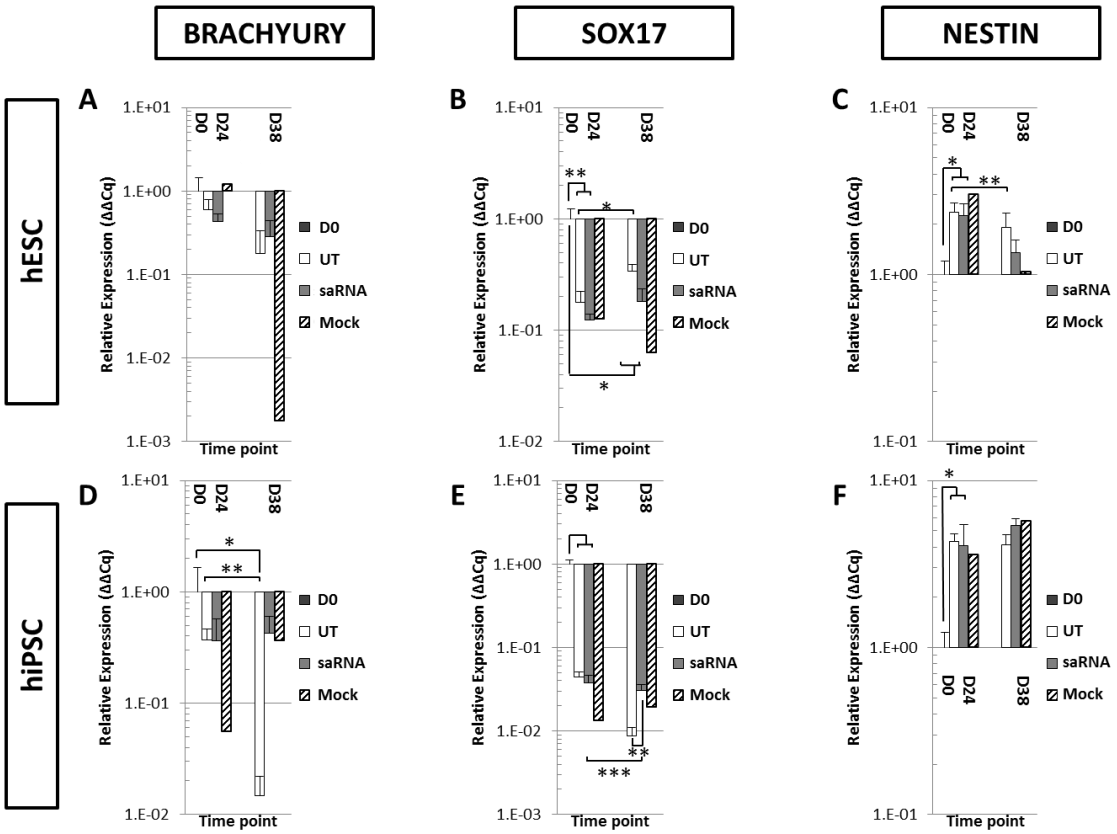


**Figure 54 - qPCR analysis of germ layer expression following the inclusion of saRNA during dopaminergic differentiation and maturation**

qPCR analysis of germ layer mRNA expression following dopaminergic differentiation (D24) and adhered maturation in DDM (D38). hESC and hiPSC derived neurosphere expression of *brachyury* **(A/D)**, *sox17* **(B/E)** and *nestin* **(C/F)** are shown relative to D0 expression. Data was normalised using *GAPDH, β-Actin* and *UBC* expression (* p≤0.05, ** p≤0.01, ***p≤0.001 and **** p≤0.0001. Bars represent Mean ± SEM. All UT and saRNA cultures n=3, hESC mock n=1 and hiPSC mock n=2).

### 6.3.6 Impact of transfecting saRNAs during the dopaminergic differentiation protocol - neuronal gene expression

Assessment of neuronal gene expression during differentiation showed *sox1* and *en1* to be significantly increased over the course of the differentiation process in both hESC (Figure 55, A-B) and hiPSC (Figure 55, E-F). Expression of *sox1* and *en1* was slightly increased in saRNA transfected hESC cultures relative to the controls, at D24; no difference was observed in hiPSC relating to culture condition. *Nurr1* expression in both hESC and hiPSC increased significantly by D38 in all conditions (Figure 55, D & H), with expression being greater in saRNA transfected hESC culture. Expression of *otx2* was shown in both cell types to decrease across all conditions (Figure 55, C & G).

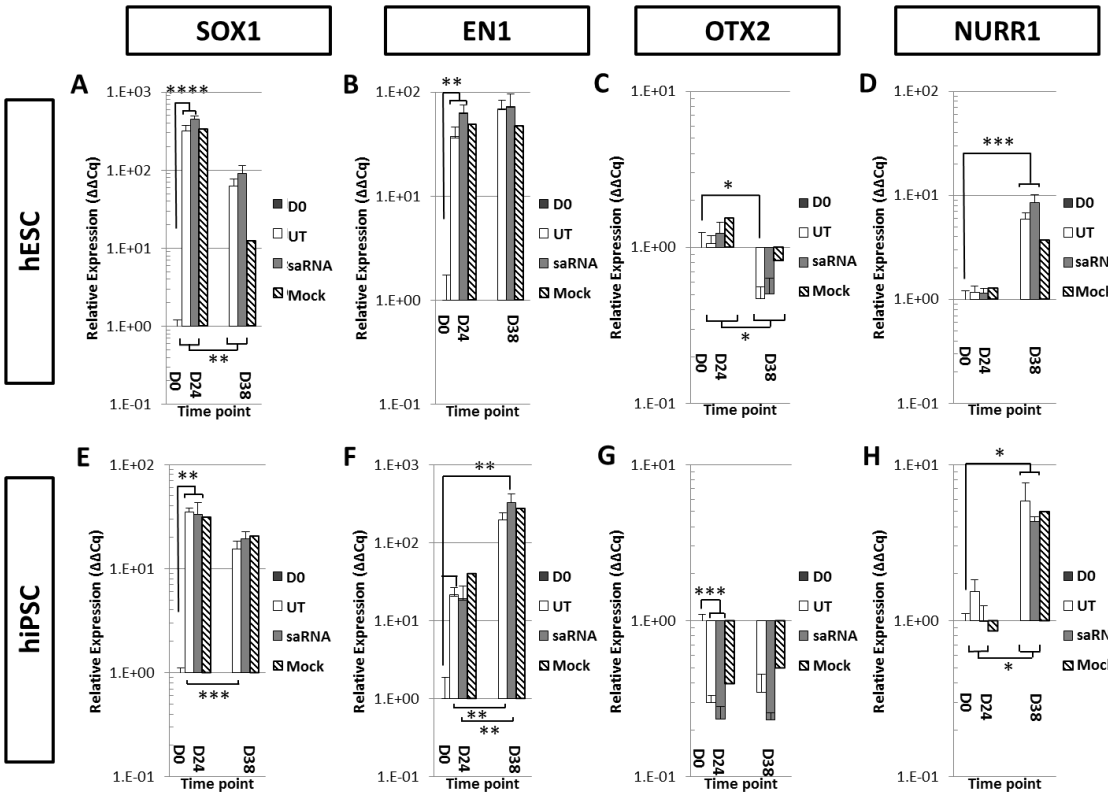


**Figure 55 - qPCR analysis of neuronal gene expression following the inclusion of saRNA during dopaminergic differentiation and maturation**

qPCR analysis of neuronal mRNA expression following dopaminergic differentiation (D24) and adhered maturation in DDM (D38) alongside the inclusion of saRNA. hESC and hiPSC derived neurosphere expression of *sox1* **(A/E)**, *en1* **(B/F)**, *otx2* **(C/G)** and *nurr1* **(D/H)** are shown relative to D0 expression. Data was normalised using GAPDH, β-Actin and UBC expression (* p≤0.05, ** p≤0.01, ***p≤0.001 and **** p≤0.0001. Bars represent Mean ± SEM. All UT and transfected cultures n=3, hESC mock n=1 and hiPSC mock n=2).

### 6.3.7 Impact of transfecting saRNAs during the dopaminergic differentiation protocol - dopaminergic gene expression

Expression of DA marker genes, *foxa2, TH* and *DRD* were shown to significantly increase in all conditions by D24 in hESC (Figure 56, A, C-D) with expression of *foxa2* being significantly greater in saRNA transfected cultures than UT cultures by D24. Expression of *lmx1a* was delayed until D38 where expression in saRNA transfected cultures appeared to be greater (Figure 56, B), though not significantly. Expression of *lmx1a, TH* and *DRD* also rose significantly in hiPSC cultures by D24 (Figure 56, F-H) but no difference was observed associated with treatment. Expression of *foxa2* was shown in both UT and mock transfected to decrease in hiPSC culture, only saRNA transfected culture increased slightly over the course of the protocol (Figure 56, E).

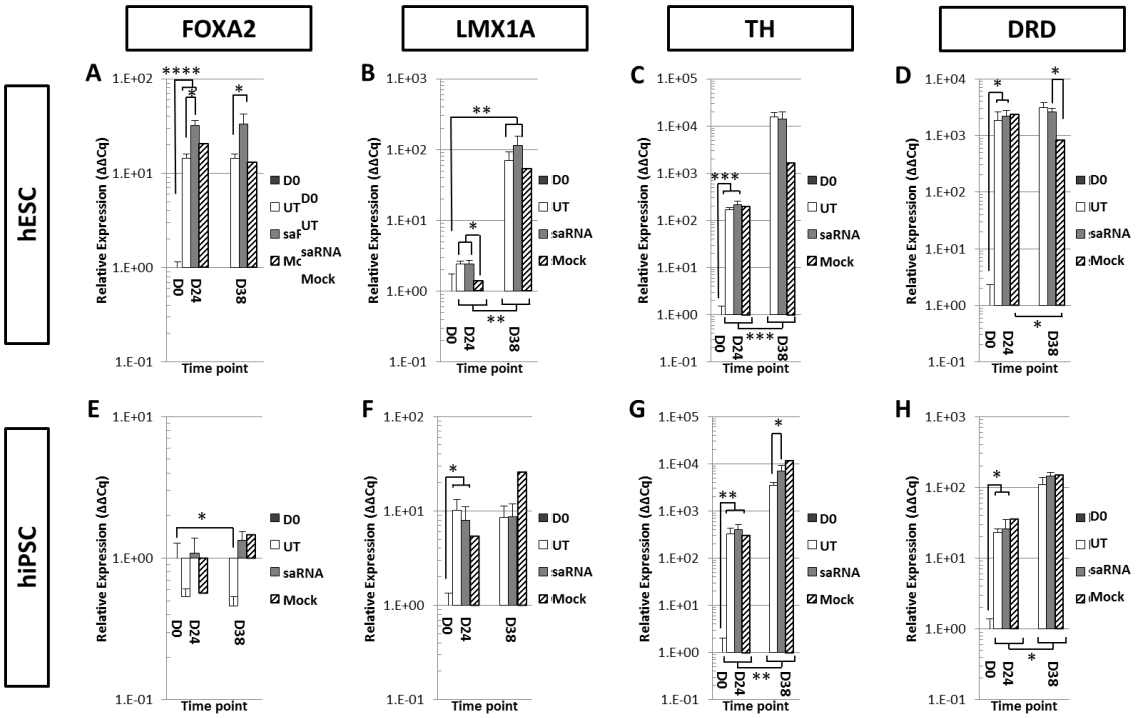


**Figure 56 -** qPCR analysis of dopaminergic gene expression **following the inclusion of saRNA during dopaminergic differentiation and maturation**

qPCR analysis of dopaminergic mRNA expression following dopaminergic differentiation (D24) and adhered maturation in DDM (D38) alongside the inclusion of saRNA. hESC and hiPSC derived neurosphere expression of *foxa2* **(A/E)**, lmx1a **(B/F),** *TH* **(C/G)** and *DRD* **(D/H)** are shown relative to D0 expression. Data was normalised using GAPDH, β-Actin and UBC expression (* p≤0.05, ** p≤0.01, ***p≤0.001 and **** p≤0.0001. Bars represent Mean ± SEM. All UT and transfected cultures n=3, hESC mock n=1 and hiPSC mock n=2).

### 6.3.8 Confocal imaging of UT versus saRNA transfected cultures

Immunofluorescent staining and confocal imaging confirmed the presence of neuronal marker β-III-Tubulin in both hESC and hiPSC cultures. No visual difference in expression of β-III-Tubulin could be distinguished between UT and saRNA transfected cultures in either cell type (Figure 57). DA marker, TH, was also assessed with expression being observed in both cell types and conditions (Figure 57). A greater number of $TH^+$ cells were seen to be present in hESC saRNA transfected cultures when compared with UT and hiPSC cultures though this was not quantified (Figure 57, C-D).

$TH^+$/$Foxa2^+$ cells were confirmed in both UT and saRNA culture conditions and cell types (Figure 58). TH staining was observed to be located to the cytoplasm of the cell whereas Foxa2 was located to the nuclei, co-stained with dapi. The majority of cells were shown to be $TH^-$ /$Foxa2^-$ but in pockets, cells could be observed to be $Foxa2^+$ with granular red staining in the nuclei. Co-association of Foxa2 and TH within a single cell was found to be low in both hESC

and hiPSC cultures. No difference in abundance of $Foxa2^{+}/TH^{+}$ cells could be discerned between UT and saRNA transfected cultures.

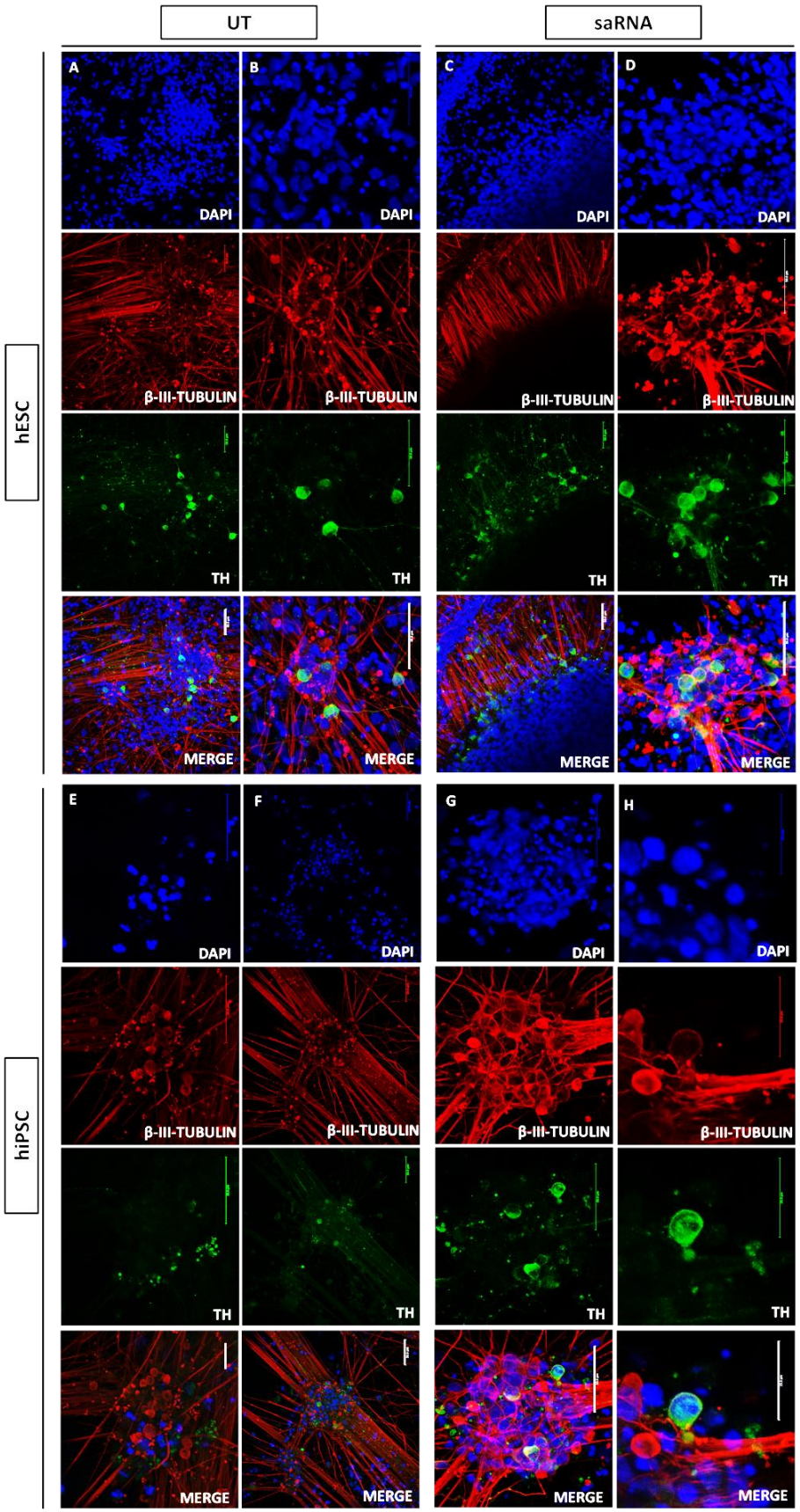


**Figure 57 - Confocal imaging of hPSC β-III-Tubulin and TH staining of untransfected and saRNA transfected cultures**

Representative confocal images of hESC (**A-D**) and hiPSC (**E-H**) UT and saRNA transfected cultures after 14 days in DDM. Cultures were affinity stained for β-III-Tubulin (red) and TH (green) antibodies. Dapi (blue) stained the nuclei (Scale bars A-G = 50µm, except H scale bar = 25µm).

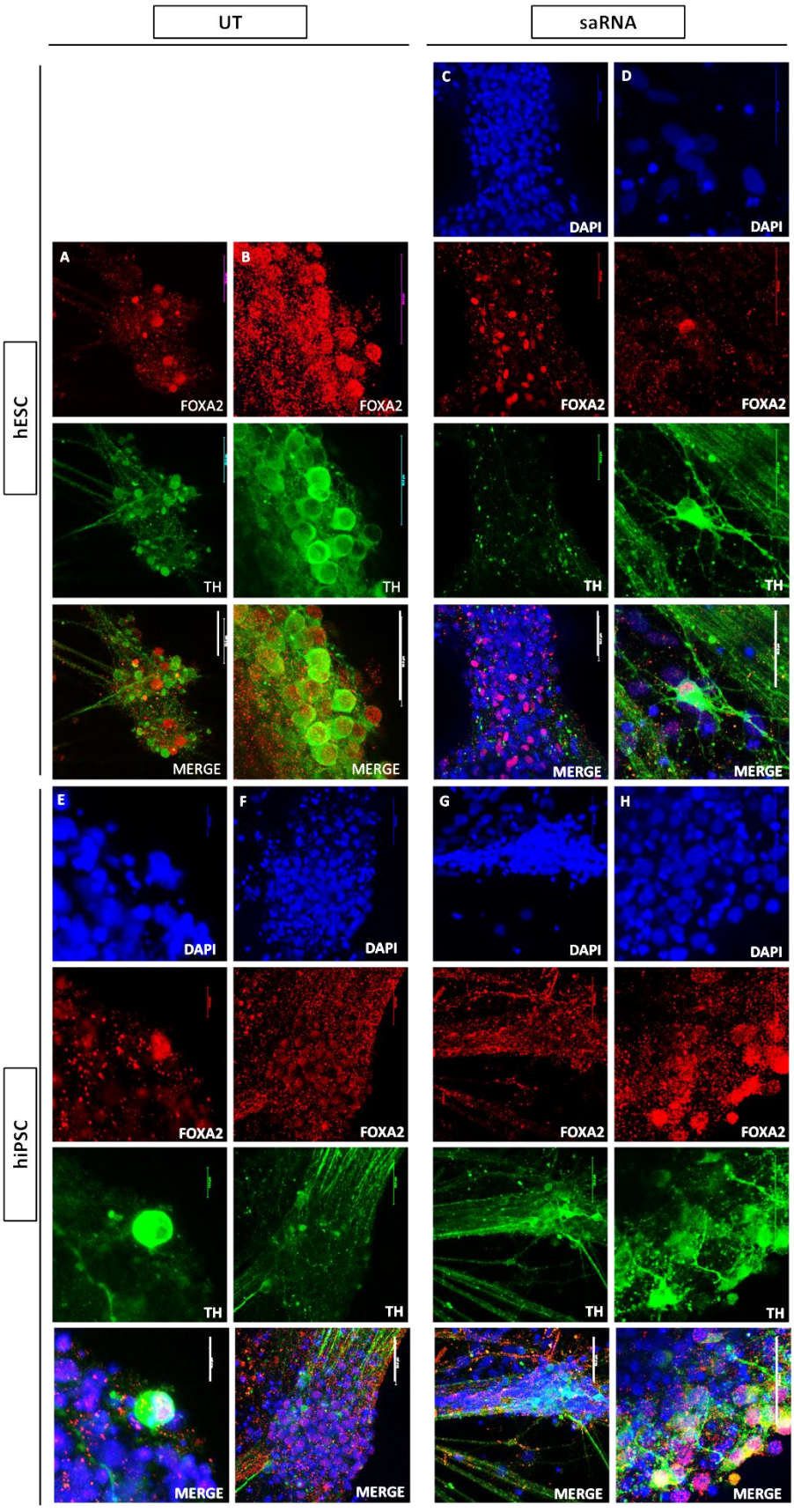


**Figure 58 - Confocal imaging of hPSC foxa2 and TH staining of untransfected and saRNA transfected cultures**

Representative confocal images of hESC (**A-D**) and hiPSC (**E-H**) cultures after 14 days UT and saRNA transfected culture in DDM stained with TH (green) and foxa2 (red) antibodies. Dapi (blue) stained the nuclei (All scale bars represent 50μm).

### 6.3.9 Co association analysis of Foxa2 and TH immunocytochemistry staining

To fully assess the ability of the DA differentiation protocol, with and without saRNA, to derive $TH^+/Foxa2^+$ neurons, confocal microscopy and Volocity software were used to quantify co-association of staining in matured neurospheres. Images were processed as described in Chapter 2, section 2.6.9. Unfortunately due to noise, for both hESC and hiPSC experimental groups no statistical difference between UT and saRNA could be ascertained (Figure 62).

Neurospheres (UT and saRNA transfected) derived from hESC and hiPSC (Figure 59/Figure 60) were shown to include $Foxa2^+$ and $TH^+$ cells. Data indicated that Foxa2 was enhanced in saRNA transfected cultures for both cell types but no significance could be identified due to noise (Figure 62). TH staining displayed the opposite trend, revealing a slight decrease in the volume of expression. Comparison with $2^o$ only confocal images in Figure 61 shows that each population contains $Foxa2^+$ and $TH^+$ cells but few were co-associated.

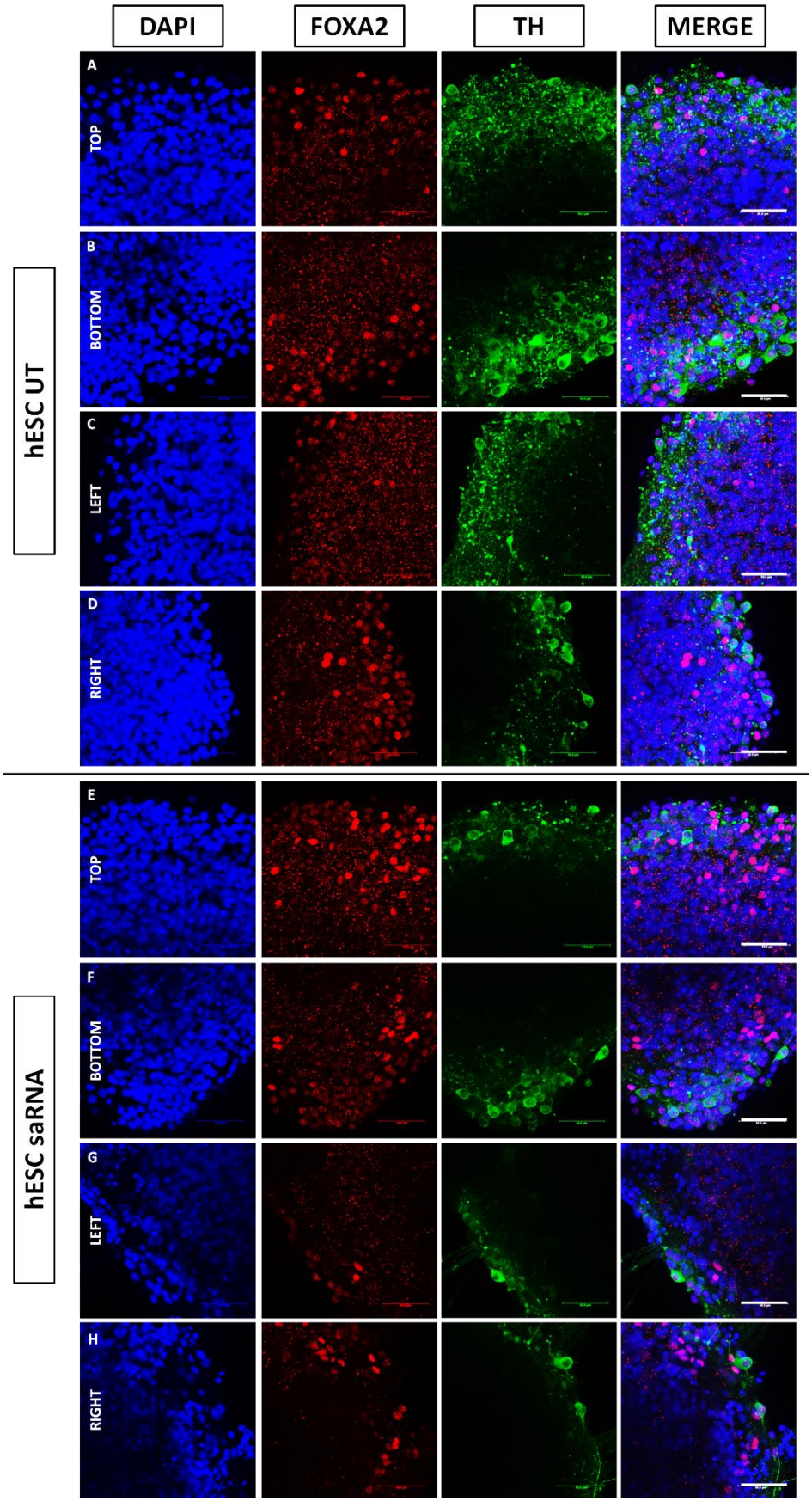


**Figure 59 - hESC foxa2 and TH confocal imaging of neurospheres**

Representative maximum intensity images of confocal images of hESC derived neurospheres cultured for 14 days in DDM. **A - D)** Representative UT neurospheres images. **E - H)** Representative images of saRNA transfected neurospheres. $Foxa2^{+}$ (red) and $TH^{+}$ (green) can be observed in all conditions with co association found to be minimal (Scale bars = 50µm).

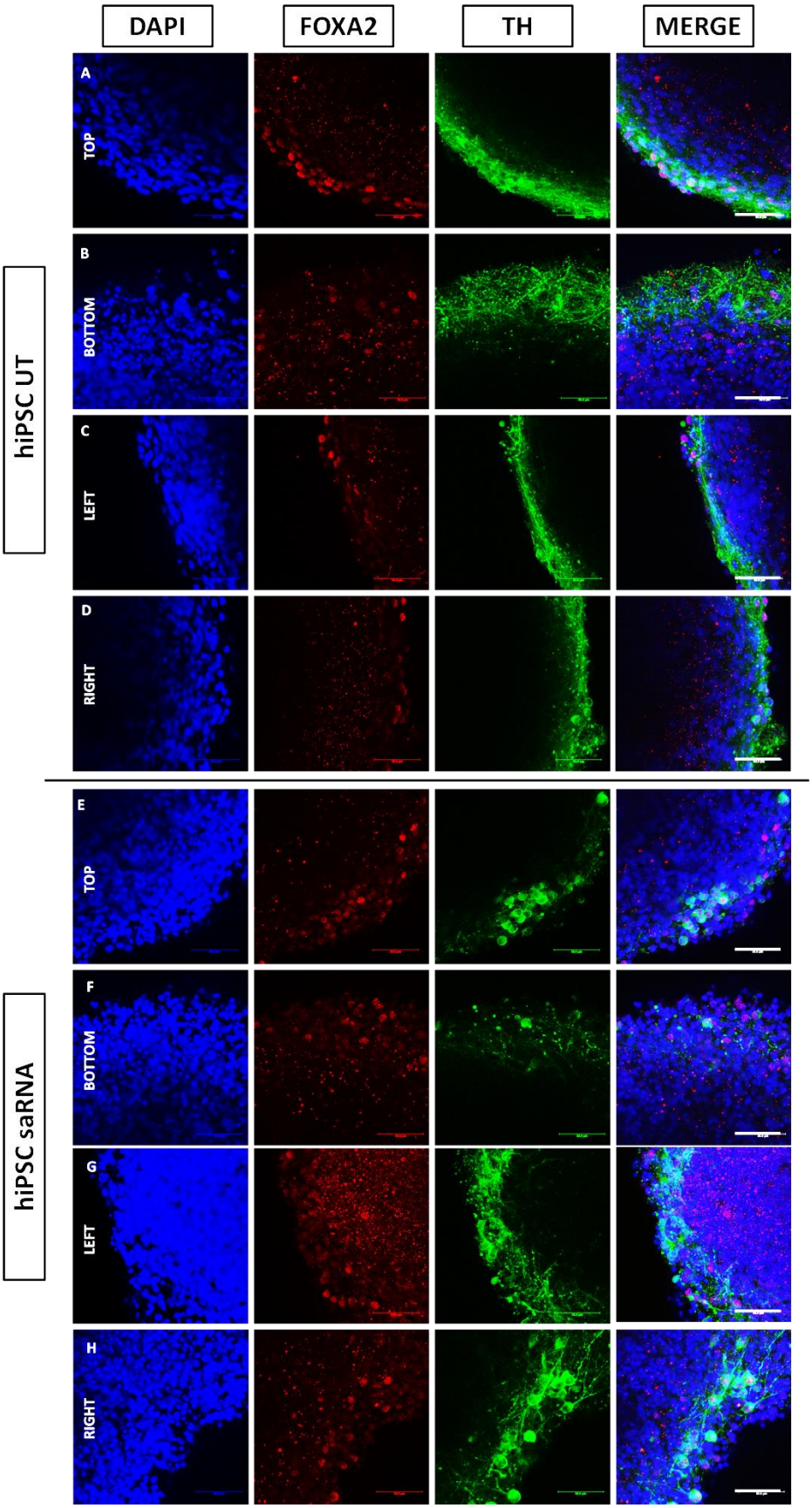


**Figure 60 - hiPSC foxa2 and TH confocal imaging of neurospheres**

Representative maximum intensity images of confocal images of hiPSC derived neurospheres cultured for 14 days in DDM. **A - D)** Representative UT neurospheres images. **E - H)** Representative images of saRNA transfected neurospheres. $Foxa2^{+}$ (red) and $TH^{+}$ (green) can be observed in all conditions with co association found to be minimal (Scale bars = 50µm).

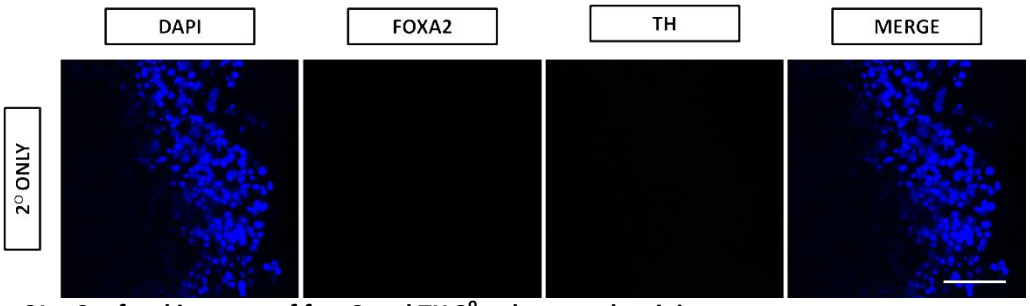


**Figure 61 – Confocal imagaes of foxa2 and TH 2° only control staining**
Representative maximum intensity images of 2° only staining for both Foxa2 and TH staining (Scale bar = 50µm).

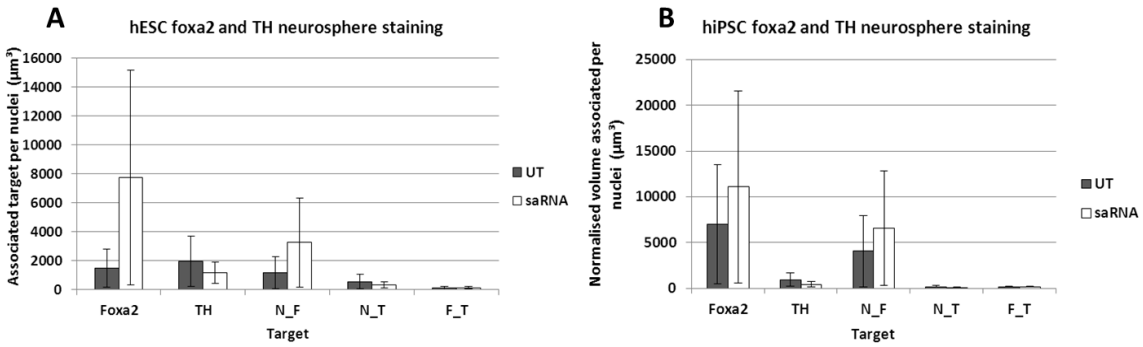


**Figure 62 - hiPSC associated volume of foxa2 and TH staining in hPSC derived neurospheres**
Graphs showing the associated volumes of positive staining for both TH and foxa2 in (A) hESC and (B) hiPSC derived neurospheres following Volocity analysis. Data is shown as volume (µm$^3$) per nuclei (Bars = SEM, n=3).

## 6.4 Investigating the impact of using a reduced number of saRNAs in enhancing target gene expression during dopaminergic differentiation

Next, we investigated the impact of the individual saRNA; we did this by reducing the number of saRNAs from the 3 target genes to 2, now targeting only *TH* and *lmx1a* and removing *foxa2*. The same transfection regime as previously used was utilised.

### 6.4.1 Impact of transfecting a reduced number of saRNA during dopaminergic differentiation - pluripotent gene expression

Analysis of mRNA expression showed pluripotent genes, *nanog* and *oct4,* in hESC and hiPSC decreased following neural induction (Figure 63, A/B & D/E). hESC, transfected with saRNA, appeared to show a greater reduction in *oct4* expression when compared with UT (Figure 63, B).

Expression of *sox2* in hESC and hiPSC marginally increased but then decreased to D0 levels by D24 in all conditions (Figure 63, C & F). With the exception of *oct4* in hESC, transfection with saRNA appeared to have little impact on pluripotent gene expression.

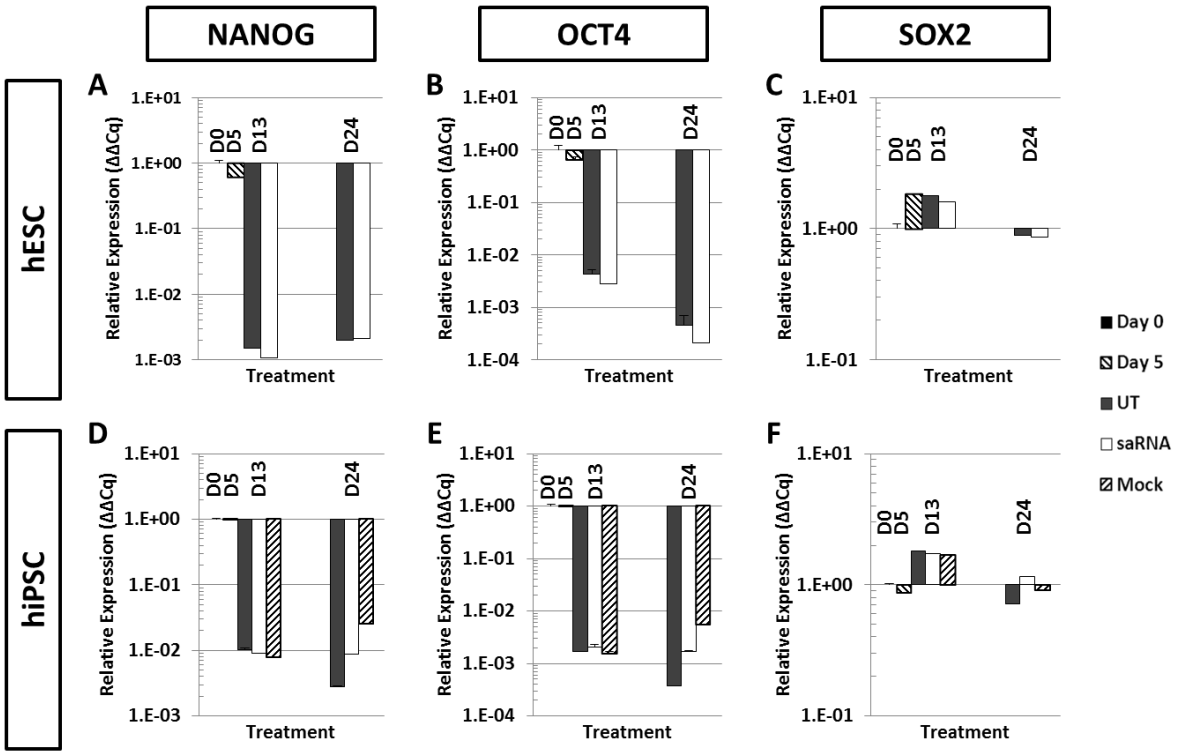


**Figure 63 - qPCR analysis of pluripotent gene expression following dopaminergic differentiation, with and without inclusion of TH and lmx1a saRNA**

qPCR analysis of pluripotent mRNA expression following dopaminergic differentiation and the inclusion with TH and lmx1a saRNA. hESC and hiPSC derived neurosphere expression of *nanog* **(A/D)**, *oct4* **(B/E)** and *sox2* **(C/F)** are shown at D5, D13 and D24 relative to D0. Data was normalised using *GAPDH, β-Actin and UBC* expression. (n=1)

### 6.4.2 Impact of transfecting a reduced number of saRNA during dopaminergic differentiation - fgf5 gene expression

Expression of *fgf5* expression in both hESC and hiPSC were observed to decrease for all conditions relative to D0 over the course of the protocol (Figure 64, A & B). Transfection with saRNA did not enhance the expression of *fgf5* by D24 when compared with D0 in either cell line.

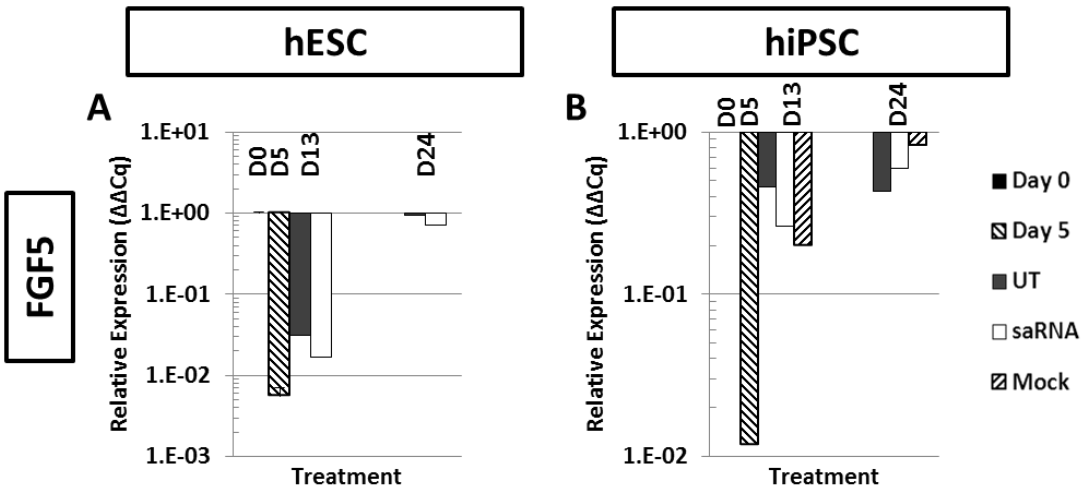


**Figure 64 - qPCR analysis of fgf5 gene expression following dopaminergic differentiation, with and without inclusion of TH and lmx1a saRNA**

qPCR analysis of *fgf5* mRNA expression following dopaminergic differentiation and transfection with TH and lmx1a saRNA. **(A)** hESC and **(B)** hiPSC derived neurosphere expression of *fgf5* was shown at D5, D13 and D24 relative to D0 expression. Data was normalised using *GAPDH, β-Actin* and *UBC* expression. (n=1)

### 6.4.3 Impact of transfecting a reduced number of saRNA during dopaminergic differentiation - germ layer gene expression

Germ layer markers *brachyury* and *sox17* were shown to reduce in both hESC and hiPSC by D24 (Figure 65, A/B & D/E) except in the case of saRNA transfected hiPSC expression of *brachyury* which was increased slightly, relative to D0. Expression of *nestin* was shown to increase in both cell types though only marginally, with hiPSC showing greater expression than that of hESC at both time points (Figure 65, C & F). hiPSC transfected with saRNA showed a marginal increase in *nestin* expression compared with UT by D24 (Figure 65, F).

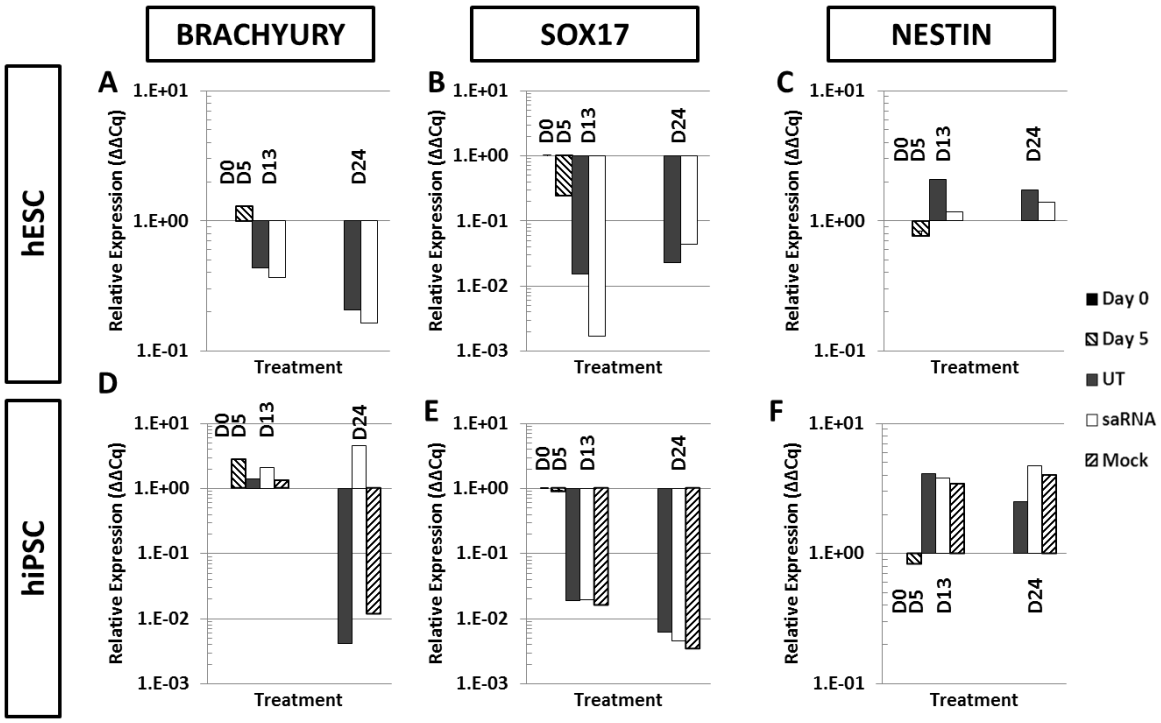


**Figure 65 - qPCR analysis of germ layer expression following dopaminergic differentiation, with and without inclusion of TH and lmx1a saRNA**

qPCR analysis of germ layer mRNA expression following dopaminergic differentiation and transfection with TH and lmx1a saRNAs. hESC and hiPSC derived neurosphere expression of *brachyury* **(A/D)**, *sox17* **(B/E)** and *nestin* **(C/F)** are shown at D5, D13 and D24 relative to D0 expression. Data was normalised using *GAPDH, β-Actin* and *UBC* expression. (n=1)

### 6.4.4 Impact of transfecting a reduced number of saRNA during dopaminergic differentiation - neuronal gene expression

Analysis of neuronal genes showed that *nurr1* and *en1* increased in expression to D24 in both hESC and hiPSC (Figure 66, A/C & D/F). *Nurr1* expression in both cell types was delayed, only showing a significant increase relative to D0 at D24. *En1* also showed a stepwise increase with expression in hESC by D24, with saRNA transfected cultures showing slighting increased levels of expression relative to UT. Expression of *otx2* was shown to decrease in both cell types though the decrease was observed to be greater in hiPSC (Figure 66, B & E).

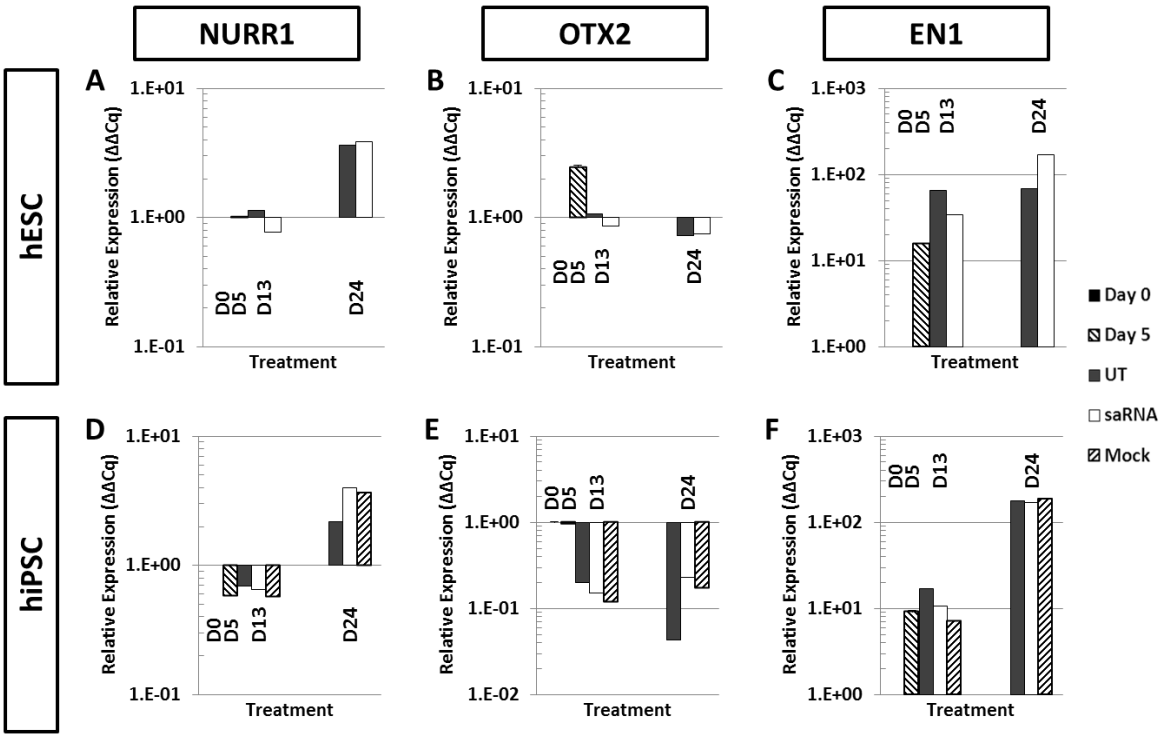


**Figure 66 - qPCR analysis of neuronal gene expression following dopaminergic differentiation, with and without inclusion of TH and lmx1a saRNA**

qPCR analysis of neuronal mRNA expression following dopaminergic differentiation and transfection with TH and lmx1a saRNAs. hESC and hiPSC derived neurosphere expression of *nurr1* **(A/D)**, *otx2* **(B/E)** and *en1* **(C/F)** are shown at D5, D13 and D24 relative to D0 expression. Data was normalised using *GAPDH, β-Actin* and *UBC* expression. (n=1)

### 6.4.5 Impact of transfecting a reduced number of saRNA during dopaminergic differentiation - dopaminergic gene expression

The expression levels of the DA genes assessed in the experiment increased relative to D0 in both cell types. *Lmx1a* in hESC and hiPSC at D24 showed greater expression in cultures that had been transfected with saRNA (Figure 67, B & F). This was also observed in *foxa2* expression with hiPSC, though in hESC this increase was only marginal (Figure 67, E & A). Expression of *TH* and *DRD* in both hESC and hiPSC gradually increased to D24 levels but no distinction could be made between expression level according to culture conditions (Figure 67, C-D & G-H).

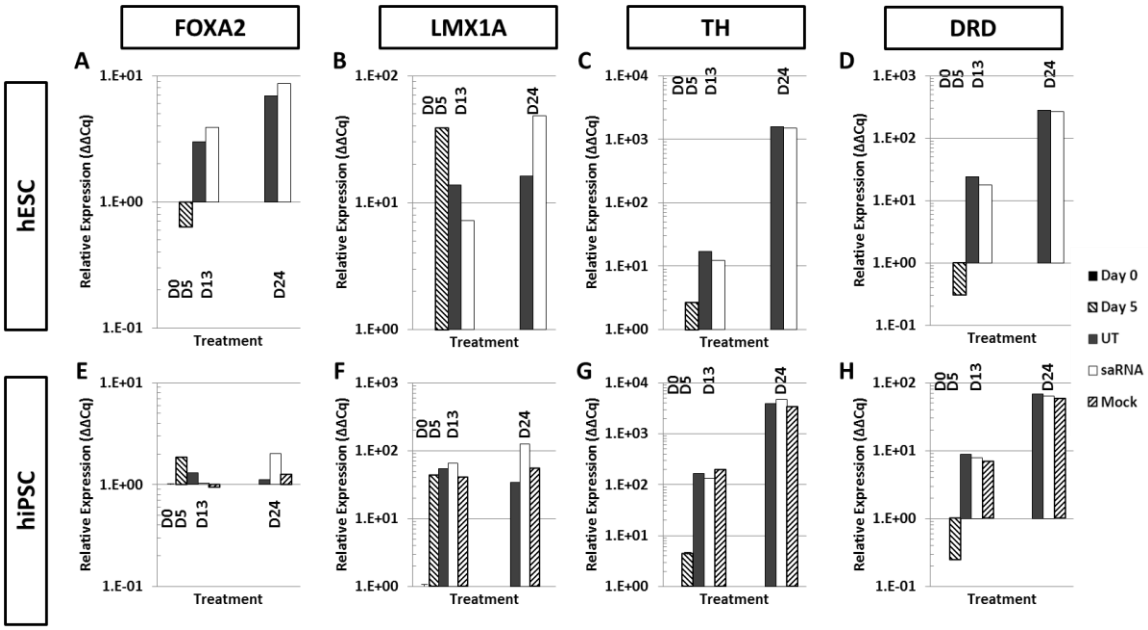


**Figure 67 - qPCR analysis of dopaminergic gene expression following dopaminergic differentiation, with and without inclusion of TH and lmx1a saRNA**

qPCR analysis of dopaminergic mRNA expression following dopaminergic differentiation and transfection with TH and lmx1a saRNAs. hESC and hiPSC derived neurosphere expression of *foxa2* **(A/E)**, lmx1a **(B/F),** *TH* **(C/G)** and *DRD* **(D/H)** are shown at D5, D13 and D24 relative to D0 expression. Data was normalised using *GAPDH, β-Actin* and *UBC* expression. (n=1)

## 6.5 Assessing the efficiency of transfecting cell aggregates in suspension

Transfection of saRNA was shown to have little impact on gene expression and so an investigation was developed to investigate the ability of nanofectin to transfect cell aggregates. This was to test the hypothesis, only the surface cells of the aggregates were affected by the saRNA. If this was the case the majority of the cells within the aggregate were not being influenced, and so the impact of the saRNA in our previous experiments would have been overshadowed.

To assess the efficiency of transfecting cell aggregates in suspension we used aggrewell technology. This technology generated uniformly sized aggregates which allowed us to tightly control and assess the impact of aggregate size on transfection efficiency (Figure 68).

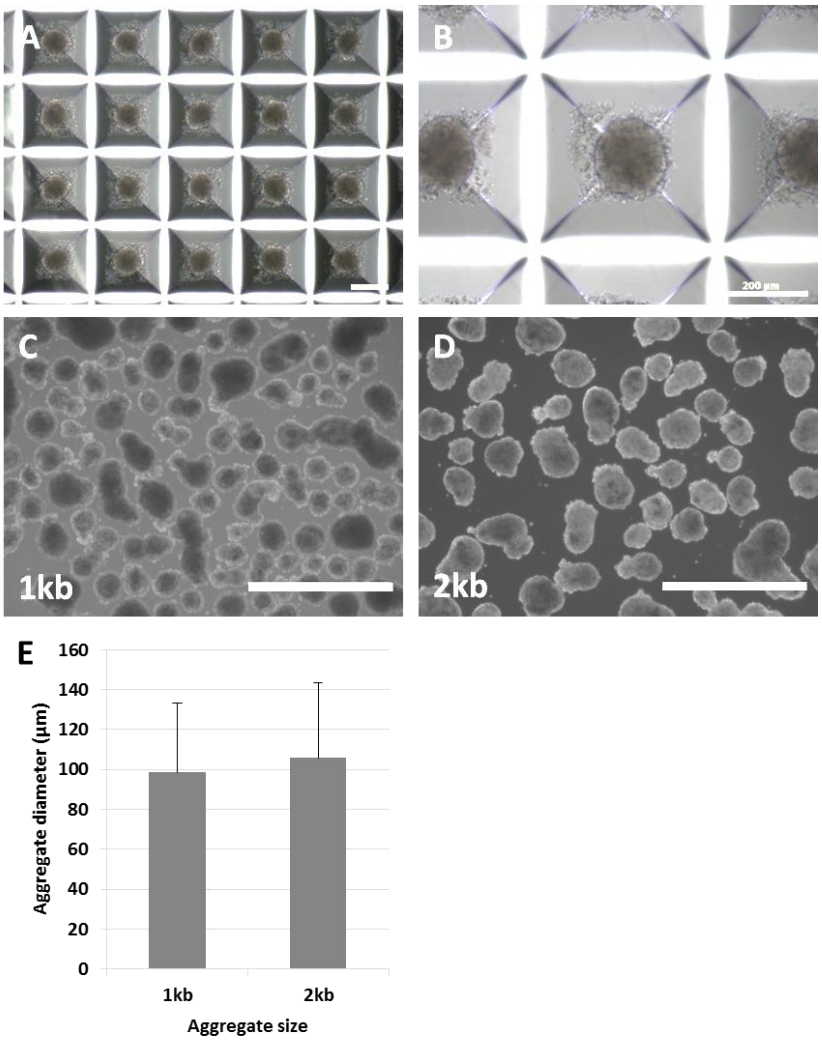


**Figure 68 - Aggrewell EB formation**
**A/B)** Representative aggrewell formation images, a single cell suspension has been applied to the aggrewell well and centrifuged to evenly distribute the cells across the wells, uniform sized EBs are generated (Scale bar = 200µm). Representative image of aggrewell generated EBs in suspension at 1kb **(C)** and 2kb **(D)** sizes (Scale bar = 1000µm). **E)** Shows EB diameter distribution of EBs of 1kb and 2kb cells (Error bars = ±SD)

### 6.5.1 Quantification of aggregate transfection efficiency

Aggregates were generated that contained 1,000 and 2,000 cells per aggregate; these were then transfected over 3 days and assessed using flow cytometry. Aggregates treated with nanofectin and siGLO were shown to be positively transfected relative to UT aggregates, confirming that nanofectin was appropriate for transfecting hPSC aggregates (Figure 69, A - D). Flow cytometry analysis showed a material difference in transfection efficiency associate with aggregate size. Transfection was shown to be more efficient in smaller 1k cell aggregates (1.57%) than in the larger aggregates of 2k (0.05%, Figure 69, E).

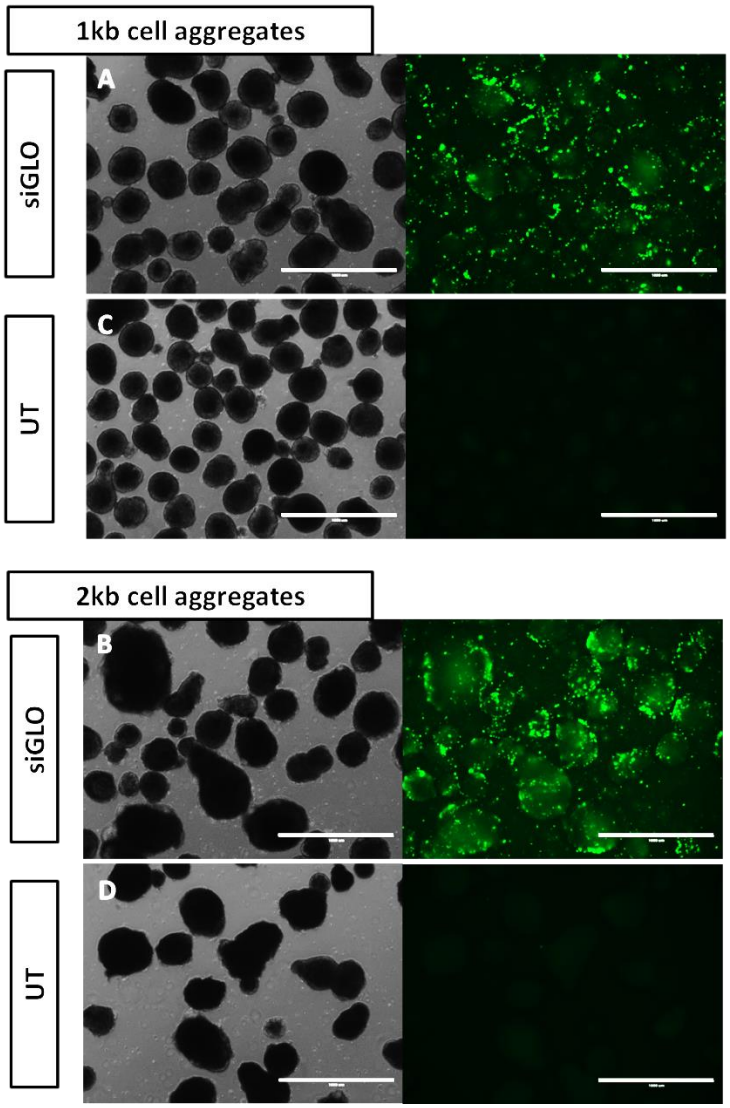


**E**

| | % positive | Average |
|---|---|---|
| **Aggregate (1k)** | | |
| UT 1 | 1.0% | |
| UT 2 | 1.9% | 1.43% |
| siGLO1 | 2.1% | |
| siGLO2 | 3.9% | 2.99% |
| Transfection efficiency | | 1.57% |
| **Aggregate (2kb)** | | |
| UT 1 | 1.1% | |
| UT 2 | 2.7% | 1.86% |
| siGLO1 | 1.6% | |
| siGLO2 | 2.2% | 1.92% |
| Transfection efficiency | | 0.05% |

**Figure 69 - Analysis of siGLO transfected cell aggregates**

Representative images of 1kb **(A)** and 2kb **(B)** siGLO transfected cell aggregates and UT controls (**C** & **D**) (Scale bars = 1000µm). **E)** Flow cytometry data collected following disassociation of cell aggregates at varying sizes and the number of viable transfected cells in the population minus the negative control.

## 6.6 Discussion

### 6.6.1 Transfection of hPSC using Nanofectin

Nanofectin was selected as the transfection reagent for this research; this was the favoured reagent by Omnicyte Ltd. and would allow them to continue to develop this work in the future. hPSC transfection efficiency was assessed using a transfection control (fluorescence emitting siGLO), and resulted in positive emission at 488nm in both hESC and hiPSC (Figure 49, C & F). A degree of cell death in the siGLO transfected cultures (absent in the UT and mock transfected cultures) indicates that the siGLO element may contribute to greater cell death (Figure 49, B & E). It is important to recognise this potential impact of the cyctoxcity of saRNAs, however if a higher efficiency of derivation of target cell populations is achieved at the expense of a small degree of cell death, the trade-off is tenable.

Results observed using fluorescent microscopy on the suspension-based culture system showed that cell aggregates were 488nm positive relative to the UT control (Figure 51). This indicated that the transfection method used for adherent cultures could be translated to our suspension differentiation system, which would be important for translating the process to industry-ready bioreactor technologies.

### 6.6.2 saRNA function confirmed using hPSC

hiPSC cultures were transfected with the candidate saRNA to assess their effect on target gene expression (Figure 50). It was shown that all target gene expression levels increased relative to UT following transfection, though *TH* expression increased only marginally. Foxa2 and TH saRNA transfected cultures increased in target gene expression relative to saRNA concentration increase (Figure 50, A & C) suggesting that the activity of these saRNAs was not saturated and could be further optimised. For the purposes of this work and with limited resources and time, and given the positive correlation between concentration and gene potency, it was decided that work should progress using the highest saRNA concentration (50nM) for transfection. All target genes were found to have the greatest increase in

expression following transfection with all three saRNA candidates (Figure 50, A-C). These investigations were performed in duplicate and confirmed previous findings by Omnicyte Ltd. (unpublished).

This work shows that using the combination of saRNA produces superior results to transfecting with the individual saRNAs. From this point all transfections were carried out in combination and at the higher concentration of 50nM.

### 6.6.3 Molecular analysis of saRNA transfected cultures versus UT cultures

Analysis of pluripotent markers was performed to assess the relative impact of saRNA inclusion compared with UT (statistically significant) and mock (indicative due to low replicative numbers) transfected cultures. The expression of both *nanog* and *oct4* in hESC and hiPSC cultures were shown to be substantially down-regulated following 24 days of differentiation culture (Figure 52, A/B & D/E) but no difference was observed between treatments, except in the case of hESC *oct4* expression where saRNA transfection resulted in a greater reduction. These results indicate that cultures are moving away from a pluripotent state and differentiating (Pan and Thomson 2007), although the qPCR methodology does not allow us to assess what proportion of the population remains pluripotent. *Sox2* expression was found to increase in both hESC and hiPSC up to D24 and then drop to D38 (Figure 52, C & F). Although *sox2* was assessed as a pluripotency marker, it is also a marker for neuronal progenitors (Graham, Khudyakov et al. 2003), and the increase in expression may indicate that cultures to D24 contain a greater proportion of neuronal progenitors, but these may be lost by D38, as the neurons develop and mature. The move from a pluripotent state is further confirmed through the expression of *fgf5*. Significantly increased expression of *fgf5* in hiPSC by D24 (Figure 53, B) and hESC by D38 (Figure 53, A) indicates early differentiation and the presence of a primitive *fgf5*$^{+}$ ectoderm population (Hitoshi, Seaberg et al. 2004). SaRNA transfected cultures showed that saRNA had no significant impact on the experimental culture's early development compared with the differentiation media itself, both pluripotent markers and

neuronal progenitor *fgf5* marker expressions suggest that saRNA does not impact the shift away from pluripotency or on early differentiation towards a neuronal lineage.

Analysis of contaminating mesoderm and endoderm markers, *brachyury* and *sox17,* indicated that all conditions resulted in a drop in expression in hESCs and hiPSC (Figure 54, A/B & D/E). *Nestin* was observed to increase significantly in both hESC and hiPSC by D24 (Figure 54, C & F) confirming again that the cultures moved towards an ectoderm lineage (Suzuki, Namiki et al. 2010). Again, saRNA transfection had no effect on germ layer marker expression above that of the differentiation media, suggesting no involvement in lineage commitment and early differentiation.

Neuronal marker gene analysis showed increased levels of *sox1, en1* and *nurr1* (Figure 55) in both hESC and hiPSC cultures, this implies that cultures are differentiating and developing down the neuronal lineage and moving towards the midbrain cell type (Sacchetti, Carpentier et al. 2006). Unfortunately, *otx2* in both cell types by D38 were lower than the original expression levels at D0. This finding is a similar result from Chapter 4, and emphasizes the need for further optimisation of the patterning process. *Otx2* being the 'master' anterior-posterior patterning module gene (Omodei, Acampora et al. 2008) implies it is an essential step in the differentiation of DA neurons.

saRNA transfected hESC cultures exhibited a slight increase relative to the control arms for a number of the neuronal markers assessed (*nurr1, en1* and *sox1*), suggesting that transfection may be increasing gene expression within the cell population. This was not the case in hiPSC where no difference was observed. These results confirm that all conditions are able to form neuronal populations that express a number of the desired neuronal markers but no significant effect on gene expression was caused by transfection with saRNA. It also suggests that the population being created may not be the A9 midbrain neuronal population, indicated by the loss of *otx2* expression which has been shown by Chung *et al*. to be a marker for the efficient generation of DA neurons (Chung, Moon et al. 2011).

Analysis of DA target genes in hESC and hiPSC confirmed the findings of Chapter 4, showing that the DA differentiation protocol generates *foxa2*$^{+}$/*lmx1a*$^{+}$/*TH*$^{+}$ populations. The inclusion of saRNA within the differentiation protocol did not result in significant changes in the majority of genes assessed. Although it was observed that marginally higher expression levels for target genes: *TH*, *lmx1a* and *DRD* (Figure 56) were found in hESC cultures when transfected, suggesting that the saRNAs did impact slightly on expression levels. Further optimisation of the process could result in significant results. *Foxa2* expression in hESC cultures was observed to be significantly impacted by transfection over that of UT cultures (Figure 56, A). *Foxa2* expression was also of note due to the disappointing findings of Chapter 4, where expression was negative by D24. *Foxa2* expression in this investigation was observed across all conditions, potentially resulting from the age of the cultures. hiPSC showed no significant difference between UT and saRNA transfected cultures for *foxa2, lmx1a* and *DRD* expression, however did show significantly enhanced expression for *TH* in saRNA transfected cultures over that of UT (Figure 56, G). hiPSC expression of *foxa2* was shown never to exceed that of D0 confirming results from Chapter 4 and implying that hiPSC, specifically MSUH001 may not be suitable for this type of cell manipulation.

These findings though not significant, suggest that saRNA transfection has some impact on the gene expression. It is possible that the effects of the saRNA in our findings are overshadowed by the total population mRNA expression. This is a limitation of the analytical technique (qPCR) employed within this work.

### 6.6.4 Confocal analysis of saRNA transfected cultures versus UT cultures

qPCR allowed us to assess gene expression at a population level but not at the individual cell level, confirming qPCR findings using immunocytochemistry was important, reflecting the translation of mRNA to protein and the locality of *foxa2* and *TH* up-regulation. Confocal microscopy confirmed that both UT DA differentiation and saRNA incorporation generated neuronal (β-III-Tubulin$^{+}$) cell types from both hESC and hiPSC (Figure 57, A-D & E-H). It was

observed that all treatments produced β-III-Tubulin$^{+}$/TH$^{+}$ cells, confirming neuronal differentiation had been achieved, and also confirmed results from the qPCR analysis, showing that *TH* was being translated to the protein level. Immunocytochemistry staining of differentiated cultures also confirmed the presence of Foxa2$^{+}$/TH$^{+}$ cells within the cultures following 14 days in DDM (Figure 58), however co-association was found to be rare (Figure 59/Figure 60). This low level of co-expression and the lack of *otx2* gene expression indicated that the cells generated within this work were not all the targeted A9 midbrain DA neurons desired.

Quantification of Foxa2$^{+}$ and TH$^{+}$ cells and their co-expression was attempted using confocal microscopy and Volocity software (Figure 59, Figure 60). Representative images were taken from four locations on the neurospheres from all culture conditions and this was repeated for all three biological replicates. This work confirmed that Foxa2$^{+}$ and TH$^{+}$ cells were present in all cultures but co-staining (Foxa2$^{+}$/TH$^{+}$) was found only rarely. saRNA transfection appeared to increase the level of Foxa2 protein expression but reduced TH protein levels relative to UT cultures. Results were so varied that significant conclusions could not be drawn. These findings indicated that though the protocols with and without saRNA could differentiate hPSC toward a DA (Foxa2$^{+}$/TH$^{+}$) lineage, consistency within the protocol had not been achieved.

### 6.6.5 The potential of reducing the saRNA incorporated into the protocol

To understand the individual impact of the saRNA and to assess the importance in their inclusion we undertook an investigation that removed foxa2 saRNA from the work. *Foxa2* gene expression was shown to be impacted the greatest when cultures were transfected with all saRNA. It was hypothesised that any changes observed were due to the foxa2 saRNA targeting that specific target gene.

qPCR analysis showed that pluripotent marker gene expression dropped in hESC and hiPSC mimicking previous findings (Figure 64). *Fgf5* expression behaved atypically during this experiment with reductions in expression observed in all conditions (Figure 65). The expression

of neuronal genes was low when compared with previous findings, with *nurr1* and *otx2* showing very little change from D0 levels in hESC and negative expression in hiPSC (Figure 66), contradictory to findings in the previous work (Figure 55).

In addition, DA marker gene expression was contrary to previous experiments: in previous work, *foxa2* in hESC and *TH* in hiPSC showed significant differences in expression for cultures transfected with saRNA (Figure 56, A & G) whereas in the reduced saRNA work, differences were not found (Figure 67, A & G). These findings suggest a vital role for the foxa2 saRNA in the protocol. This result compliments the work of Kriks *et al*. which suggests that a number of factors can be required to induce the desired response, not just one factor is always the master trigger (Kriks, Shim et al. 2011).

These results may also indicate variability in the quality of the starting material or in the reagents used. Cell types were continuously cultured from frozen samples and maintained over time in feeder-based cultures, the inherent age of the cultures could impact on their performance (Xie, Hiona et al. 2011). It is possible that the reduced saRNA experiment was performed on cells that were different genetically (due to age or cryopreservation) to those used in the previous experiments, impacting results. Karyotyping was periodically undertaken (outsourced) for the cell lines used within this work, this was done to assess the karyotypic stability of the cell lines, but this did not control against point mutations or genetic modification. Moreover, RNAi research has shown that uncharacterised off-target effects might play a role in determining gene expression responses (Jackson and Linsley 2010). The reagents used may have also been affected over time, chemical and growth factors were stored in their respective recommended conditions and freeze-thaw was kept to a minimum during this work, although effects outside of our control could have led to the degradation of reagents, impacting on results. These are all aspects that would need to be understood and mitigated if this technology is to progress towards the clinic.

### 6.6.6 Aggregate transfection efficiency

Transfection data from adhered cultures indicated that the enhancement in target gene expression in cultures transfected with saRNA should be significant. And yet cell aggregates showed neutral to low impact of saRNA on gene expression. To understand this contradiction, we artificially formed aggregates of known cell volumes, either 1,000 or 2,000 cells per aggregate using aggrewell technology (Figure 68). Aggregates were transfected with the siGLO transfection control over 3 days and then dissociated and quantified using flow cytometry. This work showed that the size of the aggregate influenced the transfection efficiency of the protocol and it is logical that the larger the aggregate the fewer cells are exposed to the transfection reagent, reducing the efficiency of the reagent (Figure 69). This observation may explain the low level of influence of the saRNA and would be an interesting area for future work. I propose that due to our protocol being based on aggregate technology and neurosphere expansion, only a small proportion of the cells on the surface were exposed to the lipid based regent and saRNA. Cells within the aggregate core will have not been in contact with the saRNA and so unaffected, resulting in the population gene study results (qPCR) being overshadowed by the mass of unaffected cells in the centre of the aggregates, influenced only by the media conditions.

## 6.7 Conclusion

hPSC can be successfully transfected using nanofectin in adhered culture and this is translatable to suspension culture. The functionality of saRNA in adhered hiPSC was found to have the greatest effect on target gene expression when all saRNA were used in conjunction. Unfortunately when this technology was used on aggregates during differentiation, transfection was inefficient and failed to promote greater effects beyond that of differentiation media alone. New strategies to penetrate beyond the outer surface layers of the aggregates need to be explored. Lipid-based transfection methods may not be optimal for aggregates due to transient functioning of saRNA and due to the need for continuous application, disassociating the cells is not an option.

# CHAPTER 7 - THE EFFECT OF INITIAL SEEDING DENSITY ON PLURIPOTENT AND NEURONAL GENE EXPRESSION DURING 11 DAYS OF NEURONAL PRIMING

This independent section of work was designed to investigate the effects of initial cell seeding density (ICSD) on the expression of neuronal genes by two hPSC populations, hESC (Shef6) and hiPSC (MSUH001), during an 11 day neuronal priming protocol.

## 7.1 Introduction

In order to successfully address the challenges of cell therapy manufacture at an industrial scale, it is important to ensure all stages of the bioprocess are optimised firstly at the bench scale. The initial stage of many expansion or differentiation processes involves the plating of the cell population onto an appropriate substrate for attachment and growth. The substrate has been shown to be critical for culture, for example hPSCs are often plated onto iMEF (Thomson, Itskovitz-Eldor et al. , Reubinoff, Pera et al. 2000) or specially adapted for survival and growth on acellular materials such as matrigel (Xu, Inokuma et al. 2001). In addition to substrate, ICSD can have a significant impact on cell behaviour and is reported to alter proliferation and differentiation responses of various adult cells during 2D culture (Peh, Toh et al. 2013) and 3D culture for tissue engineering purposes (Oh, Lee et al. 2012). In the case of hPSC it has been shown that passaging hESC colonies at a lower density of 1:8 results in a higher degree of spontaneous differentiation versus those passaged at a higher density of 1:3 (Heng, Liu et al. 2006). Using mouse 46C embryonic stem cells, Veraitch *et al.* demonstrated that lower ICSD specifically enhanced neuroectoderm differentiation, identified by enhanced *sox1* expression (Veraitch, Scott et al. 2008).

For these reasons ICSD should be addressed when investigating the scalable expansion of therapeutic cell lines to achieve the necessary clinical quantities. As cell therapy culture develops from lab scale to manufacturing scale, it will be important to address ICSD in both an

adherent and suspension-based system, this may be in the form bioreactor or micro-carrier bead culture (Abbasalizadeh, Larijani et al. 2012, Bardy, Chen et al. 2013). Scalable expansion obstacles are not just the case for primary somatic cell populations, where expansion is held back by limited replicative potential and biological changes accompanying cell aging (Salehinejad, Alitheen et al. 2013), but also for pluripotent cell lines that are prone to karyotypic abnormalities with extended periods in culture (Pera 2011, Steinemann, Gohring et al. 2013). Understanding the impact of ICSD will allow researchers to optimize and potentially reduce the starting material needed to produce a cellular therapeutic, which will be of substantial benefit to the regenerative medicine industry.

## 7.2 Aim

The aim of this study was to determine the impact of ICSD on the expression of key genes during neuronal induction of hPSC lines. Work was based on established protocols, which use smad signalling inhibition along with DA factors to induce neuronal differentiation (Chambers, Fasano et al. 2009, Kriks, Shim et al. 2011) and mapped the gene expression profile associated with the shift away from a pluripotent state, during neuronal priming and induction of a specialised phenotype over the first 11 days of differentiation.

## 7.3 ICSD Results

### 7.3.1 ICSD confluence analysis

Confluence analysis of the hESC culture population (Figure 70, A & B) showed that over the first 4 days of culture, each ICSD showed distinct cell coverage in comparison to the other ICSD investigated, however, by D6 this difference had disappeared and all cultures reached 100% confluence. No significance was observed between the three ICSD; 10k/$cm^2$, 18k/$cm^2$ and 25k/$cm^2$ at any time point.

A similar trend was observed with the hiPSC population (Figure 70, C) with cell confluence steadily increasing over the culture period, no significance was observed across the ICSD investigated.

From these findings it was decided that neuronal priming would commence at D3, although no significance was observed, distinct cell densities (associated with the different ICSD) could be observed in both cell types.

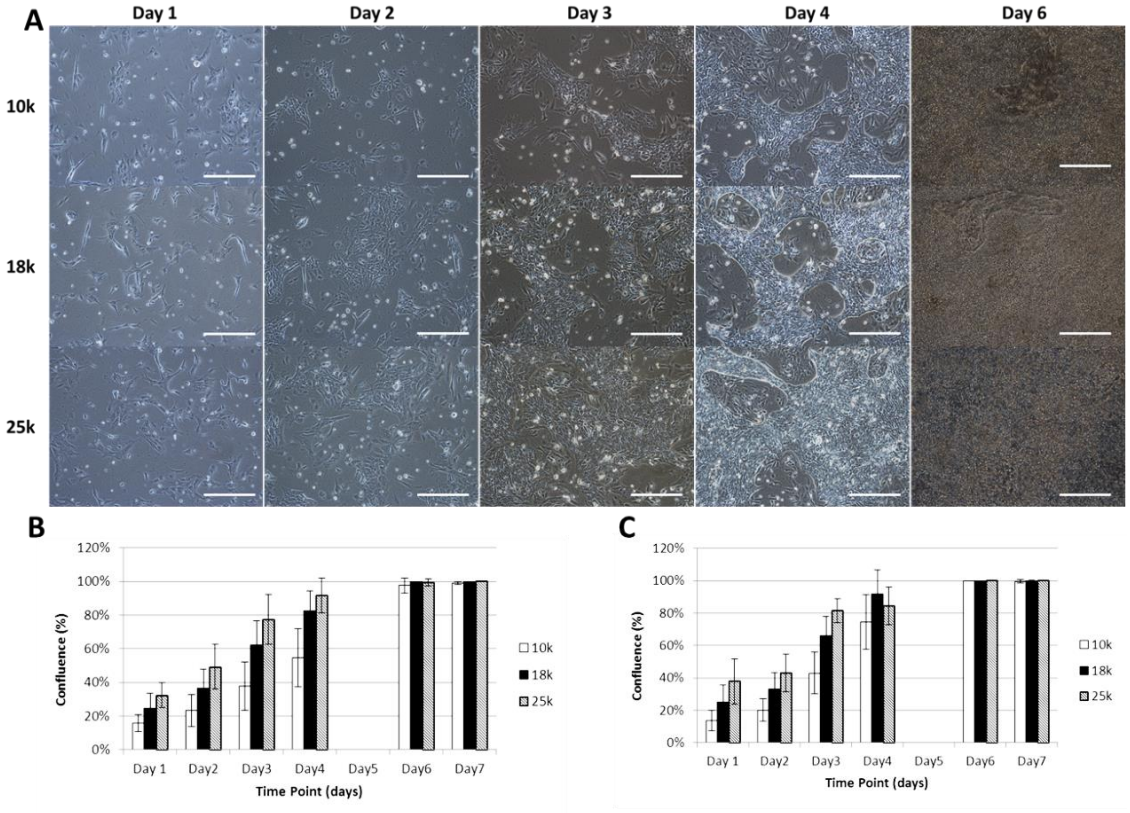


**Figure 70 - hPSC ICSD confluence over 7 days**
**A) Representative bright-field images of hESC confluence over the initial 6 days of expansion (Scale bar = 400µm). B) hESC and C) hiPSC confluence analysis performed over 7 days, 20 representative images of each cell density were taken in duplicate, daily. Confluence was assessed using Method for Automated Confluence Estimation software (Error bars represent SEM, n=2 (day 1-4) n=1 (day 6-7)).**

### 7.3.2 ICSD impact on culture population gene expression

hPSCs were cultured according to the protocol described in materials and methods. Cell samples were harvested at D0, D5 and D11 and assessed using qPCR, allowing us to track the changes in gene expression throughout the priming protocol.

### 7.3.3 Influence of ICSD on hPSC pluripotent gene expression

qPCR analysis of pluripotent mRNA expression of both *nanog* and *oct4* showed that neuronal priming with smad inhibition resulted in significant reductions of *nanog* and *oct4* gene expression across all ICSD, in both hPSC types. hESC and hiPSC expression of *nanog* was shown to decrease $>1.9^{-1}\Delta\Delta Cq$ and $>1^{-2}\Delta\Delta Cq$ fold relative to D0 by D5 (Figure 71, A, D). At D5 hESC *nanog* expression indicated that lower ICSDs resulted in a greater decrease in expression relative to 25k/cm$^2$, this trend did not continue to D11. In both cell types this reduction in expression was maintained through to D11. *Oct4* expression exhibited a stepwise reduction in

expression for both cell types. D5 expression showed significant decreases in expression with hiPSC showing the greatest reduction. This trend carried on through to D11 where hiPSC showed a $>1^{-3}\Delta\Delta Cq$ compared with hESC reduction of $>1.2x10^{-2}\Delta\Delta Cq$ (Figure 71, E, B).

Expression of *sox2* unlike *nanog* and *oct4* was shown to increase in both cell types (Figure 71, C, F). hESC analysis showed that higher ICSDs resulted in significantly greater expression of *sox2* relative to D0. At D5, 25k/cm$^2$ exhibited significantly higher levels of expression relative to other ICSD investigated, and by D11, both 18k/cm$^2$ and 25k/cm$^2$ showed similar and significantly higher expression levels relative to 10k/cm$^2$.

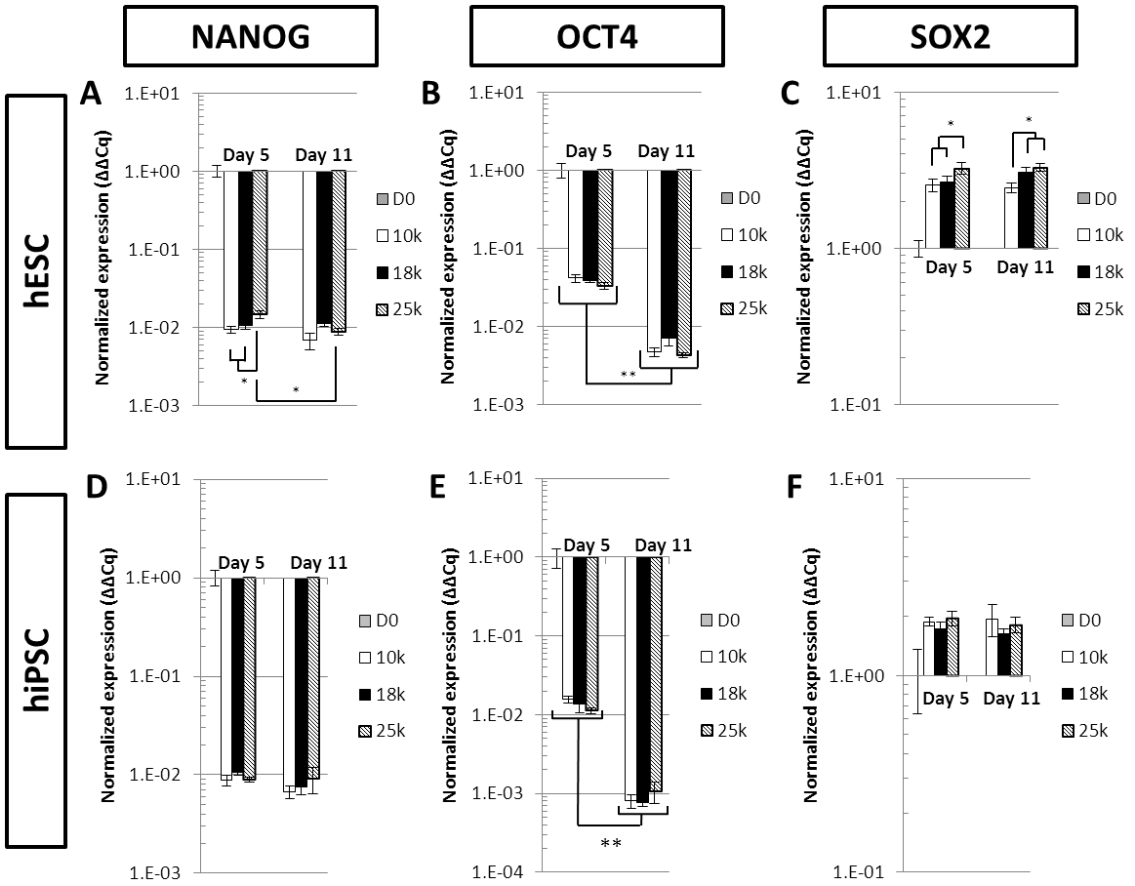


**Figure 71 - qPCR analysis of the influence of ICSD on pluripotent gene expression during neuronal priming**

qPCR analysis of pluripotent mRNA expression over the course of neuronal priming, D0 through to D11. hESC and hiPSC expression of *nanog* **(A/D)**, *oct4* **(B/E)** and *sox2* **(C/F)** are shown relative to D0 expression. Data was normalised using *GAPDH, Ubiquitin-C and β-Actin* expression (* p< 0.05 and ** p<0.01. Bars = Mean ± SEM. n=3).

### 7.3.4 Influence of ICSD on hPSC *fgf5* gene expression

hESC expression of *fgf5* was shown to significantly increase by D5 and continued to increase for the duration of the protocol at the three ICSDs. However, both 18k & 25k/cm$^2$ increased significantly whilst 10k/cm$^2$ did not over the remaining 6 day period to D11 (Figure 72, A). Expression of *fgf5* in hiPSC increased relative to D0 but did not continue to increase over time. At both the time points, *fgf5* expression was higher in 25k/cm$^2$ ICSD (Figure 72, B).

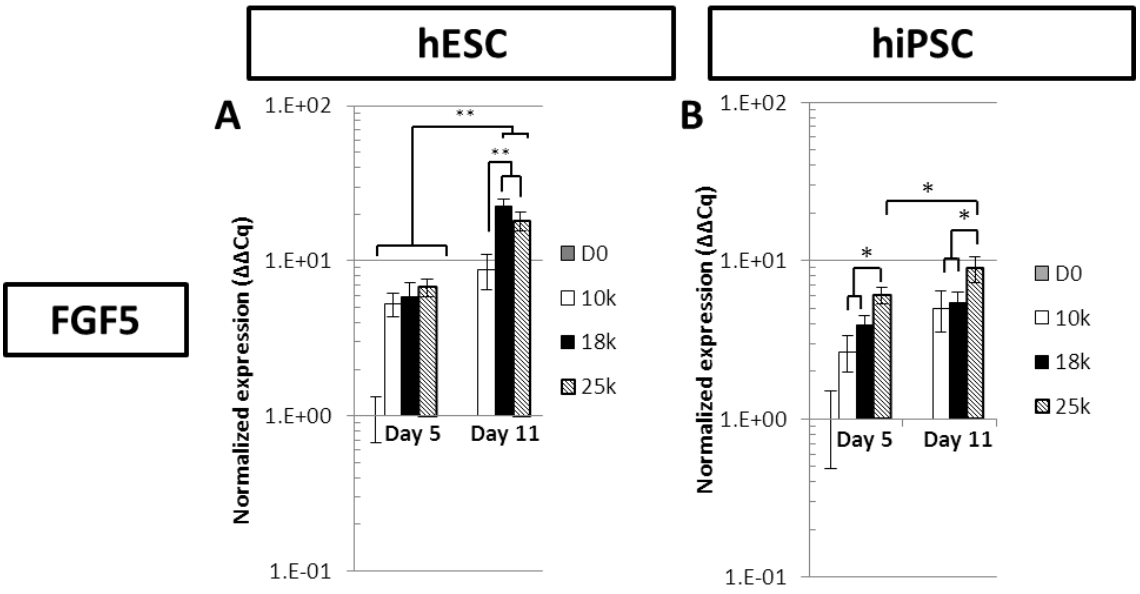


**Figure 72 - qPCR analysis of the influence of ICSD on *fgf5* expression during neuronal priming**
qPCR analysis of *fgf5* mRNA expression over the course of neuronal priming, D0 through to D11. **(A)** hESC and **(B)** hiPSC expression of *fgf5* is shown relative to D0 expression. Data was normalised using *GAPDH, Ubiquitin-C and β-Actin* expression (* p< 0.05 and ** p<0.01. Bars = Mean ± SEM. n=3).

### 7.3.5 Influence of ICSD on hPSC *sox1* and *pax6* gene expression

hESC early neuronal marker *sox1* expression (Figure 73, A) was enhanced over time for all ICSD to D11. At D11, 10k/cm$^2$ was shown to have enhanced expression relative to the two higher ICSD. *Pax6* expression also increased throughout the duration of the protocol, with no distinction identified between the ICSD by D11 (Figure 73, B).

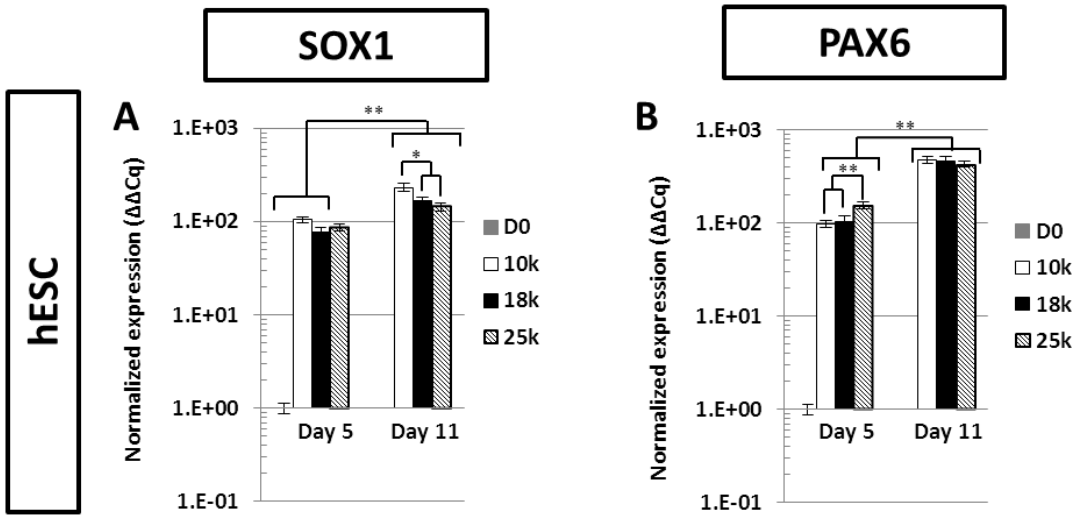


**Figure 73 - qPCR analysis of the influence of ICSD on hESC sox1 and pax6 expression during neuronal priming**

qPCR analysis of hESC mRNA expression over the course of neuronal priming, D0 through to D11. Expression of **(A)** sox1 and **(B)** pax6 are shown relative to D0 expression. Data was normalised using *GAPDH*, *Ubiquitin-C* and *β-Actin* expression (* p< 0.05 and ** p<0.01. Bars = Mean ± SEM. n=3).

S*ox1* and *pax6* expression in hiPSC (Figure 74, A & B) increased significantly over the course of the experiment.

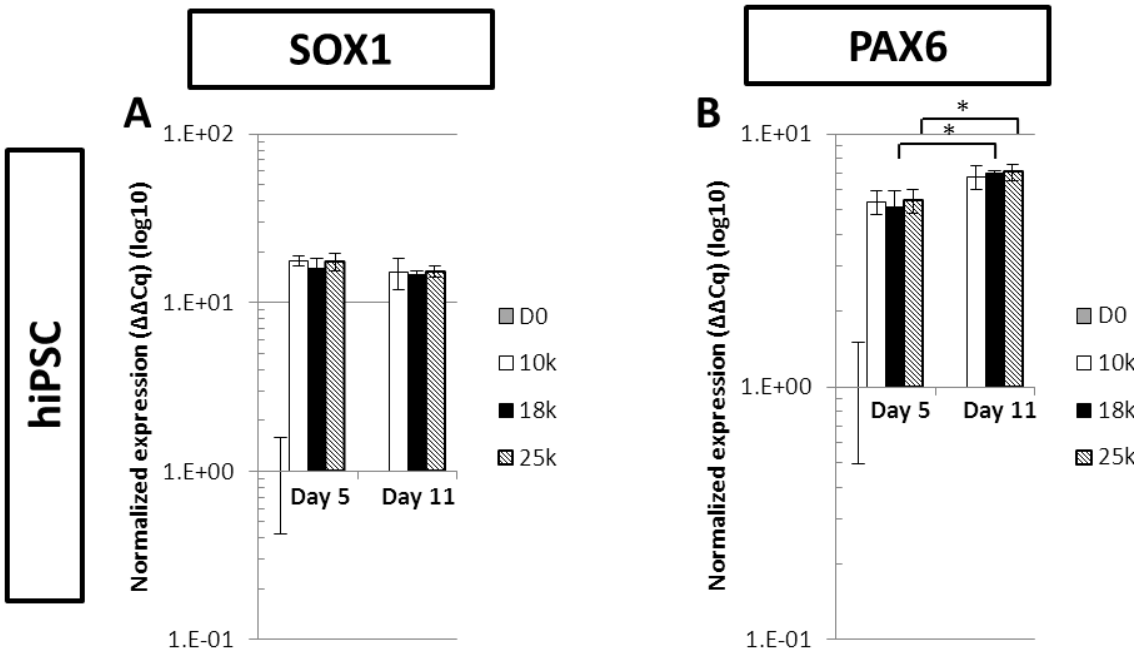


**Figure 74 - qPCR analysis of the influence of ICSD on hiPSC *sox1* and *pax6* expression during neuronal priming**

qPCR analysis of hiPSC mRNA expression over the course of neuronal priming, D0 through to D11. Expression of **(A)** *sox1* and **(B)** *pax6* are shown relative to D0 expression. Data was normalised using *GAPDH, Ubiquitin-C and β-Actin* expression (* p< 0.05. Bars represent Mean ± SEM. n=3).

### 7.3.6 Influence of ICSD on hPSC *otx2* and *foxa2* gene expression

Expression of *otx2* within the hESC population was shown to significantly increase over the course of the culture period when compared with D0. At D11, 10k/cm$^2$ was shown to have significantly greater expression than that of the two higher ICSD (Figure 75, A). hiPSC expression of the *otx2* gene (Figure 75, C) was observed to increase for the first 5 days and then drop significantly to D11. Similar to the experiment with hESC, expression of *otx2* in hiPSC was not observed to increase past $1^1$ΔΔCq. In hESC (Figure 75, B) and hiPSC (Figure 75, D), *foxa2* expression was shown to fall over the course of the culture period relative to D0.

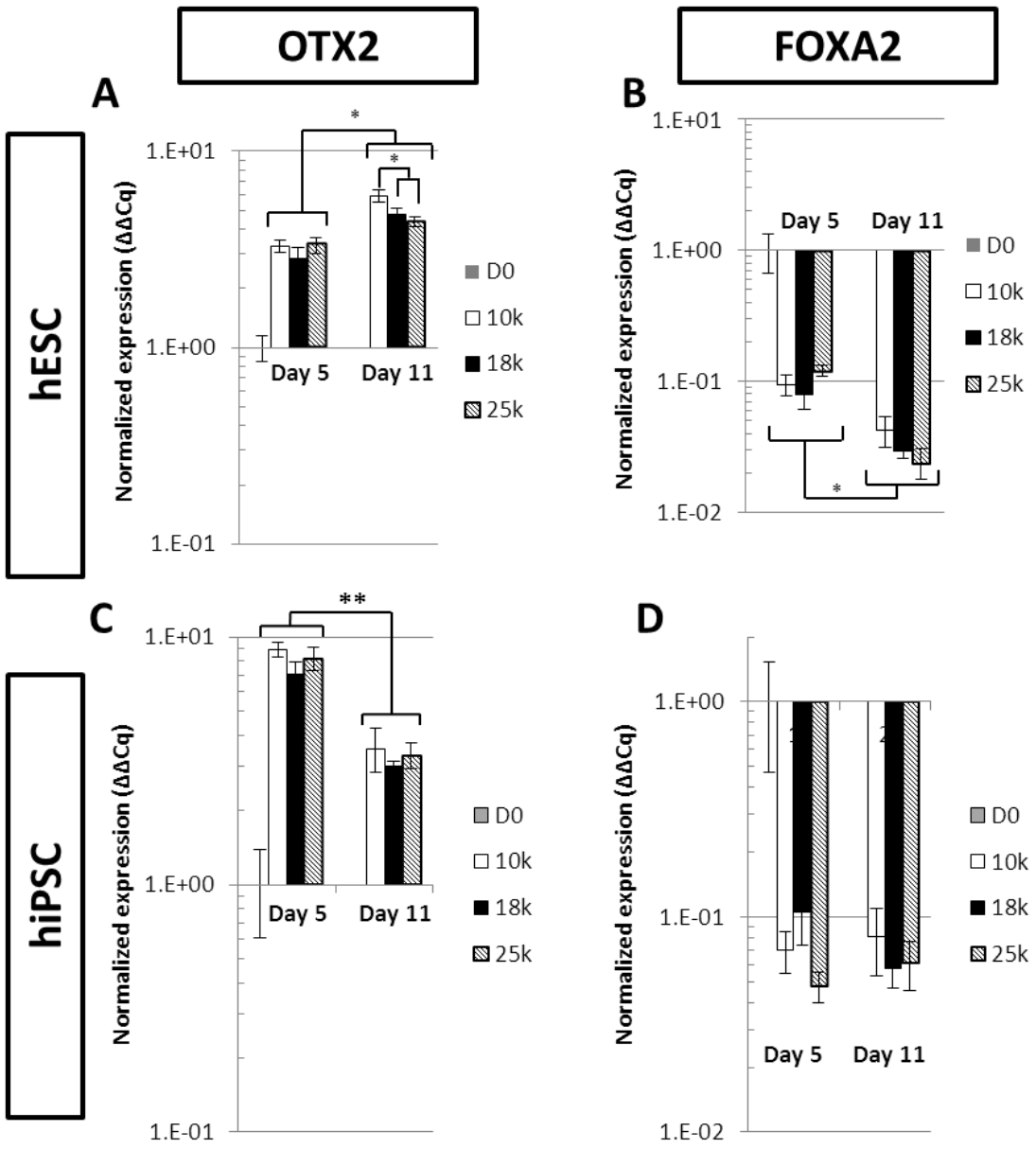


**Figure 75 - qPCR analysis of the influence of ICSD on *otx2* and *foxa2* gene expression during neuronal priming**

qPCR analysis of *otx2* and *pax6* mRNA expression over the course of neuronal priming, D0 through to D11. hESC and hiPSC expression of *otx2* **(A/C)** and *pax6* **(B/D)** are shown relative to D0 expression. Data was normalised using *GAPDH, Ubiquitin-C* and *β-Actin* expression (* p< 0.05 and ** p<0.01. Bars = Mean ± SEM. n=3).

### 7.3.7 Influence of ICSD on hPSC *TH* and *lmx1a* gene and protein expression

hESC expression of *TH* was observed to increase over the course of the priming protocol. At D11 it was shown that the lowest ICSD, 10k/cm$^2$, showed significantly greater expression compared to the other ICSD (

Figure **76**, A). Expression of *lmx1a* (

Figure **76**, B) was shown to increase relative to D0 but by D11, 25k/cm$^2$ was shown to decrease significantly relative to D5 and the other ICSD investigated; 10k/cm$^2$ was observed to have the highest levels of *lmx1a* at D11. Immunocytochemical staining for hESC was inconclusive.

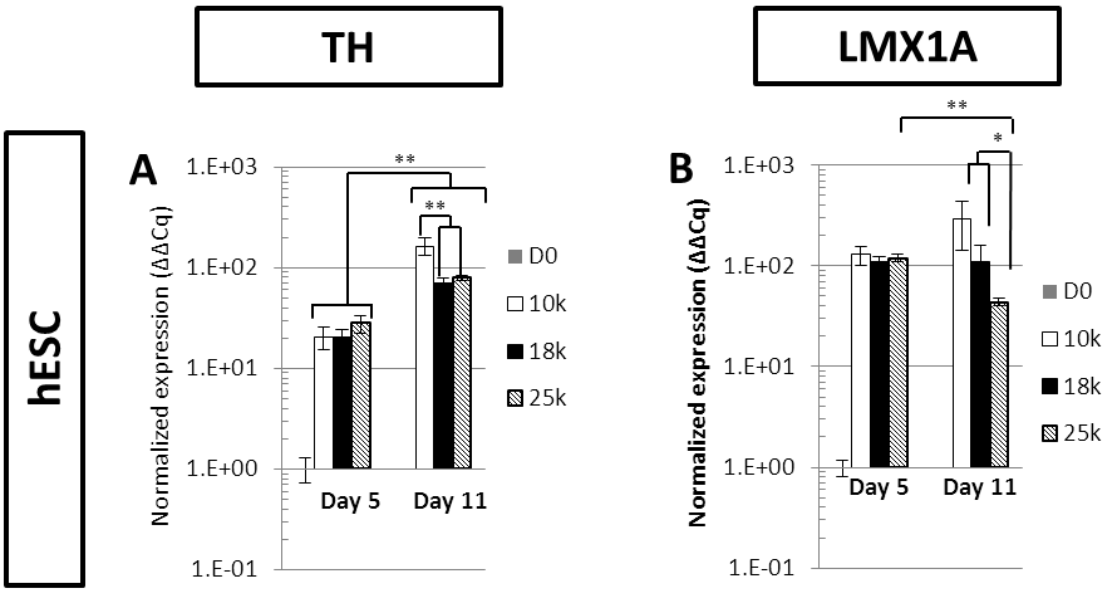


**Figure** 76 - **qPCR analysis of the influence of ICSD on hESC TH and lmx1a expression during neuronal priming**

qPCR analysis of hESC mRNA expression over the course of neuronal priming, D0 through to D11. Expression of **(A)** *TH* and **(B)** *lmx1a* are shown relative to D0 expression. Data was normalised using *GAPDH, Ubiquitin-C and β-Actin* expression (* p< 0.05 and ** p<0.01. Bars = Mean ± SEM. n=3).

While expression of *TH* in hiPSC was shown to increase throughout the protocol, no trends could be identified associated with ICSD (Figure 77, A). Expression of TH was confirmed at a protein level, with a few cells showing more developed phenotypes (Figure 77, C). At D11 it appeared that there were more TH$^+$ cells present at the lowest ICSD (10k/cm$^2$) but within the higher ICSD, mature neuronal phenotypes were present.

Expression of *lmx1a* was shown to increase to D5, however, by D11 expression of *lmx1a* fell significantly for all ICSD. No distinction could be made between the ICSD (Figure 77, B). Staining showed wide spread expression of lmx1a though no difference could be observed across the ICSD (Figure 77, C).

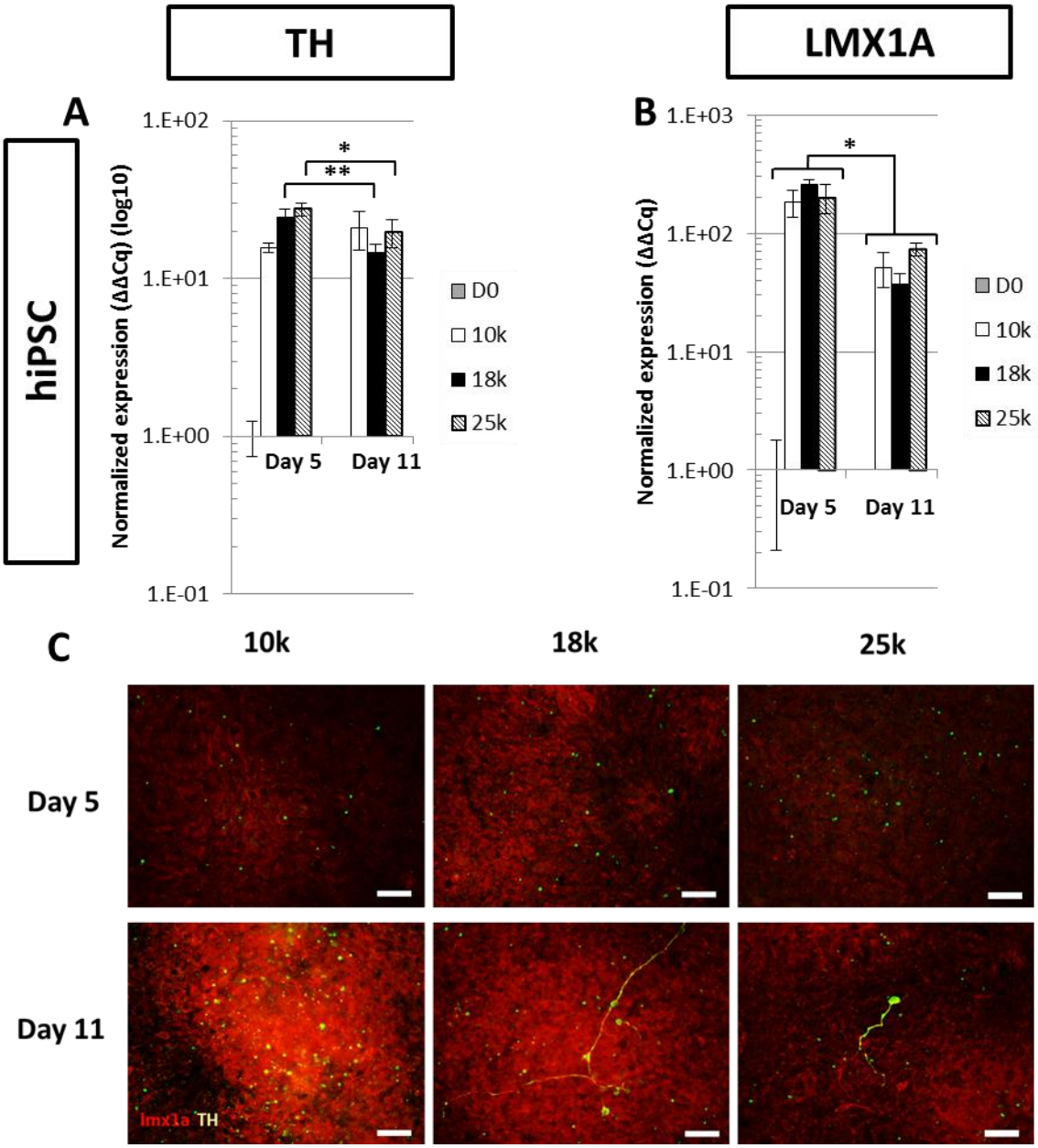


**Figure 77 - qPCR and immunocytochemical analysis of the influence of ICSD on hiPSC TH and lmx1a expression during neuronal priming**

qPCR analysis of hiPSC mRNA expression over the course of neuronal priming, D0 through to D11. Expression of **(A)** *TH* and **(B)** *lmx1a* are shown relative to D0 expression. Data was normalised using *GAPDH, Ubiquitin-C and β-Actin* expression (* p< 0.05 and ** p<0.01. Bars = Mean ± SEM. n=3). **C)** Immunocytochemical staining of hiPSC expression of TH and Lmx1a at D5 and D11 (Scale bars = 100µm)

### 7.3.8 Passage methods tested on hiPSC line

This work assessed the ability of the neuronal priming protocol in influencing neuronal gene expression of hPSC and its ability to drive hPSC towards a neuronal lineage. To exploit this protocol and any ability to drive neuronal gene expression, it was imperative that cultures could next be passaged. Over the 11 days in the priming culture, cultures had become confluent with no further capacity to expand. Two methods of passaging were trialled on hiPSC

within this work, mechanical and enzymatic; with enzymatic being the most appropriate for bioprocessing in the future because it can be carried out in a closed system and did not require manual manipulation.

Mechanical passaging with a sterile pastette was trialled, with and without ROCK inhibitor. The representative images shown in Figure 78, A, show a high level of cell death with very low adherence of cells to the culture plastic 2 days after passaging. The addition of ROCK inhibitor did not reduce cell death when compared with the culture without ROCK treatment.

Enzymatic passaging was also trialled with Tryple Express, a gentle disassociated enzyme favoured within the laboratory and appropriate for use alongside qPCR analysis. Cells were incubated for 5min (Figure 78, B), with and without ROCK inhibitor, and 10min (Figure 78, C) without ROCK inhibitor. All protocols resulted in low cell viability and low cell adhesion as represented by the bright-field images.

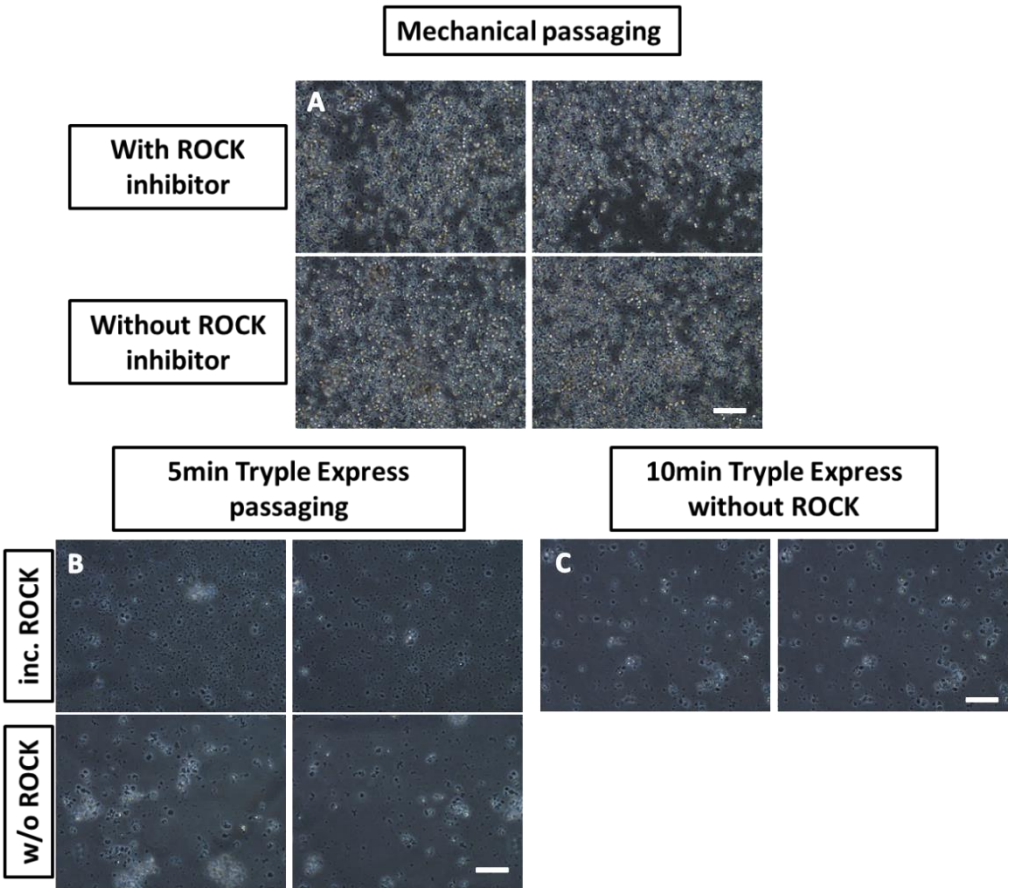


**Figure 78 - Passaging methods trialled on hiPSC cultures**

Representative bright field images of hiPSC cultures at D11, passaged mechanically (using scraper, A) or enzymatically for set time periods, (B) 5min and (C) 10min. Cells were either passaged with or without ROCK inhibitor supplemented into the media to help prevent spontaneous cell death. Images were taken 2 days post passaging (Scale bars = 100µm).

## 7.4 Discussion

Through the use of in-house confluence analysis software (Jaccard, Griffin et al. 2014), we were able to accurately assess the cell density of cultures seeded at three different ICSD over the first 6 days of culture. Using this we identified a specific time point that we felt would allow us to assess the impact of ICSD on neuronal priming of hPSC cultures.

Analysis of both hESC and hiPSC cultures identified D3 as the optimal day to start the experiment. This time point resulted in distinct and reproducible densities; ~40%, ~60% and ~80% for ICSDs 10k/cm$^2$, 18k/cm$^2$ and 25k/cm$^2$ respectively. Both cell lines followed this trend, although hiPSC were observed to expand quicker than hESC resulting in slightly higher densities at D3.

To allow us to assess the impact ICSD on the level of pluripotency and neuronal gene expression a sample was taken at D0, to act as the internal control and all gene expression levels are shown relative to this. During experimentation samples were taken at D5 and D11, to capture the impact of ICSD over the duration of the experiment.

Pluripotent gene expression analysis showed a significant drop in expression of *nanog* in hESC and hiPSC (Figure 71, A, D), as was reported by Chambers *et al.* when using a similar protocol to achieve an 80% yield in neuronal progenitors (Chambers, Fasano et al. 2009). *Nanog* within hESC was observed to show significantly lower expression in 10k & 18k/cm$^2$ when compared to 25k/cm$^2$. *Oct4* was also shown to reduce significantly over time in both cell types, again replicating results shown by Chambers *et al. Oct4* reduction in both cell types increased over time with significant reductions being shown to D5 and then to D11, this indicates that *oct4* was either slower to be impacted by the smad inhibition or was more abundant within the pluripotent population than *nanog* (Figure 71, B/E). These results indicate that the cultures moved away from expressing genes associated with maintained pluripotency towards a differentiated state. Moreover, this drop in expression was accompanied by a concurrent increase in expression of *fgf5* (Figure 72), indicating differentiation to the late epiblast stage

and early ectoderm phase (Pelton, Sharma et al. 2002). This expression increase was found to be greatest in the higher ICSD investigated, suggesting a role of ICSD in *fgf5* expression. Lower expression in the lower ICSD at D11 may suggest that these populations may have matured faster than the higher ICSDs, and passed the point of expression when measured. This is corroborated by the expression of more mature neural and neuronal markers, *sox1, otx2, TH* and *lmx1a* by D11 in 10k/cm$^2$ cultures.

*Sox2* expression was also assessed within the cohort of pluripotency genes. It was shown that the highest expression resulted from the highest ICSD investigated in hESC; however this trend was not reflected in hiPSC results (Figure 71, C, F) which showed no difference in expression relating to ICSD. Increased expression of *sox2* in both hPSC cultures is associated with the acquisition of a neuronal progenitor phenotype (Graham, Khudyakov et al. 2003) and further supports a shift away from pluripotency towards the ectodermal/neuronal lineage. The higher ICSD of 25k/cm$^2$ led to higher population-wide expression of *fgf5*, however, combined with the increased expression of later neuronal markers at lower ICSD, it is possible that in the higher ICSD investigated, a higher proportion of the population stay in this late epiblast/early ectoderm stage, whereas at 10k/cm$^2$, stagnated expression of *fgf5* possibly indicated differentiation past the epiblast stage (Figure 72).

*Sox1* an early neuroectoderm marker showed significant increases in expression over the course of the protocol, with 10k/cm$^2$ showing significantly greater expression by D11 in hESC (Figure 73, A). Enhanced expression of *sox1* was also observed in hiPSC, though no differentiation could be discerned associated with ICSD (Figure 73 & Figure 74). *Pax6*, an early neuroectoderm marker and key gene in the development of neural tissue (Walcher, Xie et al. 2013) also showed significant increases in expression when compared to the control in both cell types (Figure 73 & Figure 74). These findings replicated findings by Chambers *et al* (Chambers, Fasano et al. 2009), that smad inhibition moved hPSC towards a neural lineage and

strengthen previous findings in this work, that these cultures are moving away from a pluripotent state and towards a neuronal phenotype.

The suggestion that lower *fgf5* expression in hESCs at 10k/cm$^2$ indicates a move down the ectoderm lineage is enforced by the significant difference in *sox1* expression observed at D11. This trend was repeated for *otx2* at 10k/cm$^2$ where higher expression was noted compared to the other ICSDs (Figure 75), possibly indicating more rapid differentiation towards mature neuronal states at lower ICSD. This supports previous observations in mouse ESCs, where increased neuroectoderm differentiation was noted at lower ICSDs (Veraitch, Scott et al. 2008). Expression of neuronal genes by hiPSCs was not as prominent as those observed for hESCs, with relative expression of the majority of genes screened never showing greater than 1x10$^2$ΔΔCq increase. This may indicate a reluctance of the cell type to move down the ectoderm lineage. In the case of hiPSCs, the reduction in *otx2* expression over time (Figure 75, C) would also suggest that differentiation is not toward a mid-neural tube phenotype.

This assumption in hiPSCs is supported by the expression profile of *TH* and *lmx1a* (Figure 77), with *TH* showing significantly reduced expression at both 18k & 25k/cm$^2$ from D5 to D11 and *lmx1a* expression showing a significant drop across all ICSDs within the hiPSC populations. Protein analysis of these cultures showed a contradictory story with hiPSC exhibiting mature TH phenotypes in 18 & 25k/cm$^2$ (Figure 77, C). In the case of hESCs, the trend for *TH* and *lmx1a* (Figure 76) was similar to that found for the other pro-neuronal genes; the lowest ICSD (10k/cm$^2$) led to significantly greater expression of *TH* and *lmx1a* than the higher ICSDs. The highest ICSDs showed the only significant drop in *lmx1a* expression observed in hESCs (Figure 76, B), enforcing the hypothesis that lower ICSD and level of confluence at the commencement of differentiation can improve the efficiency of lineage specification that is needed to drive towards a DA neuronal cell phenotype.

*Foxa2* gene expression did not behave as expected and was observed to decrease in both cell types, rather than increasing, as was the case for *TH* and *lmx1a*. This observation is thought to

be a result of the smad signalling inhibition, blocking differentiation towards the endoderm lineage of which *foxa2* is associated (Burtscher and Lickert 2009).

To develop the potential of this protocol within the bioprocess of a product, we investigated the ability of hiPSC cultures to be passaged. hiPSC were used at this stage due to their greater availability and robustness compared to hESC. Mechanical and enzymatic passaging methods were trialled; these were supplemented with or without ROCK inhibition to reduce cell death. These techniques were tested three times and it was found that cultured cells could not be passaged. At this stage it was decided to discontinue this line of work, pursuing suspension culture as a more viable bioprocess alternative.

## 7.5 Conclusion

This work showed that low ICSD resulted in an overall improved neuronal differentiation in hESCs, with greater expression of a number of neuronal genes including *TH* and *lmx1a*. hESCs had a greater propensity than hiPSCs to differentiate towards an ectoderm cell type, when assessing population-wide gene expression. Even though differences were evident between the two pluripotent cell lines, this data provides evidence that ICSD can affect target gene expression and hence differentiation during neuronal lineage commitment.

The positive response under the protocol was limited by the inability to passage the resulting cultures. A number of avenues were explored to overcome this hurdle but we were not successful in passaging the cells and we moved instead to use a suspension-based system that showed true potential in scalability and bioprocessing.

# CHAPTER 8 - FINAL DISCUSSION

The CTI is a rapidly growing market with an estimated value in 2012 of $7Bn (Mason, McCall et al. 2012). This is an exciting area of research, not just because of the potential financial value being created but mainly the number of clinical indications that it could address. These include orphan indications like Stargardt's macular dystrophy, to widespread conditions such as ischemic stroke and PD (Trials.gov 2013). The CTI may provide the opportunity to make a step change in the provision of healthcare; providing a cure rather than symptomatic control for a number of conditions, resulting in long-term relief to patients and their loved ones.

This thesis studied stem cells from two classes of cell: (i) autologous cells (omnicytes) and (ii) allogeneic cells (hESC and hiPSCs). In particularly, this work focused on their respective potential to specifically derive neuronal cell populations, and the factors that enhance the yield of these populations. This study, performed within a framework, investigated the use of omnicytes in the generation of neurons for the treatment of acute ischemic stroke and the use of hPSC in the differentiation of DA neurons for the treatment of PD.

These two conditions are attractive targets for cell therapy, due to their impact on individuals and society, with the number of affected people anticipated to become greater with the ageing population. They are also natural targets because existing therapies are limited in their application.

There are very few interventions for ischemic stroke currently available. A pharmacological intervention, rt-PA (Albers, Bates et al. 2000), has a treatment window of 6hrs and mechanical interventions (Bose, Henkes et al. 2008, Cohen, Itshayek et al. 2011) that require surgeons to physically remove the embolism following stroke. The timing requirements of these treatments means a majority of patients do not receive treatment, resulting in a high level of mortality or serious disabilities following the onset (Deb, Sharma et al. 2010). An alternative treatment option is high on the agenda. *In-vivo* studies have shown the potential of HSCs within an ischemic environment, resulting in enhanced neovascularization and neurogenesis

along with reduced scaring (Taguchi, Soma et al. 2004). This study investigated the use of omnicytes, a sub-population of the HSC population, to efficiently derive functional neurons, which could then be administered to replace lost cells and function to aid endogenous recovery.

PD is not a terminal condition but does result in a gradual and irreversible deterioration of the patient, with symptoms worsening as the disease progresses (UK 2010, UK 2013). Pharmacological and surgical treatments that are currently available for this condition, do not slow or prevent the progression of the disease but serve only to control symptoms. Because PD is caused predominantly by the loss of a specific cell type within the substantia nigra, A9 DA neurons (German, Manaye et al. 1989), it is a particularly attractive target for cell therapy. Trials involving the transplantation of foetal-derived DA grafts have previously shown promising results (Lindvall and Kokaia 2009). The goal of this work was to use autologous derived cells, rather than grafts, to differentiate DA neurons, *in-vitro,* under quality controlled and efficient protocol to provide improved and a widely available treatment for patients.

This thesis investigated the potential of omnicytes and hPSCs to generate neuronal cell populations. It also investigated the potential of a novel RNA technology, saRNA, to affect the transient up-regulation of specific target genes with the intention of increasing the yield of DA neurons from hPSC.

### 8.1 The use of omnicytes in neuronal differentiation

Omnicytes were discovered in 1994 as a subpopulation of the $CD34^+$ cell population. They were speculated to contain the regenerative capabilities of the $CD34^+$ population due to their morphology and gene expression i.e. they had the potential to differentiate into all 3 germ layer lineages (Gordon 1994, Gordon, Levicar et al. 2006), similar to that of hESC.

This thesis investigates whether omnicytes have the capability to differentiate into neuronal populations due to the endogenous expression of a number of neuronal genes; and aimed to generate specialized neurons once proof of principal had been achieved.

A number of methods were investigated to exploit the proposed potential of omnicytes and achieve neuronal differentiation, including: media manipulation using smad signalling inhibition (Chambers, Fasano et al. 2009) and growth factor manipulation (Jiang, Henderson et al. 2003); as well as the inclusion on microRNA to effect change at a molecular level.

We were able to show that by using 'expansion mix' it was possible to expand the starting population six-fold, thereby establishing a population to interrogate our hypothesis. We also showed that during expansion, the majority of target neuronal genes, including, *sox1, sox2* and *otx2* were stably expressed, indicating a neuronal primed population suitable for testing our hypothesis.

Manipulation of the expanded omnicyte population using different media was observed to be largely unsuccessful, although it was shown neuronal genes including *sox1* and *otx2* could be sustained over the culture period and some cells adhered to the culture surface and changed in morphology. We were unable to induce the expression of *pax6* (Bel-Vialar, Medevielle et al. 2007), a marker gene considered essential in moving this differentiation process forwards through to mature neurons (Chambers, Fasano et al. 2009).

Due to lack of results from media manipulation, we attempted to use microRNA in an effort to manipulate the omnicytes at a molecular level and induce neuronal differentiation. We focused this work on two microRNA, miR124 and miR9. These microRNAs have now been found by Yoo *et al*. to transdifferentiate human fibroblasts into functional neurons (Yoo, Sun et al. 2011), though our work on omnicytes was less successful. Results were highly variable and largely negative.

We showed that patient variability and cryopreservation impacted on the consistency of the results. The response of cells to manipulation using these protocols depended heavily on the source cell origin and preservation techniques, and indicated that further work on this cell type would be hindered until a consistent and reliable source of cells could be ascertained.

Due to the high level of patient variability observed and rarity of the cell type restricting their use, it was decided that the research would refocus on readily available cell sources (hESC and hiPSC). The work performed on these cell sources, hPSC, would include the use of a novel RNA technology, saRNA.

### 8.2 Aggregate-based differentiation of dopaminergic neurons from hPSC

To allow us to investigate the potential of saRNA and their ability to increase the yield of differentiated neuronal populations we first needed to produce the desired neuronal population *in-vitro*. The focus of the research moved towards PD and the differentiation of DA neurons.

We showed that the cell populations (hESC and hiPSC) we were using were pluripotent, through their marker expression at both a genetic and protein level. We also showed that these cells were able to generate cells of the 3 germinal layers, through spontaneous differentiation, affirming their status as pluripotent.

Results showed that the methodology used in this project reduced key pluripotency genes along with contaminating germ layer markers in both hESC and hiPSC. The protocol also induced up-regulation of neuronal progenitor genes, *sox2* and *fgf5* indicating a move toward the ectoderm linage, which was confirmed by expression of *sox1*. Further interrogation of neuronal genes showed that the protocol was able to up-regulate key DA genes including; *nurr1, otx2, en1, TH, DRD*, *lmx1a* and *foxa2* in hESC, indicating success in driving hESC towards a DA neuronal cell type. The protocol was shown to be less successful for hiPSC cultures, with a number of key genes (*nurr1, otx2* and *foxa2*) not being expressed during the differentiation process, indicating a need for further optimization of the patterning process or the use of a different cell type.

These findings were examined at the protein level for both cell types, with expression of nestin, TH and foxa2 following maturation being observed. The ability of these differentiated cultures to respond to stimuli and express dopamine was also confirmed and quantified

through ELISA, indicating that we had been successful in generating functional DA neurons from both cell types. Results from hiPSC at a molecular and protein level did not correspond, highlighting a key limitation of this work, using qPCR; this will be discussed in more detail in the limitations section.

Experiments were also performed to understand the impact of extended culture on DA differentiation and gene expression. This was done by extending the time aggregates were cultured in suspension or by doubling the length of time neurospheres were stuck down and matured. Analysis showed that extending the time in suspension or extending stick down time had a detrimental impact on a number of the key target genes expressed, namely *foxa2* and *lmx1a*. It was hypothesized that the resultant reduction in gene expression may be a result of the increased size of the aggregates in extended culture; and that as aggregates grow, necrotic death occurs within the core. This occurs because nutrients, growth factors and oxygen cannot penetrate to the whole cell population. This hypothesis is supported by work published by Van Winkle *et al.*, that found that cell aggregate size impacts on the ability of factors to perfuse to the core, resulting in starvation (Van Winkle, Gates et al. 2012). This result suggests that extended culture without a feasible passaging method is not advisable.

### 8.3 Potential of saRNA in dopaminergic differentiation

Building on these finding using an aggregate-based differentiation programme, we re-focused to increase the yield through the incorporation of saRNA. The aim of this work was to enhance the expression of three key DA marker genes, *foxa2*, *lmx1a* and *TH* (Kriks, Shim et al. 2011), and impact on the expression of associated genes, resulting in the enhancement of DA neuron yield.

The initial optimization using cancer cell lines and omnicytes proved inconclusive. We expect the lack of consistency in results to be due to the insensitive nature of rtPCR and the inherent variability of omnicytes as mentioned above.

Optimization of saRNA in adherent hiPSC cultures, in contrast, resulted in enhanced expression of all target genes; a compilation of all saRNA transfected together resulted in the greatest increase in target gene expression.

Following the transfection of the suspension-based DA differentiation cultures for 24 days, hESC culture's expression of *sox1*, *nurr1* and *en1* were revealed to be slightly enhanced in transfected cultures relative to UT cultures. These findings were further strengthened by the increase in DA marker expression (*TH, foxa2, lmx1a* and *DRD*) observed in saRNA transfected cultures. Although not statistically significant these results indicated that saRNA transfection was impacting on gene expression. Contrary to this, hiPSC were found not to respond to saRNA manipulation, confirming finding from the previously work that the particular hiPSC line being used may not be an appropriate cell type for the differentiation of DA neuronal populations and the incorporation of this technology. Neuronal differentiation was confirmed at a protein level (β-III-Tubulin$^{+}$ and TH$^{+}$) for both cell types.

Through protein analysis cells were found to express TH$^{+}$ and foxa2$^{+}$ across the whole neurosphere but to assess the whole population was impractical resulting in the targeting of stain rich areas but this inherently skewed findings. Greater levels of foxa2 were shown to be present in both cell types when transfected with saRNA. Contrary to this, TH expression was found to drop following transfection. Although this demonstrates an impact of the saRNA, because of the method of analysis, and the inherent biased nature of the procedure, no conclusions could be drawn at a protein level.

Work done to understand the individual impact of the saRNA, found that foxa2 saRNA had a vital role in the protocol. Key genes that had previously shown a slight increase when transfected with all saRNA (*foxa2/TH/lmx1a*), did not show this response when transfected without the foxa2 saRNA. This finding suggested synergistic action of the saRNAs; to induce the desired response, multiple factors may need to be applied (Kriks, Shim et al. 2011).

Through this work it was hypothesized that aggregate size may impact on transfection efficiency, in so directly impacting on saRNA efficiency. Larger aggregates would show lower transfection efficiency when compared to smaller aggregates due to the mechanism of action of the lipid-based transfection reagent (endocytosis). Although this experiment was not performed to statistical significance, results suggest that aggregate size does impact on transfection efficiency. It is thought that by using a transfection reagent that functions via cell-lipid endocytosis, only the surface layer cells were affected by the reagent. In smaller aggregates the surface cells represent a larger proportion of the whole cell population. To maximize transfection efficiency, aggregates either need to be disassociated to a single cell layer then transfected and re-aggregated, which is not feasible or a mechanism to control aggregate size employed.

### 8.4 Impact of ICSD on neuronal priming

Investigating the impact of ICSD was an independent piece of work within the thesis. It was undertaken to understand the impact of ICSD on neuronal priming.

We showed that lower ICSD resulted in faster up-regulation of pro-neural genes including, *otx2*, *TH* and *lmx1a*. However, higher ICSD (25k/cm$^2$) showed greater expression of early neuronal progenitor markers (*sox2* and *fgf5*), over the same culture period. These findings suggest delayed differentiation within higher ICSDs; this may the result of a 'cell niche' environment. This work could not be pursued as it was found that passaging the cultures was not possible, but this work does have implications on the wider regenerative medicine industry. It demonstrates a need to account for ICSD when designing any new differentiation process as it could impact on differentiation efficiency.

### 8.5 Limitations

There were a number of limitations that were identified whilst carrying out this research. Here, they are identified, along with prospective solutions in future work:

i. The endogenous gene expression of omnicytes would suggest that they have the potential to differentiate into different lineages. The advantage of this is that the source cell type could be obtainable from the patient, negating the need for immunosuppression. However, the current availability of the cell type limits the ability to develop this technology and as shown within this work, patient variability, disease-type and preservation techniques impact on the performance of the cells. To address this, a consistent source of cells needs to be identified; $CD34^+$ cells can be acquired commercially, providing a source of consistent quality to develop this work.

ii. It has been shown that the use of lipid-based transfection reagents within this work impacted on the ability to transfect the whole cell population. Nanofectin functions via cell-lipid endocytosis; this means that only cells on the surface of the aggregates are influenced by the saRNA being transported by the nanofectin. To achieve optimal transfection, cell aggregates need to be disassociated into single cells, transfected and re-aggregated; because saRNAs only provide transient expression this process would be required every 3 days; this is not feasible as it would impact on cell viability, and would hinder scale-up. To address this limitation, the implementation of a continuous or gradual transfection method would be required, this may be in the form of retro-viral transfection as done with siRNA (Devroe and Silver 2002) or the use of slow release nanoparticles as is being developed for the distribution of growth factors by Zhang *et al.* (Zhang, Zhou et al. 2014). These methods would allow the transfection of the saRNA to be continuous within the cell population or delay the release of the saRNA until the nanoparticles have diffused to the core of the aggregate.

iii. The use of an aggregate-based system, though having the potential for scale-up does also present some issues that need to be addressed. It has been shown by Van Winkle *et al*. (Van Winkle, Gates et al. 2012) that aggregate size has a direct impact on oxygen, growth factors and nutrient diffusion into the aggregates. In this method, because there is no way to passage (in a closed system), the aggregate size was not controlled,

resulting in increasingly larger aggregates. This inherently results in aggregates over the optimal size, reducing the diffusion of factors to the whole population. To address this, aggregate size needs to be standardized at D0. This could be achieved through the use of aggrewell technology, which enables the synthesis of uniform aggregates. This would ensure that aggregates are uniformly impacted by reagents and conditions. For the continuous control of aggregate size a bioreactor, including impeller could be incorporated (Olmer, Lange et al. 2012).

iv. The main analysis method utilized within this work was PCR, both rtPCR and qPCR. Although these techniques allow the analysis of gene modification within the experimental sample, in this work gene expression analysis was limited to the whole cell population. As observed a number of times within this thesis, molecular and protein results did not reflect each other, this is likely to be a result of whole population gene expression obscuring the expression of the smaller, differentiated population. To investigate this further and to gain an accurate understanding of the changes induced using these protocol, single-cell qPCR should be incorporated. It is important for the future development of cell products that the desired markers are expressed homogenously throughout the cell population; this will not be illuminated using qPCR whole population analysis.

# CHAPTER 9 - FINAL CONCLUSION

This thesis studies a number of methods for driving omnicytes down a neuronal lineage; including, adapting the length of the culture and changing the timing of the manipulation, both by signalling pathway manipulation and molecular modification. The experiments did not show the changes in gene expression thought to be indicative of a neuronal population switch. Further, it was found that the results were not consistent, with no two replicates producing the same reading. Although we expect that the lack of consistency is a result of patient variability and the impact of storage method (cryopreservation), the lack of consistency and the general nonappearance of changes in gene expression following manipulation suggest that omnicytes are not a strong cell source for cell therapy development.

The investigation also studied cancer cell manipulation and the utilization of hPSC. DA-like neurons were derived from hPSC using a suspension-based aggregate differentiation protocol. Down-regulation of pluripotent and germ layer genes and up-regulation of key neuronal and dopaminergic genes were observed. The products of this protocol also expressed a number of neuronal and DA protein markers and responded to stimuli to release dopamine, indicating that the protocols successfully derived functional DA-like neurons though the generation of A9 dopaminergic neurons was not confirmed.

After establishing a baseline of *in-vitro* DA-like neurons, the thesis studied the potential of saRNA to increase yield. Results were disappointing. In adhered culture, notable expression changes were observed when transfected with all saRNA, though once utilized within aggregate culture these changes were insignificant: slight up-regulation was observed in hESC transfected cultures in key genes such as *nurr1, sox1, en1*, *TH, foxa2 and lmx1a,* but no significance was found. It was hypothesized that the low impact of saRNA was a result of the low penetration of the saRNA into the cell aggregates. Further work will be required to develop this protocol and the method of transfection addressed to ensure the saRNA penetrates beyond the outer surface of the aggregates and affects the whole cell population.

Alongside the derivation of neuronal populations, an independent experiment investigated the impact of ICSD on neuronal priming. We showed that lower ICSD resulted in improved neuronal priming, with enhanced expression of a number of neuronal genes including *TH* and *lmx1a* in hESC. It was observed that hESCs have a greater propensity to differentiate towards an ectoderm cell type, indicating that that hiPSC (MSUH001) are not a suitable cell type for the development of neuronal cell therapy development.

This work has shown that though omnicytes express a number of markers indicating their potential to differentiate into all germ layers and be a prime starting material for cell therapy products; the reliable sourcing of this cell type needs to be addressed, so to mitigate the effects of patient variability and storage during product development. This body of work has also provided evidence that saRNA can be used within an aggregate-based differentiation protocol to enhance gene expression and impact on DA yield. Up-regulation of key genes can be induced, though transfection efficiency needs to be addressed prior to this being fully realized.

# CHAPTER 10 - FUTURE WORK

This investigation has highlighted a number of limitations in moving this technology forwards and towards a viable product for commercial manufacture. Future work should focus on incorporating saRNA into the DA differentiation protocol.

The following investigations could be used to take this work further:

**1. Understand how aggregate size impacts on the efficiency of transfection, incorporating new techniques and technologies to mitigate the identified limitations of lipid-based reagents.**

In the development of an aggregate-based differentiation system it will be essential that future work understands the impact of aggregate size on: cell viability; the ability for aggregates to differentiate; growth factor, oxygen and nutrient perfusion; and transfection efficiency. Through work reported by Van Winkle *et al.* (Van Winkle, Gates et al. 2012) we know that different growth factors and cytokines differ in their ability to penetrate cell aggregates, for this reason a full analysis of the material being used within this protocol is required. To address these issues technology, for example, slow release nanoparticles could be investigated to deliver various factors including saRNA, allowing factors to penetrate further into the aggregates.

**2. Incorporate alternative analytical techniques at the individual cell level to understand the impact of the saRNA at a molecular and protein level.**

To fully understand the impact of new processes and additives on the end product it is important to assess at the whole-population, as well as the individual-cell level. This work was limited by our ability to only assess at the whole-population level. To take this work forwards, analytical techniques including Fluorescence-activated cell sorting (FACS) to understand protein expression at a population level and individual-cell qPCR to fully elucidate the impact of the protocols at the single-cell level should be utilized. Prior to the generation of any

therapy it is imperative that the full effects of the protocol being utilized are understood, and that homogenous cell differentiation is occurring. These protocols could eventually serve as screening methods for product release.

**3. Develop a technique for the isolation and purification of differentiated DA neurons.**

Following the confirmation and proof of principal of the technology a purification technique is required to provide high resolution purification as to generate the end product for patient treatment. It is important that this method is able to effectively remove contaminating cell types, although not to the detriment of the final end product recovery (Weil 2014). It will be important that this is addressed early in the development of the therapy as to not create an unnecessary bottleneck later in the progression of the product. This could involve the incorporation of FACS for specific antigens.

**4. Incorporate the use of an impeller driven bioreactor to allow complete and uniform control of the aggregate culture environment, controlling aggregate size and enabling the scale-up.**

Once proof of principle is achieved, this research will need to move from static flasks into an impeller driven bioreactor (enabling the technology to progress from the bench-top to bedside). The bioreactor would allow the cellular environment to be controlled (including monitoring pH, oxygen, waste gases, and nutrient and growth factor levels) and contained within a closed-system, thereby reducing the risk of infection. An impeller allows the user to control of aggregate size (Olmer, Lange et al. 2012), which in turn would allow optimal size to be maintain, allowing sufficient perfusion of growth factors, nutrient, oxygen and saRNA to the core of the aggregate.

# BIBLIOGRAPHY


Abbasalizadeh, S., M. R. Larijani, A. Samadian and H. Baharvand (2012). "Bioprocess development for mass production of size-controlled human pluripotent stem cell aggregates in stirred suspension bioreactor." Tissue engineering. Part C, Methods **18**(11): 831-851.

abcam (2014). Anti-FOXA2 antibody [EPR4466], abcam.

abcam (2014). Anti-LMX1A antibody.

abcam (2014). Anti-Tyrosine Hydroxylase antibody [EP1533Y]

Adina Michael-Titus, P. R., Peter Shortland, Ed. (2007). The Nervous System - Basic science and clinical conditions, Elsevier Limited.

Agrawal, N., P. V. Dasaradhi, A. Mohmmed, P. Malhotra, R. K. Bhatnagar and S. K. Mukherjee (2003). "RNA interference: biology, mechanism, and applications." Microbiol Mol Biol Rev **67**(4): 657-685.

Akashi, K., D. Traver, T. Miyamoto and I. L. Weissman (2000). "A clonogenic common myeloid progenitor that gives rise to all myeloid lineages." Nature **404**: 193-197.

Albers, G. W., V. E. Bates, W. M. Clark, R. Bell, P. Verro and S. A. Hamilton (2000). "Intravenous tissue-type plasminogen activator for treatment of acute stroke: the Standard Treatment with Alteplase to Reverse Stroke (STARS) study." JAMA **283**(9): 1145-1150.

Alves dos Santos, M. T. and M. P. Smidt (2011). "En1 and Wnt signaling in midbrain dopaminergic neuronal development." Neural development **6**: 23.

Ameres, S. L. and P. D. Zamore (2013). "Diversifying microRNA sequence and function." Nature reviews. Molecular cell biology **14**(8): 475-488.

Andrews, P. W., I. Damjanov, D. Simon, G. S. Banting, C. Carlin, N. C. Dracopoli and J. Fogh (1984). "Pluripotent embryonal carcinoma clones derived from the human teratocarcinoma cell line Tera-2. Differentiation in vivo and in vitro." Lab Invest **50**(2): 147-162.

Association, A. H. (2012). let's talk about - Ischemic Stroke. A. S. Association, American Heart Association.

Association, A. H. (2012, 10/23/2012). "Togther to End Stroke." Retrieved 23rd Aug 2013, 2013, from http://www.strokeassociation.org/STROKEORG/.

Association, A. S. (2013, May 29,2013). "Stroke Treatments " Retrieved 26th August 2013, 2013, from http://www.strokeassociation.org/STROKEORG/AboutStroke/Treatment/Stroke-Treatments_UCM_310892_Article.jsp.

Association, S. (2013). "About stroke." Retrieved 26th August 2013, 2013, from http://www.stroke.org.uk/about-stroke.

Association, S. (2013). Stroke statistics. S. Association, Stroke Association.

Athersys. (2013). "Clinical programs." Retrieved 26th August 2013, 2013, from http://www.athersys.com/clinicalPrograms.cfm.

Banerjee, S., P. Bentley, M. Hamady, S. Marley, J. Davis, A. Shlebak, J. Nicholls, D. A. Williamson, S. L. Jensen, M. Gordon, N. Habib and J. Chataway (2014). "Intra-Arterial Immunoselected CD34+ Stem Cells for Acute Ischemic Stroke." Stem Cells Translational Medicine.

Bang, O. Y., J. S. Lee, P. H. Lee and G. Lee (2005). "Autologous mesenchymal stem cell transplantation in stroke patients." Annals of neurology **57**(6): 874-882.

Bardy, J., A. K. Chen, Y. M. Lim, S. Wu, S. Wei, H. Weiping, K. Chan, S. Reuveny and S. K. Oh (2013). "Microcarrier suspension cultures for high-density expansion and differentiation of human pluripotent stem cells to neural progenitor cells." Tissue engineering. Part C, Methods **19**(2): 166-180.

Bartel, D. P. (2004). "MicroRNAs: genomics, biogenesis, mechanism, and function." Cell **116**(2): 281-297.

Bel-Vialar, S., F. Medevielle and F. Pituello (2007). "The on/off of Pax6 controls the tempo of neuronal differentiation in the developing spinal cord." Dev Biol **305**(2): 659-673.

Bose, A., H. Henkes, K. Alfke, W. Reith, T. E. Mayer, A. Berlis, V. Branca and S. P. Sit (2008). "The Penumbra System: a mechanical device for the treatment of acute stroke due to thromboembolism." AJNR Am J Neuroradiol **29**(7): 1409-1413.

Brafman, D. A. (2014). "Generation, Expansion, and Differentiation of Human Pluripotent Stem Cell (hPSC) Derived Neural Progenitor Cells (NPCs)." Methods Mol Biol.

Brice, J. and L. McLellan (1980). "SUPPRESSION OF INTENTION TREMOR BY CONTINGENT DEEP-BRAIN STIMULATION." The Lancet **315**(8180): 1221-1222.

Brindley, D. and C. Mason (2012). "Human embryonic stem cell therapy in the post-Geron era." Regenerative Medicine **7**(1): 17-18.

Brundin, P., G. Barbin, R. E. Strecker, O. Isacson, A. Prochiantz and A. Bjorklund (1988). "Survival and function of dissociated rat dopamine neurones grafted at different developmental stages or after being cultured in vitro." Brain research **467**(2): 233-243.

Brundin, P., O. G. Nilsson, R. E. Strecker, O. Lindvall, B. Astedt and A. Bjorklund (1986). "Behavioural effects of human fetal dopamine neurons grafted in a rat model of Parkinson's disease." Experimental brain research. Experimentelle Hirnforschung. Experimentation cerebrale **65**(1): 235-240.

Burton, K. and D. B. Calne (1984). "Dopamine agonists and Parkinson's disease." Clinical Neurology and Neurosurgery **86**(3): 172-177.

Burtscher, I. and H. Lickert (2009). "Foxa2 regulates polarity and epithelialization in the endoderm germ layer of the mouse embryo." Development **136**(6): 1029-1038.

Cai, J., A. Donaldson, M. Yang, M. S. German, G. Enikolopov and L. Iacovitti (2009). "The role of Lmx1a in the differentiation of human embryonic stem cells into midbrain dopamine neurons in culture and after transplantation into a Parkinson's disease model." Stem Cells **27**(1): 220-229.

Caiazzo, M., M. T. Dell'anno, E. Dvoretskova, D. Lazarevic, S. Taverna, D. Leo, T. D. Sotnikova, A. Menegon, P. Roncaglia, G. Colciago, G. Russo, P. Carninci, G. Pezzoli, R. R. Gainetdinov, S. Gustincich, A. Dityatev and V. Broccoli (2011). "Direct generation of functional dopaminergic neurons from mouse and human fibroblasts." Nature.

Carlsson, A., M. Lindqvist, T. Magnusson and B. Waldeck (1958). "On the presence of 3-hydroxytyramine in brain." Science **127**(3296): 471.

Catapult, C. T. (2013). VERIFIED CELL THERAPY CLINICAL TRIALS IN THE UK. Catapult. London.

Chambers, I., D. Colby, M. Robertson, J. Nichols, S. Lee, S. Tweedie and A. Smith (2003). "Functional expression cloning of Nanog, a pluripotency sustaining factor in embryonic stem cells." Cell **113**(5): 643-655.

Chambers, S. M., C. A. Fasano, E. P. Papapetrou, M. Tomishima, M. Sadelain and L. Studer (2009). "Highly efficient neural conversion of human ES and iPS cells by dual inhibition of SMAD signaling." Nat Biotechnol **27**(3): 275-280.

Chen, J., Y. Li, L. Wang, M. Lu, X. Zhang and M. Chopp (2001). "Therapeutic benefit of intracerebral transplantation of bone marrow stromal cells after cerebral ischemia in rats." Journal of the neurological sciences **189**(1-2): 49-57.

Chen, J., Z. G. Zhang, Y. Li, L. Wang, Y. X. Xu, S. C. Gautam, M. Lu, Z. Zhu and M. Chopp (2003). "Intravenous Administration of Human Bone Marrow Stromal Cells Induces Angiogenesis in the Ischemic Boundary Zone After Stroke in Rats." Circ Res **92**(6): 692-699.

Chen, M., J. Huang, X. Yang, B. Liu, W. Zhang, L. Huang, F. Deng, J. Ma, Y. Bai, R. Lu, B. Huang, Q. Gao, Y. Zhuo and J. Ge (2012). "Serum starvation induced cell cycle synchronization facilitates human somatic cells reprogramming." PLoS One **7**(4): e28203.

Cheng, L. C., E. Pastrana, M. Tavazoie and F. Doetsch (2009). "miR-124 regulates adult neurogenesis in the subventricular zone stem cell niche." Nat Neurosci **12**(4): 399-408.

Choices, N. (2012). "Stroke key facts." Retrieved 25th Aug, 2013, from http://www.nhs.uk/NHSEngland/NSF/Pages/Nationalstrokestrategy.aspx.

Chung, S., C. H. Kim and K. S. Kim (2012). "Lmx1a regulates dopamine transporter gene expression during ES cell differentiation and mouse embryonic development." Journal of neurochemistry **122**(2): 244-250.

Chung, S., J. I. Moon, A. Leung, D. Aldrich, S. Lukianov, Y. Kitayama, S. Park, Y. Li, V. Y. Bolshakov, T. Lamonerie and K. S. Kim (2011). "ES cell-derived renewable and functional midbrain dopaminergic progenitors." Proc Natl Acad Sci U S A **108**(23): 9703-9708.

Claassen, D. A., M. M. Desler and A. Rizzino (2009). "ROCK inhibition enhances the recovery and growth of cryopreserved human embryonic stem cells and human induced pluripotent stem cells." Mol Reprod Dev **76**(8): 722-732.

ClinicalTrials.gov. (2013, July 11, 2013). "TRANSEURO Open Label Transplant Study in Parkinson's Disease." Retrieved 26th August 2013, 2013, from http://clinicaltrials.gov/ct2/show/NCT01898390.

Cohen, J. E., E. Itshayek, S. Moskovici, J. M. Gomori, S. Fraifeld, R. Eichel and R. R. Leker (2011). "State-of-the-art reperfusion strategies for acute ischemic stroke." Journal of clinical neuroscience : official journal of the Neurosurgical Society of Australasia **18**(3): 319-323.

Conaco, C., S. Otto, J. J. Han and G. Mandel (2006). "Reciprocal actions of REST and a microRNA promote neuronal identity." Proc Natl Acad Sci U S A **103**(7): 2422-2427.

Cooper, O., G. Hargus, M. Deleidi, A. Blak, T. Osborn, E. Marlow, K. Lee, A. Levy, E. Perez-Torres, A. Yow and O. Isacson (2010). "Differentiation of human ES and Parkinson's disease iPS cells into ventral midbrain dopaminergic neurons requires a high activity form of SHH, FGF8a and specific regionalization by retinoic acid." Molecular and cellular neurosciences **45**(3): 258-266.

Cotzias, G. C., M. H. Van Woert and L. M. Schiffer (1967). "Aromatic amino acids and modification of parkinsonism." The New England journal of medicine **276**(7): 374-379.

Crawford, T. Q. and H. Roelink (2007). "The notch response inhibitor DAPT enhances neuronal differentiation in embryonic stem cell-derived embryoid bodies independently of sonic hedgehog signaling." Developmental dynamics : an official publication of the American Association of Anatomists **236**(3): 886-892.

Cross, M. A. and T. Enver (1997). "The lineage commitment of haemopoietic progenitor cells." Curr Opin Genet Dev **7**(5): 609-613.

Davie, C. A. (2008). "A review of Parkinson's disease." Br Med Bull **86**: 109-127.

Deb, P., S. Sharma and K. M. Hassan (2010). "Pathophysiologic mechanisms of acute ischemic stroke: An overview with emphasis on therapeutic significance beyond thrombolysis." Pathophysiology **17**(3): 197-218.

Devroe, E. and P. A. Silver (2002). "Retrovirus-delivered siRNA." BMC Biotechnol **2**: 15.

Dezawa, M., H. Kanno, M. Hoshino, H. Cho, N. Matsumoto, Y. Itokazu, N. Tajima, H. Yamada, H. Sawada, H. Ishikawa, T. Mimura, M. Kitada, Y. Suzuki and C. Ide (2004). "Specific induction of neuronal cells from bone marrow stromal cells and application for autologous transplantation." J Clin Invest **113**(12): 1701-1710.

Dirnagl, U., C. Iadecola and M. A. Moskowitz (1999). "Pathobiology of ischaemic stroke: an integrated view." Trends Neurosci **22**(9): 391-397.

Dogini, D. B., V. D. Pascoal, S. H. Avansini, A. S. Vieira, T. C. Pereira and I. Lopes-Cendes (2014). "The new world of RNAs." Genet Mol Biol **37**(1 Suppl): 285-293.

EuroStemCell. (2013). "Regulation of stem cell research in Europe." Retrieved 27thAugust 2013, 2013, from http://www.eurostemcell.org/stem-cell-regulations.

Excellence, N. I. f. H. a. C. (2010). NICE cost impact and commissioning assessment: quality standard for stroke, National Institue for Health and Clinical Excellence.

Ferri, A. L. M., W. Lin, Y. E. Mavromatakis, J. C. Wang, H. Sasaki, J. A. Whitsett and S.-L. Ang (2007). "Foxa1 and Foxa2 regulate multiple phases of midbrain dopaminergic neuron development in a dosage-dependent manner." Development **134**(15): 2761-2769.

Fiandaca, M., J. Forsayeth and K. Bankiewicz (2008). "Current status of gene therapy trials for Parkinson's disease." Exp Neurol **209**(1): 51-57.

Filipowicz, W., S. N. Bhattacharyya and N. Sonenberg (2008). "Mechanisms of post-transcriptional regulation by microRNAs: are the answers in sight?" Nat Rev Genet **9**(2): 102-114.

Findley, L. J. (2007). "The economic impact of Parkinson's disease." Parkinsonism & related disorders **13 Suppl**: S8-S12.

Foundation, B. H. (2009). "Stroke Statistics 2009: Summary " BHF Statistics database, from http://www.heartstats.org/temp/Summaryspamspglossaryhs1hs.pdf.

Friedman, J. H. (2010). "Parkinson's disease psychosis 2010: a review article." Parkinsonism Relat Disord **16**(9): 553-560.

Fu, Y. S., Y. C. Cheng, M. Y. Lin, H. Cheng, P. M. Chu, S. C. Chou, Y. H. Shih, M. H. Ko and M. S. Sung (2006). "Conversion of human umbilical cord mesenchymal stem cells in Wharton's jelly to dopaminergic neurons in vitro: potential therapeutic application for Parkinsonism." Stem Cells **24**(1): 115-124.

Gale, E. and M. Li (2008). "Midbrain dopaminergic neuron fate specification: Of mice and embryonic stem cells." Molecular brain **1**: 8.

Geiman, T. M. and K. D. Robertson (2002). "Chromatin remodeling, histone modifications, and DNA methylation-how does it all fit together?" J Cell Biochem **87**(2): 117-125.

Gensburger, C., G. Labourdette and M. Sensenbrenner (1987). "Brain basic fibroblast growth factor stimulates the proliferation of rat neuronal precursor cells in vitro." FEBS letters **217**(1): 1-5.

German, D. C., K. Manaye, W. K. Smith, D. J. Woodward and C. B. Saper (1989). "Midbrain dopaminergic cell loss in Parkinson's disease: computer visualization." Ann Neurol **26**(4): 507-514.

Gordon, M. Y. (1994). "Plastic-adherent cells in human bone marrow generate long-term hematopoiesis in vitro." Leukemia **8**(5): 865-870.

Gordon, M. Y., N. Levicar, M. Pai, P. Bachellier, I. Dimarakis, F. Al-Allaf, H. M'Hamdi, T. Thalji, J. P. Welsh, S. B. Marley, J. Davies, F. Dazzi, F. Marelli-Berg, P. Tait, R. Playford, L. Jiao, S. Jensen, J. P. Nicholls, A. Ayav, M. Nohandani, F. Farzaneh, J. Gaken, R. Dodge, M. Alison, J. F. Apperley, R. Lechler and N. A. Habib (2006). "Characterization and clinical application of human CD34+ stem/progenitor cell populations mobilized into the blood by granulocyte colony-stimulating factor." Stem Cells **24**(7): 1822-1830.

Graham, V., J. Khudyakov, P. Ellis and L. Pevny (2003). "SOX2 Functions to Maintain Neural Progenitor Identity." Neuron **39**(5): 749-765.

Graham, V., J. Khudyakov, P. Ellis and L. Pevny (2003). "SOX2 functions to maintain neural progenitor identity." Neuron **39**(5): 749-765.

Hartikka, J., M. Staufenbiel and H. Lubbert (1992). "Cyclic AMP, but not basic FGF, increases the in vitro survival of mesencephalic dopaminergic neurons and protects them from MPP(+)-induced degeneration." Journal of neuroscience research **32**(2): 190-201.

Health, N. I. o. (2013, November 14, 2011 ). "Stem Cell Information." Retrieved 26th August 2013, 2013, from http://stemcells.nih.gov/policy/Pages/Default.aspx.

Health, T. N. I. o. (2009, 28th April 2009). "Stem Cell Information." from http://stemcells.nih.gov/info.

Hellmann, M. A., R. Djaldetti, Z. Israel and E. Melamed (2006). "Effect of deep brain subthalamic stimulation on camptocormia and postural abnormalities in idiopathic Parkinson's disease." Mov Disord **21**(11): 2008-2010.

Heng, B. C., H. Liu, A. J. Rufaihah and T. Cao (2006). "Human embryonic stem cell (hES) colonies display a higher degree of spontaneous differentiation when passaged at lower densities." In vitro cellular & developmental biology. Animal **42**(3-4): 54-57.

Henry, E. Y. and C. B. Asa, Jr. (2004). "Adult stem cells." The Anatomical Record Part A: Discoveries in Molecular, Cellular, and Evolutionary Biology **276A**(1): 75-102.

Hermann, A., R. Gastl, S. Liebau, M. O. Popa, J. Fiedler, B. O. Boehm, M. Maisel, H. Lerche, J. Schwarz, R. Brenner and A. Storch (2004). "Efficient generation of neural stem cell-like cells from adult human bone marrow stromal cells." Journal of cell science **117**(Pt 19): 4411-4422.

Hindorff, L. A., P. Sethupathy, H. A. Junkins, E. M. Ramos, J. P. Mehta, F. S. Collins and T. A. Manolio (2009). "Potential etiologic and functional implications of genome-wide association loci for human diseases and traits." Proc Natl Acad Sci U S A **106**(23): 9362-9367.

Hitoshi, S., R. M. Seaberg, C. Koscik, T. Alexson, S. Kusunoki, I. Kanazawa, S. Tsuji and D. van der Kooy (2004). "Primitive neural stem cells from the mammalian epiblast differentiate to definitive neural stem cells under the control of Notch signaling." Genes & development **18**(15): 1806-1811.

Hyman, C., M. Hofer, Y. A. Barde, M. Juhasz, G. D. Yancopoulos, S. P. Squinto and R. M. Lindsay (1991). "BDNF is a neurotrophic factor for dopaminergic neurons of the substantia nigra." Nature **350**(6315): 230-232.

Inman, G. J., F. J. Nicolas, J. F. Callahan, J. D. Harling, L. M. Gaster, A. D. Reith, N. J. Laping and C. S. Hill (2002). "SB-431542 is a potent and specific inhibitor of transforming growth factor-beta superfamily type I activin receptor-like kinase (ALK) receptors ALK4, ALK5, and ALK7." Molecular pharmacology **62**(1): 65-74.

Institute, H. S. C. (2013). "StemBook." from http://www.stembook.org/.

Ives, N. J., R. L. Stowe, J. Marro, C. Counsell, A. Macleod, C. E. Clarke, R. Gray and K. Wheatley (2004). "Monoamine oxidase type B inhibitors in early Parkinson's disease: meta-analysis of 17 randomised trials involving 3525 patients." BMJ **329**(7466): 593.

Jaccard, N., L. D. Griffin, A. Keser, R. J. Macown, A. Super, F. S. Veraitch and N. Szita (2014). "Automated method for the rapid and precise estimation of adherent cell culture characteristics from phase contrast microscopy images." Biotechnol Bioeng **111**(3): 504-517.

Jackson, A. L. and P. S. Linsley (2010). "Recognizing and avoiding siRNA off-target effects for target identification and therapeutic application." Nat Rev Drug Discov **9**(1): 57-67.

Jiang, Y., D. Henderson, M. Blackstad, A. Chen, R. F. Miller and C. M. Verfaillie (2003). "Neuroectodermal differentiation from mouse multipotent adult progenitor cells." Proc Natl Acad Sci U S A **100 Suppl 1**: 11854-11860.

Joannides, A. J., C. Fiore-Heriche, A. A. Battersby, P. Athauda-Arachchi, I. A. Bouhon, L. Williams, K. Westmore, P. J. Kemp, A. Compston, N. D. Allen and S. Chandran (2007). "A scaleable and defined system for generating neural stem cells from human embryonic stem cells." Stem Cells **25**(3): 731-737.

Karlsborg, M., L. Korbo, L. Regeur and A. Glad (2010). "Duodopa pump treatment in patients with advanced Parkinson's disease." Dan Med Bull **57**(6): A4155.

Kawada, H., S. Takizawa, T. Takanashi, Y. Morita, J. Fujita, K. Fukuda, S. Takagi, H. Okano, K. Ando and T. Hotta (2006). "Administration of hematopoietic cytokines in the subacute phase after cerebral infarction is effective for functional recovery facilitating proliferation of intrinsic neural stem/progenitor cells and transition of bone marrow-derived neuronal cells." Circulation **113**(5): 701-710.

Keirstead, H. S., G. Nistor, G. Bernal, M. Totoiu, F. Cloutier, K. Sharp and O. Steward (2005). "Human embryonic stem cell-derived oligodendrocyte progenitor cell transplants remyelinate and restore locomotion after spinal cord injury." The Journal of neuroscience : the official journal of the Society for Neuroscience **25**(19): 4694-4705.

Kim, J. H., J. M. Auerbach, J. A. Rodriguez-Gomez, I. Velasco, D. Gavin, N. Lumelsky, S. H. Lee, J. Nguyen, R. Sanchez-Pernaute, K. Bankiewicz and R. McKay (2002). "Dopamine neurons derived from embryonic stem cells function in an animal model of Parkinson's disease." Nature **418**(6893): 50-56.

Kordower, J. H., J. M. Rosenstein, T. J. Collier, M. A. Burke, E. Y. Chen, J. M. Li, L. Martel, A. E. Levey, E. J. Mufson, T. B. Freeman and C. W. Olanow (1996). "Functional fetal nigral grafts in a patient with Parkinson's disease: chemoanatomic, ultrastructural, and metabolic studies." The Journal of comparative neurology **370**(2): 203-230.

Krichevsky, A. M., K. S. King, C. P. Donahue, K. Khrapko and K. S. Kosik (2003). "A microRNA array reveals extensive regulation of microRNAs during brain development." RNA **9**(10): 1274-1281.

Krichevsky, A. M., K. C. Sonntag, O. Isacson and K. S. Kosik (2006). "Specific microRNAs modulate embryonic stem cell-derived neurogenesis." Stem Cells **24**(4): 857-864.

Krieglstein, K., P. Henheik, L. Farkas, J. Jaszai, D. Galter, K. Krohn and K. Unsicker (1998). "Glial cell line-derived neurotrophic factor requires transforming growth factor-beta for exerting its full neurotrophic potential on peripheral and CNS neurons." The Journal of neuroscience : the official journal of the Society for Neuroscience **18**(23): 9822-9834.

Kriks, S., J. W. Shim, J. Piao, Y. M. Ganat, D. R. Wakeman, Z. Xie, L. Carrillo-Reid, G. Auyeung, C. Antonacci, A. Buch, L. Yang, M. F. Beal, D. J. Surmeier, J. H. Kordower, V. Tabar and L. Studer (2011). "Dopamine neurons derived from human ES cells efficiently engraft in animal models of Parkinson's disease." Nature **480**(7378): 547-551.

Lai, K., B. K. Kaspar, F. H. Gage and D. V. Schaffer (2003). "Sonic hedgehog regulates adult neural progenitor proliferation in vitro and in vivo." Nat Neurosci **6**(1): 21-27.

Lam, B. S. and G. B. Adams (2010). "Hematopoietic stem cell lodgment in the adult bone marrow stem cell niche." Int J Lab Hematol **32**(6 Pt 2): 551-558.

Lander, E. S., L. M. Linton, B. Birren, C. Nusbaum, M. C. Zody, J. Baldwin, K. Devon, K. Dewar, M. Doyle, W. FitzHugh, R. Funke, D. Gage, K. Harris, A. Heaford, J. Howland, L. Kann, J. Lehoczky, R. LeVine, P. McEwan, K. McKernan, J. Meldrim, J. P. Mesirov, C. Miranda, W. Morris, J. Naylor, C. Raymond, M. Rosetti, R. Santos, A. Sheridan, C. Sougnez, N. Stange-Thomann, N. Stojanovic, A. Subramanian, D. Wyman, J. Rogers, J. Sulston, R. Ainscough, S. Beck, D. Bentley, J. Burton, C. Clee, N. Carter, A. Coulson, R. Deadman, P. Deloukas, A. Dunham, I. Dunham, R. Durbin, L. French, D. Grafham, S. Gregory, T. Hubbard, S. Humphray, A. Hunt, M. Jones, C. Lloyd, A. McMurray, L. Matthews, S. Mercer, S. Milne, J. C. Mullikin, A. Mungall, R. Plumb, M. Ross, R. Shownkeen, S. Sims, R. H. Waterston, R. K. Wilson, L. W. Hillier, J. D. McPherson, M. A. Marra, E. R. Mardis, L. A. Fulton, A. T. Chinwalla, K. H. Pepin, W. R. Gish, S. L. Chissoe, M. C. Wendl, K. D. Delehaunty, T. L. Miner, A. Delehaunty, J. B. Kramer, L. L. Cook, R. S. Fulton, D. L. Johnson, P. J. Minx, S. W. Clifton, T. Hawkins, E. Branscomb, P. Predki, P. Richardson, S. Wenning, T. Slezak, N. Doggett, J. F. Cheng, A. Olsen, S. Lucas, C. Elkin, E. Uberbacher, M. Frazier, R. A. Gibbs, D. M. Muzny, S. E. Scherer, J. B. Bouck, E. J. Sodergren, K. C. Worley, C. M. Rives, J. H. Gorrell, M. L. Metzker, S. L. Naylor, R. S. Kucherlapati, D. L. Nelson, G. M. Weinstock, Y. Sakaki, A. Fujiyama, M. Hattori, T. Yada, A. Toyoda, T. Itoh, C. Kawagoe, H. Watanabe, Y. Totoki, T. Taylor, J. Weissenbach, R. Heilig, W. Saurin, F. Artiguenave, P. Brottier, T. Bruls, E. Pelletier, C. Robert, P. Wincker, D. R. Smith, L. Doucette-Stamm, M. Rubenfield, K. Weinstock, H. M. Lee, J. Dubois, A. Rosenthal, M. Platzer, G. Nyakatura, S. Taudien, A. Rump, H. Yang, J. Yu, J. Wang, G. Huang, J. Gu, L. Hood, L. Rowen, A. Madan, S. Qin, R. W. Davis, N. A. Federspiel, A. P. Abola, M. J. Proctor, R. M. Myers, J. Schmutz, M. Dickson, J. Grimwood, D. R. Cox, M. V. Olson, R. Kaul, C. Raymond, N. Shimizu, K. Kawasaki, S. Minoshima, G. A. Evans, M. Athanasiou, R. Schultz, B. A. Roe, F. Chen, H. Pan, J. Ramser, H. Lehrach, R. Reinhardt, W. R. McCombie, M. de la Bastide, N. Dedhia, H. Blocker, K. Hornischer, G. Nordsiek, R. Agarwala, L. Aravind, J. A. Bailey, A. Bateman, S. Batzoglou, E. Birney, P. Bork, D. G. Brown, C. B. Burge, L. Cerutti, H. C. Chen, D. Church, M. Clamp, R. R. Copley, T. Doerks, S. R. Eddy, E. E. Eichler, T. S. Furey, J. Galagan, J. G. Gilbert, C. Harmon, Y. Hayashizaki, D. Haussler, H. Hermjakob, K. Hokamp, W. Jang, L. S. Johnson, T. A. Jones, S. Kasif, A. Kaspryzk, S. Kennedy, W. J. Kent, P. Kitts, E. V. Koonin, I. Korf, D. Kulp, D. Lancet, T. M. Lowe, A. McLysaght, T. Mikkelsen, J. V. Moran, N. Mulder, V. J. Pollara, C. P. Ponting, G. Schuler, J. Schultz, G. Slater, A. F. Smit, E. Stupka, J. Szustakowski, D. Thierry-Mieg, J. Thierry-Mieg, L. Wagner, J. Wallis, R. Wheeler, A. Williams, Y. I. Wolf, K. H. Wolfe, S. P. Yang, R. F. Yeh, F. Collins, M. S. Guyer, J. Peterson, A. Felsenfeld, K. A. Wetterstrand, A. Patrinos, M. J. Morgan, P. de Jong, J. J. Catanese, K. Osoegawa, H. Shizuya, S. Choi, Y. J. Chen and C. International Human Genome Sequencing (2001). "Initial sequencing and analysis of the human genome." Nature **409**(6822): 860-921.

Laping, N. J., E. Grygielko, A. Mathur, S. Butter, J. Bomberger, C. Tweed, W. Martin, J. Fornwald, R. Lehr, J. Harling, L. Gaster, J. F. Callahan and B. A. Olson (2002). "Inhibition of transforming growth factor (TGF)-beta1-induced extracellular matrix with a novel inhibitor of the TGF-beta type I receptor kinase activity: SB-431542." Molecular pharmacology **62**(1): 58-64.

Lee, H. S., E. J. Bae, S. H. Yi, J. W. Shim, A. Y. Jo, J. S. Kang, E. H. Yoon, Y. H. Rhee, C. H. Park, H. C. Koh, H. J. Kim, H. S. Choi, J. W. Han, Y. S. Lee, J. Kim, J. Y. Li, P. Brundin and S. H. Lee (2010). "Foxa2 and Nurr1 synergistically yield A9 nigral dopamine neurons exhibiting improved differentiation, function, and cell survival." Stem Cells **28**(3): 501-512.

Lee, J. S., J. M. Hong, G. J. Moon, P. H. Lee, Y. H. Ahn and O. Y. Bang (2010). "A long-term follow-up study of intravenous autologous mesenchymal stem cell transplantation in patients with ischemic stroke." Stem Cells **28**(6): 1099-1106.

Lees, A. J., J. Hardy and T. Revesz (2009). "Parkinson's disease." Lancet **373**(9680): 2055-2066.

Levicar, N., M. Pai, N. A. Habib, P. Tait, L. R. Jiao, S. B. Marley, J. Davis, F. Dazzi, C. Smadja, S. L. Jensen, J. P. Nicholls, J. F. Apperley and M. Y. Gordon (2008). "Long-term clinical results of autologous infusion of mobilized adult bone marrow derived CD34+ cells in patients with chronic liver disease." Cell Prolif **41 Suppl 1**: 115-125.

Lin, W., E. Metzakopian, Y. E. Mavromatakis, N. Gao, N. Balaskas, H. Sasaki, J. Briscoe, J. A. Whitsett, M. Goulding, K. H. Kaestner and S.-L. Ang (2009). "Foxa1 and Foxa2 function both upstream of and cooperatively with Lmx1a and Lmx1b in a feedforward loop promoting mesodiencephalic dopaminergic neuron development." Developmental Biology **333**(2): 386-396.

Lindvall, O., P. Brundin, H. Widner, S. Rehncrona, B. Gustavii, R. Frackowiak, K. L. Leenders, G. Sawle, J. C. Rothwell, C. D. Marsden and et al. (1990). "Grafts of fetal dopamine neurons survive and improve motor function in Parkinson's disease." Science **247**(4942): 574-577.

Lindvall, O. and Z. Kokaia (2006). "Stem cells for the treatment of neurological disorders." Nature **441**(7097): 1094-1096.

Lindvall, O. and Z. Kokaia (2009). "Prospects of stem cell therapy for replacing dopamine neurons in Parkinson's disease." Trends Pharmacol Sci **30**(5): 260-267.

Lindvall, O., H. Widner, S. Rehncrona, P. Brundin, P. Odin, B. Gustavii, R. Frackowiak, K. L. Leenders, G. Sawle, J. C. Rothwell and et al. (1992). "Transplantation of fetal dopamine neurons in Parkinson's disease: one-year clinical and neurophysiological observations in two patients with putaminal implants." Annals of neurology **31**(2): 155-165.

Lopez, A. D., C. D. Mathers, M. Ezzati, D. T. Jamison and C. J. Murray (2006). "Global and regional burden of disease and risk factors, 2001: systematic analysis of population health data." Lancet **367**(9524): 1747-1757.

Lowell, S., A. Benchoua, B. Heavey and A. G. Smith (2006). "Notch promotes neural lineage entry by pluripotent embryonic stem cells." PLoS biology **4**(5): e121.

Marti, E., D. A. Bumcrot, R. Takada and A. P. McMahon (1995). "Requirement of 19K form of Sonic hedgehog for induction of distinct ventral cell types in CNS explants." Nature **375**(6529): 322-325.

Martin, G. R. (1981). "Isolation of a pluripotent cell line from early mouse embryos cultured in medium conditioned by teratocarcinoma stem cells." Proceedings of the National Academy of Sciences of the United States of America **78**(12): 7634-7638.

Martinez-Agosto, J. A., H. K. Mikkola, V. Hartenstein and U. Banerjee (2007). "The hematopoietic stem cell and its niche: a comparative view." Genes Dev **21**(23): 3044-3060.

Martino, S., I. di Girolamo, A. Orlacchio and A. Datti (2009). "MicroRNA implications across neurodevelopment and neuropathology." J Biomed Biotechnol **2009**: 654346.

Mason, C., M. J. McCall, E. J. Culme-Seymour, S. Suthasan, S. Edwards-Parton, G. A. Bonfiglio and B. C. Reeve (2012). "The global cell therapy industry continues to rise during the second and third quarters of 2012." Cell stem cell **11**(6): 735-739.

Massano, J. and K. P. Bhatia (2012). "Clinical approach to Parkinson's disease: features, diagnosis, and principles of management." Cold Spring Harb Perspect Med **2**(6): a008870.

Masui, S., Y. Nakatake, Y. Toyooka, D. Shimosato, R. Yagi, K. Takahashi, H. Okochi, A. Okuda, R. Matoba, A. A. Sharov, M. S. Ko and H. Niwa (2007). "Pluripotency governed by Sox2 via regulation of Oct3/4 expression in mouse embryonic stem cells." Nature cell biology **9**(6): 625-635.

Meza-Sosa, K. F., G. Pedraza-Alva and L. Perez-Martinez (2014). "microRNAs: key triggers of neuronal cell fate." Front Cell Neurosci **8**: 175.

Mikkola, H. K. A. and S. H. Orkin (2006). "The journey of developing hematopoietic stem cells." Development **133**(19): 3733-3744.

Mitsios, N., J. Gaffney, P. Kumar, J. Krupinski, S. Kumar and M. Slevin (2006). "Pathophysiology of acute ischaemic stroke: an analysis of common signalling mechanisms and identification of new molecular targets." Pathobiology **73**(4): 159-175.

Mitsui, K., Y. Tokuzawa, H. Itoh, K. Segawa, M. Murakami, K. Takahashi, M. Maruyama, M. Maeda and S. Yamanaka (2003). "The homeoprotein Nanog is required for maintenance of pluripotency in mouse epiblast and ES cells." Cell **113**(5): 631-642.

Morshead, C. M., B. A. Reynolds, C. G. Craig, M. W. McBurney, W. A. Staines, D. Morassutti, S. Weiss and D. van der Kooy (1994). "Neural stem cells in the adult mammalian forebrain: a relatively quiescent subpopulation of subependymal cells." Neuron **13**(5): 1071-1082.

Nakajima, M., T. Ishimuro, K. Kato, I. K. Ko, I. Hirata, Y. Arima and H. Iwata (2007). "Combinatorial protein display for the cell-based screening of biomaterials that direct neural stem cell differentiation." Biomaterials **28**(6): 1048-1060.

O'Keeffe, F. E., S. A. Scott, P. Tyers, G. W. O'Keeffe, J. W. Dalley, R. Zufferey and M. A. Caldwell (2008). "Induction of A9 dopaminergic neurons from neural stem cells improves motor function in an animal model of Parkinson's disease." Brain **131**(Pt 3): 630-641.

O'Keeffe, G. C., R. A. Barker and M. A. Caldwell (2009). "Dopaminergic modulation of neurogenesis in the subventricular zone of the adult brain." Cell Cycle **8**(18): 2888-2894.

Obeso, J. A., M. C. Rodriguez-Oroz, M. Rodriguez, R. Macias, L. Alvarez, J. Guridi, J. Vitek and M. R. DeLong (2000). "Pathophysiologic basis of surgery for Parkinson's disease." Neurology **55**(12 Suppl 6): S7-12.

Oh, S. A., H. Y. Lee, J. H. Lee, T. H. Kim, J. H. Jang, H. W. Kim and I. Wall (2012). "Collagen three-dimensional hydrogel matrix carrying basic fibroblast growth factor for the cultivation of mesenchymal stem cells and osteogenic differentiation." Tissue Eng Part A **18**(9-10): 1087-1100.

Olmer, R., A. Lange, S. Selzer, C. Kasper, A. Haverich, U. Martin and R. Zweigerdt (2012). "Suspension culture of human pluripotent stem cells in controlled, stirred bioreactors." Tissue Eng Part C Methods **18**(10): 772-784.

Omodei, D., D. Acampora, P. Mancuso, N. Prakash, L. G. Di Giovannantonio, W. Wurst and A. Simeone (2008). "Anterior-posterior graded response to Otx2 controls proliferation and differentiation of dopaminergic progenitors in the ventral mesencephalon." Development **135**(20): 3459-3470.

Packer, A. N., Y. Xing, S. Q. Harper, L. Jones and B. L. Davidson (2008). "The bifunctional microRNA miR-9/miR-9* regulates REST and CoREST and is downregulated in Huntington's disease." J Neurosci **28**(53): 14341-14346.

Pai, M., D. Zacharoulis, M. N. Milicevic, S. Helmy, L. R. Jiao, N. Levicar, P. Tait, M. Scott, S. B. Marley, K. Jestice, M. Glibetic, D. Bansi, S. A. Khan, D. Kyriakou, C. Rountas, A. Thillainayagam, J. P. Nicholls, S. Jensen, J. F. Apperley, M. Y. Gordon and N. A. Habib (2008). "Autologous infusion of expanded mobilized adult bone marrow-derived CD34+ cells into patients with alcoholic liver cirrhosis." Am J Gastroenterol **103**(8): 1952-1958.

Pan, G. and J. A. Thomson (2007). "Nanog and transcriptional networks in embryonic stem cell pluripotency." Cell Res **17**(1): 42-49.

Parish, C. L., G. Castelo-Branco, N. Rawal, J. Tonnesen, A. T. Sorensen, C. Salto, M. Kokaia, O. Lindvall and E. Arenas (2008). "Wnt5a-treated midbrain neural stem cells improve dopamine cell replacement therapy in parkinsonian mice." J Clin Invest **118**(1): 149-160.

Park, C. H., M. S. Lim, Y. H. Rhee, S. H. Yi, B. K. Kim, J. W. Shim, Y. H. Kim, S. J. Jung and S. H. Lee (2012). "In vitro generation of mature dopamine neurons by decreasing and delaying the expression of exogenous Nurr1." Development **139**(13): 2447-2451.

Parkinson, J. (1917). An Essay on the Shaking Plasy, The Royal College of Surgeons.

Peh, G. S., K. P. Toh, H. P. Ang, X. Y. Seah, B. L. George and J. S. Mehta (2013). "Optimization of human corneal endothelial cell culture: density dependency of successful cultures in vitro." BMC Res Notes **6**: 176.

Pelton, T. A., S. Sharma, T. C. Schulz, J. Rathjen and P. D. Rathjen (2002). "Transient pluripotent cell populations during primitive ectoderm formation: correlation of in vivo and in vitro pluripotent cell development." Journal of cell science **115**(Pt 2): 329-339.

Pera, M. F. (2011). "Stem cells: The dark side of induced pluripotency." Nature **471**(7336): 46-47.

Pfisterer, U., A. Kirkeby, O. Torper, J. Wood, J. Nelander, A. Dufour, A. Bjorklund, O. Lindvall, J. Jakobsson and M. Parmar (2011). "Direct conversion of human fibroblasts to dopaminergic neurons." Proc Natl Acad Sci U S A **108**(25): 10343-10348.

Pillai, R. S., S. N. Bhattacharyya and W. Filipowicz (2007). "Repression of protein synthesis by miRNAs: how many mechanisms?" Trends Cell Biol **17**(3): 118-126.

Pleasure, S. J. and V. M. Lee (1993). "NTera 2 cells: a human cell line which displays characteristics expected of a human committed neuronal progenitor cell." Journal of neuroscience research **35**(6): 585-602.

Pleasure, S. J., C. Page and V. M. Lee (1992). "Pure, postmitotic, polarized human neurons derived from NTera 2 cells provide a system for expressing exogenous proteins in terminally differentiated neurons." The Journal of neuroscience : the official journal of the Society for Neuroscience **12**(5): 1802-1815.

Reebye, V., P. Saetrom, P. J. Mintz, K. W. Huang, P. Swiderski, L. Peng, C. Liu, X. X. Liu, S. Jensen, D. Zacharoulis, N. Kostomitsopoulos, N. Kasahara, J. P. Nicholls, L. R. Jiao, M. Pai, M. Mizandari, T. Chikovani, M. M. Emara, A. Haoudi, D. A. Tomalia, J. J. Rossi, N. A. Habib and D. R. Spalding (2013). "A novel RNA oligonucleotide improves liver function and inhibits liver carcinogenesis in vivo." Hepatology.

Reebye, V., P. Saetrom, P. J. Mintz, J. J. Rossi, N. Kasahara, G. Nteliopoulos, J. Nicholls, A. Haoudi, M. Gordon and N. A. Habib (2013). "A Short-activating RNA Oligonucleotide Targeting the Islet beta-cell Transcriptional Factor MafA in CD34(+) Cells." Molecular therapy. Nucleic acids **2**: e97.

ReNeuron. (2013, 1 August 2013). "ReNeuron wins £1.5 million UK Government grant for Phase II stroke trial." Retrieved 26th August 2013, 2013, from http://www.reneuron.com/press-release/reneuron-wins-1-5-million-uk-government-grant-for-phase-ii-stroke-trial.

Reubinoff, B. E., M. F. Pera, C. Y. Fong, A. Trounson and A. Bongso (2000). "Embryonic stem cell lines from human blastocysts: somatic differentiation in vitro." Nature biotechnology **18**(4): 399-404.

Roelink, H., A. Augsburger, J. Heemskerk, V. Korzh, S. Norlin, A. Ruiz i Altaba, Y. Tanabe, M. Placzek, T. Edlund, T. M. Jessell and et al. (1994). "Floor plate and motor neuron induction by vhh-1, a vertebrate homolog of hedgehog expressed by the notochord." Cell **76**(4): 761-775.

Roybon, L., Z. Ma, F. Asztely, A. Fosum, S. E. Jacobsen, P. Brundin and J. Y. Li (2006). "Failure of transdifferentiation of adult hematopoietic stem cells into neurons." Stem Cells **24**(6): 1594-1604.

Sacchetti, P., R. Carpentier, P. Segard, C. Olive-Cren and P. Lefebvre (2006). "Multiple signaling pathways regulate the transcriptional activity of the orphan nuclear receptor NURR1." Nucleic acids research **34**(19): 5515-5527.

Salehinejad, P., N. B. Alitheen, A. Mandegary, S. N. Nematollahi-Mahani and E. Janzamin (2013). "Effect of EGF and FGF on the expansion properties of human umbilical cord mesenchymal cells." In vitro cellular & developmental biology. Animal.

Sander, M., S. Paydar, J. Ericson, J. Briscoe, E. Berber, M. German, T. M. Jessell and J. L. Rubenstein (2000). "Ventral neural patterning by Nkx homeobox genes: Nkx6.1 controls somatic motor neuron and ventral interneuron fates." Genes & development **14**(17): 2134-2139.

Savitz, S. I., V. Misra, M. Kasam, H. Juneja, C. S. Cox, Jr., S. Alderman, I. Aisiku, S. Kar, A. Gee and J. C. Grotta (2011). "Intravenous autologous bone marrow mononuclear cells for ischemic stroke." Ann Neurol **70**(1): 59-69.

Scadden, D. T. (2006). "The stem-cell niche as an entity of action." Nature **441**(7097): 1075-1079.

Schofield, R. (1978). "The relationship between the spleen colony-forming cell and the haemopoietic stem cell." Blood cells.

Schwarting, S., S. Litwak, W. Hao, M. Bahr, J. Weise and H. Neumann (2008). "Hematopoietic stem cells reduce postischemic inflammation and ameliorate ischemic brain injury." Stroke; a journal of cerebral circulation **39**(10): 2867-2875.

Shao, N. Y., H. Y. Hu, Z. Yan, Y. Xu, H. Hu, C. Menzel, N. Li, W. Chen and P. Khaitovich (2010). "Comprehensive survey of human brain microRNA by deep sequencing." BMC Genomics **11**: 409.

Shen, L. H., Y. Li, J. Chen, A. Zacharek, Q. Gao, A. Kapke, M. Lu, K. Raginski, P. Vanguri, A. Smith and M. Chopp (2007). "Therapeutic benefit of bone marrow stromal cells administered 1 month after stroke." Journal of cerebral blood flow and metabolism : official journal of the International Society of Cerebral Blood Flow and Metabolism **27**(1): 6-13.

Shim, J. W., C. H. Park, Y. C. Bae, J. Y. Bae, S. Chung, M. Y. Chang, H. C. Koh, H. S. Lee, S. J. Hwang, K. H. Lee, Y. S. Lee, C. Y. Choi and S. H. Lee (2007). "Generation of functional dopamine neurons from neural precursor cells isolated from the subventricular zone and white matter of the adult rat brain using Nurr1 overexpression." Stem Cells **25**(5): 1252-1262.

Sigurjonsson, O. E., M. C. Perreault, T. Egeland and J. C. Glover (2005). "Adult human hematopoietic stem cells produce neurons efficiently in the regenerating chicken embryo spinal cord." Proceedings of the National Academy of Sciences of the United States of America **102**(14): 5227-5232.

Siomi, M. C., K. Sato, D. Pezic and A. A. Aravin (2011). "PIWI-interacting small RNAs: the vanguard of genome defence." Nat Rev Mol Cell Biol **12**(4): 246-258.

Stanslowsky, N., A. Haase, U. Martin, M. Naujock, A. Leffler, R. Dengler and F. Wegner (2014). "Functional differentiation of midbrain neurons from human cord blood-derived induced pluripotent stem cells." Stem Cell Res Ther **5**(2): 35.

Steichen, C., E. Luce, J. Maluenda, L. Tosca, I. Moreno-Gimeno, C. Desterke, N. Dianat, S. Goulinet-Mainot, S. Awan-Toor, D. Burks, J. Marie, A. Weber, G. Tachdjian, J. Melki and A. Dubart-Kupperschmitt (2014). "Messenger RNA- versus retrovirus-based induced pluripotent stem cell reprogramming strategies: analysis of genomic integrity." Stem Cells Transl Med **3**(6): 686-691.

Steinemann, D., G. Gohring and B. Schlegelberger (2013). "Genetic instability of modified stem cells - a first step towards malignant transformation?" American journal of stem cells **2**(1): 39-51.

Suzuki, S., J. Namiki, S. Shibata, Y. Mastuzaki and H. Okano (2010). "The neural stem/progenitor cell marker nestin is expressed in proliferative endothelial cells, but not in mature vasculature." J Histochem Cytochem **58**(8): 721-730.

Svendsen C. N., E. A. E., Ed. (2008). Encyclopedia of Stem cell research, SAGE Publications.

Taguchi, A., T. Soma, H. Tanaka, T. Kanda, H. Nishimura, H. Yoshikawa, Y. Tsukamoto, H. Iso, Y. Fujimori, D. M. Stern, H. Naritomi and T. Matsuyama (2004). "Administration of CD34+ cells after stroke enhances neurogenesis via angiogenesis in a mouse model." J Clin Invest **114**(3): 330-338.

Takagi, Y., J. Takahashi, H. Saiki, A. Morizane, T. Hayashi, Y. Kishi, H. Fukuda, Y. Okamoto, M. Koyanagi, M. Ideguchi, H. Hayashi, T. Imazato, H. Kawasaki, H. Suemori, S. Omachi, H. Iida, N. Itoh, N. Nakatsuji, Y. Sasai and N. Hashimoto (2005). "Dopaminergic neurons generated from monkey embryonic stem cells function in a Parkinson primate model." J Clin Invest **115**(1): 102-109.

Takahashi, K. and S. Yamanaka (2006). "Induction of pluripotent stem cells from mouse embryonic and adult fibroblast cultures by defined factors." Cell **126**(4): 663-676.

Thanvi, B., N. Lo and T. Robinson (2007). "Levodopa-induced dyskinesia in Parkinson's disease: clinical features, pathogenesis, prevention and treatment." Postgraduate medical journal **83**(980): 384-388.

Theka, I., M. Caiazzo, E. Dvoretskova, D. Leo, F. Ungaro, S. Curreli, F. Manago, M. T. Dell'Anno, G. Pezzoli, R. R. Gainetdinov, A. Dityatev and V. Broccoli (2013). "Rapid generation of functional dopaminergic neurons from human induced pluripotent stem cells through a single-step procedure using cell lineage transcription factors." Stem cells translational medicine **2**(6): 473-479.

Therapy, C. U.-C. (2013). Verified Cell Therapy Clinical Trials in the UK. London, Catapult.

Thomson, J. A., J. Itskovitz-Eldor, S. S. Shapiro, M. A. Waknitz, J. J. Swiergiel, V. S. Marshall and J. M. Jones (1998). "Embryonic stem cell lines derived from human blastocysts." Science **282**(5391): 1145-1147.

Thomson, J. A., J. Itskovitz-Eldor, S. S. Shapiro, M. A. Waknitz, J. J. Swiergiel, V. S. Marshall and J. M. Jones (1998). "Embryonic Stem Cell Lines Derived from Human Blastocysts." Science **282**(5391): 1145-1147.

Thwaites, J. W., V. Reebye, P. Mintz, N. Levicar and N. Habib (2012). "Cellular replacement and regenerative medicine therapies in ischemic stroke." Regenerative Medicine **7**(3): 387-395.

Trials.gov, C. (2013, February 1, 2013). "Safety and Tolerability of Sub-retinal Transplantation of hESC Derived RPE (MA09-hRPE) Cells in Patients With Advanced Dry Age Related Macular Degeneration (Dry AMD)." Retrieved 26th August 2013, 2013, from http://clinicaltrials.gov/ct2/show/NCT01344993?term=rpe+advanced+cell+technology&rank=1.

Trials.gov, C. (2013, February 1, 2013). "Sub-retinal Transplantation of hESC Derived RPE(MA09-hRPE)Cells in Patients With Stargardt's Macular Dystrophy." Retrieved 26th August 2013, 2013, from http://clinicaltrials.gov/ct2/show/NCT01345006?term=NCT01345006&rank=1.

UK, P. s. (2010). What is Parkinson's?

UK, P. s. (2013). "Parkinson's Symptoms." Retrieved 26th August 2013, 2013, from http://www.parkinsons.org.uk/content/parkinsons-symptoms.

UK, P. s. (2013). "Treatments and Therapies for Parkinson's." Retrieved 23rd August 2013, 2013, from http://www.parkinsons.org.uk/content/treatments-and-therapies-parkinsons.

UK, P. s. (2013). "What is Parkinson's?" Retrieved 26th August 2013, 2013, from http://www.parkinsons.org.uk/content/what-parkinsons.

Van Winkle, A. P., I. D. Gates and M. S. Kallos (2012). "Mass transfer limitations in embryoid bodies during human embryonic stem cell differentiation." Cells Tissues Organs **196**(1): 34-47.

Veraitch, F. S., R. Scott, J. W. Wong, G. J. Lye and C. Mason (2008). "The impact of manual processing on the expansion and directed differentiation of embryonic stem cells." Biotechnology and bioengineering **99**(5): 1216-1229.

Vitek, J. L. (2008). "Deep brain stimulation: how does it work?" Cleve Clin J Med **75 Suppl 2**: S59-65.

Wagers, A. J. and I. L. Weissman (2004). "Plasticity of Adult Stem Cells." Cell **116**(5): 639-648.

Walcher, T., Q. Xie, J. Sun, M. Irmler, J. Beckers, T. Ozturk, D. Niessing, A. Stoykova, A. Cvekl, J. Ninkovic and M. Gotz (2013). "Functional dissection of the paired domain of Pax6 reveals molecular mechanisms of coordinating neurogenesis and proliferation." Development **140**(5): 1123-1136.

Watt, F. M., Hogan, L. Brigid, nbsp and M (2000). "Out of Eden: Stem Cells and Their Niches." Science **287**(5457): 1427-1430.

Weil, B. V., FS (2014). Bioprocessing Challenges Associated with the Purification of Cellular Therapies. Stem Cells and Cell Therapy, Springer.

Wernig, M., J. P. Zhao, J. Pruszak, E. Hedlund, D. Fu, F. Soldner, V. Broccoli, M. Constantine-Paton, O. Isacson and R. Jaenisch (2008). "Neurons derived from reprogrammed fibroblasts functionally integrate into the fetal brain and improve symptoms of rats with Parkinson's disease." Proc Natl Acad Sci U S A **105**(15): 5856-5861.

Wesselschmidt, R. L. (2011). "The teratoma assay: an in vivo assessment of pluripotency." Methods in molecular biology **767**: 231-241.

WHO. (2013). "Pharmaceutical Industry." Retrieved 27th August 2013, 2013, from http://www.who.int/trade/glossary/story073/en/index.html.

Woodbury, D., E. J. Schwarz, D. J. Prockop and I. B. Black (2000). "Adult rat and human bone marrow stromal cells differentiate into neurons." Journal of neuroscience research **61**(4): 364-370.

Xie, X., A. Hiona, A. S. Lee, F. Cao, M. Huang, Z. Li, A. Cherry, X. Pei and J. C. Wu (2011). "Effects of long-term culture on human embryonic stem cell aging." Stem Cells Dev **20**(1): 127-138.

Xu, C., M. S. Inokuma, J. Denham, K. Golds, P. Kundu, J. D. Gold and M. K. Carpenter (2001). "Feeder-free growth of undifferentiated human embryonic stem cells." Nature biotechnology **19**(10): 971-974.

Yan, Y., D. Yang, E. D. Zarnowska, Z. Du, B. Werbel, C. Valliere, R. A. Pearce, J. A. Thomson and S. C. Zhang (2005). "Directed differentiation of dopaminergic neuronal subtypes from human embryonic stem cells." Stem Cells **23**(6): 781-790.

Yoo, A. S., A. X. Sun, L. Li, A. Shcheglovitov, T. Portmann, Y. Li, C. Lee-Messer, R. E. Dolmetsch, R. W. Tsien and G. R. Crabtree (2011). "MicroRNA-mediated conversion of human fibroblasts to neurons." Nature **476**(7359): 228-231.

Zeng, X., J. Cai, J. Chen, Y. Luo, Z. B. You, E. Fotter, Y. Wang, B. Harvey, T. Miura, C. Backman, G. J. Chen, M. S. Rao and W. J. Freed (2004). "Dopaminergic differentiation of human embryonic stem cells." Stem Cells **22**(6): 925-940.

Zhang, L., Y. Zhou, G. Li, Y. Zhao, X. Gu and Y. Yang (2014). "Nanoparticle mediated controlled delivery of dual growth factors." Sci China Life Sci **57**(2): 256-262.

Zhao, C., G. Sun, S. Li and Y. Shi (2009). "A feedback regulatory loop involving microRNA-9 and nuclear receptor TLX in neural stem cell fate determination." Nat Struct Mol Biol **16**(4): 365-371.

Ziello, J. E., Y. Huang and I. S. Jovin (2010). "Cellular endocytosis and gene delivery." Mol Med **16**(5-6): 222-229.

Zuba-Surma, E. K., M. Kucia, J. Ratajczak and M. Z. Ratajczak (2009). ""Small stem cells" in adult tissues: very small embryonic-like stem cells stand up!" Cytometry A **75**(1): 4-13.